
Monitoring Large Conservation Areas with Imaging Spectroscopy: Combining Discrete and Non-discrete Approaches

Carola Weiß



München 2008

Monitoring Large Conservation Areas with Imaging Spectroscopy: Combining Discrete and Non-discrete Approaches

Carola Weiß

Dissertation
der Fakultät für Geowissenschaften
der Ludwig-Maximilians-Universität
München

vorgelegt von
Carola Weiß
aus München

München, den 14. April 2008



1. Gutachter: Prof. Dr. Friedrich Wieneke
 2. Gutachter: Prof. Dr. Ralf Ludwig
 3. Gutachter: Prof. Dr. Sebastian Schmidlein
- Tag der Disputation: 26. Juni 2008

Contents

List of Figures	x
List of Tables	xi
Abbreviations	xiii
Summary	xv
Zusammenfassung	xxi
1 Monitoring Large Conservation Areas	1
1.1 The Commitment of the FFH-Directive	1
1.2 The Continuum Problem	2
1.3 Combining Discrete and Non-discrete Approaches	2
2 Mapping Natural and Semi-natural Vegetation	5
2.1 Habitat Monitoring	5
2.2 Plant Communities versus Continuum Concept	6
2.3 Imaging Spectroscopy for Vegetation Mapping	8
3 The Murnauer Moos	13
3.1 Genesis and Geologic, Pedologic, and Climatic Realities	14
3.2 Fauna, Flora and Habitats	15
3.3 Utilisation and Conservation	16
4 Materials and Methods	19
4.1 Scene Data	19
4.1.1 Preprocessing Steps	19
4.1.2 Radiance Log Transformation and Band Selection	22
4.2 Vegetation Data	22
4.2.1 Sampling Steps	23
4.2.2 Vegetation Period 2004	23

4.2.3	Vegetation Period 2005	28
4.2.4	Extracting Spectra	30
4.3	Ordination and its Mapping	31
4.3.1	Indirect Ordination in Reduced Space	32
4.3.2	NMS - Non-metric Multidimensional Scaling	33
4.3.3	PLS Regression Models	34
4.3.4	Constructing Borderless Maps	37
4.4	Classification and its Mapping	38
4.4.1	Vegetation Classification	38
4.4.2	Pixelbased Supervised Image Classification	40
4.5	Synthesis	48
4.5.1	Complementary Analysis: Constructing Colour Legends	48
4.5.2	Combining Discrete and Non-discrete Approaches	49
5	Results	51
5.1	Ordination and its Mapping	51
5.1.1	Ordination Results: NMS	51
5.1.2	PLS Regression Models	61
5.1.3	Constructing Borderless Maps	62
5.2	Classification and its Mapping	65
5.2.1	Phytosociological Classification	66
5.2.2	Sociation Concept	76
5.2.3	Delineation of Fauna-Flora-Habitats	80
5.2.4	Image Classification Results	87
5.3	Synthesis	97
5.3.1	Complementary Analysis	97
5.3.2	Synthesis Maps	102
6	Discussion and Outlook	105
6.1	Data Collection	105
6.2	Ordination and its Mapping	108
6.3	Classification and its Mapping	110
6.4	Synthesis	115
6.5	Usage for Conservancy Purposes	116
	Bibliography	117
A	Tables	141
A.1	MRPP: Tests on homogeneity	142
A.2	NMS Axis Scores	147
A.2.1	Data 2004	147

A.2.2	Data 2005	149
A.3	Plot Header Data	151
A.4	Vegetation Classification Tables	155
A.4.1	Phytosociology	155
A.4.2	Sociation	155
A.4.3	Fauna-Flora-Habitats	155
B	Synthesis Maps	157
	Acknowledgements	159

List of Figures

2.1	Characteristic sample spectra of green vegetation	9
3.1	The Murnauer Moos	14
3.2	Mining at Langer Köchel	17
4.1	The project's workflow	20
4.2	The raw image data before and after preprocessing	21
4.3	Systematic sampling raster	25
4.4	Sampling grids of 2004	26
4.5	Subplot design 2004	27
4.6	Map of ISODATA strata	30
4.7	Stratified random sampling design of 2005	32
4.8	Extracting spectra 2005	33
4.9	Red-green colour space	37
4.10	Sample MSD spectrum	43
4.11	Sample ISD spectra	44
4.12	Sample RMSE matrix	45
4.13	Sample BRSD spectrum	45
5.1	Stress values of NMS ordination	52
5.2	NMS ordination scatterplot of the subarea 2004 north.	53
5.3	Species cover values I, NMS 2004 north	55
5.4	Species cover values II, NMS 2004 north	56
5.5	NMS ordination scatterplot of the subarea 2004 south.	57
5.6	Species cover values, NMS 2004 south	58
5.7	NMS ordination scatterplot of the subarea 2005	59
5.8	Species cover values - NMS 2005	60
5.9	Colour composites of regression models of 2004 and 2005	64
5.10	Disposition of communities	65
5.11	Photos of <i>Phragmitetalia</i> communities	68
5.12	Photos of the <i>Molinietum caeruleae</i> , and of the <i>Molinia</i> -Stadium	72

5.13	Photos of species of the <i>Sphagnion magellanicum</i> communities . . .	74
5.14	Photos of <i>Molinia caer.</i> , <i>Trichophorum cesp.</i> , and <i>Calluna vulg.</i>	79
5.15	Map of degraded raised bogs	83
5.16	Photos of depressions on peat substrates	84
5.17	Photos of species of alkaline fens	86
5.18	Vegetation type polygons of the subarea 2004 north	89
5.19	Vegetation type polygons of the subarea 2004 south	90
5.20	Vegetation type polygons of the subarea 2005	91
5.21	Results of image classification: phytosoc. vegetation types . . .	92
5.22	Spectral differentiability between phytosociological types . . .	93
5.23	Results of image classification: sociation vegetation types . . .	94
5.24	Spectral differentiability between sociation vegetation types . .	94
5.25	Results of image classification: Fauna-Flora-Habitat types . . .	96
5.26	Spectral differentiability between sociation vegetation types . .	96
5.27	Complementary analysis of the subarea 2004 north	98
5.28	Complementary analysis of the subarea 2004 south	99
5.29	Complementary analysis of the subarea 2005	101
5.30	Detail Synthesis maps, subarea 2004 north	103
6.1	Fractions of vegetation types within ISODATA strata	107
A.1	Header Data 2004 north	151
A.2	Header Data 2004 south	152
A.3	Header Data 2005 I	153
A.4	Header Data 2005 II	154

List of Tables

4.1	Sensor and flight information of the imaging spectroscopy data	21
4.2	Parameters taken <i>in situ</i>	24
4.3	Stratum sample numbers according to standard deviation . . .	31
4.4	Sample confusion matrix	47
5.1	NMS ordination results of the vegetation data 2004 and 2005 .	52
5.2	PLS regression model results	62
5.3	Occurring phytosociological plant communities	67
5.4	Occurring plant sociations	76
5.5	Occurring Fauna-Flora-Habitats	80
5.6	Image classification results	87
A.1	MRPP test: floristic homogeneities among subplots 2004 . . .	142
A.2	MRPP test: Spectral homogeneity among subplots 2004 . . .	144
A.3	MRPP test: Spectral homogeneity among plots 2005	145
A.4	NMS axis scores 2004 north	147
A.5	NMS axis scores 2004 south	148
A.6	NMS axis scores 2005	149

Abbreviations

BRSD	Best Reference Spectra Determination
FFH	Fauna-Flora-Habitat
ISD	Individual Spectra Determination
ISODATA	Iterative Self-Organizing Data Analysis Technique
LSU	Linear Spectral Unmixing
MESMA	Multiple Endmember Spectral Mixture Analysis
MIR	Middle Infrared Region
MNF	Minimum Noise Fraction
MRPP	Multi-Response Permutation Procedure
MSD	Mean Spectra Determination
NIR	Near Infrared Region
NMS	Non-metric Multidimensional Scaling
PCA	Principal Component Analysis
PHY	Phytosociological Classification
PLS	Partial Least Squares
RMSE	Root Mean Squared Error
SAM	Spectral Angle Mapper
SD	Standard Deviation
SOC	Sociation Concept, Classification for Dominance Aspects
VIS	Visual wavelength range

Abbreviations used in the phytosociological classification

AR	<i>Arrhenatherion</i>
CE	<i>Caricetum elatae</i>
CM	<i>Cladietum marisci</i>
ET	<i>Eriophoro-Trichophoretum cespitosi</i>
MC	<i>Molinetum caeruleae</i>
MSt*b	<i>Molinia</i> -Stadium (abandoned fen meadows)
MSt*f	<i>Molinia</i> -Stadium (desiccated bogs)
PC	<i>Phragmitetum communis</i>
PM	<i>Pino mugo-Sphagnetum magellanicum</i>
PS	<i>Primulo-Schoenetum ferruginei</i>
SM	<i>Sphagnetum magellanicum</i>
SR	<i>Sphagnetum magellanicum-Rhynchosporion</i> -Complex

Abbreviations used in the sociation classification

Cl	<i>Phragmites comm.-Cladium mar.-Molinia caer.</i> -Sociation
CE	<i>Carex elata</i> -(Con-)Sociation
C	<i>Calluna vulgaris</i> -Consociation
CS	<i>Calluna vulgaris-Sphagnum</i> -Association
F	Tall Forbs-Association
M	<i>Molinia caerulea</i> -Consociation
MPH	<i>Molinia caerulea-Phragmites communis</i> -Subconsociation
MS	<i>Molinia caerulea-Sphagnum</i> -Association
MT	<i>Molinia caerulea-Trichophorum cesp.</i> -Subconsociation
Pin	<i>Pinus mugo-Sphagnum</i> -Association
Ph	<i>Phragmites communis-Carex elata</i> -Sociation
T	<i>Trichophorum cespitosum</i> -Consociation

Acronyms used in the FFH-/biotope classification

GR	Reeds
GP00BK	Secondary developed <i>Molinia</i> -meadows
VC00BK	Large sedge formation of siltation zone
6410	<i>Molinia</i> -meadows on calcareous soils
6430	Tall herb fringe communities
6510	Hay meadows of the planar level
6520	Mountain hay meadows
7110	Active raised bogs
7120	Degraded raised bogs still capable of natural regeneration
7150	Depressions on peat substrates of the <i>Rhynchosporion</i>
7210	Calcareous fens with <i>Cladium mariscus</i>
7230	Alkaline fens
91D3	Mountain pine bog woods

Summary

In all member states of the European Union the enactment of the European Fauna-Flora-Habitats Directive gave reason for the development of new monitoring approaches. The Habitats Directive (Council of the European Union/ Der Rat der Europäischen Gemeinschaften, 1992) is part of the Natura 2000, a network of conservation areas in all member states of the European Union. To maintain endangered habitats and biodiversity (listed in the Appendix I and II of the Habitats Directive), monitoring is a main postulate, and has been set by a reporting commitment (article 17 of the FFH-Directive). Each member state has to designate conservation areas of common interest. These areas have to be mapped and monitored intensely on a stand level, i.e. on a level of plant communities. Traditional field methods are cost-intensive, and do not account for an area-wide high spatial resolution. To fulfil the reporting commitment of the European Fauna-Flora-Habitats Directive, we propose a technique that reforms the approved traditional field methods by the use of spatially and spectrally highly resolved remote sensing data (imaging spectroscopy data). Hence, the potential of airborne imaging spectroscopy for openland vegetation mapping and monitoring in conservancy was investigated.

Vegetation maps need discrete class information to give names and areas to stands. As well, vegetation maps need continuous information to allow for the continuous reality of nature and the important role of ecotones in monitoring. Main aim of this project was to solve this apparent contradiction.

The new method was developed and evaluated using image and field data taken in the wetland complex Murnauer Moos area, Upper Bavaria. This large conservation area comprises various intertwined habitat types of European Community importance, among them reeds, fringe communities, large sedge beds, fens, meadows, margin lag and raised bog communities.

The airborne imagery had been gathered using the imaging spectrometer HyMapTM. The scene was taken during the vegetation period 2003, and provides spectral information in the wavelength range from VIS to MIR (438 - 2500 nm) within 128 bands, each having a spectral resolution of 15 - 20 nm.

After preprocessing and georeferencing steps, 105 spectral bands remained with a spatial resolution of $4 \times 4 \text{ m}^2$.

Field data collection was based on different sampling designs on ground. One data set was taken with a systematic sampling grid in 2004, whereas a second data set, taken in 2005, was based on restricted random sampling.

The data set of the vegetation period 2004 comprised 112 relevés gained from two systematic sampling grids. Errors that possibly occur when linking GPS-geolocalised relevés with spectra of the georeferenced scene, were reduced by the application of a subplot design. Each plot contained three circular relevés (subplots) of 4 m^2 that formed a triangle. By MRPP test (Multi-Response Permutation Procedure, Biondini et al. 1985), the plots were tested on within-plot homogeneity, and averaged. Heterogeneous plots were discarded. Where the GPS-coordinates of the subplot centres hit the scene, pixels were extracted, also tested on homogeneity (MRPP), and averaged. Thereby, 104 out of 112 plots of the two test sites remained for further analyses.

For the restricted random sampling design 2005, stratification was done by unsupervised ISODATA (Iterative Self-Organizing Data Analysis Technique, Duda and Hart 1973) classification of the imagery. Eight stable strata were calculated, and between 10 and 20 plots were randomly distributed within the strata, according to the standard deviation of each stratum. The data set of the vegetation period 2005 included 100 circular relevés of 4 m^2 . The reference spectra were taken from the scene pixels that were hit by the GPS-coordinates of the relevés centres. Possible wrong pixel assignment was reduced by the extraction of four neighbouring pixels per plot. These four spectra were tested on homogeneity (MRPP), and averaged. Of originally 100 plots of the data set 2005, 97 were used in further analyses.

To gain maps of gradients and transitions, field data were ordinated and linked with spectra via multiple regression. With ordination techniques, the complex, multidimensional plot versus taxa-matrix can be reduced to few dimensions, and its structure can be displayed in the ordination space. We used NMS (Non-metric multidimensional scaling, Shepard 1962; Kruskal 1964) ordination, because it bears the advantage that the numbers of dimensions of the ordination can be pre-defined. This was of interest in respect of a later legend generation. Solutions were calculated to display the variance of the original and the log-transformed vegetation data sets by two dimensions. Log-transformed vegetation data sets always performed better. The resulting solutions explained 82 - 95 % of the variance. Each axis was regressed against spectra via PLS1 (Partial Least Squares) -regression. Model performance was validated by a full cross-validation. Long gradients, with high explanatory power in NMS ordination, lead to better models than short gra-

dients. R^2 of 0.6 to 0.93 could be gained for the longer gradients, whereas R^2 of 0.29 to 0.44 were obtained for the shorter gradients. The resulting models were applied to the full scene. To gain maps of gradients and transitions, we combined both gray-scale regression models of the two NMS axes to a red-green colour composite.

To gain maps of discrete vegetation type information, we classified the field data, and used the spectra of the resulting categories to supervise image classifications. Three different vegetation classification schemes were applied to the vegetation data sets. Diagnostic taxa established a relationship to the phytosociological system of Central Europe (Braun-Blanquet, 1928). A classification by the sociation concept of Du Rietz (1930) appeared advantageous for remote sensing matters as it is based on dominant species and dominant species contribute most to the mainly reflected structures. We sorted into Fauna-Flora-Habitat types using classification keys set up by the Habitats Committee (European Commission DG Environment, 2003) or by the federal states (Lang and Walentowski, 2007) that were mainly based on diagnostic species. Results were used to supervise pixelbased image classification algorithms. We tested SAM (Spectral Angle Mapper, Kruse et al. 1993) and MESMA (Multiple Endmember Spectral Mixture Analysis, Roberts et al. 1998) with full cross-validation, and calculated the quality of the image classification procedures (κ and overall accuracy).

Three methods of reference spectra determination were applied. The MSD (Mean Spectra Determination) method averages all spectra of a class, i.e. vegetation type. The ISD (Individual Spectra Determination) method is based on the idea of de Lange et al. (2004). All spectra of a vegetation type are used as reference. Only after image classification, vegetation type memberships are regarded. The BRSD (Best Reference Spectra Determination) follows the concept of Dennison et al. (2004), and determines the spectrum which represents its vegetation type best. Each spectrum is unmixed with each other spectrum that belongs to the same vegetation type. The spectrum that unmixes the components of its vegetation type with the least RMS Error (Root Mean Squared Error) is used as reference spectrum for this certain vegetation type in the image classification procedure.

Image classification performed well with all three applied vegetation classification schemes. Reference spectra derived from well defined, or well characterised structures are able to differentiate the vegetation types of the two testing areas of 2004 and the one of 2005 with high quality. Spectra of relevés of transition zones as well as mixed stands which can not be properly assigned to vegetation types show also confusions in image classifications. Hence, these reference spectra are not appropriate, or pure enough, to separate. This applies to all vegetation classifications.

SAM classification with an individual reference spectra determination approach (ISD) gained best κ results between 0.51 and 0.93, and overall accuracy results between 61 and 95 % in cross-validation. The ISD approach takes into account the heterogeneity of natural vegetation stands. This heterogeneity applies to most of the vegetation types of all three applied vegetation classifications. Deeper investigations on stand level show that homogeneous stands can be better classified by SAM classification using average reference spectra per vegetation type (MSD). Some weakly defined structures are best detected by the use of the best reference spectra determination (BRSD) approach.

To gain Synthesis maps that combine discrete and non-discrete mapping approaches, we combined the polygons derived from image classifications as transparent overlays with the red-green colour composites of the regression models. The resulting Synthesis maps display informations on the continuous attributes of natural vegetation as well as on vegetation types. The maps can be interpreted with a two-fold legend. On the one hand, PLS regression models display all existing habitats that have been sampled in their variance, defined by a two-dimensional colour space, where also the centroids of the mapped vegetation types are displayed. Homogeneous as well as heterogeneous areas with transitions in between can be identified. All colours can be referred to positions in the two-dimensional ordination space and indicate habitat definition and species composition. The quality of the models is given by the coefficient of determination (R^2) for each axis as well as by the explanatory power of the ordination. On the other hand, vegetation stands are mapped by polygons derived from different image classifications. Vegetation type colours in the map depend on the colour space of the NMS ordination. Homogeneous areas show more or less homogeneous colours whereas transition zones and mixed stands show graduated colours and dispersions (Salt-and-Pepper-Effects). Types that are closely related to each other, show similar colour space positions and are difficult to separate. Therefore, different hatchures are overlaid. In case of vegetation types that have very similar species composition, equal hatchures are overlaid but coloured, e.g. point signatures in blue, white or black. The quality of image classifications κ applies for each pixel of the scene, and can be projected for each type as percentage of correctly classified relevés. This enables deeper research, if individual structures shall be mapped in more detail for a certain monitoring approach.

With this study, we succeeded in developing a reproducible method that solves the apparent contradiction between maps containing continuous information and maps containing class information. We produced Synthesis maps that deliver two-fold information on pixel basis: vegetation type membership

on the one side, stand position in the context of the continuous field of the vegetation on the other. Hence, ecotones can be monitored within habitats. We were able to show that with the use of high spatial and spectral resolution of the imagery, this information is given in the same spatial detail for a large area, and the quality of the given details is measurable. Producing maps of this level of detail and spatial extent is not possible by traditional field methods.

Field data are an important component, as PLS regression models are based on ordination axes that have been calculated from relevés data. Also, in the context of supervised image classifications, for each monitoring study, a new spectral library should be formed by the collection of samples to account for the local realities of vegetation. It is advised against the use of extant spectral libraries from other regions, because the same vegetation types of different areas can highly differ from each other, e.g. concerning species composition and phenology. Field data can be taken from extant mapping projects in the area under investigation, if sampling and scene acquisition interval allows for.

In the course of the reporting commitment of article 17 of the FFH-Directive, a combined relevé utilisation is supposable in the context of systematic inventarisations of biotopes. For a complete map, the sampling design should ensure that all habitats are included in the relevés data that occur in the area of investigation, and well characterised samples should ensure a spectral differentiation. To base mapping on objective data, but best allow for the mentioned conditions, we propose a restricted random sampling design, where unsupervised image classifications of the image data deliver the stratum informations. The number of samples for each stratum should be calculated according to the variance of each stratum.

Zusammenfassung

In allen Mitgliedstaaten der EU gibt die Umsetzung der Fauna-Flora-Habitat (FFH)-Richtlinie des Europäischen Rates Anlass, neue Monitoringmethoden zu entwickeln. Die FFH-Richtlinie (Council of the European Union/ Der Rat der Europäischen Gemeinschaften, 1992) ist Bestandteil der Natura 2000, eines Netzwerkes von Naturschutzgebieten in allen Mitgliedstaaten der EU. Um gefährdete Lebensräume nach Anhang I der Richtlinie und die darin enthaltene Biodiversität zu erhalten, ist die dauerhafte Beobachtung dieser Schutzgebiete Voraussetzung. Demzufolge wurde die Beobachtung dieser Flächen und deren Dokumentation in der FFH-Richtlinie festgeschrieben (Berichtspflicht nach Artikel 17 der FFH Richtlinie). Die EU-Mitgliedstaaten sind verpflichtet, Naturschutzgebiete von gemeinschaftlicher Bedeutung gemäß ihres Arten- und Lebensrauminventars zu melden (Anhang I und II der Richtlinie). Diese Gebiete müssen kartiert und dauerhaft mit hoher räumlicher Auflösung beobachtet werden. Traditionelle Methoden der Feldkartierung sind sehr kostenintensiv und werden der geforderten gebietsweiten hohen räumlichen Auflösung nicht gerecht. Um die Berichtspflicht der FFH-Richtlinie umzusetzen, verhelfen wir den bewährten Feldmethoden zu größerer Effizienz durch die Kombination mit sowohl räumlich als auch spektral hoch aufgelösten Fernerkundungsdaten (Hyperspektraldaten). Dafür wurde das Potential von flugzeuggestützten Hyperspektraldaten für die Vegetationsbeobachtung von Offenlandtypen untersucht.

Vegetationskarten benötigen diskrete Klasseninformation, um Bestände zu benennen und abzugrenzen. Ebenso sollen Informationen abgebildet werden, die den kontinuierlichen Gegebenheiten der Natur und der wichtigen Rolle, die Ökotope (Übergänge) für das Monitoring spielen, gerecht werden. Im Vordergrund dieser Arbeit stand daher, diesen scheinbaren Widerspruch aufzulösen und beide Ansätze in einer Karte zu vereinen.

Als Untersuchungsgebiet für die Methodenentwicklung und -evaluierung wurde das Murnauer Moos in Oberbayern gewählt. Es stellt den größten zusammenhängenden Moorkomplex der nördlichen Alpenrandmoore dar. Enthalten sind zahlreiche Lebensraumtypen von gemeinschaftlicher Bedeutung,

darunter Schilf- und Uferbestände, Großseggenriede, Niedermoore, Streuwiesen, Randlagg- und Hochmoorbestände.

Das hyperspektrale Datenmaterial wurde mit dem flugzeuggestützten Sensor HyMapTM in der Vegetationsperiode 2003 aufgenommen. Die Szene enthält die spektrale Information über den Wellenlängenbereich vom VIS bis MIR (438 - 2500 nm) in 128 Bändern. Jedes Band hat eine spektrale Auflösung zwischen 15 - 20 nm. Nach Vorprozessierung und Georeferenzierung wurden 105 spektrale Bänder für die Methodenentwicklung des Projekts verwendet. Die Auflösung am Grund betrug $4 \times 4 \text{ m}^2$.

Felddaten wurden mit zwei verschiedenen Stichprobenstrategien erhoben. Mit einem systematischen Raster wurde der Datensatz 2004 aufgenommen, der Datensatz 2005 hingegen basierte auf einem stratifiziert-zufälligen Sampling-Design.

In der Vegetationsperiode 2004 wurden 112 Vegetationsaufnahmen (Plots) mittels zweier systematischer Samplingraster aufgenommen. Um eventuell auftretende Fehler bei der Inbezugsetzung von Vegetationsaufnahmen zu den Spektren der georeferenzierten Szene zu verringern, wurde ein aufwändiges Subplotdesign angewandt. Jeder Plot enthielt drei kreisförmige Vegetationsaufnahmen von 4 m^2 , die sich in Form eines Dreiecks anordneten. Die Plots wurden mittels MRPP-Test (Multi-Response Permutation Procedure, Biondini et al. 1985) auf ihre Homogenität überprüft und gemittelt. Heterogene Plots wurden verworfen. Über die GPS-Koordinaten der Subplotmittelpunkte wurden die Spektren der zugehörigen Pixel aus der Szene extrahiert, ebenfalls mittels MRPP-Test auf Homogenität überprüft und gemittelt. Von den ursprünglichen 112 Plots der zwei Testgebiete des Datensatzes der Vegetationsperiode 2004 gingen schließlich 104 Plots in die weiteren Auswertungen ein.

Für ein stratifiziert-zufälliges Sampling 2005 erfolgte die Stratifizierung durch eine unüberwachte ISODATA (Iterative Self-Organizing Data Analysis Technique, Duda and Hart 1973) Klassifikation der hyperspektralen Szene. Es konnten acht stabile Straten ermittelt werden, in denen zwischen 10 und 20 Plots zufällig verteilt wurden. Die Anzahl der Vegetationsaufnahmen pro Stratum richtete sich nach der jeweiligen Varianz der Straten. Der Datensatz von 2005 enthielt 100 kreisförmige Plots von je 4 m^2 . Die zugehörigen Spektren wurden an den Pixeln der Szene extrahiert, die durch die GPS-Koordinaten der Plotmittelpunkte getroffen wurden. Um Fehlzuordnungen abzuschwächen, wurden zusätzlich die Spektren von dreier weiterer Nachbarpixel extrahiert. Diese vier Spektren wurden mittels MRPP-Test auf Homogenität geprüft. Nach diesen Schritten gingen 97 von 100 Plots des Datensatzes von 2005 in die weiteren Analysen mit ein.

Um Karten zu erhalten, die Gradienten und Übergänge abbilden, wur-

den die Felddaten ordiniert und mit den Spektren regrediert. Mit Ordinationsverfahren kann die komplexe, vieldimensionale Plot x Taxa-Matrix auf wenige Dimensionen reduziert und deren Struktur im Ordinationsraum dargestellt werden. Hier wurde die indirekte NMS (Non-metric Multidimensional Scaling, Kruskal 1964) Ordination verwendet, die den Vorteil bietet, dass die Anzahl der gewünschten Dimensionen der Ordination voreingestellt werden kann. Dies war für eine spätere Legendengenerierung zielführend. Es wurden Lösungen berechnet, die die Varianz der originalen und der log-transformierten Vegetationsdatensätze in zwei Dimensionen darstellen. Log-transformierte Datensätze lieferten stets die besseren Ergebnisse. Die errechneten Lösungen erklärten 82 - 95 % der Varianz. Mit PLS 1 (Partial Least Squares) Regression wurden die Ordinationsachsenwerte mit den Spektren regrediert. Die Güte der errechneten Modelle konnte mit einer kompletten Cross-Validierung geprüft werden. Lange Gradienten mit großer Erklärungskraft lieferten bessere Modelle als kurze Gradienten. R^2 von 0.6 bis 0.93 konnten für die Modellierung langer Gradienten erzielt werden, R^2 von 0.29 bis 0.44 für kurze Gradienten. Die errechneten Regressionsmodelle wurden auf die volle Szene angewandt. Um Karten von Gradienten und Übergängen zu erhalten, wurden die Graustufenmodelle beider NMS Achsen übereinandergelegt und zu einer Rot-Grün-Farbkombination vereinigt.

Um Karten zu erhalten, die diskrete Klasseninformation abbilden, klassifizierten wir die Vegetationsaufnahmen und benutzten die Spektren der resultierenden Vegetationstypen als Referenzen, um die Bildklassifikationen zu überwachen. Die Vegetationsdaten wurden mit drei verschiedenen Vegetationsklassifikationen eingeteilt. Diagnostische Arten stellten den Bezug zum pflanzensoziologischen System Mitteleuropas her (Braun-Blanquet, 1928). Eine Klassifikation nach dem Soziationskonzept von Du Rietz (1930) schien zweckmäßig für fernerkundliche Fragestellungen, da diese auf dominanten Arten beruht und dominante Arten auch die hauptsächlich reflektierten Strukturen bilden. Eine Einteilung nach Fauna-Flora-Habitaten erfolgte mittels Klassifikationsschlüsseln der EU-Arbeitsgemeinschaften (European Commission DG Environment, 2003) und der der Länder (Lang and Walentowski, 2007). Diese beruhen weitgehend auf Einteilungen nach Lebensräumen, den darin enthaltenen diagnostischen Arten und dem Erhaltungszustand des Lebensraums. Die Ergebnisse wurden zur Überwachung der Bildklassifikationen herangezogen. SAM (Spectral Angle Mapper, Kruse et al. 1993) und MESMA (Multiple Endmember Spectral Mixture Analysis, Roberts et al. 1998) wurden angewandt und mit voller Cross-Validierung getestet. Hierbei wurde die Güte der Bildklassifikationen errechnet (κ und overall accuracy)

Es wurden drei Methoden angewandt, die Referenzspektren für die überwachte Bildklassifikation aufzubereiten. Als MSD (Mean Spectra Determi-

nation) Methode bezeichnen wir die Mittelung der Spektren einer Klasse, d.h. eines Vegetationstyps. Die ISD (Individual Spectra Determination) Methode basiert auf der Idee von de Lange et al. 2004. Es werden alle Spektren aller Vegetationstypen als Referenz genutzt. Erst nach der Bildklassifikation werden Klassenzugehörigkeiten beachtet. Ein Ansatz, den wir BRSD (Best Reference Spectra Determination) Methode bezeichnen, ermittelt das repräsentativste Spektrum eines Vegetationstyps (nach dem Konzept von Dennison et al. 2004). Mit spektraler Entmischung wird jedes Spektrum mit jedem entmischt, das zu seinem Vegetationstyp gehört. Das Spektrum, das die Komponenten seines Vegetationstyps mit dem geringsten RMS Fehler (Root Mean Squared Error) entmischt, wird als Referenzspektrum für die Bildklassifikation herangezogen.

Alle drei Vegetationsklassifikationen lieferten gute Ergebnisse in der Bildklassifikation. Referenzspektren gut definierter oder gut charakterisierter Bestände konnten die beiden Testgebiete des Datensatzes 2004 und den von 2005 mit hoher Qualität differenzieren. Vegetationsaufnahmen von Übergangszonen und gemischten Beständen, die sich schwer den Vegetationstypen zuordnen ließen, zeigten ebenso Konfusion in der Bildklassifikation. Deswegen waren ihre Referenzspektren nicht geeignet, oder nicht rein genug, um zu differenzieren. Dies galt für alle Vegetationsklassifikationen.

Beste κ zwischen 0.51 und 0.93 und overall accuracy Ergebnisse zwischen 61 und 95 % in der Cross-Validierung wurden mit SAM erzielt in Kombination mit der ISD Methode. Dieser Ansatz berücksichtigt die Heterogenität natürlicher Vegetationsbestände, was der Heterogenität entspricht, die der Großteil der Vegetationstypen der drei angewandten Vegetationsklassifikationen aufweist. Tiefere Untersuchungen auf Bestandesebene zeigten, dass homogene Bestände besser differenziert wurden, wenn das gemittelte Spektrum eines Vegetationstyps benutzt wurde (MSD). Sehr schwach charakterisierte Strukturen konnten am besten mit der BRSD Methode differenziert werden.

Die Grenzen, die die Bildklassifikationen produzierten, wurden als durchsichtige Polygone über die Rot-Grün-Farbkompositionen der Regressionsmodelle gelegt. Die resultierenden Synthesekarten zeigen sowohl Informationen über kontinuierliche Attribute natürlicher Vegetationsbestände als auch über Vegetationstypen. Die Karten können durch eine zweigeteilte Legende interpretiert werden. Zum einen zeigen die PLS Regressionsmodelle alle Strukturen, die aufgenommen wurden in ihrer Varianz, definiert durch einen zwei-dimensionalen Farbraum, in dem auch die Zentren der kartierten Vegetationstypen im Ordinationsraum dargestellt sind. Sowohl homogene als auch heterogene Bestände mit Übergängen dazwischen können unterschieden werden. Alle Farben der Karte können den Positionen auf den Ordina-

tionsachsen zugeordnet werden, und somit auch Lebensräumen und Arteninventar. Die Modellqualität ist durch das Bestimmtheitsmaß (R^2) und die erklärte Varianz der zugrunde liegenden Ordination in Prozent angegeben. Zum anderen werden Vegetationsbestände angezeigt mit Polygonen, deren Grenzen aus den Bildklassifikationen resultieren. Die Farben der Vegetationstypen hängen vom Farbraum der Regressionsmodelle ab. Homogene Bestände zeigen homogene Farben, gemischte Bestände und Übergangszonen werden durch Farbübergänge und Streueffekte (Salt-and-Pepper-Effects) gekennzeichnet. Ähnliche Bestände zeigen ähnliche Farbgebungen und sind auf der Karte schwer zu unterscheiden. Durchsichtige Schraffuren verschiedener Signaturen helfen hier. Bei sehr ähnlichem Arteninventar zweier Vegetationstypen empfiehlt es sich, gleiche Schraffuren in unterschiedlicher Farbgebung anzuwenden, z.B. Punktsignaturen in blauer, weißer oder schwarzer Farbgebung.

Die Güte der Bildklassifikation κ gilt für jedes Pixel des klassifizierten Gebiets und kann auch in Prozent für jeden einzelnen Vegetationstyp angezeigt werden. Dies ermöglicht tiefergehende Untersuchungen, falls einzelne Bestände Gegenstand von gesonderten Untersuchungen sind.

Mit dieser Arbeit ist es uns gelungen, eine reproduzierbare Methode zu entwickeln, die den scheinbaren Widerspruch auflöst zwischen einer Karte, die Informationen zu Übergängen enthält und einer Karte, die Informationen zu Klassen abzubilden vermag. Wir erstellten Synthesekarten, die sowohl Informationen zu abrupten als auch zu kontinuierlichen Vegetationsübergängen enthalten. Mit ihrer Hilfe können für jeden Bestand sowohl Klassenzugehörigkeiten ermittelt werden, als auch dessen Position im Kontinuitätsgefüge natürlicher Vegetation. Folglich können Ökotope in ihrem Lebensraum überwacht werden. Die Verwendung von sowohl räumlich als auch spektral hochaufgelösten Bilddaten gibt die oben genannten Informationen in gleicher räumlicher Auflösung auch für sehr große Gebiete wieder. Die räumliche Auflösung der Karten entspricht der Größe der Pixel aus der eingegangenen hyperspektralen Szene. Die Güte der abgebildeten Informationen ist messbar. Eine Kartengenerierung in dieser Detailschärfe und räumlicher Ausdehnung ist mit herkömmlichen Feldmethoden alleine nicht möglich.

Feldaufnahmen bleiben ein unverzichtbares Werkzeug: zum einen bilden sie die Basismatrix (Plot x Taxa) für Ordinationen, auf denen die Regressionsmodelle beruhen. Zum anderen sollten zur Überwachung von Bildklassifikationen für jede Monitoring-Studie neue Felddaten erhoben werden, um den Gegebenheiten vor Ort gerecht zu werden. Die Verwendung von bereits vorhandenen Spektralen Bibliotheken aus anderen Gebieten ist als kritisch zu bewerten, da gleiche Vegetationstypen unterschiedlicher Gebiete starke lokale Differenzen aufweisen können, z.B. hinsichtlich Artenzusammensetzung und

Phänologie. Vegetationsdaten können auch aus vergleichbaren Kartierprojekten stammen, falls Aufnahme-Design und der Zeitunterschied zur Hyperpektralszene dies erlauben.

Im Zuge der FFH-Berichtspflicht nach Art. 17 der Richtlinie ist eine sinnvolle, kombinierte Nutzung bereits bestehender Kartierungen und Feldaufnahmen denkbar, z.B. gemeinsam mit systematischen Biotopkartierungen. Um vollständige Synthesekarten zu erhalten, sollte durch das Sampling-Design sichergestellt werden, dass alle im Untersuchungsgebiet vorhandenen Bestände auch im Vegetationsdatenmaterial vorhanden sind. Ebenso sollten gut charakterisierte Vegetationsaufnahmen deren spektrale Differenzierung ermöglichen. Um objektive Felddaten zu erhalten und den genannten Bedingungen gerecht zu werden, empfehlen wir die Verwendung eines stratifiziert-zufälligen Sampling-Designs mit einer Stratifizierung über eine unüberwachte Bildklassifikation des Bilddatenmaterials. Die Anzahl der Vegetationsaufnahmen kann entsprechend der Varianz pro Stratum gewichtet verteilt werden.

Chapter 1

Monitoring Large Conservation Areas with Imaging Spectroscopy

1.1 The Commitment of the Fauna-Flora-Habitats Directive

In all member states of the European Union the enactment of the European Fauna-Flora-Habitats Directive (Council of the European Union/ Der Rat der Europäischen Gemeinschaften, 1992) gave reason for the development of new monitoring approaches. The Habitats Directive is part of the Natura 2000, a network of conservation areas in all member states of the European Union. To maintain endangered habitats and biodiversity, monitoring is a main postulate, and has been set by a reporting commitment (article 17 of the FFH-Directive). Each member state has to designate conservation areas of common interest. These areas have to be mapped and monitored intensely on a stand level, i.e. on a level of plant communities.

In the face of the reporting commitment of the European Fauna-Flora-Habitats Directive, the question to pose is how it can be fulfilled (Fartmann et al., 2001; Kehrein, 2002). The actual size of the terrestrial European FFH-areas is about 56.000.000 ha (European Commission, 2007). Traditional field methods are cost-intensive, and do not account for an area-wide high spatial resolution. Consequently arises the necessity, or the chance, to strike a new path in vegetation mapping and monitoring. We propose a technique that reforms the approved traditional field methods by the use of remote sensing data with both high spatial and high spectral resolution, i.e. imaging spectroscopy data.

1.2 The Continuum Problem

”An arbitrary classification can also be justified as a practical convenience, provided one does not lose sight of the fact that dividing lines have been drawn where Nature put none.”

(Goodall, 1963, 298)

Mapping natural and semi-natural vegetation means dealing with highly complex structures. Homogeneous areas alternate with heterogeneous parts, mixed formations, and various transition zones inbetween. To fulfil the Habitats Directive, conservation managers are forced to determine boundaries. Habitats have to be defined, characterised, and labelled. That means that class information is highly important when mapping habitat types. Unfortunately, any crisp classification draws a boundary where Nature put none - to say it with the words of Goodall (1963). Transitions, the so-called ecotones, are the most interesting regions when monitoring vegetation. Changes of these transition zones can give information on slightest shifts, for example, of nutrient input, or draw down of ground water level. One can see that changes happen and one can see in which direction they happen. That means that vegetation maps must also allow for continuous vegetation information.

Altogether, vegetation maps need class information to give names and areas to vegetation types. As well, vegetation maps need continuous information to allow for the continuous reality of nature and the important role of ecotones in monitoring. Main challenge of this project was to solve this apparent contradiction.

1.3 Combining Discrete and Non-discrete Approaches

This study dealt with urgent problems of conservancy. Large areas have to be mapped and monitored in high spatial detail. Therefore, data derived from imaging spectroscopy were linked with field data. Hence, two basic approaches in the preparation of field data and in image processing respectively were combined to pay attention for both discrete information on habitat classes as well as continuous information on transitions and within-habitat variation. Furthermore, it was in the main focus to develop reproducible methods.

Aims of the Project

Summarising, two main goals stood in the focus of this study:

1. analysing the potential of imaging spectroscopy for vegetation mapping and monitoring in conservancy
2. developing a new mapping approach that combines discrete spatial information on vegetation classes with non-discrete information on the vegetation as a continuum

Proceeding of the Work

The workflow of this study is shown in fig. 4.1. Chapter 2 gives the current state of the art in respect to mapping natural and semi-natural vegetation. Habitat monitoring, the important role of ecotones, and the application of imaging spectrometry for vegetation mapping purposes are specified. Chapter 3 describes the area of investigation, the Murnauer Moos in Upper Bavaria, and details realities of the area. In chapter 4, materials and methods are presented, parted into scene data acquirement and preprocessing steps, followed by the vegetation data collection. Sampling strategies of two vegetation periods are described. Methods are explained in two sections, Ordination and its Mapping and Classification and its Mapping. First, with Non-metric Multidimensional Scaling (NMS) ordination techniques and Partial Least Squares (PLS) regression attention is paid to gradual vegetation transitions and within-habitat variation. Second, there are vegetation classification techniques that are suited to distinguish spatially discrete habitats. Three common vegetation classification keys are applied to the same data sets. They are used for supervised image classification algorithms like Spectral Angle Mapper (SAM) and Multiple Endmember Spectral Mixture Analysis (MESMA). Certain emphasis is placed upon the possibilities of endmember determination. The synthesis of both, namely of methods that deal with continuous structures, and methods that deal with discrete class information, forms the third part of the methods sections. In chapter 5, results are shown following the schedule line of the methods. Data collection, methods, and results are discussed in chapter 6. As well, the usage for conservancy purposes is treated, and an outlook is given.

Chapter 2

Mapping Natural and Semi-natural Vegetation

”No scheme can claim more than practical convenience and *relatively* little violence done to the facts.”

(Tansley and Chipp, 1926, 6)

This study combines methods of different fields. The basic motivation with its political background originates from nature conservancy, i.e. the commitment of the Fauna-Flora-Habitats Directive. Mapping natural vegetation bears continuum problems that can be solved with methods from vegetation science that can be applied in the field of remote sensing. The linkage with data derived from airborne imaging spectrometry combines the evaluation of field studies with applications of remote sensing and digital cartography.

2.1 Habitat Monitoring

Monitoring of vegetation is presumed to be an essential instrument of conservancy to inform and control (Traxler, 1998, 13ff). Common consensus consists that applicable methods have to be designed for attaining reproducible results that allow comparison over several years and decades. Coevally, expenditure of time and costs should be in due proportion to the achieved outcomes (Ssymank, 1997).

Monitoring of Fauna-Flora-Habitats comprises the control of the state of preservation of natural and semi-natural habitats according to article 11 of the FFH-Directive (Rückriem and Roscher, 1999; Fartmann et al., 2001). The acquisition of extent and condition of the areas has to be carried out

every 6 years. That amounts to an enormous effort in view of the expansive areas that have to be monitored. The responsibility of data collection lies within the federal states. To allow the assembly of all monitoring results to form a national report, data have to be comparable. Commendations have been framed from the EU, and LANA (AG conservancy of state department of environments) initiated workshops to evaluate the habitats of common interest, e.g. European Commission DG Environment (2003); Balzer et al. (2004); Stellmach and Langensiepen (2006, 2007); Lang and Walentowski (2007). For mapping purposes on a large scale, this study deals with relating the developed vegetation classification keys to remote sensing applications.

2.2 Plant Communities versus Continuum Concept

Since Clements (1916) published his studies on the succession of plant communities, the main focus of (European) phytosociological research laid on the distinction and classification of homogeneous units (e.g. Gams 1918; Du Rietz 1921). Furthermore, the established sampling strategies for setting out field plots focused on homogeneous and representative parts of the vegetation (e.g. reminded of Goodall 1963, 299). Vegetation scientists divided into two rivalling schools. On the one side were scientists that opined the existence of homogeneous plant communities, with some successional or fragmentary stages inbetween (e.g. Braun-Blanquet 1921; Williams and Lambert 1939; Ellenberg 1956; Williams and Lambert 1959; Daubenmire 1960; Kuchler 1973). Others, mainly Anglo-American scientists, described vegetation as continuous phenomena, denying the existence of plant communities (see e.g. Gleason 1926; Ramenski 1930; Whittaker 1956; Austin 1985). Ponyatovskaya (1961), Anderson (1965) and Glavac (1992) gave detailed views of the matter.

The Important Role of Ecotones

Ecotones (in between plant communities) were rather left beside (Daubenmire, 1968; Mueller-Dombois and Ellenberg, 1974; Stohlgren et al., 2000), and were more or less regarded as static structures (Risser, 1995). During the first decades of the 20th century, early approaches to investigate ecotones were made only in certain specific settings, e.g. wildlife habitats (Leopold, 1933), and treelines (Griggs, 1938). Not until the seventies of the last century, ecotones attracted broader notice to vegetation scientists. It became clear since, that ecotones are important dynamic components, which was backed by some investigations, e.g. works of Swanson and Sparks (1990); Holland

et al. (1991); Cornelius and Reynolds (1991); Hansen and diCatri (1992); Gosz (1993), and Fortin et al. (2000) among many others. Risser (1995) cites their sensitivity concerning flows of water, nutrients, and other important factors that influence vegetation. Ecotones function as ecological indicators, and research seems therefore challenging, especially for monitoring reasons and change detection of natural vegetation in the context of climate change. Ecotones help maintain species diversity as they expand the geophysiological range of certain types (Stohlgren et al., 2000). It is therefore of main interest to concentrate not only on the mapping of vegetation communities. Focus has to be laid onto transition zones inbetween as well, to enable monitoring of small changes in time.

Dealing with Gradients

Today, phytosociologists agree to the view that vegetation can be a continuous as well as a discontinuous phenomenon. The gradient along which plant communities occur can variegate, e.g. depending on environmental factors, on the viewpoint of the analysis, and on the self organisation of vegetation itself (Fortin et al., 2000). Vegetation scientists have found ways to deal with abrupt changes as well as with continuous transitions. Classifications are made to describe discrete patterns, whereas ordination methods display transitions of abrupt and of continuous nature.

Remote sensing has to cope with both abrupt and continuous structures as well. Abrupt structures can be analysed with crisp image classifications, where pixels of the imagery are assigned to a single class only. Already Treitz et al. (1992), and later Lewis (1998), correlated numerical classification methods of phytosociology with classification methods of image processing. That allowed for dominance aspects of the different species within the image classification. This approach has also been followed by Jacobsen (2000) and Jacobsen et al. (2000), who integrated the spectral classification with vegetation and land use categories. Thomas et al. (2002) added ordination methods that come from phytosociology, but without using this application for mapping yet.

The application of crisp image classifications to continuous gradients certainly leads to false information. For this purpose, other methods are appropriate. Possibilities are fuzzy image classification algorithms, where single pixels can be assigned to more classes on a subpixel level (fractions). Pixels are composite signals of species or plant communities that can be extracted by spectral unmixing processes. This has been subject of many investigations, e.g. Adams et al. (1986); Gamon et al. (1993); Tompkins et al. (1997); Wessman et al. (1997); Roberts et al. (1998); Jacobsen (2000), and Denni-

son and Roberts (2003a). Alternatively, Fuzzy Logic (Foody, 1996, 1999; Townsend, 2000), Spectral Angle Mapper or Maximum Likelihood (e.g. applied by Foody and Arora 1996) are possibilities to classify on subpixel level. On the other hand, methods to map transitions can be used that are not based on the definition of classes at all, i.e. regression models. Regression models can link floristic data derived from relevés to remote sensing spectra. Beforehand, the floristic data matrix (relevés x taxa) has to be converted to metric data, e.g. as done by ordination. Armitage et al. (2005) described correlations from ordination results with spectral band information without applying the results to a map. Applications of models for mapping purposes have been done e.g. by works of Schmidtlein (2003) with PLS (Partial Least Squares) regression models, and by Thessler et al. (2005) with knn (k-nearest neighbour) estimation.

2.3 Imaging Spectroscopy for Vegetation Mapping

Airborne imaging spectrometer data combine high spatial with high spectral resolution (van der Meer and de Jong, 2001, 54). High spectral resolution is defined by the number and widths of given bands of a system, i.e. high spectral resolution is derived by many bands of narrow contiguous spectral ranges (Wieneke et al., 1988). Reflectance from ground is passively recorded in the wavelength range from visual spectral range to mid and thermal infrared in numerous narrow, contiguous bands. From the band information a spectral curve, or spectrum, can be constructed for each pixel of the scene (Lillesand and Kiefer, 2004, 363). Due to its multidimensionality and its mass of information, this method of image data collection is called hyperspectral (Boardman and Green, 2000). End of the eighties of the last century the new sensors opened up the possibility of automated image processing on a high spatial resolution as well as a very high density of information per unit, i.e. per pixel of a scene. Examples are following sensors: AVIRIS (Nasa/ JPL U.S.A. since 1987), CASI (Itres Research Canada, since 1989), DAIS (DLR Germany, since 1994), HyMap (HyVista Corp. Australia, since 1997), and AVIS (IGGF, LMU University of Munich, since 1999). In future, image data with high spectral and spatial resolution (approx. $4 \times 4 \text{ m}^2$) will be globally as well as cost-efficiently supplied by satellites (van der Meer and de Jong, 2001; Hirano et al., 2003). So far, airborne systems enable method development.

Reflectance Attributes of Vegetation

A characteristic sample spectrum of green vegetation is shown in fig. 2.1. Three broad wavelength intervals, namely the visible region between 400 and 700 nm, the near infrared region between 700 and 1300 nm, and the mid infrared region between 1300 and 2500 nm, are cited to be appropriate for the discrimination of vegetation (Gausman et al., 1973), and have been subject of some investigations in the past (e.g. Gates et al. 1965; Gausman et al. 1969; Myers 1970; Sinclair et al. 1971; Hoffer 1978; Belward 1991; Verdebout et al. 1994), and shall be shortly described. Concise information can be gained from Kumar et al. (2001). The reflectance in the visual wavelength region is characterised by chlorophyll contents as well as other pigments of the plants. At 700 nm, the so-called red edge (Collins, 1978) shows the sharp interface between high red absorption of chlorophyll and strong near-infrared reflectance which merely depends on foliar cell structures, e.g. volume of intercellular air spaces. The reflectance curve of the mid infrared region is mainly influenced by water contents of the plants. It is dissected by the absorption ranges of atmospheric water at 1450, 1900 and 2500 nm (Lillesand and Kiefer, 2004; Albertz, 1996).

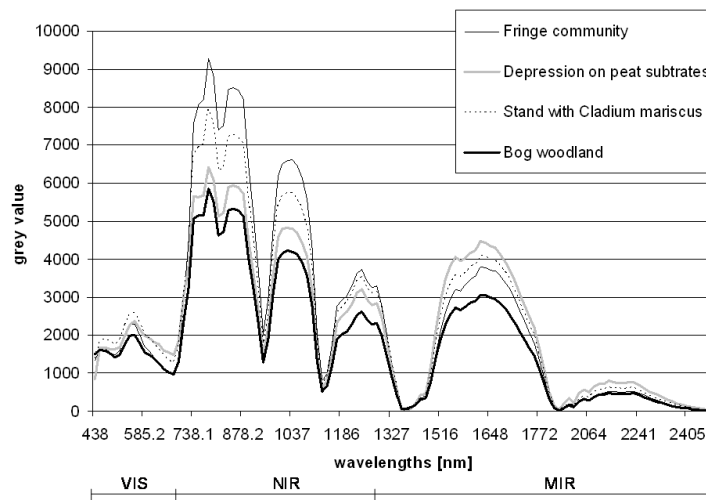


Figure 2.1: Characteristic sample hyperspectral signatures of green vegetation: Green vegetation shows a small peak in the visual wavelength range of green (around 500 nm), the ascent (Red Edge) to a high maximum in the begin of near-infrared and a slow decline towards the middle infrared region with the typical absorption minima around 1450, 1900 and 2500 nm. Source: project imagery 2003

With imaging spectrometer data insights can be gained on the spatial

distribution of numerous vegetation parameters. The different reflectance attributes of vegetation are traced back to biochemical reasons on the one hand (Gates et al., 1965; Wooley, 1971)), water contents (Peñuelas et al., 1993), structure of cells and tissue morphology (Wessman, 1994), and to canopy architecture and growth of the plants on the other. Cell components, mainly chlorophyll and other pigments, as well as others like water, proteins, starch, waxes, lignin, cellulose etc. have different reflectance attributes according to their composition and fractions. This topic was object of multiple investigations (e.g. Elvidge 1990; Aber and Martin 1995; Peñuelas et al. 1997; Ustin et al. 1998; Blackburn 1998; Curran et al. 1998; Jago et al. 1999; Serrano et al. 2000; Zarco-Tejada et al. 2001, and others). The differentiation of plant communities and ecosystems by their reflectances depends on the sum of biochemical and structural differences and their characteristic changes within a seasonal cycle. Biochemical and structural parameters variegate with the condition of the vegetation and with the combination of species. Different cell components, different cell structure and different shape of the different species cause different reflectances on a stand level. That means that with highly spatially resolved data derived from imaging spectrometer it is basically possible to differentiate vegetation on a species level or on a level of recurring species that form a certain plant community, even if heterogeneities complicate the subject (e.g. Treitz et al. 1992; Lewis 1994; Goodin and Henebrey 1997; Spanglet et al. 1998; Neuenschwander et al. 1998; Lewis 2000; Thomas et al. 2002; Underwood et al. 2003).

Hyperspectral data show a high sensitivity in respect to canopy cover, canopy structure, angle of leaf growth and leaf area index (LAI) (e.g. Asner 1998; Asner et al. 1998; Innanen and Miller 1998; Broge and Leblanc 2000; Fernandes et al. 2002). This sensitivity bears problems, namely the influence of reflectances due to bidirectional effects (sensor view-angle, Kennedy et al. 1997). The so-called BRDF (Bidirectional reflectance distribution function) effects cause different implications on the reflectance of different structures. This can be positively used to differentiate biophysical vegetation types with various canopy closure conditions and diverse plant architecture (Kumar et al., 2001, 11f), e.g. with contemporary imagery that has been collected from different perspectives (Mauser, 2003).

Applications to Differentiate on a Stand Level

The possibility to give information on vitality or stress of vegetation lead to the application of imaging spectroscopy in agricultural matters (precision farming, e.g. Brisco et al. 1998; Council 1998; Oppelt and Mauser 2004; Dobrowski et al. 2000; Mariscal et al. 2000) and forest management (Sampson

et al., 2001; Zarco-Tejada et al., 2001). Here, the usage of hyperspectral data has proven to be practicable. Over the past years endeavours were made to map plant communities with the help of imaging spectroscopy (e.g. Alberotanza et al. 1999; Schmidt and Skidmore 2001; Underwood et al. 2003; Yamano et al. 2003; Williams et al. 2003). Mostly researches were limited to species-poor systems like boreal forests, semi-deserts, steppes or submersed aquatic vegetation. The differentiation of more complex plant communities was only little investigated yet (Hirano et al., 2003; Schmidt and Skidmore, 2003; Schmidtlein, 2003).

In nature conservation, the differentiation of vegetation structures with high spatial resolution was and is still done by traditional field methods and visual interpretation of orthophotos (Wagner et al., 2000a; Strohwasser, 2006). Of course, numerous analyses based on digital remote sensing data with high spatial resolutions have been seen against the background of a later applicability for conservancy purposes (e.g. Neuenschwander et al. 1998; Merényi et al. 2000; Lewis 2000). But any detection of structures that are of conservation importance was hardly in the main focus of research. Jacobsen (2000) tested the sensitivity of CASI data with respect to shrub encroachment in grassland fallows. By maximum likelihood classification and linear unmixing analyses, she tried to monitor succession stages on a species level. In this regard, some classification deepness could be yielded if monitored objects were large enough, but individuals (e.g. coniferous shrubs) were not mapped. However, supervised image classification showed promising results that hyperspectral data were adequate to perform heterogeneous vegetation mapping on a plant community level (Jacobsen, 2000, 48).

The ProSmart-Project BIOTOPE mapped rare dry grassland biotopes on the German island Rügen with a combination of digital elevation models, multispectral data and imaging spectroscopy. Image classifications used were spectral unmixing algorithms (Kaptein et al., 1999) and promising results could be gained. However, the resulting maps do not allow for the discrimination of vegetation types according to the FFH Directive yet. Birger (1998) performed monitoring approaches with hyperspectral CASI and HyMap data in post-mining landscapes. The classification results satisfied to estimate successional stages. Still, a discrepancy exists between frequent considerations of the applicability of imaging spectrometry for conservancy purposes (e.g. Wenkel et al. 2003) and its real application.

Chapter 3

The Murnauer Moos

In this chapter, the selection of the area under investigation is explained, followed by a description of its natural and physical attributes.

In regard to the project's motivation, a proper area of investigation should fulfil the following conditions: First of all, the area of investigation should be designated as area of conservation within the framework of the Natura 2000 due to its natural habitats, wild animals and plant species of Community importance. Secondly, the usage of airborne imaging spectrometer data requires the existence of openland vegetation. In order to map ecotones in particular, various intertwined vegetation types, with differently natured transition zones inbetween, are of essential importance.

The Murnauer Moos (see fig. 3.1, at 47°39' N, 11°11' E, ca. 630 m a.s.l.), Upper Bavaria, meets all listed requirements. It is located about 60 km south of Munich and belongs to the administrative district of Garmisch-Partenkirchen. By reason of its expanse (about 3000 ha) and the diversity of habitat types covered with rare and endangered species, it takes an exceptional position among conservation areas (Strohwasser, 1994). Jeschke (2003) mentions the Murnauer Moos to be the largest interrelated wetland complex of Central Europe, Burmeister (1982) cites its seminatural state of preservation. The area comprises a mosaic of different wetland types, e.g. raised bogs, poor fens, tall sedge beds, reed swamps, and wet meadows (Kaule, 1974). It is naturally bounded due to its position in a glacially formed depression in the Oligocen Molasse terrain (see subsection 3.1).

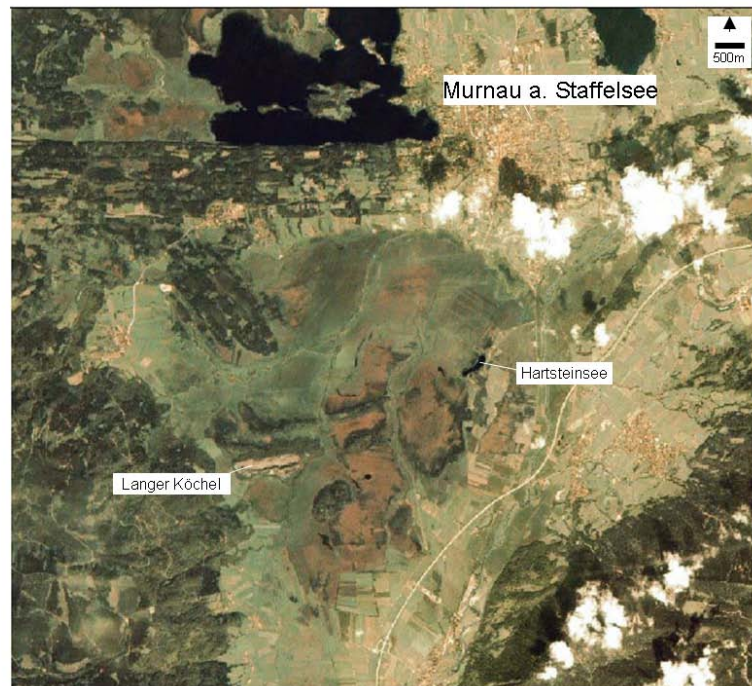


Figure 3.1: The Murnauer Moos within its position in a depression of the terrain (Source: GeoFachdatenAtlas www.bis.bayern.de, adapted)

3.1 Postglacial Genesis as well as Geologic, Pedologic, and Climatic Realities

During Günz-, Mindel-, Riß- and Würm-ice ages, the pleistocenic glaciers scraped deep depressions along the northern edge of the Alps (Habbe, 1995). Such a depression was formed under the Isar-Loisach glacier. Its shape was a funnel with its open side northwards, due to geological reasons. Molasse barriers with harder morphologic qualities, that strike transverse to the flow direction of the ice, restricted the glacier in the north. The Murnauer Moos was formed after the melting of the ice by siltation of a large postglacial lake (terrestrialisation mire) with manifold rivulet and spring fed percolation mires within (see e.g. Gams 1947; Succow and Jeschle 1990, 156; Strohwasser 1994; Habbe 1995; Jeschke 2003, 10f).

Since the end of the Würm-ice age, peat was accumulated to an average thickness of 16 to 19 m, with its various kinds of mires in different states of trophy (Strohwasser, 1994). Sporadically, roches moutonnées (Köchel) protrude about 90 m high from the peat soils. These Cretaceous monad-

nocks (Barrême - Alb) are allocated to the Helvetic zone of the North Alpine Foreland Basin that is tectonically scaled in between the Folded Molasse northward and the Flysch Zone south of Murnau. More details can be found in Lagally et al. (1994) and Engelbrecht (2003).

Primarily, bog and fen peat form the biggest part of the area's soil types. Fen soils are permanently waterlogged and peat formation occurs, therefore, infra-aquatic, and the soil attributes depend on groundwater qualities. In the case of the Murnau watershed, groundwaters are influenced from the calcareous region of the Northern Alps which means alkaline base-rich water supplies. Bogs are ombrotrophic, i.e. they depend merely on precipitation due to their growth over the water table (e.g. Du Rietz 1954; Dierßen and Dierßen 2001). So, cut off from mineralic waters, the Murnau bog soils are nutrient poor and very acidic. Peat formation occurs by deposition of dead plant material, predominantly *Sphagnum* mosses and types of sour grasses, namely *Eriophorum*, *Trichophorum* and *Carex* species. Intermediate between soligenous and ombrogenous types, transition mires occur, mostly influenced by oligotrophic to mesotrophic waters. Although they belong to soligenous types, they are often interrelated with bogs and, in parts, lead to their genesis (see e.g. Ellenberg 1996, 477; European Commission DG Environment 2003, 74). Also, alluvial soils occur along the rivulets that spate irregularly but often in times of rainy seasons. At the foot of the Köchel slopes gley soils, and on top brown soils, are found. Concerning this study, they are of less importance, because they are usually covered with forest vegetation.

The Murnauer Moos falls climatically into the temperate humid zone (Walter and Lieth, 1967). High precipitation sums derive from its vicinity to the Alps, as maritime air masses retain in front of the barrier of the Alpine north ridge (Fartmann et al., 2001). Murnau (622 m a.s.l., 11°13' E', 47°40' N) measured averaged precipitations of 1257 mm/a over the period from 1961 - 1990 (Deutscher Wetterdienst, 2007) with a maximum in summer (July and August). The mean annual temperature averages about 6.5° C (Deutscher Wetterdienst, 2007).

3.2 Fauna, Flora and Habitats

Faunistic studies (e.g. Dingler et al. 1943; Burmeister 1982) estimate the occurrence of 4000 species in the different wetland types of the area. Of great richness are fish and bird species (the seldom *Crex crex* among them, Burmeister 1982) as well as insects, e.g. 50 dragonfly species can be found in the area (Reitter-Welter, 2004). According to Braun et al. (1984), Quinger

(1986) and Strohwasser (1990), more than 800 vascular plant species occur in the area, and about 160 plants are registered as critical on the IUCN Red List of Threatened Species (Reitter-Welter, 2004). These numbers approve the area's importance for conservancy. Some taxa (most probably *Cladium mariscus* and *Rhynchospora fusca* (Strohwasser, 1994)) have the main occurrence of Germany within the area.

The plants' origins are diverse, Strohwasser (1994) cites 16 % of the plants to be pre-alpine, and 32 % of nordic origin. Others are glacial relict plants, e.g. *Betula nana* and *Pedicularis sceptrum-carolinum*. Additionally, numerous moss species as well as lichens and funghi occur but have not been in the focus of comprehensive investigations yet (Strohwasser, 1994).

The area contains numerous open-land plant communities that are intertwined in, partly small-scaled, mosaics (Wagner et al., 2000a). Freshwater and alluvial habitats can be found as well as all stages of eutrophic and calcareous-oligotrophic terrestrialisation, transition mires, and bogs.

Aside the natural wetland habitats, agriculturally used fen meadows and pastures cover big parts of the area. The extensive cultivation of the fen meadows to produce litter is a centuries-old tradition. Parts of the natural fens as well as originally cleared bog forests and carrs have been mown once a year. This led to the development and spread of species-rich fen meadows (Succow and Jeschke, 1990). These characteristic habitats of the Murnauer Moos are endangered due to structural changes of agriculture. Since the mowing of the meadows is not profitable any longer, only parts of it can be sustained by contracts between the local conservancy authority and local farmers (Schmidtlein et al., 2007). In parts where the mowing tradition has not continued any longer, changes can be monitored lately, e.g. the spread of *Phragmites communis* agg. (Jeschke, 2003).

A complete list of occurring plant communities is given by Vollmar (1947) as well as by Braun (1983), and more recently, by Wagner et al. (2000a) who have mapped the area in the context of a conservancy project. Comparative studies on changes in the vegetation composition from 1947 to 2000 have not been published so far.

3.3 Agricultural and Industrial Utilisation as well as Conservation Efforts

Whereas the old tradition of litter production increased the biodiversity of the area, turf cutting destroyed not only peat accumulation of millennia but led to the drainage of water. However, turf cutting was of minor focus

and was stopped in 1974 (turf cutting leaseholds of the commune Murnau, Geiersberger 2002), and in 1982 (medical purposes of Kurhaus Ludwigsbad, Murnau, König 2007).

From 1926 until 2000, two roches moutonnées (Langer Köchel and Moosberg) were mined for glauco-quartz that was used to produce sands, high-quality gritting materials, and road and railway ballast (Kuisle, 2000; Scharl, 2000b,a). Although parts of the Murnauer Moos were already subject of conservation efforts (e.g. Dingler et al. 1943), the Moosberg was excavated totally. Only the Hartsteinsee is a sign of its former existence (see fig. 3.1).

At Langer Köchel, about 24 M tons were digged during this period (see fig. 3.2). Finally, the exposure had to be stopped due to lack of space. To the north, the mining could not be widened to sustain the panorama for touristical interests according to an order from 1940. To the south, industrial buildings etc. refused an expansion. Nowadays, the remainder of the mining at Langer Köchel has geotope status and shall be preserved (Lagally et al., 1994). Anyway, the dust contamination of 70 years affects the area lastingly. Moreover, the autobahn close-by as well as the gliderport near Eschenlohe exert polluting influence. Altogether, Jeschke (2003) assesses the listed impacts as moderate which can, amongst others, be traced back to high precipitations of the pre-alpine region (Gremer, 2001, 463).



Figure 3.2: Since 1930, glauco-quartz was mined at Langer Köchel. (Source, by courtesy of: Schloßmuseum des Marktes Murnau am Staffelsee 2002)

In 1980, a small part of the Murnauer Moos (about 2355 ha, Jeschke 2003) became nature conservation area. Between 1992 and 2003, the Murnauer Moos was subject of a sustainability project of the German Federal Agency for Nature Conservation (BfN). Management plans were developed (Wagner et al., 2000a) and the conservation area could be widened (to ca. 4300 ha) due to land acquisition and long-termed landscape conservation contracts

with special focus on the sustainment of the fen meadows. According to the Fauna-Flora-Habitats Directive, the Murnauer Moos was officially accounted for FFH-conservation area in 2000 (FFH-Code: DE8332301). Lately, Jeschke (2003) proposes the nomination of the Murnauer Moos for national park.

Chapter 4

Materials and Methods

First, this chapter details data collection. The recording and preprocessing of the imaging spectrometer data are described as well as sampling designs and relevant parameters of two vegetation periods. Then, methods are described how field data will be evaluated, and linked with the hyperspectral scene. On the one hand, ordination methods and their mapping by regression modelling are presented. On the other hand, vegetation classification keys are described. The results build the base for the applied image classification algorithms that will be explained. Finally, synthesis aspects of ordination and classification methods are presented. The workflow of the project is shown in fig. 4.1.

4.1 Scene Data

During the vegetation period 2003, the imaging spectroscopy data were gathered from the airborne sensor HyMapTM (HyVista, Australia). The scene was taken on July 22nd at cloud-free atmospheric conditions at 11:25 a.m. by the DLR Oberpfaffenhofen. All sensor and flight information can be taken from table 4.1.

4.1.1 Preprocessing Steps

HyMapTM is a hyperspectral scanner that consists of four sensors with each 32 channels (Clark, 1999). Radiance, expressed in so-called grey values, was measured in 128 bands in the wavelength region between 438 and 2483 nm with bandwidths of 15-20 nm. The raw image data yielded a spatial resolution of 4 x 6 m².

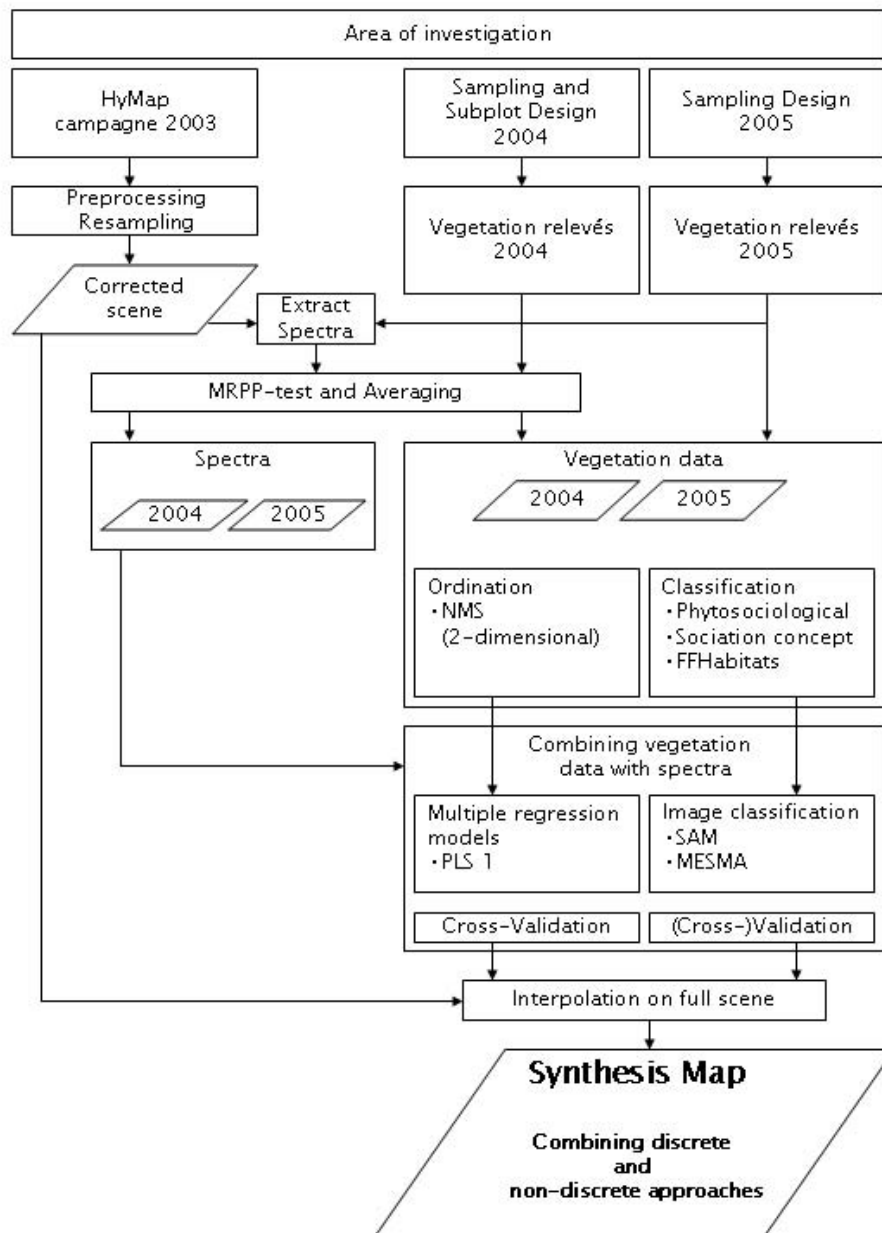


Figure 4.1: The project's workflow

Wavelength range	438 to 2483 nm
No. of bands	128
Spectral resolution	15 to 20 nm
Spatial resolution	4 x 6 m^2
Signal to Noise ratio	< 500:1
Flying altitude	2712 m a.s.l.
Date of flight	22nd of July 2003
Time of flight	11:25 a.m. MESZ

Table 4.1: Sensor and flight information of the scene data (DLR Oberpfaffenhofen)

Initially, aircraft disturbances (rolling, pitching, yawing) were corrected by the help of ephemeris data. The resulting image was recalculated with nearest-neighbour assignment, only 126 bands remained.

Secondly, with the orthorectification software PARGE (ReSe) the image was directly geocoded to an accurate digital elevation model (DGM 25) from the Bavarian Survey Department (LVG). After this recalculation with bilinear interpolation, the correctly oriented image had a spatial resolution of 4 x 4 m^2 (see fig. 4.2). These first standard geocorrection steps were processed at DLR Oberpfaffenhofen.

The flatness of the area, for the part of this study, rendered any additional topographic correction of the image data unnecessary. Atmospheric corrections were not executed since no other imagery but the very scene was used for training, allocation, and testing stages altogether (Aspinall et al., 2002). That means that all evaluations of the project were quantitatively calculated with radiance values, and not with reflectance values instead.

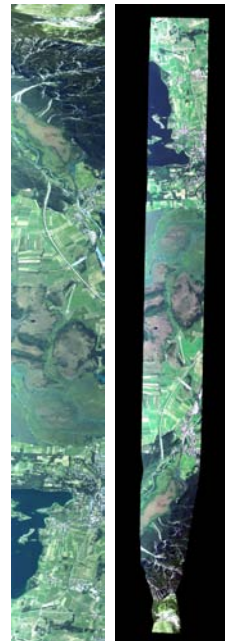


Figure 4.2: The raw image data before (left) and, correctly oriented, after preprocessing steps at DLR Oberpfaffenhofen (right).

A final fine-scaled geocorrection was subjected to two subsets of the scene that comprised the inner parts of the conservation area Murnauer Moos. They were registered to an ortho image from the Bavarian Survey Depart-

ment (LVG) with $0.4 \times 0.4 \text{ m}^2$ spatial resolution. The Root Mean Squared error of position constituted approx. 0.66 m with 9 ground control points each. To sustain radiometric fidelity (Fogel and Tinney, 1996), nearest-neighbour assignment was used as 2nd grade polynomial resampling method.

4.1.2 Radiance Log Transformation and Band Selection

The log transformation $\text{Log}_{10}(1/R)$ (also called ‘Pseudo-absorbance’) of the radiance values R is an almost linear relation to true absorbances of the materials under investigation (Hruschka, 1987; Myneni et al., 1995; Blackburn, 1998). Deeper insights can be taken from Smith et al. (2002). All further analyses were, for comparison reasons, calculated with the log-transformed as well as the original final rectified image subsets.

Band selection was done optically following Zimmermann (2005). Bands showed strong noise in the beginning and end of the spectral range due to technical reasons. Bands around the wavelength ranges of 1404 to 1475 nm and 1795 to 2009 were disturbed by atmospheric water absorption (e.g. Kumar et al. 2001; Lillesand and Kiefer 2004). After band selection, 105 bands remained for further analyses (see e.g. figs 2.1, 4.10, 4.11, and 4.13).

4.2 Vegetation Data

The collection of relevé data means a careful planning of the sampling strategy. It is fundamental if basic knowledge on the area of investigation is to be gained or if any parameters already exist to underlie the intended investigations. Therefore, the sampling design defines the spatial range of the results (Traxler, 1998, 53). Basically, sampling designs differ according to subjective, random and systematic strategies (Glavac, 1996, 78-81).

Depending on the issue one of the three possibilities is adequate. With a subjective sampling strategy one tries to cover all vegetation stands of the area of investigation in their homogeneous and characteristic forming. Hence the results are influenced by the decisions of the person that collects the data. A prior knowledge of the area is essential.

Discussion

The term ”homogeneity of a stand” implicates another subjective valuation of the data-collecting person because under an adequate extension any vegetation stand can be interpreted as heterogeneous (Du Rietz, 1930, 341). The

section under investigation must correspond to the issue of the project.

Random and systematic strategies exclude subjectivity from the analyses concerning plot positioning, but complicate a complete registration of the vegetation structure on the other side. Random sampling means that relevés are randomly distributed in a certain area. For systematic relevés, plots are positioned according to a systematic pattern, e.g. an even knit reticule can be laid over the area of investigation. In each case stratified or non-stratified methods can be performed. Stratified methods require the random or subjective pre-definition of strata, usually according to independent properties of the area. In each stratum the relevés are distributed subjectively, randomly or systematically.

4.2.1 Sampling Steps

Sampling design is a highly time-consuming matter. By the assistance of two graduands from the University of Bayreuth in 2004, and one graduand from the Ludwig-Maximilians-Universität München in 2005, it was possible to gain two adequate data sets of 2004 and one of 2005. Patrick Zimmermann (Bayreuth) and Jörg Wunsch (München) focused on ordination and PLS regression techniques, whereas Uwe Friedel (Bayreuth) followed phytosociological classification approaches and SAM image classification. Evaluations can be taken from Zimmermann (2005), Wunsch (2006), and Friedel (2005). As the data set 2004 was collected by three persons, first relevés were taken together to adjust the estimations of cover values. The following table 4.2 gives an overview about sampled areas and shows all parameters taken *in situ* during the vegetation periods 2004 and 2005. For the determination of vascular plants the following references were used: Oberdorfer (1994); Lauber and Wagner (1998); Jäger and Werner (1999, 2002). Moss species were determined with: Frahm and Frey (2004); Smith (2004). Field data were entered into and accessed with the data base management system TurboVeg Vers. 2.07a, Alterra, Green World Research, Wageningen, NL (Hennekens and Schaminée, 2001). The species list "Ellenberg" was used.

4.2.2 Vegetation Period 2004

As careful vegetation data collection is needed to build a base for the methodology of the project, the sampling design should meet two important conditions: One term of the analysis was to map floristically differentiable stands and to comprise vegetation transitions of variable continuity inbetween. The

parameters subarea	2004		2005
	north	south	
areas	40 ha	22.5 ha	250 ha
# of relevés (subplots)	68 (204)	44 (132)	100
size of relevés (subplots) [m^2]	12 (4)		4
time of sampling	June - July		August
data collecting persons	U. Friedel, P. Zimmermann, C. Weiß		J. Wunsch
covers [%]			
water	v	v	v
bare soil	v	v	v
litter	v	v	v
vegetation	v	v	v
tree layer	v	v	v
shrub layer	v	v	v
herb layer	v	v	v
moss layer (dominant taxa)	v	v	v
<i>Sphagnum</i> moss colours	v	v	-
all occurring taxa	v	v	v
av. height of herbs [cm]	v	v	v
av. height of trees [m]	v	v	v
# of <i>Phragmites comm.</i> individuals	v	v	-

Table 4.2: Parameters taken *in situ*

variation of the vegetation structure of the area of investigation should be reflected in the data. This implied the initial reconnaissance of the overall distribution of stands at a broad scale. A high density of relevés should enable later tests, how a thinned out data set would perform in PLS regression modelling (see the work of Zimmermann 2005).

Discussion

No subjective criteria concerning plot location should influence the analysis to allow for statistical evaluations. Therefore the systematic non-stratified sampling approach was used.

A systematic grid covers the variation of the vegetation in an objective manner as samples do not underlie subjective criteria (see 4.3). The grid design of equilateral triangles has proven to be useful in former analyses (Weiss, 2003). Autocorrelation tests are possible as sampling points have

equal distances to each other.

It is to be pointed out, however, that the usual statistic procedure to sample randomly, or systematically in order to provide a probability structure in the data set for some statistical evaluation models used, means disregarding true natural patterns that are known to be mostly non-random (Gillison and Brewer, 1985), and non-systematic. To receive data sets that give credits to all communities in their variance, representative sampling would include subjective knowledge. As this study concentrates on evaluations by statistical models, and furthermore develops a method for objective monitoring, missing communities in the data set are accepted.

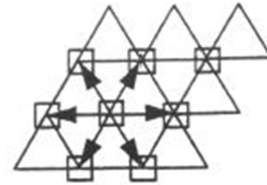


Figure 4.3: A net of equilateral triangles (Traxler, 1998, 54).

To position the vegetation relevés as reasonably as possible, the available extant vegetation map of Wagner et al. (2000b) was used as template. The application of extant classifications in vegetation mapping surveys is most advantageous in ecosystem management (e.g. Küchler 1967; Banner et al. 1996; Uhlig and Jordan 1996; "top-down approach" Smith and Carpenter 1996; Cherril and McClean 1999). Two grids were laid over parts of the area of investigation, one grid with 68 vegetation relevés that covered northern parts of the area (40 ha) and one grid with 44 relevés that covered the southern part of the area (22.5 ha). The distances of the grid points averaged about 80 m. The positioning of the grid by the help of the extant vegetation map implicated some subjectivity in sample selection. This was neutralised by two factors: on the one side by the relative impreciseness of the GPS-console Garmin GPSMap 76 in situ (approximately 1-4 metres) that was used to find the relevés first, on the other side by the interpolation of vegetation boundaries on the map itself. Fig. 4.4 shows the two sampling grids. According to the extant map of Wagner et al. (2000a), the two grids comprised the following vegetation types and complexes in their different formations, respectively:

- reeds with *Phragmites communis*, and with *Cladium mariscus*
- large sedge beds with *Carex elata*
- fen vegetation with *Schoenus* species, *Carex lasiocarpa*, and *C. fusca*

- species-rich and species-poor *Molinia caerulea* meadows
- bog communities with *Sphagnum* species, with *Calluna vulgaris* dominance, and complexes of bog hummocks and hollows

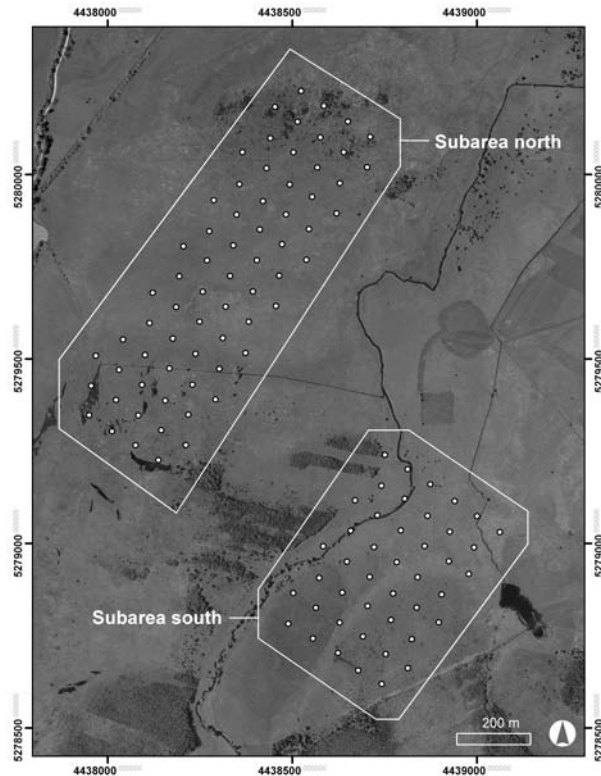


Figure 4.4: Two sampling grids were positioned in that way to cover important parts of the habitat structure of the area of investigation. Source of orthophoto: Bavarian Survey Department (LVG)

Each of the 112 plots consisted of three circular subplots. By the help of the subplot design (see fig. 4.5) tests on plot homogeneity are possible. It is important to have information on plot homogeneity before relating ground plot data (ground truth) to the imagery (Schmidtlein and Sassin, 2004; Schmidtlein et al., 2007). The centres of the three subplots were arranged in a triangle of 5 metres side length, with each subplot having an area of 4 m^2 . The first subplot was pointing north, the others laid 120° south east and 240° south west according to the first (see fig. 4.5). All subplot centres were marked with stakes and magnetic markers and localised afterwards at

an accuracy of approx. 0.3 m using the differential GPS-console dGPS Leica GS5.

Discussion

To lessen efforts the circular shape of plots has proven to be useful, as only the centre has to be marked to recover the sites. In comparison to common plot shapes like squares and rectangles, the estimation of lower cover percentages needs more exercise. Estimators automatically subdivide square plots into small squares, which simplifies estimation. According to Traxler (1998, 45), the intuitive division of a circle into slices affects the estimation process negatively.

In all 336 subplots all occurring vascular plants and the dominant mosses were registered, and their covers were estimated in percentage from 1 to 100 percent. Covers less than one percent were estimated with 0.5 percent. Moss species as well as unassured classified vascular plants were post-classified by Eduard Hertel and Pedro Gerstberger (both University of Bayreuth), and Sebastian Schmidlein (University of Bonn).

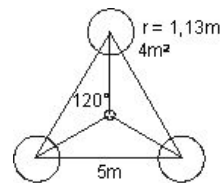


Figure 4.5: Subplot design 2004

Discussion

With well established semi-quantitative cover scales (e.g. Braun-Blanquet 1928 and its modified version Barkman et al. 1964) vegetation covers can be estimated easily and therefore fast, but have subsequently be transformed from semi-quantitative values to quantitative table formats. Each transformation step means a loss of accuracy, especially the scales upper mentioned have a rough graduation at higher cover percentages. However, the estimation of covers in percentages *in situ* demands for some routine and levelling of the estimating persons. It means more expenditure of time and makes sense only with small (maximal 4 m^2) plot sizes (Traxler, 1998, 115f).

One plot had to be excluded from further analyses because two of its subplots lay in a rivulet. The cover values of the other relevés were averaged and log-transformed at the plot level with $\log_{10}[\text{cover value}]$. All following analyses were performed with both data subsets north and south. The common setting for ecological community data is the Bray-Curtis distance

that was used here to calculate the homogeneity between the original sub-plot data (Multi-Response Permutation Procedure MRPP; Biondini et al. 1985). In heterogeneous data sets, Bray-Curtis distance retains sensitivity, and gives, compared to Euclidean distance, less weight to outliers (McCune and Mefford, 1999, 69). The homogeneity was tested within original and log-transformed data, as well with original first three axis values of results from the ordination method DCA (Detrended Correspondence Analysis, Hill and Gauch 1980), and log-transformed DCA axis values. The indirect gradient analysis DCA is a common tool for detecting outliers in a data set. Distances among DCA values were calculated with Euclidean distance. Five plots showed high heterogeneity and were therefore subjectively excluded from further calculations (see appendix table A.1 and see fig. 5.9 for heterogeneous plot locations on the map), leaving 106 plots from the vegetation data 2004 that were parted in two, the northern area comprising 65 plots and the southern area comprising 41 plots.

4.2.3 Vegetation Period 2005

The vegetation data of 2004 served well for the development of the methodology of this project. Additional field data were taken during the vegetation period 2005. Aim was to test resulting methods on a second data set that corresponded better with the operating expenses a conservation manager would have when mapping areas of large size and habitat inventory. Therefore a second field campaign was done to cover another part of the area of investigation. According to own experiences, and the extant map of Wagner et al. (2000a), this area comprises many relevant habitat types and overlaps with the sampling of 2004. The following list shows vegetation types that are comprised by the sampling area 2005 according to the map of Wagner et al. (2000a).

- reeds with *Phragmites communis*, and with *Cladium mariscus*
- large sedge beds with *Carex elata*
- fen vegetation with *Schoenus* species, *Carex lasiocarpa*, and *C. fusca*
- species-rich and species-poor *Molinia caerulea* meadows
- bog woodland with *Pinus mugo agg.*
- bog communities with *Sphagnum* species, with *Calluna vulgaris* dominance, and complexes of bog hummocks and hollows

Stratified random sampling was chosen. It has proven to be of value in comparable investigations (e.g. Congalton 1991) as it stays on objective sides for statistical reasons but prevails clustering of plots and therefore under-sampling of small but important areas. For stratification, the imagery data were processed by the common classification tool ISODATA (Iterative Self-Organizing Data Analysis Technique). ISODATA, first described by Duda and Hart (1973), is an unsupervised classification algorithm that works step-wise. First, normally distributed central vectors (of predefined quantity, if desired) are set in feature space, whereas the vector dimensionality depends on the number of bands of the imagery. Second, all pixels of the image are assigned to their proximate central vector using minimum distance techniques. Third, the central vectors are recalculated according to the pixels that were assigned to them. The latter two steps are iterated until stable class assignment is reached (e.g. Lillesand and Kiefer 2004, 575; Campbell 2002, 342). Results can be improved consecutively. A class can be divided when its standard deviation exceeds a certain threshold. Likewise can classes be merged if the number of assigned pixels is too little (Jensen, 1996). A first ISODATA classification separated open-land vegetation from areas that were not relevant for this investigation, like dense forest stands, water bodies, roads and buildings. The mentioned structures differ significantly from the spectral signature of open-land vegetation and can be masked easily by unsupervised classification algorithms. By re-running ISODATA on only open-land vegetation, eight stable strata could be defined. Fig. 4.6 shows the location of the eight strata on an orthophoto of the Murnauer Moos.

The $N = 100$ samples were distributed among the $m = 8$ strata according to the standard deviation of each stratum SD_h , and the area A_h of each stratum. By the following equation of Scott and Köhl (1994), the number N_h of samples for each stratum was calculated:

$$N_h = N \frac{A_h SD_h}{\sum_{i=1}^m A_i SD_i}$$

By limiting sample numbers between 10 and 20, each stratum should be represented sufficiently as e.g. postulated by Pfadenhauer (1997). Table 4.3 shows how sample numbers corresponded to stratum standard deviations.

The random samples were set by the help of the Random Point Extension of Beyer (2006) for ArcGIS. For reasons of economy, a three-parted subplot design like 2004 could not be accomplished. Therefore a common sample approach was used, where each circular plot had the size of 4 m^2 . Minimum distance between samples was set to 40 m to avoid pseudoreplications (Wiegleb, 1992). All plots were found by the GPS-console Garmin GPSMap 76 in situ

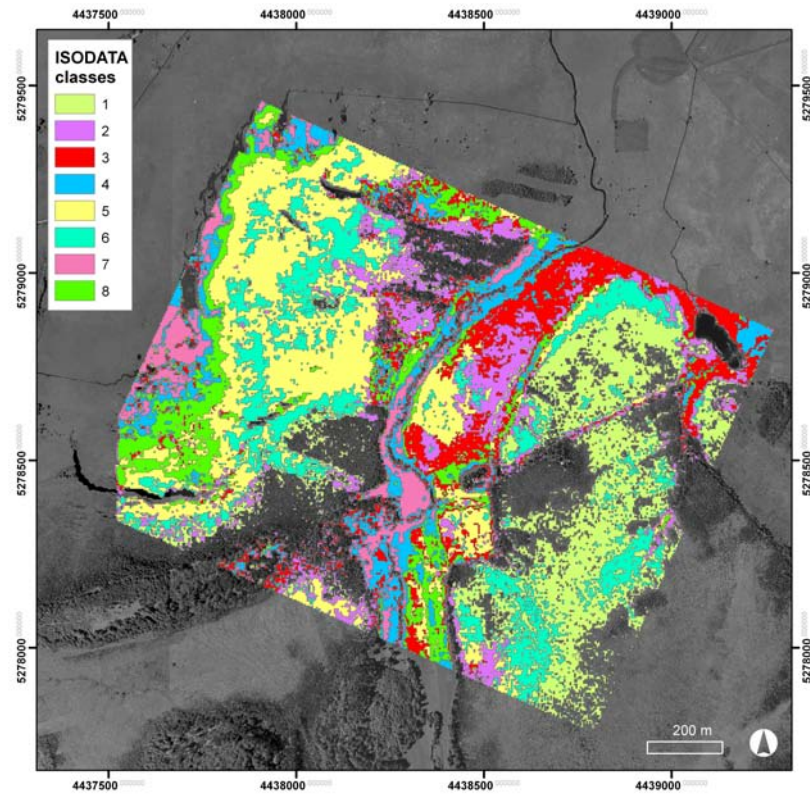


Figure 4.6: Map of strata derived from ISODATA image classification - transparent polygons show the masked pixels. Source of orthophoto: Bavarian Survey Department (LVG)

with an accuracy of 1-4 metres. In all 100 plots we registered all occurring vascular plants and the dominant mosses and estimated their covers in percentage from 1 to 100. Moss species as well as unassured classified vascular plants were post-classified by Eduard Hertel and Pedro Gerstberger (both University of Bayreuth). Covers less than one percent were estimated with 0.5 percent. 94 plots were localised afterwards at an accuracy of approx. 1 m using the differential GPS-console dGPS Leica GS5. The remaining six plots could not be recovered due to mowing reasons. For comparison reasons, the plot data were used untransformed and log-transformed $\log_{10}[\text{cover value}]$.

4.2.4 Extracting Spectra

Reference spectra were extracted from the scene. In case of the subplot design of the data set 2004, subplot centres were related to the hit pixels and

Stratum h	$Area_h[km^2] * SD_h$	$\#of\ Samples$
1	7.88	14
2	6.16	11
3	7.26	13
4	5.45	10
5	11.65	20
6	6.69	12
7	4.11	10
8	5.37	10

Table 4.3: Defining sample numbers according to stratum area A_h and standard deviation SD_h

averaged to one spectrum for each wholeplot, i.e. the spectra of three pixels were averaged and related to the averaged vegetation data of three subplots. Before averaging, spectra were examined for homogeneity by MRPP test (see appendix table A.2 and see fig. 5.9 for heterogeneous plot locations on the map). Hence, two spectrally heterogeneous wholeplots were omitted from further analyses, leaving 64 plots (northern area) and 40 plots (southern area) to continue with.

In case of the data set 2005, plot centres were related to the hit pixels, and to three neighboured pixels as well, i.e. one vegetation plot was related to four pixels, whose spectra were averaged. This was done to balance GPS- as well as georeferencing errors. Pixel neighbourhood was defined by the position of the vegetation relevé centre on the scene pixel. If the centre fell into corners of the pixel, the three surrounding pixels of this quadrant were extracted as well. If middle positions were hit, the row of three nearest pixels was extracted. Fig. 4.8 shows the spectra extracting strategy of 2005. MRPP test, calculated with Euclidean distance, showed high heterogeneity within three plots. They were therefore omitted from further analyses (see appendix table A.3 and see fig. 5.9 for heterogeneous plot locations on the map). This left 97 plots of the data set 2005 to continue.

4.3 Ordination and its Mapping

Ordination and classification are different ways to reduce the complexity of nature to comprehensible order (Anderson, 1965). Any classification is based on certain principles of arrangement or classificatory factors (Egler, 1942) and means a typification with clear zones. Ordination smoothly arranges data

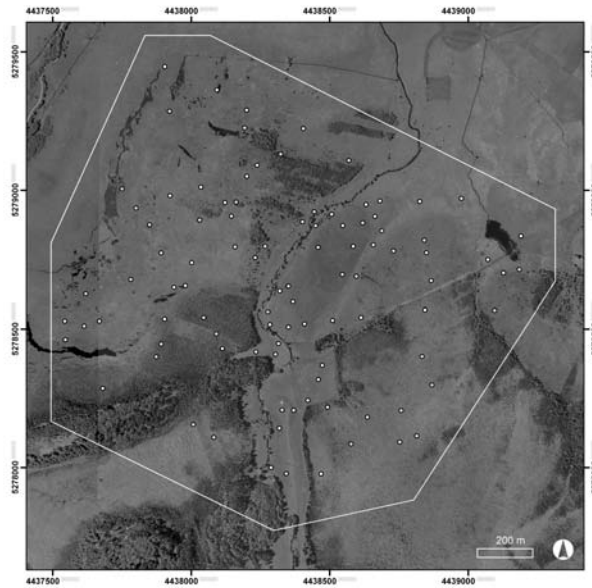


Figure 4.7: Stratified random sampling design of 2005: The vegetation data 2005 comprised a large area of 250 ha. Source of orthophoto: Bavarian Survey Department (LVG)

according to similarities and allows therefore for mixed stands and transitions (see section 2.2). Both forms are well-established in vegetation science and manifold applications express that vegetation science found its way to handle various vegetation formations.

4.3.1 Indirect Ordination in Reduced Space

”Field data must be high dimensional because of the large numbers of species and samples, whereas the final results must be low dimensional because of the human limitations.”

(Gauch, 1982, 118)

Generally speaking, ordination - the arrangement of units in some order (Goodall, 1954) - displays the relationships of complex data matrices in a multidimensional scatter plot. By reducing dimensions to few parameters, scatter objects are projected in an ordination space with only two or three dimensions, where its axes show the main trends of variation and allow for deriving quantitative information on the quality of the ordination (Legendre and Legendre, 1998, 387).

	x	x			x
	•	x		•	x
					x

Figure 4.8: Plot centres (dots) within pixel environment. The spectra of the three nearest pixels were extracted as well (x).

We distinguish between indirect (unconstrained) and direct (constrained or canonical) ordination methods. Indirect methods compute ordination results from the primary data matrix containing species composition. Due to the floristic relations that are displayed the ordination axes can be parallelised with environmental gradients (Glavac, 1996, 159). Gauch (1982, 118) describes the work flow of an indirect ordination as a two-tier analysis: first, the main structures of the data matrix are computed by ordination and second, the ordination axes and their relation to environmental gradients are interpreted. Direct methods correlate the matrix of species composition with a second matrix containing additional environmental information taken at the relevés' sites. This direct comparison allows for accounting the influence of measured variables on the vegetation (Kent and Coker 1992; Legendre and Legendre 1998, 575). As for this study no additional ecological variables were collected, only indirect ordination methods were applied.

4.3.2 NMS - Non-metric Multidimensional Scaling

The Non-metric Multidimensional Scaling method (NMS, or NMDS) - firstly devised by Shepard (1962) and Kruskal (1964) in psychometrics - computes distances of the entities of a data matrix based on their floristic similarities.

Data objects are arranged iteratively until the rank order of floristic similarities corresponds to the rank order of Euclidean distances in the ordination space. The so-computed arrangement of the objects in ordination space represents best the true distance relationships among the relevés (Schmidtlein et al., 2007). A stress value is calculated that measures the relationship between the distances within the measurement space of the original data matrix and the distances within the reduced measurement space of the NMS solution. Stress values are given from 0 to 100 without units. The closer the stress value is to 0, the better performs the calculated NMS solution. Concise stress calculation information can be gained from McCune and Mefford (1999, 112f). In this case, Bray-Curtis distance was used to measure the original data similarities which is an appropriate measure for community data (see also section 4.2.2). The number of axes can be constrained. If stress values allow for, in order to develop a vegetation map, two dimensions build an adequate base regarding facility of inspection as well as legend generation. Therefore, results were processed for two dimensions by 9999 iterations. For comparison reasons, also three dimensional solutions were calculated. All NMS calculation was performed with the programme package PC-ORD Vers. 4. MjM Software Design, Glendon Beach, OR, (McCune and Mefford, 1999) that is developed for multivariate analyses of ecological data.

4.3.3 PLS Regression Models

A short introduction to regression modelling will be given. Deeper insights with certain emphasis on ecological applications can e.g. be found in Legendre and Legendre (1998, 73ff and 497ff).

The simplest form of regression is the simple linear regression, where the relationship between a response variable y and a single explanatory variable x and its regression coefficient r is described by the following model

$$y_{\text{model}} = r_0 + r_1 x. \quad (4.1)$$

If there are p observations, then p equations result from the model which can be comprised in vector notation:

$$\vec{y}_{\text{model}} = \begin{pmatrix} y_1 \\ y_2 \\ \vdots \\ y_p \end{pmatrix}, \text{ and } \vec{x} = \begin{pmatrix} x_1 \\ x_2 \\ \vdots \\ x_p \end{pmatrix}. \quad (4.2)$$

The regression coefficients r_0 and r_1 can be estimated by the method of least squares (Gauss, 1795; Legendre, 1805). The result of the model is a straight

line that satisfies the linear regression model's equation and minimises the sum of squares of the vertical offset between measured values \vec{y} and the predicted values \vec{y}_{model} of the regression line itself.

In multiple linear regression, not only one but several (say n) explanatory variables \vec{x}_i are to be put into relationship with the response variable vector \vec{y} by the model's equation

$$\vec{y}_{\text{model}} = \begin{pmatrix} r_0 \\ \vdots \\ r_0 \end{pmatrix} + r_1\vec{x}_1 + r_2\vec{x}_2 + \cdots + r_n\vec{x}_n, \quad (4.3)$$

which, when combining the vectors \vec{x}_1 to \vec{x}_n into the matrix X , takes the form:

$$\vec{y}_{\text{model}} = X\vec{r} \quad (4.4)$$

where

$$\vec{y}_{\text{model}} = \begin{pmatrix} y_1 \\ y_2 \\ \vdots \\ y_p \end{pmatrix}, \quad X = \begin{pmatrix} 1 & x_{11} & \cdots & x_{1n} \\ 1 & x_{21} & \cdots & x_{2n} \\ \vdots & \vdots & \ddots & \vdots \\ 1 & x_{p1} & \cdots & x_{pn} \end{pmatrix}, \quad \text{and } \vec{r} = \begin{pmatrix} r_0 \\ r_1 \\ \vdots \\ r_n \end{pmatrix}. \quad (4.5)$$

With ordinary least squares (OLS), the minimisation of the offset between measured values \vec{y} and the predicted values \vec{y}_{model} can be done by first multiplying the transpose X' of X to the regression equation, i.e.

$$X'\vec{y}_{\text{model}} = X'X\vec{r}. \quad (4.6)$$

Then, the values of coefficients \vec{r} can be solved by

$$\vec{r} = [X' \cdot X]^{-1}[X'\vec{y}]. \quad (4.7)$$

Referring to this study, the ordination results are the response variables \vec{y} . With ordination methods (see section 4.3.1) the complex floristic composition data can be described by only two or three metric variables, i.e. the values on ordination axes per sample. The reflectance data that are available for each plot (spectral bands) act as explanatory variables X . Conventionally, multiple linear regression would be used here. This simple linear relationship gives good results if only few independent explanatory variables are available. The number of explanatory variables n should be well below the number of samples p to prevent multicollinearity and, therefore, model overfitting. If we use the hyperspectral information of the contiguous wavelength bands as

explanatory variables, the above mentioned assumptions do not apply, because the wavelength bands are interdependent and way too many in relation to the number of plots.

The PLS-regression (Partial Least Squares regression by Wold 1966), an expanded version of the multiple linear regression, comes into play as it can deal with numerous, correlated predictors (Hoeskuldsson, 1988; Abdi, 2003). In this study, each ordination axis is regressed against radiance data independently (PLS 1). To regard the huge number n of explanatory variables (spectral bands) independently, they are decomposed by PCA (Principal Component Analysis - Greig-Smith 1983) into latent, independent variables. As not necessarily only the first principal component describes all relevant effects, each component is treated independently as factor and is tested on its significance in respect to the response variable.

In terms of the above notation (equation 4.5), PLS uses principal components to decompose the matrix X into a score matrix T and a loading matrix W :

$$X = TW'.$$

The original model (equation 4.4) is now expressed as a regression problem with independent variables T instead of X :

$$\begin{aligned} \vec{y}_{\text{model}} &= X\vec{r} \\ &= \underbrace{X(W')^{-1}}_{=T} W'\vec{r} \\ &= TW'\vec{r} \\ &= T\vec{c}, \quad \text{with } \vec{c} = W'\vec{r}. \end{aligned}$$

With this transformed regression model, all relevant components T are integrated, and can be recalculated to the original factors X , i.e. the spectral band information.

All regression models, one of each ordination axis of each subarea, were validated by a full leave-one-out cross-validation, i.e. for each sample a sub-model was calculated to predict its value without including it into the model's computation (see section 4.4.2 and e.g. Efron and Tibshirani 1993 for more information). As, like mentioned above, too many explanatory variables cause overfitting, the number of latent variables that should be included in the model had to be estimated. Therefore, the cross-validation procedure was iterated including more and more latent variables. Then, the best model, i.e. the model with the number of latent variables causing the smallest validation errors, could be selected (Wold et al., 2001). Furthermore, a proper wavelength band selection with Marten's uncertainty test (Martens

and Martens, 2000; Davies, 2001) improved the models' results. By this test all wavelength bands were determined whose regression coefficient showed no significance in the regression model, i.e. the variables' stability was estimated by comparing the submodel regression coefficients versus the overall model coefficients. An iterative exclusion of these variables lead to final models with least validation errors. The regression models were calculated with THE UNSCRAMBLER® software Vers. 8.0, Camo, Oslo.

4.3.4 Constructing Borderless Maps

The resulting model equations were each applied to the full scene. Hence, for each ordination axis a greyscale image was produced, i.e. for each pixel of the scene its value on the ordination axis was predicted. To derive a map that contained the two-dimensional information, a colour composite was produced. Each greyscale image was displayed in colour (red or green) and displayed in combination with the other. Fig. 4.9 shows how red and green colours are mixed additively in a two-dimensional colour space. Hence, the corners of the colour space are determined by black, red, yellow and green. To bring out as much contrast as possible from the displayed patterns, the colour space of the image composites was individually adjusted to the NMS ordination extents of the axes according to minima and maxima of the data sets.



Figure 4.9: A two-dimensional colour space formed by additive colour mixture of red and green.

4.4 Classification and its Mapping

”The tendency of the human species is to crystallize and to classify his knowledge; to arrange it in pigeon-holes.”

(Gleason 1926 citing Cooper 1926).

4.4.1 Vegetation Classification

Vegetation classification can be carried out in manifold ways and by diverse criteria. In this study three common classification keys have been applied. By help of diagnostic taxa the classification of Braun-Blanquet (1928) establishes a relationship to the phytosociological system of Central Europe. A classification by the sociation concept of Du Rietz (1930) appears advantageous for remote sensing matters as it is based on dominant species, and dominant species build the mainly reflected structures. To sort vegetation into Fauna-Flora-Habitat types, classification keys have been set up by the Habitats Committee, and are mainly based on diagnostic species. For ease of all classifications, the sorting program JUICE 6.2 (Thichy, 2002) has been used.

Phytosociological Classification

The relevé data are structured by specific diagnostic species and thereupon arranged into phytosociological categories that are representative for the plant associations of Central Europe. Following the extant vegetation classification of Wagner et al. (2000b), the vegetation types are arranged in formations and complexes. This means a deviation of the traditional method of Braun-Blanquet (1928). The plant sociology organises vegetation hierarchically into classes, orders, alliances, and associations. This was done following Oberdorfer (1977a), and Oberdorfer (1977b). As the present structures often are small-scaled (less than 1 m^2) and closely intertwined with each other, also complexes and formations are described as so-called plant communities. In particular when classifying areas with bog hummocks and hollows, this is a well-established variation (Schuckert, 1998).

The systematic sampling design complicated the phytosociological classification. Depending on where the raster dots had fallen to, relevés contained components of diverse plant communities. Helpful classification routines, like e.g. TWINSpan (Two-way Indicator Species Analysis, an hierarchical divisive clustering technique developed by Hill 1979 and published by Gauch and Whittaker 1981), yielded reasonable results that had to be sorted by hand afterwards.

Sociation Concept

In the species-poor region Scandinavia it is common to classify by the sociation concept of Du Rietz (1930). This approach is based on the dominance of few species that form the main structure of vegetation in each layer. It seems reasonable to build vegetation types by dominance aspects instead of searching for sparsely occurring character species (Du Rietz, 1930, 315). It gives consideration to dominance structures and can therefore be linked well with remote sensing data. Du Rietz (1930) defines homogeneous sociations that are composed of constant dominants in each layer. Further he differs consociations that show homogeneity in only one layer, and subconsociations with two homogeneous layers. If only one layer shows homogeneity by a group of species with strong sociological affinity to each other, but with variegating coverages, it is called association.

Classification of Fauna-Flora-Habitats

A division by Fauna-Flora-Habitats and their subtypes is of essential interest concerning this project. For each member state of the European Union, classification keys have been developed on purpose to support ecologists in their countries. In Germany, monitoring responsibilities lie within the federal states. In the case of this study, the Bavarian FFH-mapping manual of Lang and Walentowski (2007) forms the base of the classification. This manual was developed from the Interpretation Manual of European Habitats (European Commission DG Environment, 2003) and the BfN-Manual from Ssymank et al. (1998), amended by Balzer et al. (2004). According to the manual, habitats are mainly classified by the composition of diagnostic species, their abundance as well as their dominance. Separations of similar habitats are eased. Although faunistic observations complete the assignment of a relevé to a certain habitat type, they are not obligatory (Lang and Walentowski, 2007, 7). Additionally, the condition of the habitats plays a major role and can be evaluated by specific criteria, e.g. the occurrence of indicator species or the degree of agricultural operations. However, the FFH manual does not include all habitats that occur in conservation areas as not every habitat is of ecological interest. For this reason, an extended version (Stellmach and Langensiepen, 2006, 2007) of the traditional guidance to mapping biotopes has been developed in 2006. It enables the combined registration of Fauna-Flora-Habitat types and biotope types and supports monitoring of conservation areas in whole.

4.4.2 Pixelbased Supervised Image Classification

Pixelbased image classification means to assign each pixel - according to its spectral information - to a category. Unsupervised methods like ISODATA (4.2.3) group the pixels corresponding to similarities among each other without any predefined classes. Supervised methods, instead, use the information given by a spectral library to compare each pixel of a scene with. Spectral libraries can contain the spectra from ground truth pixels (i.e. pixels where pretaken and classified field data exist) or extant spectra from field spectrometer or laboratory measurements. Class membership is then assigned to the pixel according to some similarity measurement. It is a precondition that the training data is representative and complete to cover all the variability of the scene to be classified (Lillesand and Kiefer, 2004, 545). Here, two common classification algorithms, namely Spectral Angle Mapper (SAM) and Multiple Endmember Spectral Mixture Analysis (MESMA), based on Linear Spectral Unmixing (LSU), have been tested on the same set of data to discover which performs best with natural openland vegetation.

With crisp methods, a pixel is assigned to one class only, whereas fuzzy methods (like MESMA) can compute the fraction a vegetation type has in the pixel's spectral information. Algorithms like Maximum Likelihood classification and Spectral Angle Mapper can produce crisp as well as fuzzy outputs (e.g. Wang 1990; Foody and Arora 1996; de Lange et al. 2004). In our case, only crisp outputs have been produced. All image classifications and their validations were performed with the software package ENVI 4.0 RSI, Boulder, USA 2004 and the programming language IDL (Interactive Data Language). In parts, the into ENVI 4.0 implemented classification routines were run, partly - as in the case of the Spectral Angle Mapper - its algorithm was self programmed to gain insight into intermediate data. All self programmed routines could be validated via the ENVI 4.0 user level.

The Spectral Angle Mapper algorithm and the MESMA model were designed for hyperspectral imagery and could therefore be applied to the full scene.

SAM (Spectral Angle Mapper)

This classification method was developed for hyperspectral imagery by Kruse et al. (1993) and is most popular in remote sensing applications (de Lange et al., 2004). The spectral signature of a test pixel with n bands can be regarded as a n -dimensional vector. The direction of the test vector is compared to the direction of the vectors of the reference spectra in the spectral library. If the angle between the test vector and the reference vector falls

below a predefined threshold (in case of this study, thresholds were considered to be 1 for all members in the spectral library), the test pixel is assigned to this class. This procedure is iterated for each pixel of the scene. It is in particular advantageous that this method performs independently from illumination effects of the imagery as not lengths but directions of the vectors are compared with each other. The spectral angle is given by the arc cosine (\cos^{-1}) of the following algorithm with \vec{t} being the n -dimensional vector of the test pixel and \vec{r} the vector of the reference pixel with n referring to the number of bands.

$$\cos^{-1} \left(\frac{\sum_{i=1}^n t_i r_i}{\sqrt{\sum_{i=1}^n t_i^2} \sqrt{\sum_{i=1}^n r_i^2}} \right)$$

MESMA (Multiple Endmember Spectral Mixture Analysis)

MESMA (Roberts et al., 1998) is an enhancement of the LSU (Linear Spectral Unmixing) algorithm. The LSU process regards each pixel as a linear combination of so-called endmember spectra contained in a spectral library, that means the algorithm calculates the fraction a certain endmember (class) has within the spectrum of a pixel. When using unmixing methods, it is advisable to use pure components in the spectral library. The term endmember refers to the spectrum of a more or less homogeneous feature. As the extraction of spectra from the scene itself always means taking a mixture of components, it is appropriate to speak of reference spectra instead.

This linear mixture model is expressed by the following equation

$$\vec{t} = \sum_{j=1}^k f_j \vec{r}_j + \vec{\epsilon},$$

where f_j indicates the fraction the reference spectrum \vec{r}_j has within the spectrum of the test pixel \vec{t} . k describes the number of different reference spectra in the spectral library. $\vec{\epsilon}$ expresses the residual, i.e. the unmodeled portion of the test pixel (Roberts et al., 1998). The sum of fractions is constrained to be 1:

$$\sum_{j=1}^k f_j = 1.$$

As it is a fuzzy method it outputs not one classification image but as many as classes, i.e. reference spectra, are in the spectral library. Additionally, the Root Mean Squared (RMS) error per pixel is computed that estimates how

well the fractions of the reference spectra unmix the test pixel. It is defined by the following equation with n being the number of bands:

$$\text{RMS error} = \sqrt{\frac{\sum_{i=1}^n (\epsilon_i)^2}{n}}.$$

With its large amount of spectral bands, spectral unmixing can be performed successfully with imaging spectrometer data (Keshava and Mustard, 2002). This means to be an overdetermined system (Okin et al., 2001) as the number of reference spectra in the spectral library is much lower than the number of useful bands, i.e. the number of equations outnumbers the number of the unknown fractions. A deeper description of this method can be found in Adams et al. (1986) and Kruse et al. (1993).

MESMA performs the above described LSU algorithm in that way that each pixel of the scene is unmixed with the most suitable model, i.e. with a subversion of the spectral library that performs with the least RMS error. That means that the spectral library consists of a pool of reference spectra. All possible class combinations (models) are tested on each pixel. A model is only applied to a pixel if the RMS error stays under a certain threshold. Furthermore, class fractions must have reasonable values between -0.01 and 1.01. If these assumptions do not apply, the model is discarded for this pixel. Roberts et al. (1998) propose a three-step approach. One begins with only one-class models to give consideration to pure stands. With all pixels of the scene that have not been unmixed satisfyingly, two-class models are performed. Still remaining pixels are then unmixed with three-class models. After that, still left pixels that can not be unmixed with good RMS error results are regarded as not-classifiable, as the differentiation of mixtures of more than three vegetation classes is not realistic (Roberts et al., 1998). Crisp class affiliation of the pixels can be computed by assigning a pixel to the class that contains the largest fraction of the best unmixing, i.e. the most suitable model of that pixel.

The number of possible models can be described by the following equation:

$$\sum_{k=1}^n \binom{n}{k},$$

with n being the number of all possible reference spectra in the spectral library and k describing the model combinations with the limitation to maximal three-class models $k = 1, 2, 3$ and $n_{max} = 3$.

The tryout of model combinations per pixel needs long computing time. That means the pool of possible reference spectra has to be limited to the

smallest amount that is possible, i.e. the number of classes that have to be distinguished. In this case that was done by the EAR-method (Endmember Average Root Mean Squared Error-method) proposed by Dennison et al. (2004) that is described in the following subsection.

MESMA has proven to be a useful classification method for soil (e.g. sludge derivatives (García-Haro et al., 2005)) as well as natural vegetation spectra in arid and semi-arid environments (Okin et al., 2001; Dennison et al., 2004; Bachmann et al., 2005). Its ability to distinguish Mid European natural openland vegetation has not been tested in the literature yet. We programmed MESMA using the LSU algorithm that is a standard routine in ENVI 4.0.

Determination of Reference Spectra

The spectral library contains spectra where reference information is available. For this project, all reference spectra are taken from the scene itself. That means that ground truth data have been surveyed beforehand. After field work and the classification of the relevé data, the spectra of the appropriate pixels are extracted from the scene and edited. The processing of the spectra for their entry into the spectral library can occur variedly.

Commonly, the arithmetic mean of all spectra per class is used (see fig. 4.10). That means that all spectra of the relevés that have been assigned to the same vegetation type are averaged per band to build up one reference spectra for this class in the spectral library. We will refer to this method as ‘MSD Mean Spectra Determination’.

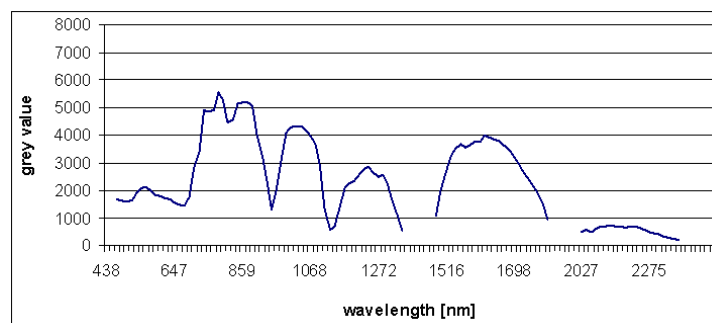


Figure 4.10: A sample MSD spectrum of the FFH type 7120 of the subarea 2004 south. The average of the spectra of 18 relevés is used in the spectral library.

If every pixel where vegetation information exists is regarded as an own subclass of a certain vegetation type, we receive a large spectral library without any modification of the spectra due to computational reasons (see

fig. 4.11). After supervised image classification, the individual subclasses are combined to form the former vegetation type again. Following de Lange et al. (2004), this method is called ‘Individual Vector Determination’, referring to its usage as band-dimensional vector for the SAM classification algorithm. As in this case, not only SAM but other supervised classification algorithms have been tested, this method is hence called ‘ISD Individual Spectra Determination’.

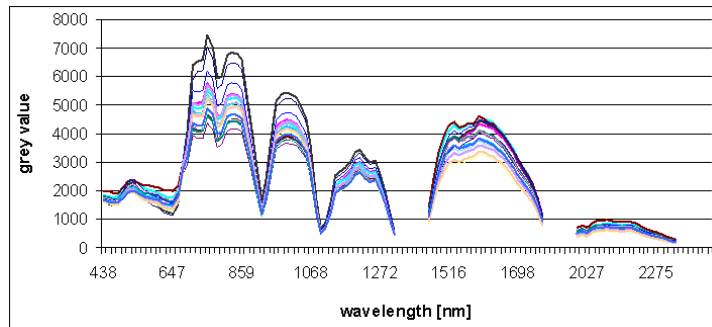


Figure 4.11: Sample ISD spectra of the FFH type 7120 of the subarea 2004 south. All 18 relevés are used in the spectral library.

Another possibility to build up the spectral library was proposed by Dennison and Roberts (2003a) and originally called EAR (Endmember Average Root Mean Squared Error). Due to above mentioned reasons the term ‘end-member’ is not appropriate here and therefore the method is called ‘BRSD Best Representative Spectra Determination’. It was meant to be used with the MESMA algorithm (Dennison and Roberts, 2003b) but has been applicable with SAM as well (Dennison et al., 2004). From a pool of reference spectra, the best spectrum per class is chosen, i.e. the spectrum that can represent its class best. That is done by averaging the RMSE that result when a spectrum unmixes all spectra of its own class with the above described method LSU (see section 4.4.2 for RMSE and LSU computation). The BRSD method is expressed by the following equation:

$$\text{BRSD}_{A_i,A} = \frac{\sum_{j=1}^k \text{RMSE}_{A_i,A_j}}{k-1},$$

where the vegetation type A has k members. The denominator $k - 1$ refers to the zero RMSE that is produced when a class member unmixes itself. Figure 4.12 shows the RMSE matrix that is produced by the unmixing routine of the class members against each other (Dennison and Roberts 2003a,b), and in fig. 4.13 a sample BRSD spectrum is given.

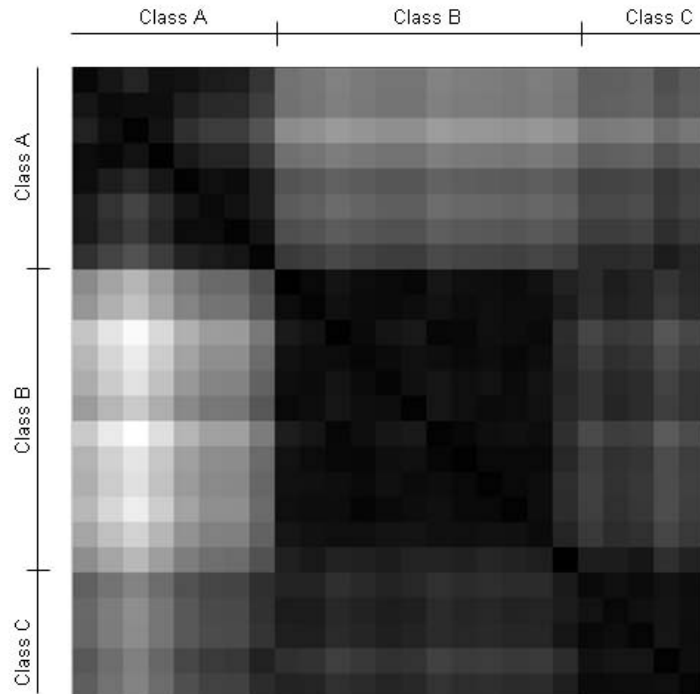


Figure 4.12: The RMSE matrix of class A, B and C shows dark pixels where the RMSE is small, and light pixels where the RMSE is high. Class assignment can therefore be seen easily, as class members unmix each other rather good. The zero diagonal refers to each spectrum unmixing itself.

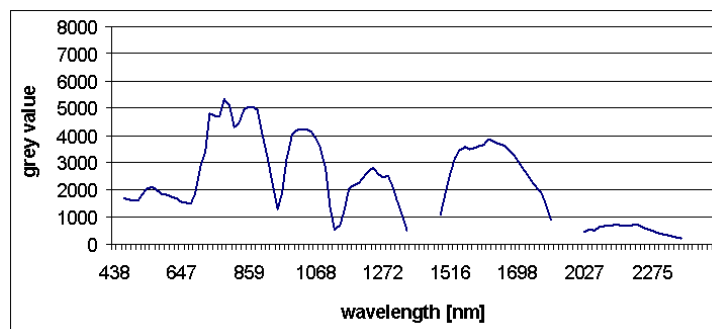


Figure 4.13: A sample BRSD spectrum of the FFH type 7120 of the subarea 2004 south. The spectrum of the relevé that represents best its class is used in the spectral library.

Accuracy Assessment

Leave-one-out Cross-validation

All results of the supervised image classification were assessed of their significance to complete the classification procedure (Lillesand and Kiefer, 2004, 568). A common approach is to part the data into a training set with which the spectral library is built and a validation set that is to be classified. This seems only reasonable with large plot numbers per class, i.e. vegetation type (at least 30 relevés per vegetation type). If smaller data sets are to be classified and assessed, they can be validated with a full leave-one-out cross validation that has been used as well to validate the PLS regression models described in section 4.3.3. The history of using cross-validation assessment goes back to the first half of the 20th century. Stone (1974) gives a detailed overview of the methods and its manifold applications in statistics. Also named predictive sample reuse (Geisser, 1975), it means to remove a sample from the data to predict its own value. Applications can be found at Lachenbruch and Mickey (1968); Lachenbruch (1968); Efron (1983) and, more recently, Steele et al. (2003). As cross-validation methods are not standard routines in ENVI 4.0, it was self programmed in IDL and linked with all applied supervised classification routines.

The leave-one-out cross-validation was used with MSD and ISD methods. Iteratively, one plot, and so its spectrum, was left in turn from the making of the spectral library. After image classification, the value of the left-out plot was investigated to which vegetation type it had been assigned to. After re-running the classification procedure for each plot, a confusion matrix was arranged and evaluated.

Cross-validation was not applied to classifications that were run with a BRSD spectral library, as the pre-defined best reference plot per class was left from the analysis and was, therefore, not included into the arrangement of the confusion matrix.

The Confusion Matrix and Cohen's Kappa of Agreement

A confusion matrix, or error matrix, is the most common method of accuracy assessment (Foody, 2002; Fritz and See, 2004). According to Strahler (2002), it is a design-based inference, as it means to assess the accuracy of the classification against samples on ground that were designed for doing so. A confusion matrix (see table 4.4) is a class-dimensional square array that gives evidence about right and wrong assignments a classification has done. All samples are listed with their true destination (according to ground truth

data) and their classification results. Numbers on the matrix diagonal refer to correctly classified samples.

		reference	data			
		Class A	Class B	...	Class Q	Row Σ
classification results	Class A	S_{11}	S_{12}	...	S_{1k}	S_{k+}
	Class B	S_{21}	S_{22}	...	S_{2k}	S_{k+}
	\vdots	\vdots	\vdots	\ddots	\vdots	\vdots
	Class Q	S_{k1}	S_{k2}	...	S_{kk}	S_{k+}
Column Σ		S_{+k}	S_{+k}	...	S_{+k}	S

Table 4.4: A confusion matrix consists of columns that represent the reference data whereas the lines illustrate the classification results. All entries show the quantity of all samples S that are assigned to all classes A, B and Q respectively. The red marked diagonal displays the correctly classified number of samples per class, i.e. vegetation type.

A simple descriptive technique of analysing the results that are displayed in a confusion matrix is the Overall Accuracy. It is a weak measure of accuracy, as wrongly classified values are neglected. It only refers to the diagonal values of the confusion matrix, and expresses the percentage of correctly classified samples. It can be calculated with the following equation:

$$\text{Overall Accuracy} = \frac{\sum_{k=1}^q S_{kk}}{S} \cdot 100,$$

with S being the total number of samples and q the number of classes.

Among many analyses, the *Kappa* analysis (Cohen's *Kappa* of Agreement, Cohen 1960) is a powerful, and therefore popular, method to measure not only the performance of a single matrix but to compare different confusion matrices from different classifications (Congalton, 1991; Smits et al., 1999). The estimation of *Kappa* from the confusion matrix means to include information on the number of samples per class and, if not correctly classified, to which category they were assigned to.

In his extended review, Congalton (1991) quotes the problem of *Kappa* estimation being designed for multinominal sampling models, which is only completely satisfied by ground truth data derived with simple random sampling. However, it has negligible bias when systematic sampling is used (Stehman, 1992), i.e. classification results based on ground truth data of the vegetation period 2004 can be analysed with the *Kappa* coefficient, which is calculated as follows:

$$Kappa = \frac{S \cdot \sum_{k=1}^q S_{kk} - \sum_{k=1}^q (S_{k+} \cdot S_{+k})}{S^2 - \sum_{k=1}^q (S_{k+} \cdot S_{+k})},$$

with q expressing the number of categories in the spectral library. Usually, the *Kappa* coefficient ranks between 0 and 1. The closer *Kappa* approximates 1, the better is the performance of the image classification.

Discussion

Though, as the ground truth data of the vegetation period 2005 were collected using stratified random sampling, its classification results should be calculated with a modification of the conventional *Kappa* coefficient that was developed by Stehman (1996). The *Kappa_{stratified}* equation brings into play the role of samples per stratum in the assumption that all strata correspond with the vegetation classes of the spectral libraries. In our case, this is not true, because strata have been formed by unsupervised classification of the hyperspectral scene beforehand (see 4.2.3) without knowledge of any vegetation classification afterwards (Wunsch, 2006). This means that in our case, strata do not correspond with vegetation classes by all means. Secondly, different vegetation keys have been used on the same data set to bring out different objectives of this study (see 4.4.1), which means that for each vegetation classification, different samples belong to different vegetation types and strata. Therefore, we have to accept the fact that the sampling design can influence kappa calculations and, hence, the comparison between different classifications concerning ground truth data of 2005.

4.5 Synthesis

This section describes how all building blocks of this study that have been developed are combined, how ordination and vegetation classification are put together without remote sensing applications, as well as how borderless maps derived from regression modelling are synthesised with vegetation type polygons derived from supervised image classification.

4.5.1 Complementary Analysis: Constructing Colour Legends

On vegetation level, classification results can be projected in ordination space (see fig. 5.27, 5.28, and 5.29). This has been described by Kent and Ballard (1988) as complementary analysis. It is a first step in combining discrete

with non-discrete information and will be done to complete the description of species composition as well as to introduce to the synthesis of PLS regression models with image classifications. It builds the base of the legends for the maps that will be created in the following section 4.5.2. To ease vegetation type colour interpretation in the Synthesis maps, the centroids of the vegetation types are displayed in NMS ordination colour space (see the Synthesis maps B in the Appendix).

4.5.2 Combining Discrete and Non-discrete Approaches

By PLS regression modelling, maps of the sampled areas are produced that contain continuous information. Vegetation type polygons are overlaid as fully transparent polygons to enable the colours of the PLS regression models to build the main structure of the map. Equal looking vegetation type colours are added with legend hatchures. Large polygons of more or less homogeneous types are best overlaid by stripes. This allows for fast type assignment, and does not mask the regression model colour underneath. Small polygons (Salt-and-Pepper-Effects) are better characterised by pointed hatchures, as points can be detected in small areas as well. Similar vegetation types are provided with similar hatchures, or with the same hatchure in a different colour.

The legend is two-fold: class definition is given by hatchure boxes on the one hand, and by a coloured ordination space via complementary analysis on the other. Concerning maps of Fauna-Flora habitats, non-relevant habitat types are displayed with a transparency level of 60 %. This eases first differentiation between relevant and non-relevant patterns, but gradients and transitions can still be distinguished. Map production was performed with the GIS software package ArcMAPTM Vers. 9.1, ESRI Inc., USA.

Chapter 5

Results

This chapter presents results from ordination methods and their linkage with hyperspectral imagery via regression modelling. Then, results of vegetation classification, as well as results of supervised image classifications are illustrated. The synthesis of ordination and its mapping with classification and its mapping builds the final core of the chapter.

5.1 Ordination and its Mapping

5.1.1 Ordination Results: NMS

The indirect ordination method NMS has been applied for two vegetation periods 2004 and 2005. The vegetation data (see table 5.1) performed better with log-transformed data than with untransformed. This became apparent in both data sets of 2004 and 2005. Similar results could be yielded by evaluations from Zimmermann (2005) and Wunsch (2006). Therefore, all subsequent structure interpretation and regression modelling was based on log-transformed vegetation data.

Aim of the indirect ordination was to receive a two-dimensional solution that displayed as much variance of the original data as possible. Both areas of 2004 showed high percentages of variance regarding the log-transformed data. 92.4 % (subarea north) and 95.2 % (subarea south) of variance could be explained by two axes. The three-dimensional results performed slightly better with increases of 2 % (subarea north) and 3 % (subarea south). With the log-transformed data set of 2005, 82.3 % of variance could be explained with a two-dimensional solution, 89 % of variance could be explained with a three-dimensional solution.

Fig. 5.1 displays NMS stress values (see section 4.3.2) plotted against di-

Data set	Dim.	$\log_{10}[\text{cover}]$	variance explained [%]			Σ
			Axis 1	Axis 2	Axis 3	
north 2004	2	v	23.0	65.6	-	88.7
			82.8	9.6	-	92.4
	3	v	72.5	11.5	9.2	93.2
			83.1	7.1	4.2	94.4
south 2004	2	v	22.7	67.3	-	90.1
			25.3	69.9	-	95.2
	3	v	56.8	28.0	10.3	95.1
			70.7	18.7	8.7	98.1
2005	2	v	32.0	43.9	-	75.9
			22.8	59.5	-	82.3
	3	v	24.1	43.9	16.8	84.7
			22.7	50.0	16.6	89.2

Table 5.1: NMS results of the vegetation data 2004 and 2005

mensionality. For all data sets, stress values stayed below 20 (apart from the one-dimensional solution of the subarea 2005), and the change of stress values decreased from two- to three dimensional solutions. Therefore, the substantive aspect of mapping convenience can be underlined with the statistical recommendation to proceed with two dimensions.

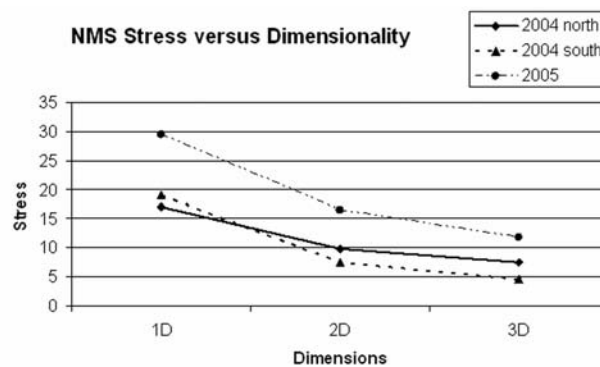


Figure 5.1: Stress of NMS ordination for vegetation data of 2004 and 2005 against dimensionality

Interpreting Structures

Figs. 5.2, 5.5, and 5.7 give an overview, how the relevés are dispersed in the ordination space formed by two NMS axes. Plot arrangement will be explained in the following. Figs. 5.3, 5.4, 5.6, and 5.8 show the cover values of selected species of the areas. Displayed plot sizes refer to the occurrence of the selected taxa in NMS ordination space. Plot dispersion and axis values correspond to the overview scatter plots 5.2, 5.5, and 5.7.

Fig. 5.2 shows dispersions of the relevés in species ordination space of the calculated NMS ordinations of the data subset 2004 north. Cover values of selected single species of this subarea can be found in fig. 5.3 and 5.4.

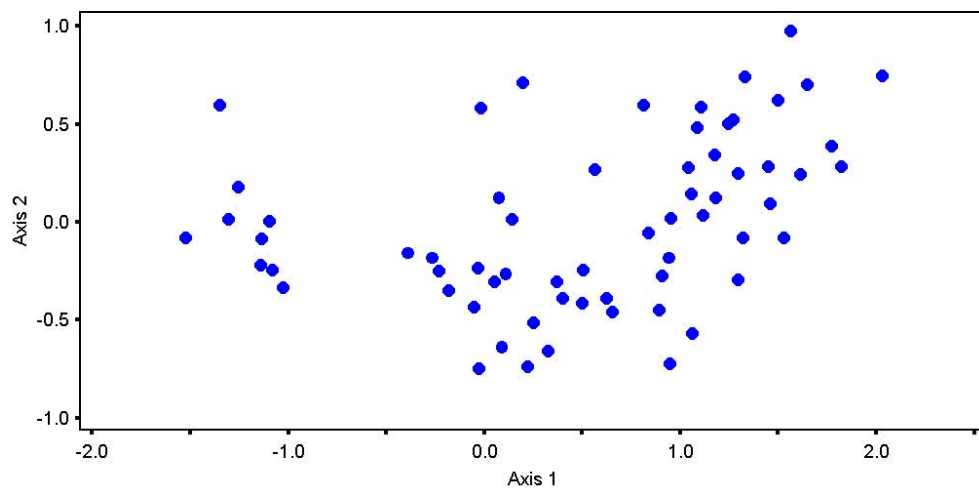


Figure 5.2: NMS ordination scatterplot of the subarea 2004 north.

The first NMS axis of the northern subarea shows a very strong gradient that explains nearly 83 % of the data variance. To the left side of the diagram (axis scores of -1.5 to -1.0), wet and eutrophic habitats along rivulets are displayed. The discrete group of concerned plots contains hydro- and nitrophilous taxa like *Urtica dioica* and *Eupatorium cannabinum*. Strong dominance of *Phragmites communis* can be found in all plots that are displayed on the left half of the diagram. Although its cover values decrease in plots of the right half, its presence is visible in nearly any plot of the data set.

The middle part of the ordination diagram (axis scores of -0.5 to 1) shows plots on fen peats. It is indicated by the occurrence of species like *Carex panicea*, *C. lasiocarpa* as well as alkaline fen species like *Schoenus ferrugineus* and *S. nigricans*. The right part of the diagram (axis values of 1 to 2.2) shows relevés on bog peats, indicated by bog character species like

Vaccinium oxycoccus, *Andromeda polifolia*, *Drosera rotundifolia* and *Eriophorum vaginatum* as well as *Calluna vulgaris*. In general, high influence of *Molinia caerulea* and *Trichophorum cespitosum* can be observed. Both taxa are abundant from the middle of the diagram to the right parts. They show the close interlocking of fen and transition mire inventory to the plots that primarily contain bog species.

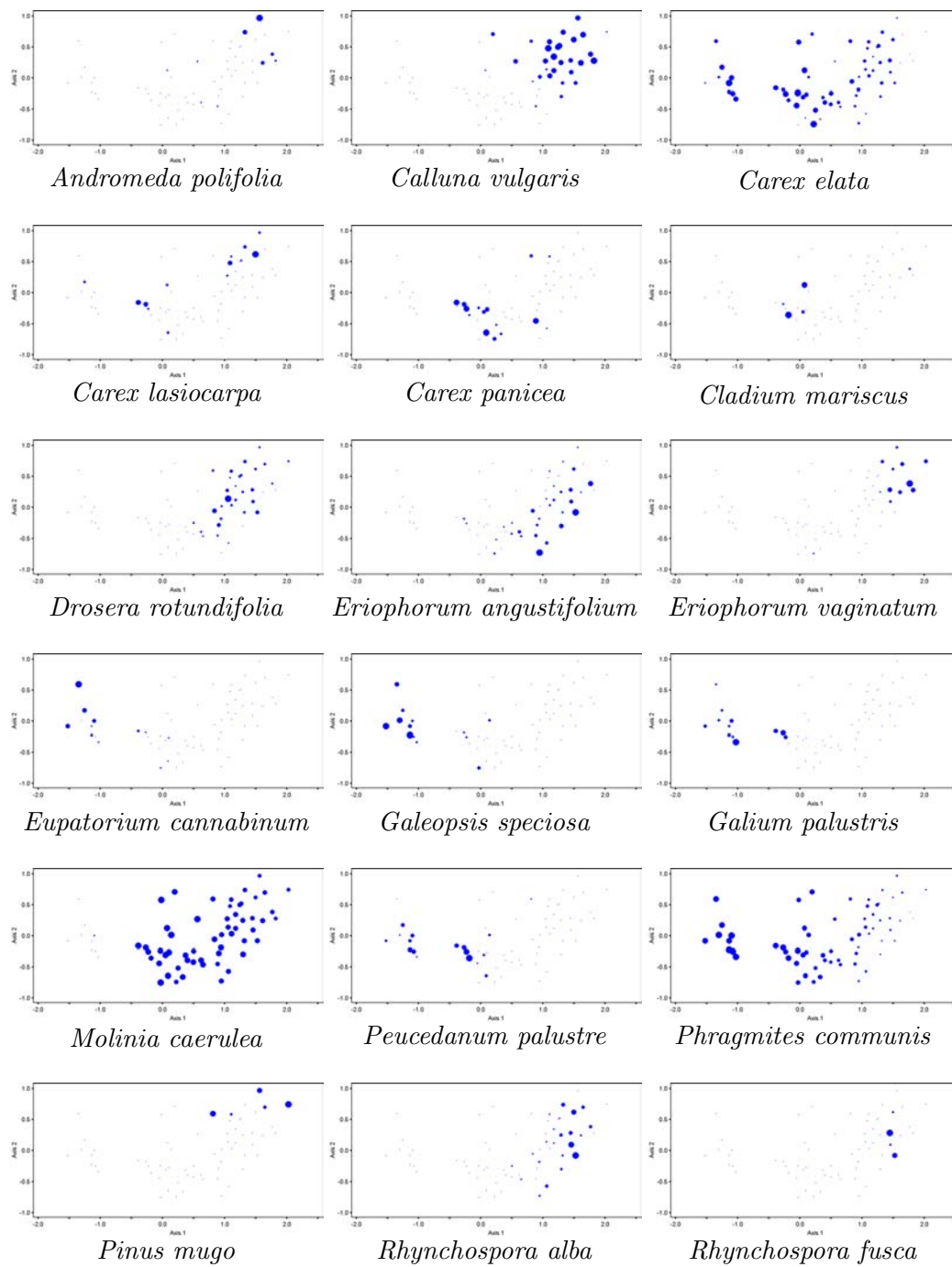


Figure 5.3: NMS: Cover values of selected species of the subarea 2004 north

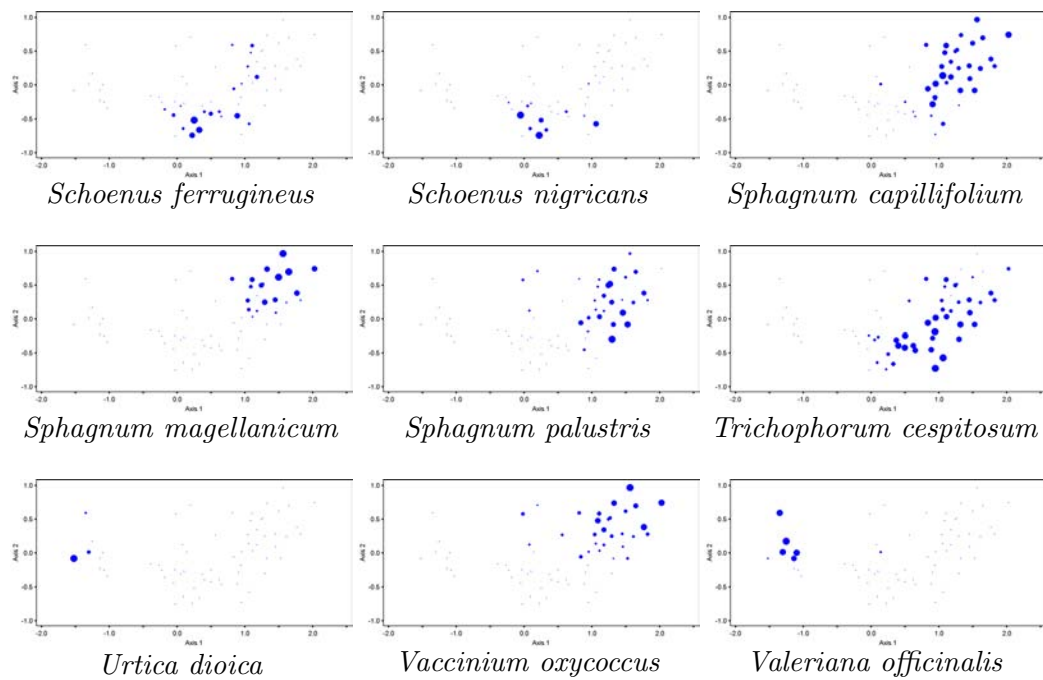


Figure 5.4: NMS: Cover values of selected species of the subarea 2004 north

The second axis explains 9.6 % of the total variance. It defines the eutrophic plots on the left side into bottom plots with *Galeopsis speciosa*, *Peucedanum palustre* and *Galium palustre* versus upper plots with species of the *Filipendulion* like *Valeriana officinalis* and *Eupatorium cannabinum*. The second axis parts the middle of the diagram into the bottom plots with *Schoenus* species and the upper plots with *Cladium mariscus*. The bottom plots at the right side of the ordination have high cover values of *Eriophorum angustifolium* and hollow species like *Rhynchospora alba*, *Rhynchospora fusca*, *Sphagnum palustre* and *Sphagnum capillifolium*. Upper lying plots are defined by hummock species like *Sphagnum magellanicum*, *Vaccinium oxycoccus* and *Eriophorum vaginatum*. Plots that contain *Pinus mugo* covers can be found on top of the right side of the diagram.

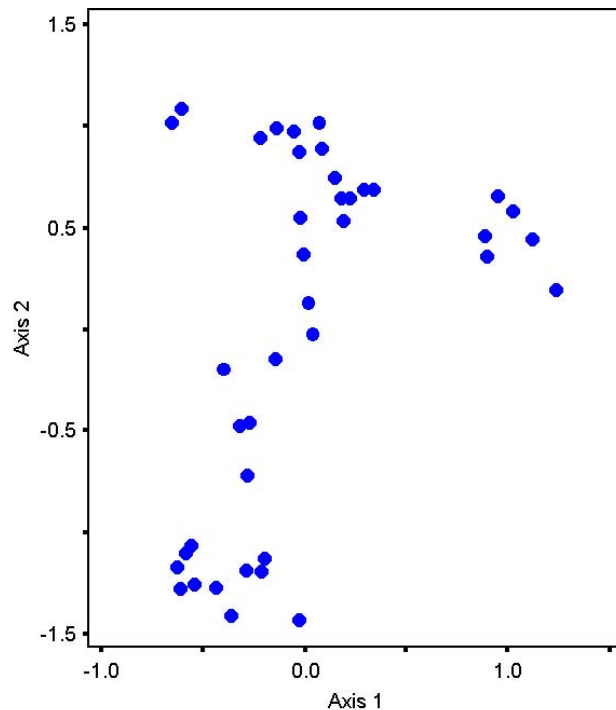


Figure 5.5: NMS ordination scatterplot of the subarea 2004 south.

The scatterplot of the southern area of the data 2004 (see fig. 5.5, and see figs. 5.6 for cover values of selected single species of this subarea) shows a strong gradient along the second NMS axis. It explains nearly 70 % of the variance and shows the vegetation transition from used and abandoned fen meadows to bog habitats. This is indicated by the occurrence of *Molinia caerulea* in the upper half of the scatterplot, whereas *Calluna vulgaris* dominates relevés that are displayed on the bottom. Finer differentiations can be made easily due to the discrete groups of plots that are formed: the topmost part of the second axis (axis scores of 1.0 to 0.5) is characterised by the occurrence of hydrophileous taxa like *Phragmites communis*, *Galium palustris* as well as *Peucedanum palustre*, followed by relevés on fen peats with *Schoenus* species and *Eriophorum angustifolium* (axis scores around 0.5). The transition to relevés on bog peats are displayed by relevés with high covers of *Trichophorum cespitosum* (axis scores of 0.5 to -0.5). The relevés on the very bottom (axis scores of -1.0 to -1.5) are dominated by bog character species like *Vaccinium oxycoccus*, *Eriophorum vaginatum* and *Pinus mugo* (shrub layer).

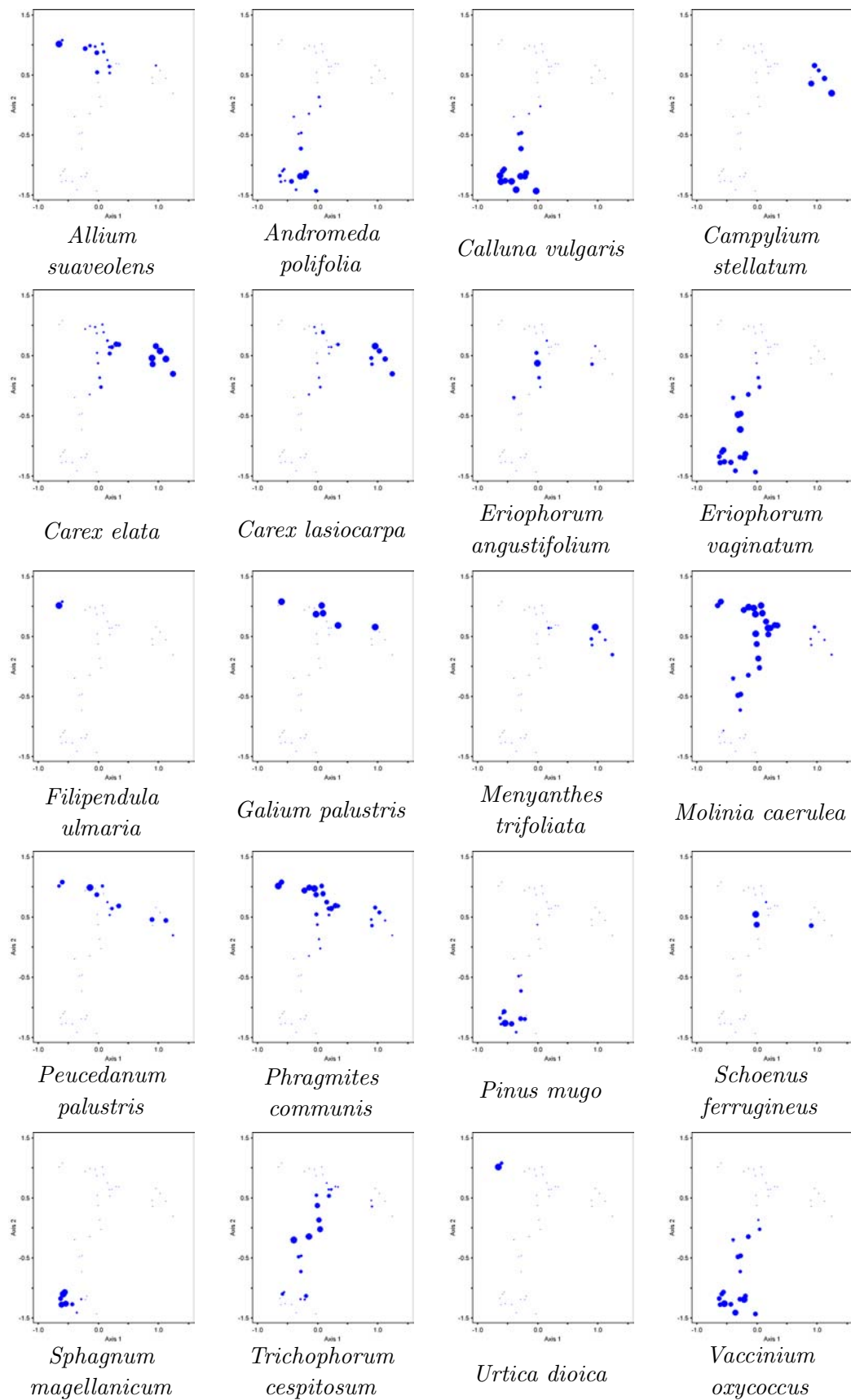


Figure 5.6: NMS: Cover values of selected species of the subarea 2004 south

The first axis explains about 25 % of the variance and shows discrete fragmentation in the upper half of the scatter. The left part of the first axis (axis scores of -1.0 to 0.5) shows plots with *Allium suaveolens*, and high cover values of *Molinia caerulea*. The two relevés that are situated at the left edge (axis scores of -0.75) differ from the others by the occurrence of e.g. *Filipendula ulmaria* and *Urtica dioica*. They refer to eutrophic parts of the area along rivulets. The group of six relevés that are located at the right side of the first axis (axis scores of 0.5 to 1) is characterised by the occurrence of *Carex elata*, *C. lasiocarpa*, *Menyanthes trifoliata* and *Campyllum stellatum*. The relevés of raised bogs split into plots that contain *Sphagnum magellanicum* to the left side of the scatter, and plots with more influence of *Andromeda polifolia* to the right side.

Fig. 5.7 displays plot dispersion in NMS ordination space of the subarea 2005. Cover values of selected single species of this subarea can be found in fig. 5.8.

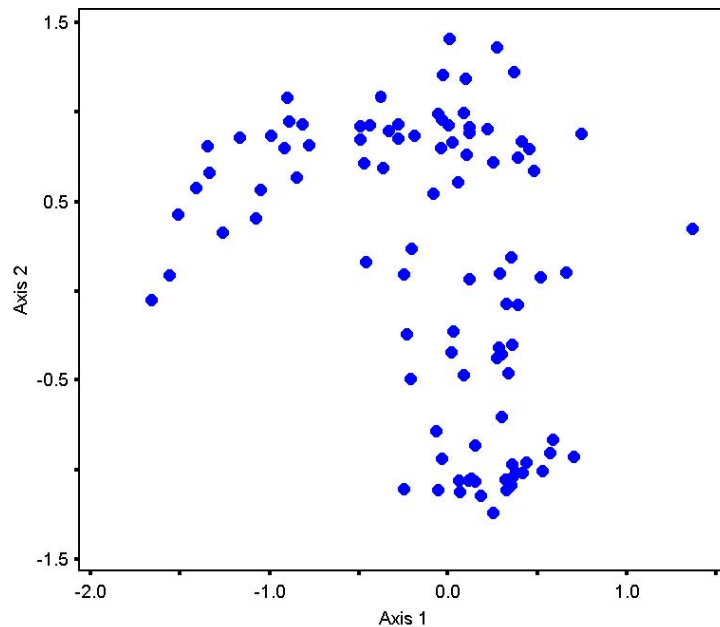


Figure 5.7: NMS ordination scatterplot of the subarea 2005

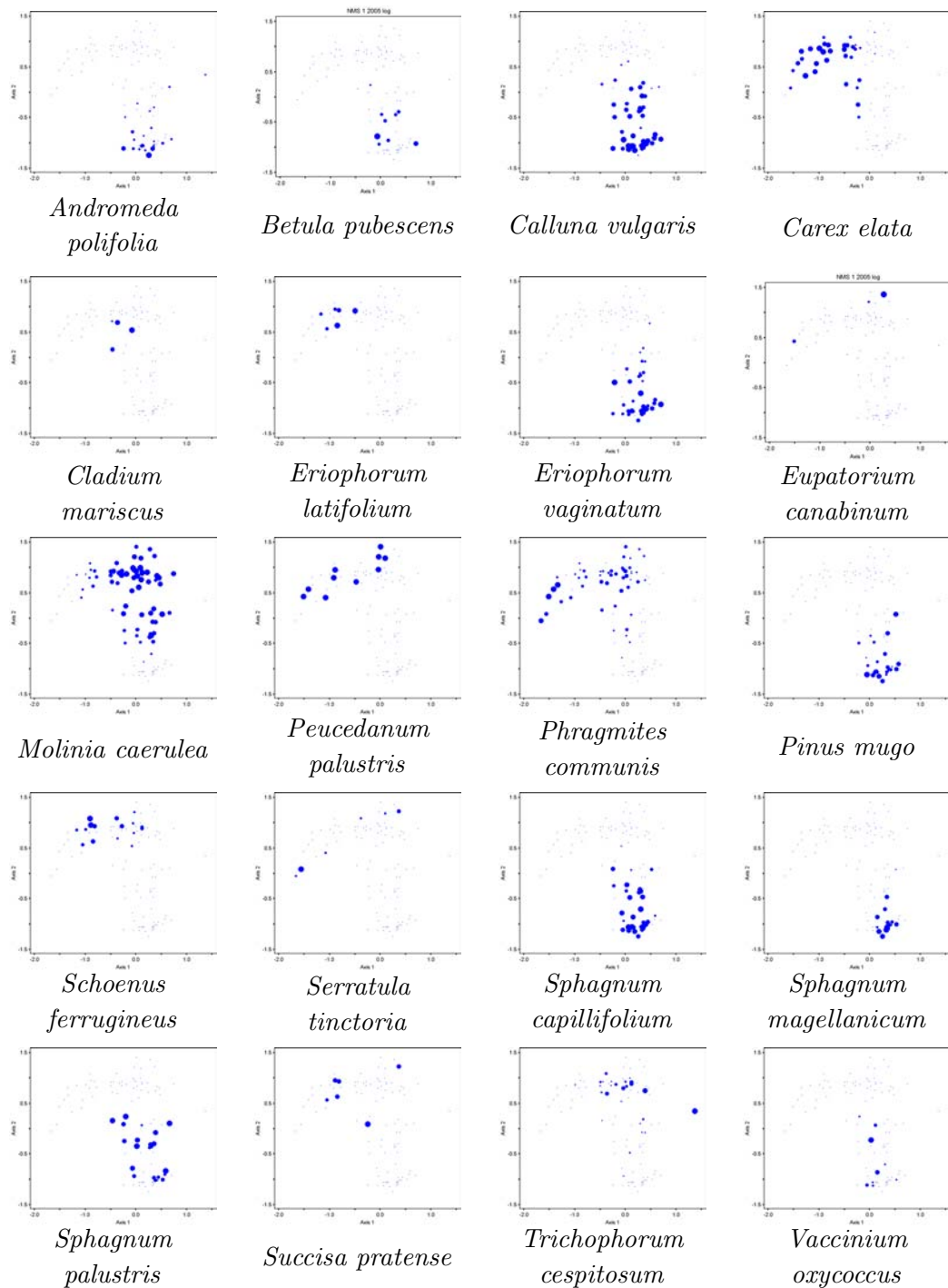


Figure 5.8: NMS: Cover values of selected species of the subarea 2005

The second axis of the data set 2005 explains 59.5 % of the variance. It shows the environmental gradient from wet, alkaline influenced habitats with *Molinia caerulea*-dominated relevés on the upper part (axis scores of 1.5 to 0) with *Eupatorium cannabinum* defining the top-most plot, transition zones with *Trichophorum cespitosum* in the middle part (axis scores of 0 to -0.5) to relevés on bog peats in the bottom half of the scatterplot (axis scores of -0.5 to -1.5), indicated by *Calluna vulgaris*, *Eriophorum vaginatum* and other bog character species like *Vaccinium oxycoccus* and *Sphagnum* species, where *Sphagnum palustris* and the bog degradation indicator species like *Betula pubescens* occur in relevés from the middle of the axis to axis scores of -1.0. *Sphagnum magellanicum* dominates below, together with *Andromeda polifolia* and *Pinus mugo*.

The first axis explains nearly 23 % of variance in the data set 2005. It mainly differentiates *Molinia caerulea*-dominated relevés in the upper half of the scatter plot. Dominant species of relevés in the left half of the first axis are *Carex elata* and *Phragmites communis*. Relevés on the very left side (axis scores of -1.5 to -1.0) are characterised by the occurrence of *Molinia* species like *Serratula tinctoria* as well as *Succisa pratense*. Relevés on wetter habitats (axis scores around 0) show cover values of *Peucedanum palustre*, *Eriophorum latifolium* and *Schoenus* species, and below of *Cladium mariscus*. The single relevé on the very right side (axis score of 1.5) is dominated by *Trichophorum cespitosum*. Bog relevés can be split into plots with high influence of *Vaccinium oxycoccus* to the left, and plots with *Sphagnum magellanicum* to the right side.

5.1.2 Mapping Ordination Results: PLS Regression Models

Table 5.2 shows the best model results from ordination axis values regressed against spectra taken from the imagery. Five of the six models performed better with log-transformed spectra ('pseudo-absorbance', see section 4.1.2). High R^2 results could be yielded for NMS axes that represented the main (longer) gradient with higher fraction of the total variance, i.e. the first NMS axis of the northern area could be modelled with R^2 of 0.93 as well as the second NMS axis of the southern area with R^2 of 0.92 in cross-validation. The first axis of the southern area could be modelled with R^2 of 0.68 whereas the second axis of the northern area received R^2 of 0.44 in cross-validation. The data of 2005 performed not as good as the data sets of 2004. The second axis could be modelled with R^2 of 0.60 and the first axis received 0.29 in cross-validation.

Subarea NMS Axis	north 2004		south 2004		2005	
	NMS1	NMS2	NMS1	NMS2	NMS1	NMS2
# bands	41	8	7	20	24	11
log[10]1/R	log	1	log	log	log	log
Min	-1.52	-0.75	-0.66	-1.43	-1.45	-1.37
Max	2.03	0.97	1.23	1.08	1.58	1.28
# PC	4	3	3	4	3	3
RV_{val}						
PC 0	0.85	0.19	0.27	0.78	0.35	0.67
PC 1	0.24	0.17	0.25	0.24	0.25	0.38
PC 2	0.13	0.13	0.09	0.07	0.25	0.33
PC 3	0.07	0.10	0.08	0.06	0.25	0.26
PC 4	0.06	0.11	0.10	0.06	0.26	0.29
PC 5	0.06	0.10	0.09	0.06	0.29	0.29
PC 6	0.06	0.11	0.09	0.06	0.28	0.30
PC 7	0.66	0.11	0.09	0.07	0.28	0.30
PC 8	0.79	0.11	-	0.08	0.30	0.30
$RMSE_{val}$	0.24	0.32	0.29	0.25	0.50	0.51
$RMSE_{\%}$	7	19	15	10	17	19
R_{cal}^2	0.95	0.51	0.75	0.93	0.35	0.64
R_{val}^2	0.93	0.44	0.68	0.92	0.29	0.60

Table 5.2: PLS regression model results of the vegetation periods 2004 and 2005. Bold values show the chosen best models with least RV in cross-validation. All R^2 values are highly significant with $\alpha < 0.001$. (Min, Max = minimum, maximum of data space, PC = principal components, RV_{val} = rest variance in cross-validation, $RMSE_{val}$ = Root Mean Squared Error in cross-validation, $RMSE_{\%}$ = Root mean Squared Error in percentage of the data space, R_{cal}^2 = Coefficient of determination in calibration data, R_{val}^2 = Coefficient of determination in cross-validation).

5.1.3 Constructing Borderless Maps

Figures 5.9 show the PLS models that were applied to the scene data. For each axis a grey scale image corresponding to NMS axis values was produced and combined with the other to a colour composition.

The resulting maps show all variance that could be found in the data sets by reducing dimensions to two. The change of colours gives an insight how vegetation types are intertwined and shows transition zones as well as homogeneous areas. The legends have been accompanied with the scatter plots from NMS ordination. In this way, the interpretation of species composition

(see section 5.1.1) can be applied to the maps as well.

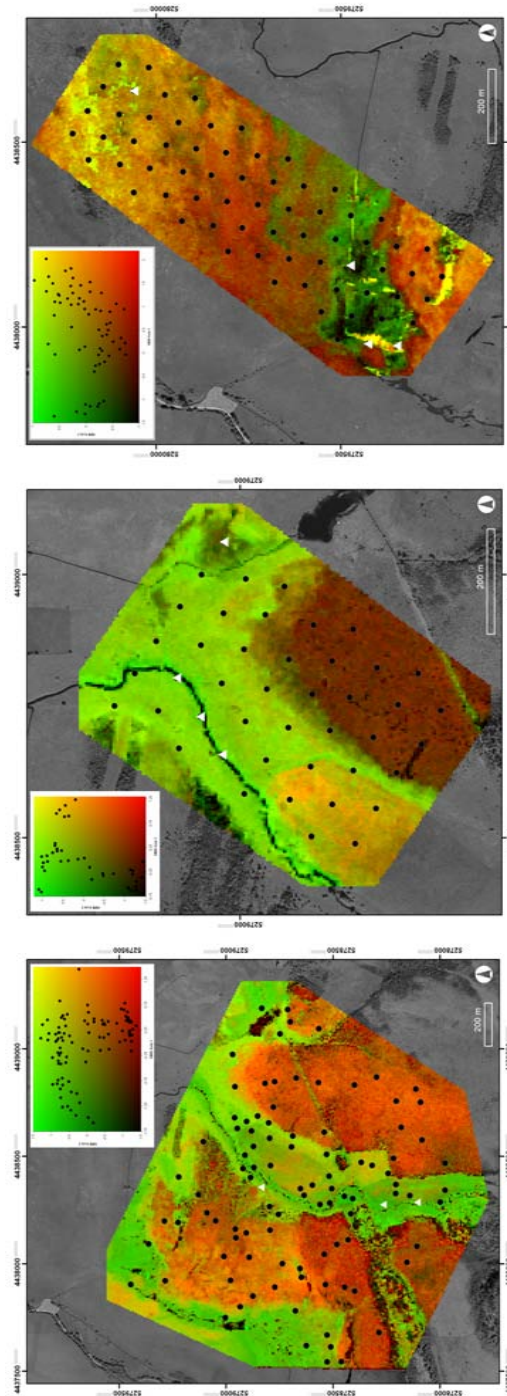


Figure 5.9: Colour composites of PLS regression models of the NMS axis 1 (red) and axis 2 (green) of the data subsets 2004 north (top), 2004 south (middle), and 2005 (bottom). The colour legend shows how color composition corresponds to plot dispersion on NMS axis values, and species composition respectively. Heterogeneous plots (derived with MRPP tests) are marked as white triangles.

5.2 Classification and its Mapping

The area under investigation comprises a high diversity of vegetation types that are closely intertwined. The vegetation data of 2004 and 2005 show the most open-land communities of the area under investigation that are of conservation importance. In the following, three possible classification schemes are applied to the same data sets. Fig. 5.10 shows the disposition of the communities in a catena along the hydrological gradient.

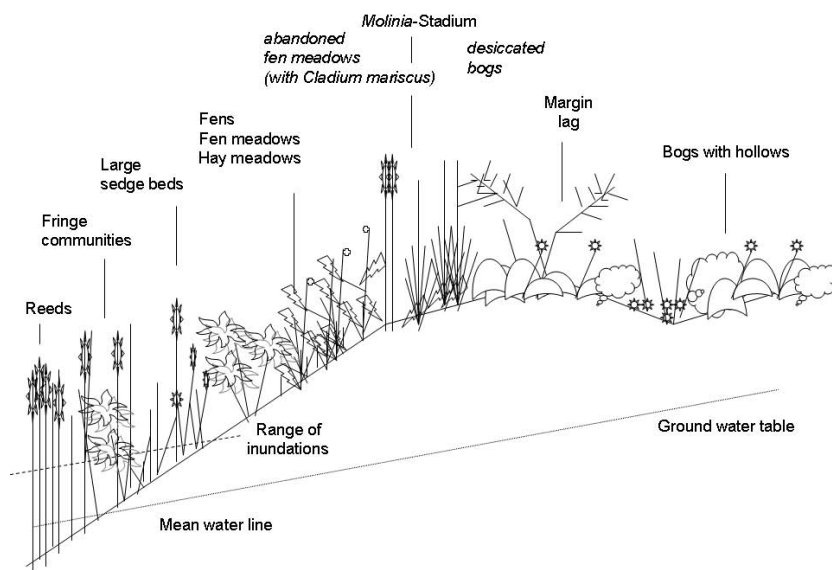


Figure 5.10: Overview of the disposition of the communities that are classified from the data sets of 2004 and 2005

Along rivulets and in the range of former turf cuttings, the species-poor association of the *Phragmitetum communis* can be found at, and curtly below, the mean water line. Due to its absolute dominance of *Phragmites communis*, it is assigned to the *Phragmites communis-Carex elata*-Sociation, and correspondingly to the non-FFH relevant biotope type GR. Drier formations build the transition to occurring associations of the *Magnocaricion* that are situated in the range of episodal inundations, i.e. the *Caricetum elatae* and its formations. It corresponds to the non-FFH relevant biotope type VC00BK. It is part of sociations formed by the dominance of *Carex elata*. Parts of the area that lie above flooded areas, with steady contact to ground waters, are covered with fen communities of the *Caricion davallianae*, i.e. the FFH-type 7230, and with utilised fen meadows of the *Molinietum caeruleae*, i.e. the

FFH-type 6410 as well as fringe communities and hay meadows with species of the *Arrhenatherion*, i.e. the FFH-types 6430, and 6510-6520. These communities are assigned to sociations formed by the dominance of *Carex elata*, *Molinia caerulea* and tall forbs. Following of fen meadows can lead to the formation of the *Cladietum marisci* on wetter parts, i.e. the FFH-type 7210, and to the development of an extremely species-poor *Molinia caerulea*-Stadium. This stadium is caused as well by dessication of the bogs. Both correspond to the non-FFH relevant biotope type GP00BK, and its relevés are assigned to subtypes of the *Molinia caerulea*-Consociation. Lag vegetation like the *Pino mugo-Sphagnetum* occurs widely along margins as well as on the bog plateaus where it builds isles in the otherwise treeless bog communities, i.e. the FFH-type 91D3. The bogs in its active (i.e. the FFH-type 7110) and degraded stadium (i.e. the FFH-type 7120) are mainly formed by complexes of other associations of the *Sphagnion magellanici* with hollow communities of the *Rhynchosporion*, i.e. the FFH-type 7150. The bog communities are assigned to sociations formed by the dominance of *Trichophorum cespitosum*, *Calluna vulgaris*, and to associations of dominant *Sphagnum* species. All mentioned communities are explained in the following. From the 104 plots of the data set 2004, one had to be excluded due to high coverages of *Picea abies* in the tree layer. As well, from the 97 plots of the data set 2005, three plots had to be discarded by reason of high coverages (> 20%) of *Alnus glutinosa*, *Alnus incana* and *Betula pendula* in the tree layer.

5.2.1 Vegetation Classification Results: Phytosociological Classification

At large, 12 different vegetation types on alliance or association level can be distinguished from the data sets. The data of 2004 north show 8 phytosociological communities, 2004 south can be classified into 5, and the data of 2005 show 11 phytosociological communities. Table 5.3 gives an overview of the occurring plant communities in their context of classes, orders and alliances as well as the number of relevés of all data sets that have been assigned to them. The phytosociological classification table A.4.1 is included in the Appendix of this work.

All phytosociological communities that could be classified from the data sets belong to the following classes, or untitled Stadia: *Phragmitetea*, *Scheuchzerio-Caricetea fuscae*, *Molinio-Arrhenatheretea*, the untitled *Molinia caerulea*-Stadia, and the *Sphagnetetea magellanici*. Abbreviations will be used for character species of classes (CC), of orders (CO), of alliances (CA), and of associations (CS) that characterise the listed communities in the vegetation

data of 2004 and 2005. To avoid the confusion of the phytosociological term ‘class’ with classified units, the identified communities are henceforth titled as ‘vegetation types’.

class	Phragmitetea			Scheuchzerio-Caricetea fusc.
order	Phragmitetalia			Tophieldietalia
alliance	Phragmition		Magnocaricion	Caricion davall.
association	Phragmitetum communis	Cladietum marisci	Caricetum elatae	Primulo-Schoenetum ferr.
abbrev.	PC	CM	CE	PS
2004 north	9	1		6
2004 south			6	
2005	1	2	4	10

class	Molinio-Arrhenatheretea			
order	Molinio-Arrhenateretalia			
alliance	Arrhenatherion	Molinion	Molinia-Stadium	
association/ Stadium		Molinietum caeruleae	abandoned fen meadows	desiccated bogs
abbrev.	AR	MC	MSt*f	MSt*b
2004 north			11	8
2004 south		2	14	
2005	2	8	13	10

class	Oxycocco-Sphagnetea			
order	Sphagnetalia magellanici			
alliance	Sphagnion magellanici			
association	Pino mugo-Sphagnetum magellanici	Eriophoro-Trichophoretum cespitosi	Sphagnetum Rhynchosporion complex	Sphagnetum magellanici
abbrev.	PM	ET	SR	SM
2004 north	1		4	22
2004 south		10		8
2005	6	7	1	30

Table 5.3: Occurring plant communities in their phytosociological context and number of relevés of the data sets of 2004 and 2005 that have been assigned to them.

Reed Formations and Large Sedge Beds of the *Phragmitetea*

class: *Phragmitetea* Tx. et Prsg. 1942

order: *Phragmitetalia* W. Koch 1926

Reeds with mainly *Phragmites communis*, *Cladium mariscus* formations and large sedge beds with *Carex elata* belong to the order of the *Phragmitetalia*.

alliance: *Phragmition* W. Koch 1926
 association: *Phragmitetum communis* Schmale 1939
 formation: typical formation of the planar level

Character species: (CC,CO,CA) *Phragmites communis*, *Galium palustre*, *Mentha aquatica*, *Lycopus europaeus*, *Peucedanum palustre*, *Scutellaria galericulata*, *Carex elata*, *Lysimachia thyrsoifolia*

The *Phragmitetum communis* is located along rivulets and former turf cuttings and has its range from the mean water line to depths of 0.4 m. It is a species-poor association of extreme habitats (see fig. 5.11, left). Oberdorfer (1977a, 127) describes this community as weakly characterised by *Phragmites communis*. It has, therefore, to be handled critically. Nevertheless, the typical subassociation of planar levels can be supposed due to very high coverages of *Phragmites communis*, small cover values of *Urtica dioica* and lack of *Phalaris arundinacea*. *Valeriana officinalis* and *Eupatorium cannabinum*, species of the *Filipendulion ulmariae* Segal 1966, are important attendants.



Figure 5.11: (left) The *Phragmitetum communis* Schmale 1939 is a species-poor association of extreme habitats. *Phragmites* plants reach heights of more than 2 m. (middle) *Cladium mariscus* is a strictly endangered species. In the Murnauer Moos, it occurs on stands of abandoned fen meadows with *Molinia caerulea* and *Phragmites communis*. (right) In the *Caricetum elatae* W. Koch 1926 of the area of investigation, *Carex lasiocarpa* is an important attendant species. (source of photos: P. Zimmermann)

alliance: *Phragmition* W. Koch 1926
association: *Cladietum marisci* Allorge 1922
formation: succession stage of former extensively utilised fen meadows

Character species: (CS) *Cladium mariscus*, (CA of the *Phragmition*) *Phragmites communis*, (CA of the *Magnocaricion*) *Galium palustre*, *Carex elata*, *Peucedanum palustre*, *Mentha aquatica*, (CS of the *Primulo-Schoenetum*) *Schoenus ferrugineus*

The *Cladietum marisci* usually occurs at the mean water level of calcareous waters, where it is closely intertwined with communities of the *Phragmition*, the *Magnocaricion* and alkaline fen vegetation. In the area of investigation, it occurs on succession stages of abandoned fen meadows. It is only weakly defined by the relevé data with cover values below 40 % of *Cladium mariscus* (see fig. 5.11, middle). Plots that are assigned to this association show high cover values of *Molinia caerulea* indicating the former usage as extensive fen meadows (see section 5.2.3).

alliance: *Magnocaricion* W. Koch 1926
association: *Caricetum elatae* W. Koch 1926

Character species: (CS) *Carex elata*, (CA) *Galium palustris*, *Peucedanum palustre*, *Mentha aquatica*, *Lycopus europaeus*, (CO) *Phragmites communis*

In the area of investigation, *Carex elata* is located on areas that lie curtly above the mean water line. Inundations occur episodically with calcareous waters. Attendant species with some influence are *Carex lasiocarpa* (see fig. 5.11, right) as well as *Carex panicea*, *Molinia caerulea* and the mosses *Campylium stellatum* and *Calliergonella cuspidata*. This community is recorded by four plots of 2005, and six plots of the southern subarea 2004 where mowing regimes both enable the occurrence of species of the *Caricion davallianae* and hinder *Phragmites communis* to overgrow.

Fens, Fen and Hay Meadows of the *Scheuchzerio-Caricetea fuscae* and of the *Molinio-Arrhenatheretea*

class: *Scheuchzerio-Caricetea fuscae*
 (Nordhag. 1937) Tüxen 1937
 order: *Tophieldietalia* Preisg. apud Oberdorfer 1949
 alliance: *Caricion davallianae* Klika 1934
 association: *Primulo-Schoenetum ferruginei*
 (Koch 1926) Oberdorfer 1957 em. 1962

Character species: (CS) *Schoenus ferrugineus*, *Schoenus nigricans*, (CA) *Tophieldia calyculata*, *Eriophorum latifolium*, *Epipactis palustris*, (CO) *Parnassia palustris*, *Pinguicula vulgaris*, *Carex davalliana*, *Primula farinosa*, *Carex flava* coll., *Campylium stellatum*, (CC) *Drepanocladus revolvens*, *Menyanthes trifoliata*, *Fissidens adianthoides*, *Carex echinata*

On peat substrates with steady contact to alkaline ground waters, fen communities of the *Primulo-Schoenetum ferruginei* can be classified from the relevé data. Plot data that belong to the association show covers of *Schoenus ferrugineus* and *Schoenus nigricans* as well as *Carex davalliana*, but other defining character species of the associations lack (e.g. *Gentiana utriculosa*, *Orchis palustris*). Nevertheless, all fen plots can, although weakly characterised, be assigned to the *Primulo-Schoenetum ferruginei* (Koch 1926) Oberdorfer 1957 em. 1962. Steady cover values of *Carex panicea* refer to fluctuations of ground water (Oberdorfer, 1977a, 252). Influences of non-calcareous waters advantage the growth of *Carex lasiocarpa*. Covers of *Trichophorum cespitosum* show parts where soils are cut off from supply of minerals due to accumulation of humus (Oberdorfer, 1977a, 253), wetter parts, instead, and the transition to the *Magnocaricion*, are indicated by high coverages of *Carex elata*. Mown parts are closely related to the *Molinietum caeruleae* and, therefore, show high fractions of character species of the latter. Fig. 5.17(right) shows the class character species *Epipactis palustris*. It could be found in only few of the relevés.

class: *Molinio-Arrhenatheretea* Tx. 1937
 order: *Molinietalia caeruleae* W. Koch 1926
 alliance: *Molinion caeruleae* W. Koch 1926
 association: *Molinietum caeruleae* W. Koch 1926

Character species: (CS, CA) *Galium boreale*, *Allium suaveolens*, (CO) *Molinia caerulea*, *Succisa pratensis*, *Gentiana pneumonanthe*, *Stachys officinale*, *Serratula tinctoria*, *Iris sibirica*, *Sanguisorba officinale*, *Juncus subnodulosus*

The communities of the *Molinion caeruleae* are situated on infertile, wet gley or pseudogley soils. They belong to species-rich fen meadows and are usually mown once a year. Therefore, in the area of investigation, they are closely related to communities of the *Caricion davallianae* due to combined mowing regimes over long periods. One association, the *Molinietum caeruleae*, can be found in the data of 2004 and 2005.

The *Molinietum caeruleae* W. Koch 1926 is dominated by *Molinia caerulea* and shows all above mentioned characteristic species of its order and alliance. The pre-alpine subtype of the area of investigation is defined by *Veratrum album*, *Primula farinosa* and *Trichophorum alpinum* (see fig. 5.12, left). In wet parts, the occurrence of *Carex davalliana* and *Schoenus ferrugineus* shows base-rich water supply whereas the occurrence of *Galeopsis speciosa* refers to nutrient-richer sites. Transitions to a weakly characterised *Allio suaveolentis-Molinietum* Görs 1979 can be found in some of the plots of 2004 and 2005. *Allium suaveolens* occurs steadily, but with poor cover values. Also *Ranunculus montanus*, and *Allium carlinum* on drier parts, define this pre-alpine association (Oberdorfer, 1977b, 385ff). It is, nevertheless, difficult to be differentiated from the typical formation of the *Molinietum caerulea* and the plots concerned are therefore assigned to the latter. On wetter parts, transitions occur to the *Magnocaricion* with *Phragmites communis* and *Carex elata*.

class: *Molinio-Arrhenatheretea* Tx. 1937
order: *Arrhenatheretalia* Pawl. 1928
alliance: *Arrhenatherion elatioris* W. Koch 1926

Character species: (CA) *Pimpinella major ssp. major*, (CA of the *Calthion*) *Chaerophyllum hirsutum*, (CO, CA of the *Molinion*) *Molinia caerulea*, *Serratula tinctoria*, *Sanguisorba officinalis*, *Cirsium oleraceum*, *Galium uliginosum*, (CC) *Aconitum variegatum*, *Vicia cracca*, *Ranunculus acris* agg.

Due to fen desiccation and eutrophication, the *Molinia caerulea*-dominated fen meadows show transitions to hay meadow communities of the *Calthion* as well as of the *Arrhenatherion elatioris*. These habitats are species-rich. Although weakly characterised by some coverages of *Pimpinella major ssp. major* and *Chaerophyllum hirsutum*, two relevés of the data set 2005 are assigned to this alliance.



Figure 5.12: (left) *Trichophorum alpinum* characterises the pre-alpine subtype of the *Molinietum caeruleae* W. Koch 1926 in the area under investigation. (middle) Fen meadows in the Murnauer Moos. (right) The desiccated bog margin with *Calluna vulgaris* and *Pinus mugo* merges to wetter parts where *Molinia caerulea* dominates. (source of photos: P. Zimmermann, C. Weiß, C. Weiß)

Molinia caerulea-Stadium

Character species: *Molinia caerulea*

Molinia caerulea-Stadium on abandoned fen meadows

Parts of the area of investigation where the mowing regime ceased, show species-poor *Molinia* stands with some residual taxa of formerly species-rich fen meadows like *Allium suaveolens*. Fallowing can lead to dominance of large sedges and reeds as well as strong tussock formation of single taxa, e.g. *Molinia caerulea* (see fig. 5.14, left) if conditions are favourable (Nowotny and Tröster, 2002). Due to high litter accumulation, seedling and germination of other taxa is inhibited (e.g. investigations of Maas 1988; Bosshard et al. 1988; Billeter et al. 2003).

Dominant taxa of the relevés that have been assigned to this formation are *Molinia caerulea*, *Phragmites communis* and *Carex elata*. Occurrences of species of the *Molinietum caeruleae* and the *Caricion davallianae* with attendance of *Carex lasiocarpa*, *Trichophorum cespitosum* and *Carex panicea* give evidence of the formerly richer stands. Number of species as well as the habitus of *Molinia caerulea* tussocks depend on the time since the meadows have lain fallow. In the range of rivulets, nitrophilous species occur, like e.g. *Eupatorium cannabinum*, *Urtica dioica* and *Galeopsis speciosa*. Steady attendance of *Potentilla erecta* refers to its ability to assert despite above mentioned conditions.

Molinia caerulea-Stadium on desiccated bogs

Already a small lowering of the water level of bogs and the involved mesotrophication blocks *Sphagnum* species and enables dwarf-shrubs and tussock-forming plants (Ellenberg, 1996, 501). *Molinia caerulea* in particular, obtains best premises to grow on large parts of desiccated structures in the area of investigation (see fig. 5.12, right). The lower water level means better aerated humus, and high precipitations lead to the required humidity. Edom (2001, 535) also cites the ability of *Molinia* to grow well on habitats with changing water levels. Oxidation processes lead to smaller pore sizes of the topsoil which means increases of water level oscillation. Relevés that have been assigned to this vegetation type, show very high coverages of *Molinia caerulea* and some influence of residual bog species like *Calluna vulgaris*, *Vaccinium oxycoccus*, *Andromeda polifolia*, *Eriophorum vaginatum* and *Sphagnum* species.

Margin Lag and Bog Communities of the *Oxycocco-Sphagnetea*

class: *Oxycocco-Sphagnetea* Braun-Blanquet et R. Tüxen 1943
 order: *Sphagnetalia magellanici* (Pawłowski 1928) Moore 1968
 alliance: *Sphagnion magellanici* Kästner und Flößner 1933 emend.

Character species: (CA, CO, CC) *Vaccinium oxycoccus*, *Eriophorum vaginatum*, *Polytrichum strictum*, *Sphagnum magellanicum*, *Sphagnum angustifolium*, *Andromeda polifolia*, *Drosera rotundifolia*, *Aulacomnium palustre*, *Dicranum bergeri*, *Odontoschisma sphagni*,

This alliance on ombrotrophic bog peats is characterised by the occurrence of *Vaccinium oxycoccus*, *Eriophorum vaginatum*, *Andromeda polifolia* (fig. 5.13, right) and turf moss species *Sphagnum magellanicum* (fig. 5.13, left) and *Sphagnum angustifolium*, though the latter does hardly occur in the vegetation data. Three associations, and formations respectively, of the communities of the *Sphagnion magellanici* have been classified from the vegetation data, as well as one complex with species of the *Sphagnion magellanici* and the *Rhynchosporion albae*.



Figure 5.13: (left) *Drosera rotundifolia* and *Sphagnum magellanicum*, (middle) *Polytrichum strictum* and *Vaccinium oxycoccus*, and *Andromeda polifolia* (right) are class, order, and alliance character species of the *Sphagnion magellanici* Kästner und Flößner 1933 emend. (source of photos: P. Zimmermann, P. Zimmermann, C. Weiß)

association: *Pino mugo-Sphagnetum*
Kästner und Flößner 1933 em. Neuhäusl 1969 corr. Dierßen

Character species:

(CS) *Pinus mugo* (tree layer)

In close relation to the *Sphagnetum magellanici*, the *Pino mugo-Sphagnetum* differs from the latter by the occurrence of *Pinus mugo* with cover values of 5 - 50 % in the tree layer. Some plots indicate transitions to the *Vaccinio uliginosi-Pinetum rotundatae* Kleist 1929 em. Matuskiewicz 1962 with the taxa *Picea abies*, *Melampyrum pratense*, *Pleurozium schreberi*, *Bazzania trilobata* and *Vaccinium* species. This community occurs at the margin lag and on the bogs where it builds isles in the otherwise treeless vegetation.

association: *Sphagnetum magellanici* Kästner und Flößner 1933

Character species: (CS) *Eriophorum vaginatum*, *Vaccinium oxycoccus*, *Vaccinium uliginosum*, *Sphagnum* species

The *Sphagnetum magellanici* (Malcuit 1929) Kästner and Flößner 1933 is the characteristic bog community of the pre-alpine region. This treeless association builds out formations depending on water supply. On subplot-level, wetter habitats with *Rhynchospora alba* and *Eriophorum angustifolium* can be differentiated from drier parts with dominant *Sphagnum* species, *Calluna*

vulgaris, *Molinia caerulea* and hummocks of *Polytrichum strictum* (Oberdorfer, 1977a, 282ff) (see fig. 5.13, middle). Cover values of more than 75 % of *Calluna vulgaris* indicate bog desiccation. Attendances of *Polytrichum strictum* and *Dicranum bergeri* show ombrotrophic parts, *Phragmites communis*, *Carex elata* and high coverages of *Molinia caerulea* characterise minerotrophic formations (Wagner et al., 2000a; Friedel, 2005). Affected plots still show high quantities of the above mentioned character species and are, therefore, assigned to this association.

association: Complex of the *Sphagnetum magellanicum* Kästner und Flößner 1933 with the *Rhynchosporion albae* W. Koch 1926

Character species: (CS of the *Sphagnetum magellanicum*) *Eriophorum vaginatum*, *Vaccinium oxycoccus*, *Vaccinium uliginosum*, *Sphagnum* species, (CA of the *Rhynchosporion*) *Rhynchospora alba*, *Rhynchospora fusca*, *Lycopodiella inundata*, *Drosera intermedia*

Plots have been assigned to this complex that show above mentioned diagnostic species of the bogs as well as of the hollow communities of the *Rhynchosporion albae* W. Koch 1926 like *Rhynchospora alba*, *Rhynchospora fusca* and *Lycopodiella inundata* (e.g. Oberdorfer (1977a, 225f)). The creation of a complex follows the extant map of Wagner et al. (2000a).

association: *Eriophoro-Trichophoretum cespitosum* (Zlatnik 1928, Rudolph et al. 1928) Rübél 1933 em.

Character species: (CS) *Eriophorum vaginatum*, *Trichophorum cespitosum*

The *Eriophoro-Trichophoretum* Rübél 1933 em. can be seen as a subassociation of the *Sphagnetum magellanicum*. Oberdorfer (1977a, 287) calls it the formation on sub-alpine levels. Characteristic high coverages of *Trichophorum cespitosum* (see fig. 5.14) as well as poor continuity of characteristic species of the *Sphagnetum magellanicum* allow for the assignment of certain plots to this association (Friedel, 2005). Plots of the southern data set of 2004 show high covers of *Calluna vulgaris*, *Molinia caerulea* and hummocks of *Sphagnum capillifolium* referring to drier habitats, the occurrence of *Sphagnum palustre* describes hollow structures. Plots of this association of the data set of 2005 are dominated by *Trichophorum cespitosum*, *Eriophorum vaginatum* and *Molinia caerulea*, whereas *Sphagnum* species do not occur. *Calluna vulgaris* mostly shows poor cover values. Relevés from the data set of the southern area 2004 show a typical subassociation with high values of *Trichophorum cespitosum*, and poor or no covers of *Vaccinium oxycoccus*, *Andromeda polifolia* and *Eriophorum vaginatum*. *Sphagnum teres* attends some of the assigned relevés.

5.2.2 Vegetation Classification Results: Sociation Concept

The classification for dominance aspects divided the data into seven different vegetation types, with finer subdivision into 14 subtypes. Mainly *Phragmites communis*, *Carex elata*, *Molinia caerulea*, *Trichophorum cespitosum*, *Pinus mugo*, *Calluna vulgaris* and turf moss species (*Sphagnum*) represent the associations that are explained as follows. Table 5.4 gives an overview of the plant communities in their context of consociations and associations, as well as the number of relevés of each data set that have been assigned to them. The sociation classification table A.4.2 is included in the Appendix of this work.

	Phragmites communis-Consociation			Carex elata-Consociation	Trich. cesp.-Consociation
	Phragmites comm.-Carex elata-Sociation	Tall forbs-Association	Cladium mar.-Molinia caer.-Sociation		
abbrev.	Ph	F	Cl	CE	T
2004 north	9				
2004 south				6	
2005	1	4	2	16	2

	Molinia caerulea-Consociation				Pinus mugo-Sphagnum-Association
	Carex elata-Molinia caer.-Subconsociation	Phragmites comm.-Molinia caer.-Subconsociation	Molinia caer.-Trich. cesp.-Subconsociation	Molinia caer. Subconsociation	
abbrev.	M	MPh	MT	M	Pin
2004 north		16	10		1
2004 south		14	5		
2005	4	8		13	8

	Calluna vulgaris-Consociation			Sphagnum-Association
	Calluna vulg.-Molinia caer.-Subconsociation	Calluna vulg.-Erioph. vag.-Subconsociation	Calluna vulg.-Sphagnum-Association	Molinia caer.-Sphagnum-Association
abbrev.	C		CS	MS
2004 north			21	5
2004 south		9	5	
2005	4	3	29	

Table 5.4: Occurring plant sociations and number of relevés of the data sets of 2004 and 2005 that have been assigned to them.

Vegetation Types Defined by *Phragmites communis*

Phragmites communis-*Carex elata*-Sociation

This species-poor sociation is mainly characterised by very high coverages of *Phragmites communis* in the upper herb layer and steady attendancy of *Carex elata* in the middle herb layer. Plot assignment corresponds to the *Phragmitetum communis* of the phytosociological classification.

Tall Forbs-Association

Four relevés of the data set 2005 show, apart from dominance of *Phragmites communis* in the upper herb layer, high coverages of tall forb species, namely *Cirsium oleraceum*, *Pimpinella major* and *Chaerophyllum hirsutum* in the middle herb layer. They are, therefore, treated as an own category with some species richness of 20 species per plot. The moss layer shows influence of *Brachythecium velutinum* which prospers in the shadows of the tall forbs. This type corresponds partly to the phytosociological alliance of the *Arrhenatherion*, and to the *Molinietum caeruleae* association.

Phragmites communis-*Cladium mariscus*-*Molinia caerulea*-Sociation

Corresponding to the phytosociological classification, two relevés of the data set 2005 are assigned to this type. All show high cover values of *Phragmites communis* and *Cladium mariscus* in the upper herb layer and *Molinia caerulea* in the middle herb layer.

Vegetation Type Defined by *Carex elata*

Carex elata-Sociation and -Consociation

Dominance of *Carex elata* in the middle herb layer combine relevés that are applied to this category. Concerning the data set 2004 south, it corresponds to the *Caricetum elatae* association assignment of the phytosociological classification. These relevés form a stable *Carex elata*-*Carex lasiocarpa*-*Campylium stellatum*-Sociation. In the data of 2005, it has to be called a *Carex elata*-Consociation due to high diversity in species richness and attendants of lower herb and moss layers. Variantly, *Molinia caerulea*, *Carex lasiocarpa* and *Schoenus ferrugineus* (see fig. 5.17, left) build the dominant species in the lower herb layer, the moss layer is formed by *Campylium stellatum* v. *protensum*, *Drepanocladus revolvens*, *Calliergonella cuspidata* and

Pleurozium schreberi in different quantities. Finer differentiation into homogeneous categories, as proposed by Du Rietz (1930, 375), would be possible. In the context of a later image classification, it is not of interest here.

Vegetation Types Defined by *Molinia caerulea*

Molinia caerulea-Consociation

Molinia caerulea dominates 38 % of the relevés of both data sets 2004 and 2005. Most of the plots that are assigned to the phytosociological categories of the *Molinietum caeruleae*, *Primulo-Schoenetum ferrugineae* and the *Molinia caerulea*-Stadia are included. At large, a *Molinia caerulea*-Consociation can be assumed. Subdivision into a subconsociation with each *Phragmites communis*, *Carex elata* and *Trichophorum cespitosum* as well as into a formation with no specific dominant taxa in the other layers can be made. Some varying influence of *Schoenus ferrugineus* in the lower herb layer occurs. The moss layer does hardly play a role at all. In the context of bog habitats, an association with *Sphagnum* species occurs and will be described later.

Vegetation Types Defined by *Trichophorum cespitosum*

Trichophorum cespitosum-Consociation

The *Trichophorum cespitosum*-Consociation shows high dominance in the lower herb layer in two plots of the data set 2005 (see fig. 5.14, middle). Other layers have heterogeneous species composition with small cover values. No moss occurs. Both relevés are species-poor with species numbers of 13 and 7 respectively.

Vegetation Type Defined by *Pinus mugo*

Pinus mugo-*Sphagnum*-Association

Corresponding to the phytosociological classification, relevés that have been assigned to the *Pino mugo-Sphagnetum magellanicum* are classified into the *Pinus mugo-Sphagnum*-Subconsociation. The concerned relevés of 2005 all show stable dominance in tree and moss layer, but the herb layer is covered by *Calluna vulgaris*, *Molinia caerulea* and *Eriophorum vaginatum* with variable percentages. Only one plot of 2004 is assigned to this category. Its herb layer is dominated by *Vaccinium myrtillus*.

Vegetation Types Defined by *Calluna vulgaris* and by *Sphagnum* species

Calluna vulgaris-Consociation

Within the context of a later image classification, the stable dominance of *Calluna vulgaris* in the herb layer (see fig. 5.14, right) leads to the definition of a *Calluna*-Consociation. On the botanical level, three subdivisions can be made. Two Subconsociations are characterised by lack of *Sphagnum* species and variable parts of *Molinia caerulea* as well as *Eriophorum vaginatum* in the lower herb layer and variable attendance of other bog species. The latter corresponds to the phytosociological vegetation types of the *Eriophoro-Trichophoretum cespitosi*. A *Calluna vulgaris*-*Sphagnum*-Association is shortly outlined within the context of the *Sphagnum* dominated vegetation types.

Sphagnum-Association

Most bog relevés are classified as *Sphagnum*-Association, as the moss layer is formed by a carpet of different *Sphagnum* species. These relevés can be divided into parts where *Calluna vulgaris* forms the main structure of the herb layer (mainly the bog relevés of the data set 2004 north and of 2005), and into parts where *Molinia caerulea* dominates (five relevés of the data set 2004 north).



Figure 5.14: (left) Tussock forming *Molinia caerulea*, *Trichophorum cespitosum* (middle), and *Calluna vulgaris* (right) are dominant plant species in the area under investigation. (source of photos: C. Weiß)

5.2.3 Vegetation Classification Results: Delineation of Fauna-Flora-Habitats

The vegetation data sets of 2004 and 2005 could be assigned to nine Fauna-Flora-Habitat types. They correspond in most parts to the phytosociological classification. Table 5.5 gives an overview over the types and the number of relevés of the data sets 2004 and 2005 that have been assigned to them. The FFH classification table A.4.3 is included in the Appendix of this work. The classified habitat types belong to natural and semi-natural grassland formations, to raised bogs, mires and fens, and to bog woodlands. As not all occurring habitats are of common interest, three non-relevant biotope types were treated differently and can be found at the end of this section.

Natural and semi-natural grassland formations					
	Semi-natural tall herb humid meadows			Mesophile grassland	
description	<i>Molinia</i> meadows on calcareous soils	Hydrophilous tall herb fringe communities		Lowland hay meadows / Mountain hay meadows	
FFH acr.	6410	6430		6510/ 6520	
2004 north	2				
2004 south					
2005	6	3		1	

Raised Bogs and Mires and Fens					
	<i>Sphagnum</i> acid bogs			Calcareous fens	
description	Active raised bogs	Degraded raised bogs	Depressions on peat substrates of the <i>Rhynchosporion</i>	Calcareous fens with <i>Cladium mar.</i>	Alkaline fens
FFH acr.	7110	7120	7150	7210	7230
2004 north		18	4 (complex with 7120)		
2004 south	3	20		1	6
2005	24	3	1 (complex with 7110)	2	10

	Bog Woodland	non FFH-relevant structures			
description	Mountain pine bog woods	Reeds	Secondarily developed <i>Molinia caer.</i> meadows	Large sedge formations of siltation zones	
FFH acr.	91D3	GR (*)	GP00BK (*)	VC00BK (*)	
2004 north	1		14	6	
2004 south		9	19		
2005	8	1	33	4	

Table 5.5: Occurring habitats in their environmental context and number of relevés of the data sets of 2004 and 2005 that have been assigned to them. (* Acronyms according to the German biotopes, Stellmach and Langensiepen 2006, 62)

6410 - *Molinia* Meadows on Calcareous, Peaty or Clayey-silt-laden Soils (*Molinion caeruleae*)

Semi-natural *Molinia* meadows that occur in the area of investigation stem from extensive, late (one-time) mowing per year. This subtype of the plain

level (see fig. 5.12, middle) is defined by the dominance of *Molinia caerulea* and the occurrence of characteristic species like *Allium suaveolens*, *Betonica officinalis*, *Carex panicea*, *Colchicum autumnale*, *Crepis paludosa*, *Galium boreale*, *Galium uliginosum*, *Gentiana pneumonanthe*, *Iris sibirica*, *Luzula multiflora*, *Sanguisorba officinalis*, *Serratula tinctoria ssp. tinctoria* and *Succisa pratense*. Plots that have been applied to this habitat type contain up to 34 species. Analogue to the phytosociological classification, relevés that have been assigned to the *Molinietum caeruleae* are classified as habitat type 6410.

Concerning the data set 2005, relevés of the *Molinietum* are intertwined with plots of the *Primulo-Schoenetum ferruginei* due to combined mowing regimes. In this case, relevés of the *Molinietum caeruleae* can be assigned to the habitat type 7230 (alkaline fens), as it is proposed by Lang and Walentowski (2007, 78).

Formations on mineralised bog peats as well as on areas where mowing management stopped are species-poor and lack of characteristic taxa. They are, therefore, excluded from this habitat type (European Commission DG Environment, 2003, 76). They will be defined within the context of non-FFH-relevant types.

6430 - Hydrophilous Tall Herb Fringe Communities of Plains and of the Montane to Alpine Levels

Ssymank et al. (2003) describe this type as wet tall herb and grass community on eutrophic locations along edges of rivulets and forests. Its need of nutrient is expressed by the tall shapes of the taxa. Periodical to episodic inundations naturally fertilise these habitats that comprise both eutrophic zones with species of the *Filipendulion ulmariae* Segal 66 and the very eutrophic zones with species of the orders *Convolvuletalia sepium* Tx. 50 und *Glechometalia heraceae* Tx. in Tx. et Brun-Hool 75. These communities grow on gley and fen soils between the mean water line and the mean high water line, i.e. they follow right above the zone of the *Phragmitetalia* communities (Oberdorfer, 1977b, 137,157,361). Important species of this habitat type are *Angelica sylvestris*, *Chaerophyllum hirsutum ssp. hirsutum*, *Cirsium oleraceum*, *Eupatorium cannabinum*, *Lysimachia vulgaris*, *Symphytum officinale* and *Valeriana officinalis agg.*. Also taxa of the alpine subtype of this habitat can be found in the vegetation data, e.g. *Aconitum napellus* and *Aconitum variegatum*. Mixed stands with *Phragmites communis agg.* and with species of the *Magnocaricion* are only of common interest, if tall herbs dominate (Lang and Walentowski, 2007, 82). Transition to lowland hay meadows (habitat type 6510) can be found in some relevés.

6510 - Hay Meadows of the Planar Level/ 6520 - Mountain Hay Meadows

These extensive grasslands are species-rich and usually mown once a year. Associations of the *Arrhenatherion* and of the *Brachypodio-Centaureion nemoralis* are assigned to this type. The European Commission DG Environment (2003, 72f) define mountain hay meadows to be situated above 600 m a.s.l. As the area of investigation lies curly above, typical species of both planar and mountain type occur, i.e. *Pimpinella major ssp. major*, *Centaurea jacea*, *Lathyrus pratensis*, *Ranunculus acris* and *Vicia cracca*. Therefore, the concerned plots are combined to one habitat type that mostly corresponds to the phytosociological alliance of the *Arrhenatherion*, and to the tall forbs-Association of the sociation concept categorisation.

7110 - Active Raised Bogs

This habitat type comprises natural and semi-natural bog complexes of hollows and hummocks, scours and pools, with mainly ombrotrophic water and nutrient input. High precipitation allows for the growth of the habitats that are confined by the margin lag with *Pinus* or *Picea* stands. They are located on bog peats that have accumulated since the end of the Würm-ice age (see section 3). Their water table lies above the surrounding ground water level (Ssymank et al., 1998, 276ff). The term "active" refers to center zones where active peat formation occurs. Species of the *Sphagnetalia magellanici*, *Scheuchzerietalia palustris*, *Utricularietalia intermedio-minoris* and of the *Caricetalia fuscae* characterise this habitat type, like *Andromeda polifolia*, *Calluna vulgaris*, *Carex nigra*, *Drosera ssp.*(see fig. 5.13, left), *Eriophorum vaginatum*, *Lycopodiella inundata*, *Rhynchospora alba*, *Rhynchospora fusca*, *Trichophorum cespitosum*, *Utricularia ochroleuca*, *Vaccinium oxycoccos agg.*, *Vaccinium uliginosum* as well as the moss species *Aulacomnium palustre*, *Odontoschisma sphagni*, *Polytrichum strictum* and *Sphagnum* species, e.g. *Sphagnum angustifolium*, *Sphagnum cuspidatum*, *Sphagnum fuscum*, *Sphagnum magellanicum* and *Sphagnum rubellum*. Deeper insights are given by Malmer (1956); Tüxen et al. (1972), and Schouten (1984).

7120 - Degraded Raised Bogs Still Capable of Natural Regeneration

Degradation of raised bogs is usually anthropogenic and occurs when the natural hydrology has been disturbed, e.g. by peat cutting and drainages. The desiccation of the surfaces leads to peat mineralisation. To include areas into this habitat types, a re-establishment of the former water balance shall permit the regeneration within 30 years.

Characteristic species of the habitat type 7110 dominate, but the occurrence of plants like *Betula pubescens*, *Molinia caerulea*, *Potentilla erecta*, *Frangula alnus*, *Pinus sylvestris*, *Salix repens* agg., mosses like *Leucobryum glaucum*, *Pleurozium schreberi* as well as high cover values of *Calluna vulgaris*, *Vaccinium myrtillus* and *Vaccinium vitis-idaea* indicate bog degradation. As in case of this habitat type the surroundings of the plots play an important role, plot assignment includes the knowledge about intact center zones of the bogs as well as about conservation efforts.

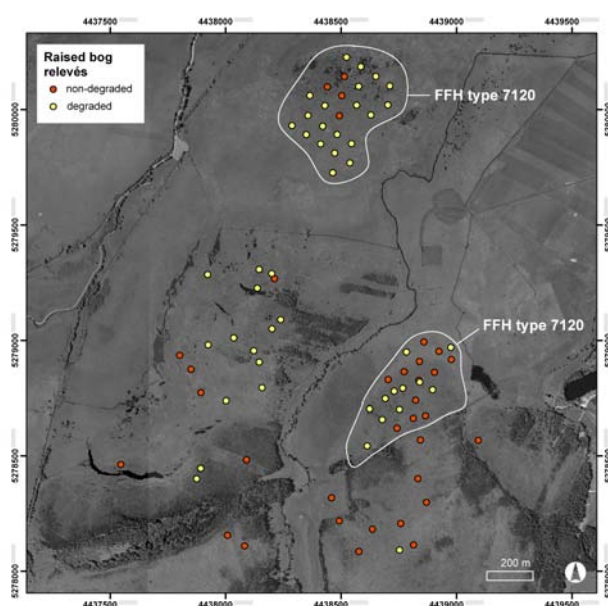


Figure 5.15: Raised bog relevés of the data sets 2004 and 2005. Two bog areas were assigned to the degraded raised bog FFH type 7120. Source of orthophoto: Bavarian Survey Department (LVG)

Apart from some relevés of the data of 2005, all plots show more or less stronger signs of degradation. On the one hand, *Calluna vulgaris* covers more than 70 % of many relevés, on the other hand, *Molinia caerulea* occurs forming main structures of the very plots. Other degradation indicators occur, like *Frangula alnus*, *Betula pubescens* and *Pleurozium schreberi*. Mapped in the context of all bog relevés, the strongly degraded regions can be identified (see fig. 5.15).

7150 - Depressions on Peat Substrates of the *Rhynchosporion*

This habitat type occurs on humid exposed peat, caused naturally seep- or frost-eroded, or anthropogenically by peat cutting, or induced by trampling

erosion and is characterised by species of the pioneer community *Rhynchosporion*. It appears at very small scales, i.e. often below one m^2 . Very similar to bog hollows and transition mires, characteristic plant species are *Drosera rotundifolia*, *Lycopodiella inundata*, *Rhynchospora alba* (see fig. 5.16, left) and *Rhynchospora fusca* (see fig. 5.16, middle). Often intertwined with bogs (see fig. 5.16, right), plots that show the characteristic features of this habitat type have been applied to a community complex of the bog habitat types 7120/7150 following the mapping proposition of Lang and Walentowski (2007, 96). This type corresponds to the phytosociological complex of the *Sphagnetum magellanici* with the *Rhynchosporion* and mainly occurs, as a stand-alone type, in the data set 2004 north. The single plot, and therefore small extent, of the habitat type 7150 of the data set 2005 has been assigned to the habitat type 7110.



Figure 5.16: Depressions on peat substrates are e.g. characterised by the occurrence of *Rhynchospora alba* (left), and *Rhynchospora fusca* (middle), and are often intertwined with bogs (right) (source of photos: C. Weiß, P. Zimmermann, P. Zimmermann)

7210 - Calcareous Fens with *Cladium mariscus* and Species of the *Caricion davallianae*

Along terrestrialisation zones of lakes, reeds that are influenced by calcareous, but nutrient-poorer waters form this habitat type. Apart from the dominance of *Cladium mariscus* with covers of at least 25 % (Lang and Walentowski, 2007, 97), other species of the *Phragmition* like *Phragmites communis*, species of large sedge beds like *Carex elata*, *Peucedanum palustre* and species of calcareous fens like *Carex davalliana*, *Carex flava* agg., *Carex panicea*, *Schoenus ferrugineus*, *Schoenus nigricans* characterise this habitat. In the area of investigation, this habitat type occurs, weakly defined though,

on succession stages of former extensive fen meadows. Therefore, high covers of *Molinia caerulea* can be found in plots that are applied to this habitat type. Habitat assignment corresponds to the *Cladium mariscus-Molinia caerulea*-Subconsociation as well as to the phytosociological categorisation, but one plot of the data set 2004 north has to be excluded as *Cladium mariscus* covers less than 25 %.

7230 - Alkaline Fens

Ssymank et al. (1998) define this habitat type as permanently waterlogged communities of small sedges and brown moss. Calcareous water supply allows for a rich development of calciphile taxa of the *Caricion davallianae* like *Carex davalliana*, *Carex flava*, *Carex lepidocarpa*, *Carex panicea*, *Dactylorhiza incarnata*, *Eleocharis quinqueflora*, *Equisetum palustre*, *Equisetum variegatum*, *Epipactis palustris* (see fig. 5.17), right), *Eriophorum latifolium*, *Juncus subnodulosus*, *Liparis loeselii*, *Mentha aquatica*, *Pinguicula vulgaris*, (see fig. 5.17), *Primula farinosa*, *Tofieldia calyculata*, *Schoenus nigricans*, *S. ferrugineus* (see fig. 5.17, left) and the brown moss species *Bryum pseudotriquetrum*, *Campylium stellatum*, *Drepanocladus revolvens*, *Fissidens adianthoides*, *Philonotis calcarea*, *Scorpidium scorpioides* and *Sphagnum teres*.

Alkaline fens include many specialised and strictly restricted species, e.g. *Dactylorhiza incarnata* and *Schoenus nigricans*. Relevé assignment corresponds to the phytosociological association *Primulo-Schoenetum ferruginei*. As mentioned before, due to combined mowing regime, plots of the *Molinietum caeruleae* can be assigned to this type as well (Lang and Walentowski, 2007, 78). This is practicable concerning the data set 2005, where both types occur.



Figure 5.17: Alkaline fens in the Murnauer Moos are e.g. characterised by the occurrence of *Schoenus ferrugineus* (left), *Pinguicula vulgaris* (middle), and *Epipactis palustris* (right) (source of photos: F. Kestler, C. Weiß, P. Zimmermann)

91D3 - Bog Woodland, Mountain Pine Bog Woods

This habitat type on nutrient poor raised bogs is characterised by a combination of water balance and extremely acidic, nutrient-poor peat soil (Ssymank et al., 1998, 355). It mostly defines the margin lag. More information can be taken from Dierßen and Dierßen (1982). In the area of investigation, it also covers large areas of the bog plateaus. Relevés can be assigned to this type if bog character species like *Vaccinium oxycoccus*, *Andromeda polifolia*, *Eriophorum vaginatum* and *Sphagnum* species occur with covers of at least 10 % and if non-bog species cover maximal 10 %. Degradation indicators like high cover values of *Calluna vulgaris* and *Molinia caerulea* can occur if above mentioned criteria are met.

Pinus mugo is assessed as poorly performing in competition, and geographically as well locally restricted. It is displaced to bog habitats where wood species can barely survive if water supply allows for. Therefore, Lang and Walentowski (2007, 145) propose habitat assignment, if *Pinus mugo* covers at least 10 %. This means that more relevés are assigned to this habitat type than those that have been categorised to the phytosociological association of the *Pino mugo-Sphagnetum magellanici*.

Non FFH-relevant Vegetation Structures

Relevé data that could not be assigned to the FFH categories are dominated by *Molinia caerulea*, *Phragmites communis* or *Carex elata*. According to Stellmach and Langensiepen (2006, 62), abandoned fen meadows can be assigned to the biotope type GP00BK (secondarily developed *Molinia caerulea*

meadows). Also *Molinia-Stadia* on desiccated bogs were assigned to this vegetation type. The *Phragmitetum communis* was assigned to the biotope type GR (Reeds) and the *Caricetum elatae* corresponded to the biotope type VC00BK (Large sedge formations of siltation zones). As they absolutely corresponded to the phytosociological vegetation types of the *Molinia caerulea-Stadia* on abandoned fen meadows or desiccated bogs, of the *Phragmitetum communis* and of the *Caricetum elatae*, untitled types assignment could be overtaken (see section 5.2.1).

5.2.4 Mapping Classifications: Image Classification Results

Table 5.6 gives an overview how well the above explained classification keys performed with different image classification algorithms, and reference spectra determination methods respectively. At large, for all data sets, the heterogeneous composition of the different vegetation types could be best differentiated by the SAM ISD (see 4.4.2) method. Best κ and overall accuracy % values could be yielded for any vegetation scheme of the smallest and most discrete data set 2004 south. The relevés of the vegetation period 2004 responded best to the sociation classification scheme, whereas the data of 2005 performed nearly equally with all vegetation categorisations. For all data subsets, the different classification keys will be closer examined in the following.

method		north 2004			south 2004			2005		
		PHY	SOC	FFH	PHY	SOC	FFH	PHY	SOC	FFH
# of veg.		7	6	6	5	4	4	10	8	9
types										
SAM	κ	0.39	0.54	0.40	0.55	0.66	0.64	0.43	0.32	0.51
MSD	%	49	63	50	65	75	75	53	43	62
SAM	κ	0.53	0.61	0.53	0.83	0.93	0.89	0.51	0.53	0.54
ISD	%	66	69	65	88	95	93	61	66	65
SAM	κ	0.32	0.52	0.31	0.60	0.92	0.68	0.34	0.45	0.47
BRSD	%	45	63	46	69	94	78	42	56	60
MESMA	κ	0.23	0.28	0.22	0.41	0.40	0.43	0.18	0.21	0.29
BRSD	%	29	37	28	49	50	56	24	31	40

Table 5.6: Image classification results for all vegetation classification keys and reference spectra determination methods used.

In general, wrong image classifications took place in structures where similar plant species composition hindered a vegetation classification as well. Strong overlapping occurred mainly in *Molinia caerulea*-dominated vegetation types. Also, bog types showed interferences with contiguous types, due to high *Calluna* and *Sphagnum* coverages. In the complementary analysis section 5.3.1, these interferences are visualised in fig. 5.27, 5.28, and 5.29.

Figs. 5.18 show SAM ISD image classification outputs of the subarea 2004 north. Large homogeneous areas can be made out, mainly the *Phragmites communis* dominated types PC (PHY-), Ph (SOC-), and GR (FFH-vegetation classification), the bog type CS (SOC) or the active raised bog at the southern part of this subarea (FFH type 7110, see fig. 5.15), and the raised bog complex SR (PHY) and 7150 (FFH). The large area of vegetation types with *Molinia caerulea* dominance in the middle parts of the subarea north show Salt-and-Pepper-Effects that indicate transition zones between the types. In the raised bog in the northern part of this subarea (FFH type 7120), degradation is displayed by the spread of *Molinia*.

Figs. 5.19 show SAM ISD image classification maps of the subarea 2004 south. Large homogeneous areas can be seen, sharp edges indicate discrete boundaries (e.g. mowing edges in the case of the *Carex elata*-dominated parts. Transition zones, indicated by Salt-and-Pepper-Effects, only occur between the phytosociological vegetation types *Eriophoro-Trichophoretum cespitosi* and the *Sphagnetum magellanicum*. As the sampling did not include fen relevés, these areas in the south of the *Carex elata*-dominated parts were wrongly image classified as bog habitats. The classification of the subarea 2005 (fig. 5.20) gives evidence of the fact that if the spectral library contains both reference spectra of bogs and fens, correct assignment is possible.

Figs. 5.20 map image classification outputs derived with SAM ISD method of the subarea 2005. Homogeneous areas, e.g. the *Carex elata*-dominated area, alternate with transition zones, e.g. *Molinia* dominated areas of the fen meadows and *Stadia*, indicated by Salt-and-Pepper-Effects.

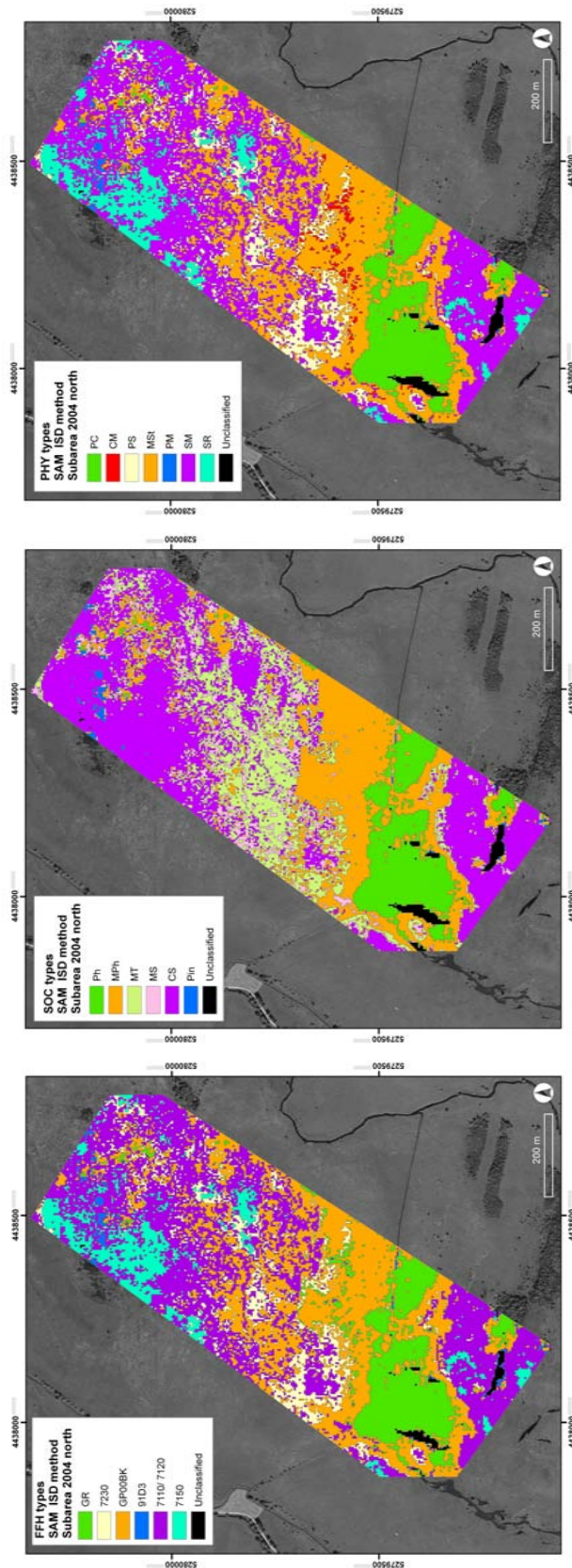


Figure 5.18: Vegetation type polygons of the subarea 2004 north derived from SAM ISD image classification.(top) PHY, (middle) SOC, (bottom) FFH

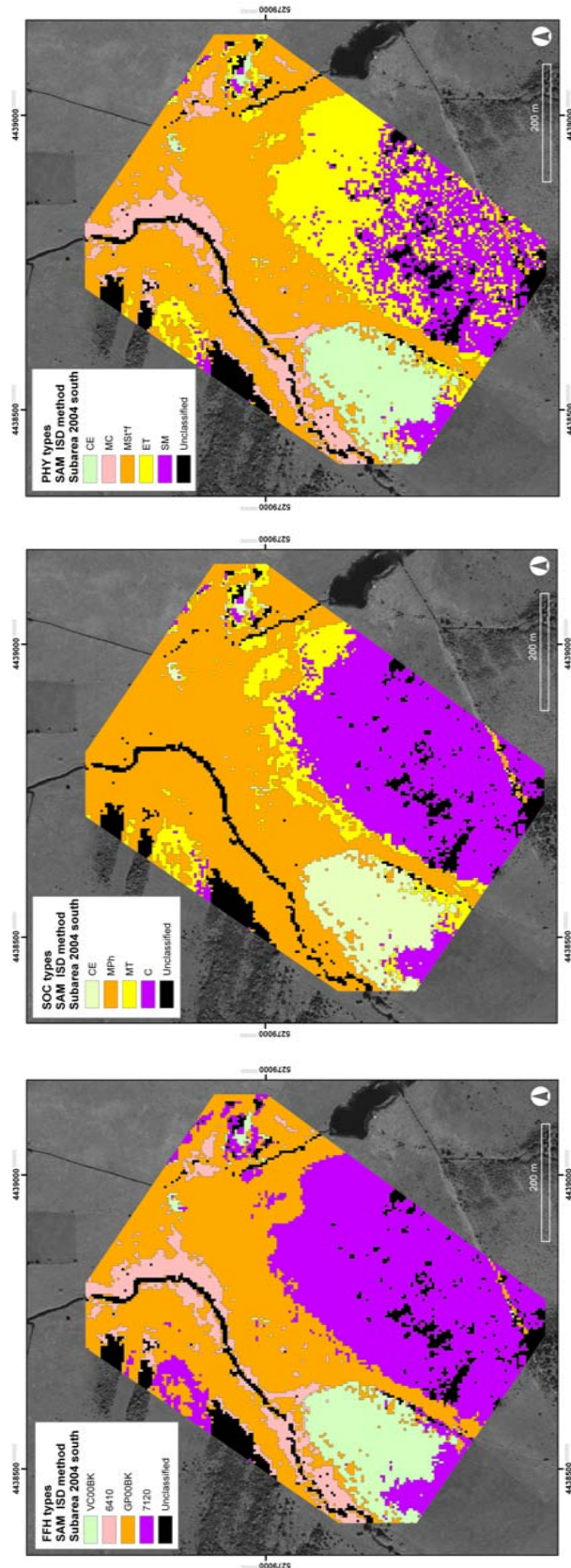


Figure 5.19: Vegetation type polygons of the subarea 2004 south derived from SAM ISD image classification. (top) PHY, (middle) SOC, (bottom) FFH

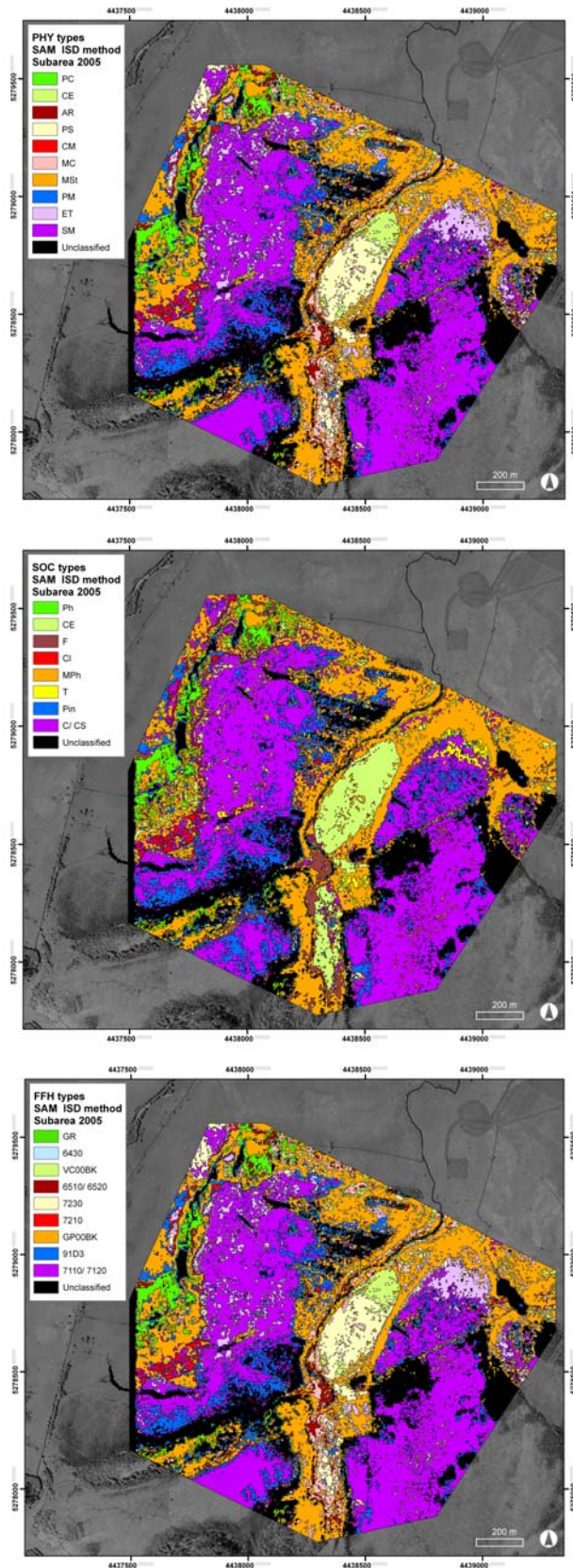


Figure 5.20: Vegetation type polygons of the subarea 2005 derived from SAM ISD image classification. (top) PHY, (middle) SOC, (bottom) FFH

Image Classification: Mapping Phytosociological Vegetation Types

The phytosociological vegetation types could be detected with κ of 51 to 83, and with an overall accuracy of 61 to 88 % for all three data sets by the SAM ISD method. The diagram in fig. 5.21 gives an overview about methods performance per data set and vegetation type. Homogeneous types like the *Rhynchosporion* complex of the data set 2004 north, and the *Caricetum elatae* of the data set 2005, showed best results when classified by an averaged reference spectrum per type (MSD). Other homogeneous types like the *Phragmitetum communis* of the data set 2004 north were best described when classified by methods that use one spectrum per vegetation type (MSD, BRSD). This was as well the case in weakly defined vegetation types like the *Primulo-Schoenetum ferruginei* of the data set 2004 north, the *Arrhenatherion*, and the *Molinietum caeruleae* of the data set 2005. The weakly characterised *Eriophoro-Trichophoretum cespitosi* of the data set 2005 could be best detected by BRSD method. Vegetation types with heterogeneous species composition like the *Molinia*-Stadia, and the *Sphagnetum magellanici* of all data sets could be best classified using the ISD method of reference spectra determination. As this was the case in most of the phytosociological categories, ISD yielded best κ and overall accuracy results.

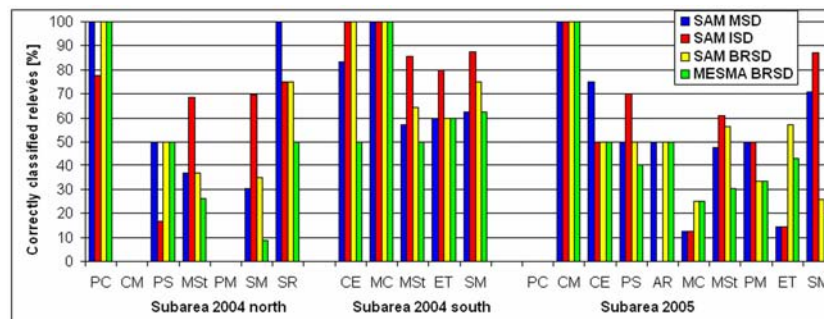


Figure 5.21: Results of image classification: phytosociological vegetation types (table of vegetation type names can be found in fig. 5.22).

The diagrams in figs. 5.22 are normalised and coloured confusion matrices. Vegetation type assignment is visualised in detail for the SAM ISD method, and it is shown which types interfered with each other. A spectral differentiation between the two different *Molinia*-Stadia could not be made, as the dominance of *Molinia caerulea* overgrows relicts of bog or fen meadow structures. Interferences between other *Molinia* rich types happened with wrong assignments of more than 40 % in the data set 2005. Types of bog

habitats were wrongly assigned to each other with more than 20 %.

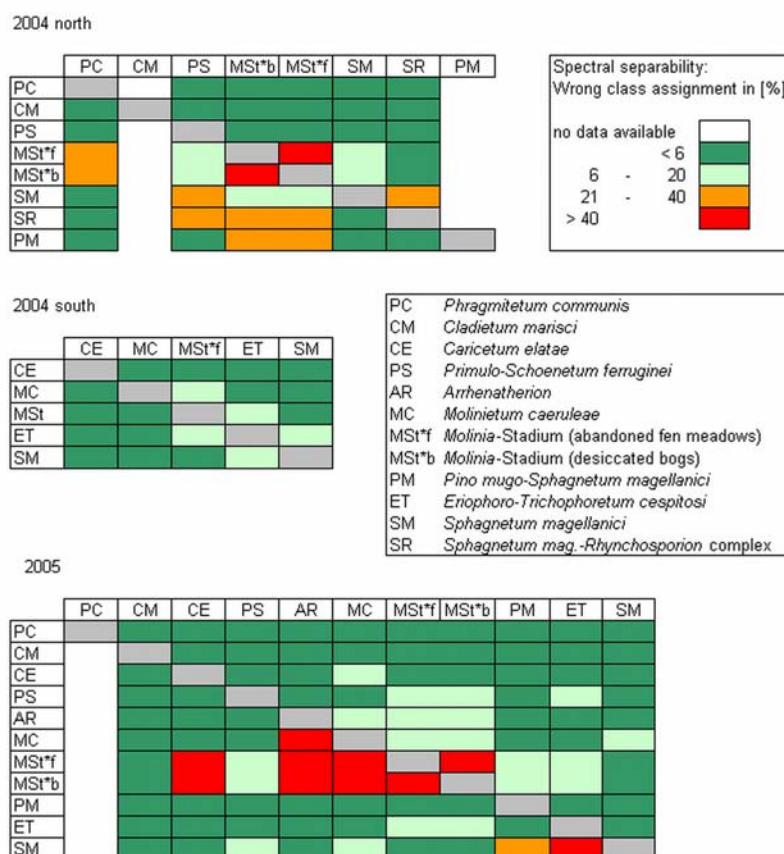


Figure 5.22: Spectral differentiability between phytosociological vegetation types in [%], gained with SAM ISD method.

Image Classification: Mapping Sociation Vegetation Types

Dominance aspects could be classified with validation results of κ of 0.53 to 0.93 and overall accuracy of 66 to 95 % for all three data sets by the SAM ISD method. Fig. 5.23 gives an overview about vegetation type performance per data set and methods.

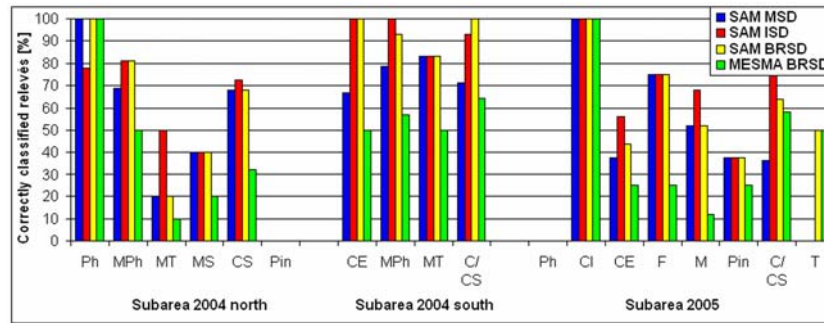


Figure 5.23: Results of image classification: sociation vegetation types (table of class names can be found in fig. 5.24).

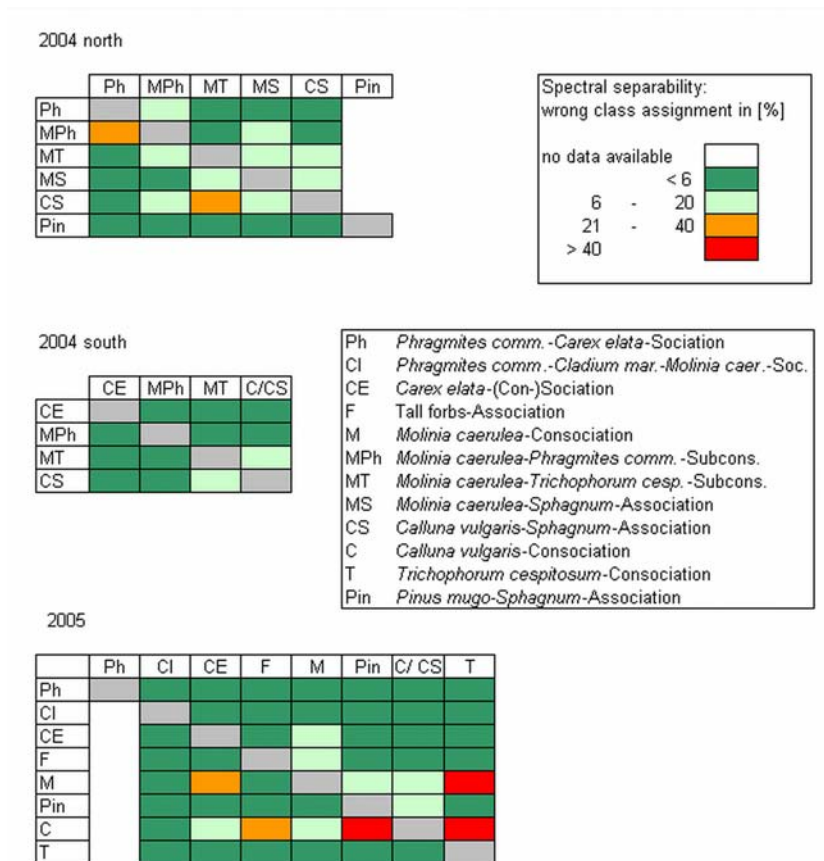


Figure 5.24: Spectral differentiability between sociation vegetation types in [%], gained with SAM ISD method.

According to the phytosociological categories, reference spectra determination methods that use only one spectrum per vegetation type (MSD, BRSD), performed better when classifying homogeneous stands (like the *Phragmites*-sociation of the data set 2004 north. As well BRSD with SAM and MESMA algorithm could separate the two plots of the very heterogeneous *Trichophorum cespitosum*-Consociation of the data set 2005, where dominance of *Trichophorum cespitosum* varied from 45 to 80 % cover. All other types of the three data sets could be best separated using SAM ISD image classification which balanced within-type heterogeneities. This result corresponds to the phytosociological image classification.

Diagrams 5.24 are normalised, coloured confusion matrices. Vegetation type assignment is visualised in detail for the SAM ISD method, and it is shown which types interfered with each other. Above mentioned problems occurred concerning differentiating *Molinia* rich types with *Phragmites* types (data set 2004 north) and *Carex elata* stands (data set 2005) with wrong assignments below 40 %. Types of bog habitats were wrongly assigned with more than 40 %. At large, the diagrams show only little overlapping between the vegetation types of the sociation classification.

Image Classification: Mapping Fauna-Flora-Habitats

The classification of Fauna-Flora-Habitats could be done with validation results of κ of 0.53 to 0.89 and overall accuracy of 65 to 93 % for all three data sets.

Diagram 5.25 gives an overview about habitat performance per data set and methods. The heterogeneity of most types was best described with SAM ISD image classification. According to the phytosociological and sociation categories, MSD and BRSD methods worked better for the classification of homogeneous stands (GR and 7230 of the data set 2004 north, VC00BK of the data set 2005).

Diagrams 5.26 are normalised and coloured confusion matrices. Vegetation type assignment is visualised in detail for the SAM ISD method, and it is shown which types interfered with each other.

Molinia caerulea dominated habitats like 6410, 7230 and GP00BK show overlapping in the range of 6 to 40 %. The raised bog types 7110 and 7120 could not be separated spectrally. The mountain pine bog woods 91D3 were mostly assigned to the raised bog types.

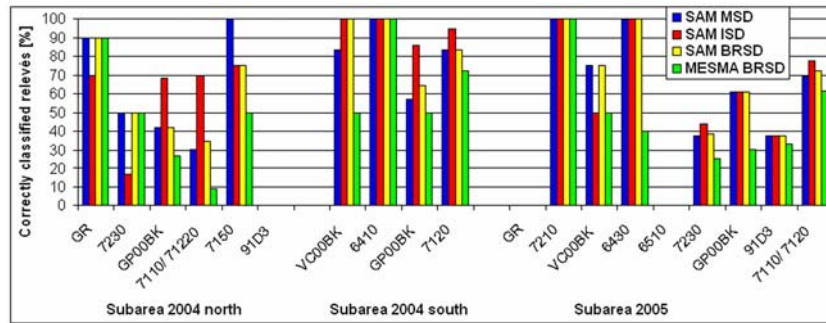


Figure 5.25: Results of image classification: Fauna-Flora-Habitat types (table of habitat names can be found in fig. 5.26).

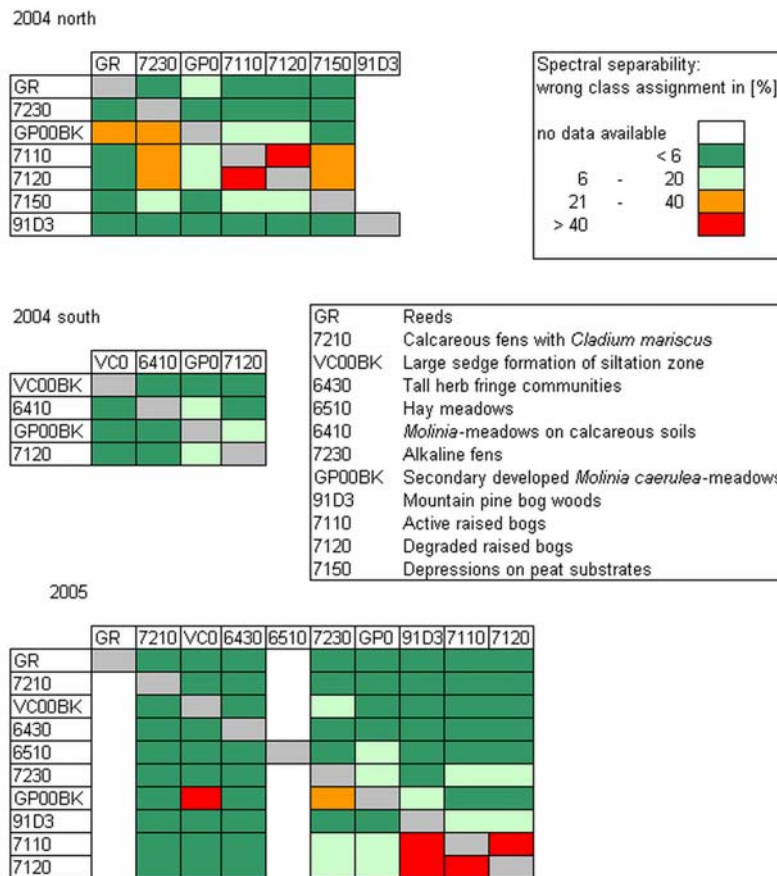


Figure 5.26: Spectral differentiability between Fauna-Flora-Habitat types in [%], gained with SAM ISD method.

5.3 Synthesis

5.3.1 Complementary Analysis: Vegetation Types in Ordination Space

The first step to combine ordination results with classification results can be done on pure vegetation level. The relevés are projected in NMS ordination space and their vegetation type assignment shows how the species dispersion follows the axis gradients.

Figs. 5.27 show the expected arrangement of vegetation types of the data subset 2004 north in feature space: discrete groups of relevés in ordination space could be easily classified in vegetation classification, i.e. mainly the discrete group of *Phragmites communis* dominated relevés on the left side of the scatterplot, i.e. the low scores of the first NMS axis. Highly dispersed relevés were mostly dominated by *Molinia caerulea* (see the middle part of the first axis), or by *Calluna vulgaris* (see the bog relevés of the right part of the first NMS axis).

Best relevé separation could be formed by the classification for dominance aspects (see fig. 5.27 middle). It clearly shows the catena from the stands with *Molinia* and high influence of *Phragmites communis* to stands with *Molinia* and *Trichophorum cespitosum*. It is followed by stands that indicate the desiccated bog margin with *Molinia* and *Sphagnum* species, intertwined with *Calluna vulgaris* dominated plots.

The FFH classification shows the habitat type 7150 as a borderline between the active raised bog 7110, and the degraded bog 7120. Regarding fig. 5.3, it is the border between plots where *Carex elata* occurs (7120), and where it is absent (7110).

Figs. 5.28 give evidence of the fact that the subarea 2004 south has a very discrete habitat structure. Vegetation classification could be easily applied for all vegetation classification keys, and this can be taken from all three complementary analyses. Dispersion of classes is not visible in any of the vegetation classifications, although some types are narrowly located due to similar species composition, e.g. the phytosociological bog communities of the *Sphagnetum magellanicum* and the *Eriophoro-Trichophoretum* at the bottom part of the second NMS axis.

Fig. 5.29 shows the complementary analyses for the data subset 2005. Here, relevés show high dispersion, and show the difficulties of this data set when performing vegetation classifications.

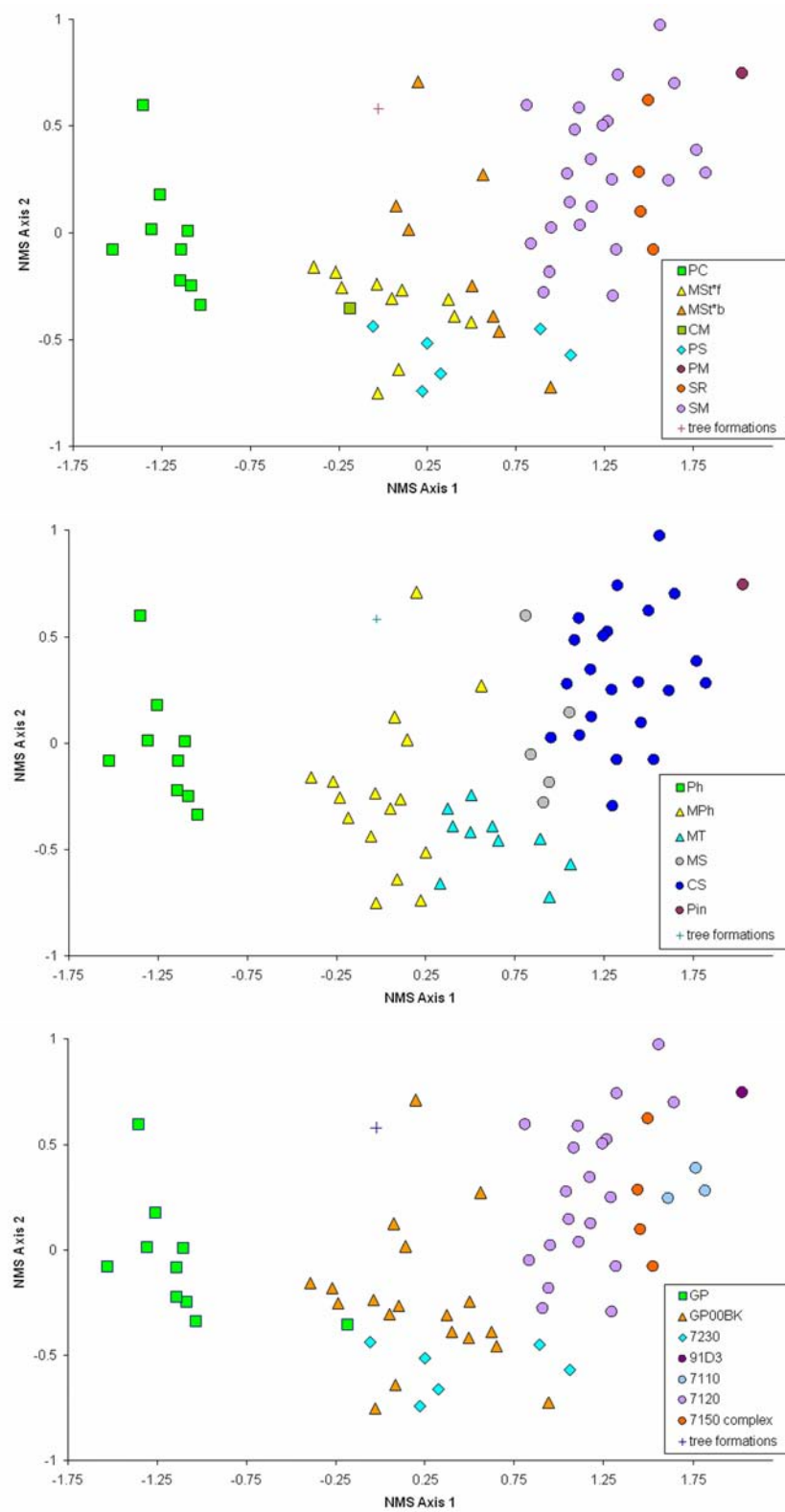


Figure 5.27: Complementary analysis of the subarea 2004 north. PHY (top), SOC (middle), FFH (bottom) vegetation types

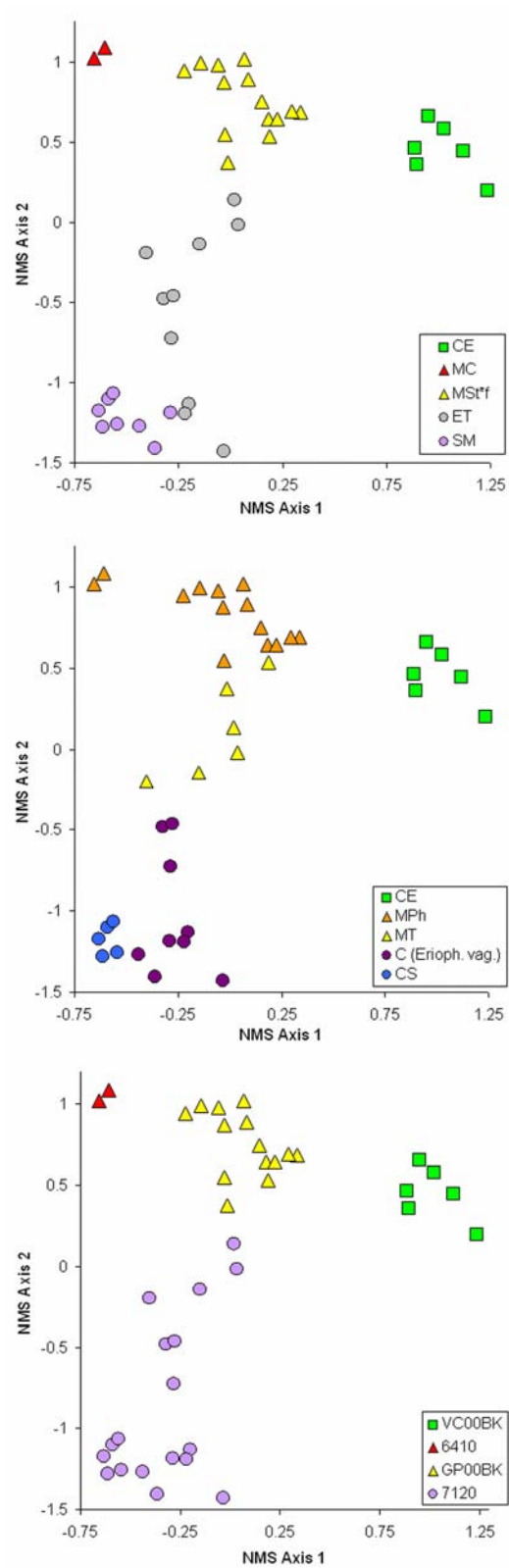


Figure 5.28: Complementary analysis of the subarea 2004 south. PHY (top), SOC (middle), FFH (bottom) vegetation types

The clear separation between bog and non-bog types is best described by the classification for dominance aspects. *Molinia* dominated plots show high dispersion in any of the three applied vegetation classifications: the phytosociological classification shows a well-defined transition along the second axis from top relevés of the *Molinietum caeruleae* to the *Molinia*-Stadium on abandoned fen meadows that disperse with relevés of the *Primulo-Schoenetum ferruginei* to the left side. The *Molinia*-Stadium on desiccated bogs follows the one of abandoned fen meadows and intertwines with relevés of the raised bogs. Relevés of the *Eriophoro-Trichophoretum* are too weakly defined, and do not show type relation to each other. Also, two relevés of the *Molinietum caeruleae* are not included in the group of the other plots due to coverages of *Carex elata* (see fig. 5.8)

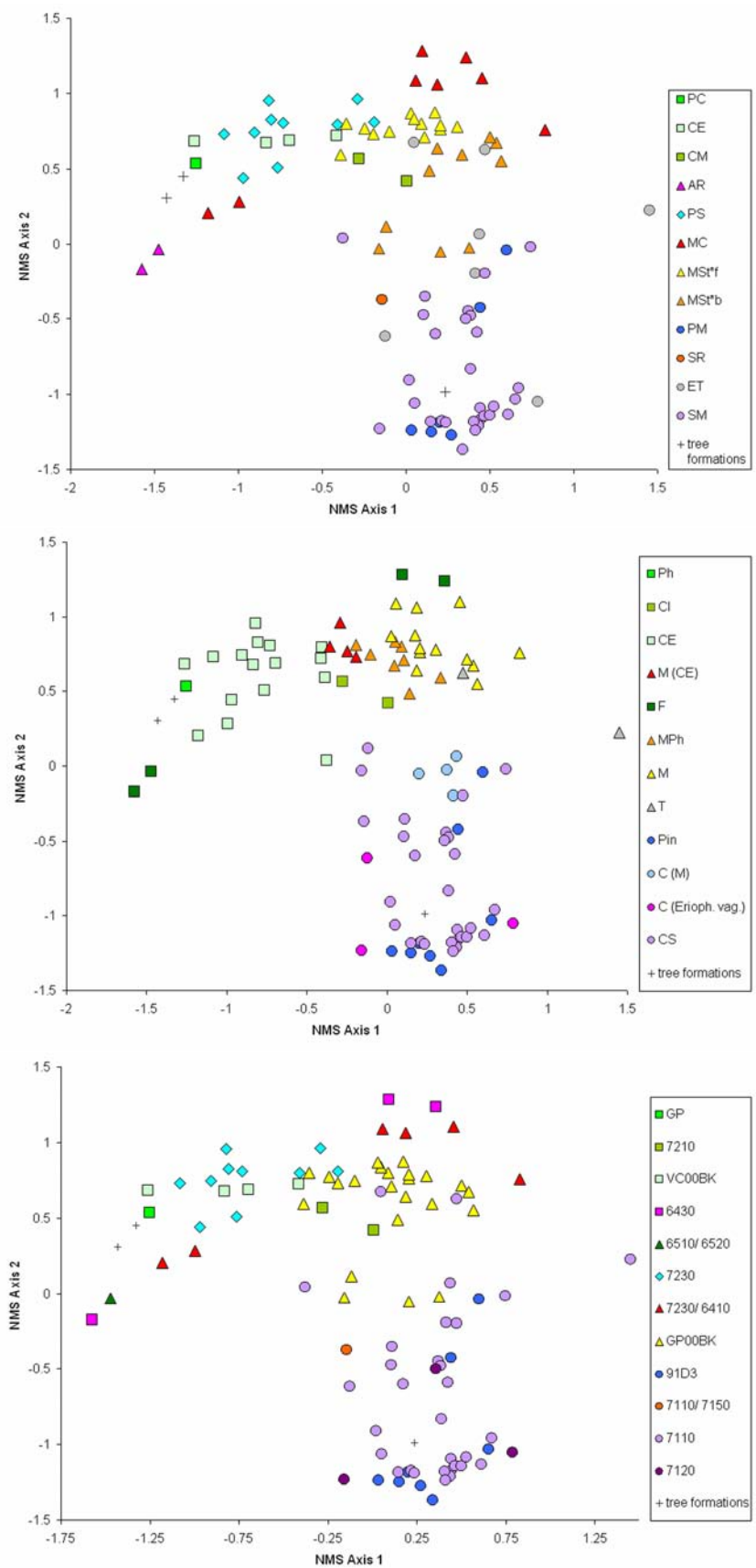


Figure 5.29: Complementary analysis of the subarea 2005. PHY (top), SOC (middle), FFH (bottom) vegetation types

5.3.2 Synthesis Maps: Combining Discrete and Non-discrete Approaches

The resulting Synthesis Maps can be found in Appendix B as folded attachments in the back cover. The two-fold legend gives information on colours derived from PLS regression models of the different data sets. Centroids of the vegetation types help to correlate colours with types. Vegetation type polygons are derived from the best image classification (SAM ISD method). As similar types show similar colours, different hatchures are overlaid that enable the differentiation of each vegetation type.

Figs. 5.30 show a detail Synthesis map of the subarea 2004 north. This detail of a bog margin has been chosen to give an example, how transition zones can be mapped with the developed synthesis approach of discrete and non-discrete techniques. Regarding the colours of the maps, green and dark parts are dominated by vegetation types defined by high coverages of *Molinia caerulea*, red and orange parts are defined by species of the raised bogs. The play of colours mirror the ecotone between the mentioned vegetation types. Vegetation type polygons show dispersion (Salt-and-Pepper-Effects) which indicates transitions as well. Concerning the detail map with phytosociological vegetation type polygons overlaid (fig. 5.30, top), it can be noticed that pixels that have been assigned to the *Molinia*-Stadium and the *Sphagnetum magellanicum* share a wide range of colours, and are highly intertwined with each other. The Synthesis map visualises transitions within both vegetation types, and shows the direction of the transition towards the other.

The detail map fig. 5.30, (middle) shows that sociation polygons correspond best to the shapes hinted by the colour composition of the models. The colour range within vegetation types does not variate as much as within polygons derived from the image classification of a phytosociological vegetation types. Here, transition zones are primarily indicated by pixel dispersion.

Fig. 5.30 (bottom) shows the polygons of FF-habitat types as overlay. The half-transparent vegetation type GP00BK is easily distinguishable from the FFH-relevant types. Within-type variances can still be detected. For deeper investigations, the half-transparency can be switched off by the GIS-software.

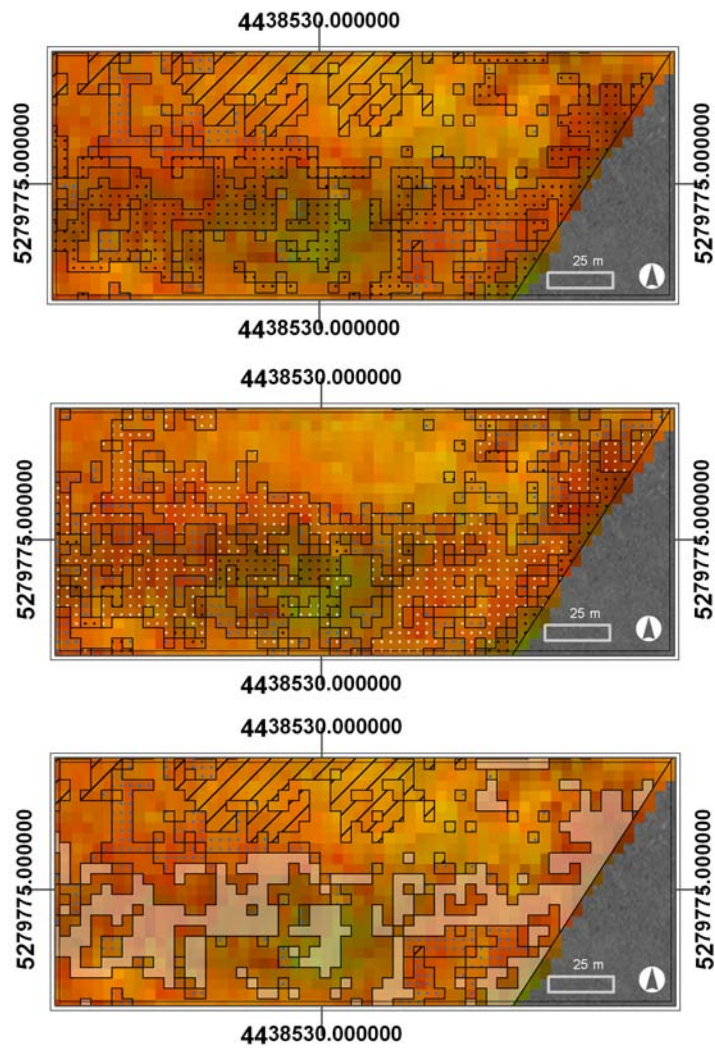


Figure 5.30: Detail Synthesis maps of the subarea 2004 north. PHY (top), SOC (middle), FFH (bottom) vegetation types. Appendant legends can be found in the Appendix maps B

Chapter 6

Discussion and Outlook

With a combination of discrete and non-discrete approaches, natural and semi-natural vegetation has been mapped on a stand level. This chapter will regard data collection as well as evaluation to line out advantages of the applied methods, and their problems. Then, results will be discussed, with certain emphasis to the utilisation of the mapping method in nature conservancy.

6.1 Data Collection

Image data derived from airborne imaging spectroscopy (see section 4.1) bear advantages for the differentiation of natural vegetation due to a high spatial as well as spectral resolution (Ustin et al., 2004). To differentiate radiance values on a band level with nanometer distances gives best basic requirements for both regression modelling and image classification, because fine differences between different vegetation types can be detected. Certainly, the usage of multitemporal image data could yield further improvements (Townsend and Walsh, 2001; Schmidtlein et al., 2007). This would embrace phenological changes as well as balance different conditions of the vegetation due to drought (Carter, 1993) or rainy periods, i.e. water content of the *Sphagnum* species.

The spatial resolution of the geocorrected imagery is $4 \times 4 \text{ m}^2$. This means that each pixel is a mixture of floristic composition, i.e. it represents the radiance on a stand level if homogeneous, or it represents the radiance values of mixed stands, if heterogeneous. To prevent the representation of very heterogeneous vegetation by one single spectrum, the elaborate wholeplot design of the relevés 2004 was used for the method development of this project. Furthermore, it was applied to outbalance errors of geocorrection.

Image data were taken end of July 2003 whereas field data for method development were taken during the vegetation period 2004. All reference spectra were taken from the scene itself. Therefore, it was possible to temporally part image data acquisition and sampling, assuming that the vegetation did not change inbetween. In this respect, the interval of one year can be seen as negligible as the investigated habitats, especially the bog structures, are slowly changing structures. The results seem to confirm this supposition.

Phenological changes during relevés collection (June to July 2004) happened. Especially *Phragmites communis* covers increased. This was balanced by an extra cover estimation of *Phragmites* within three days in August 2004 to make the whole data set comparable.

Generally speaking, a pre-stratification by an unsupervised ISODATA image classification is a helpful tool. Coarse structures can be made out with small expenditure of time.

In respect to the data collection 2005, the previous stratification of the scene data by ISODATA, and the number of relevés in dependency on the variance of each stratum, advantaged the likelihood that all occurring habitats were sampled to some number. Figures 6.1 visualise, how the eight ISODATA categories corresponded to the three applied vegetation classifications. It becomes visible though that vegetation types that cover large areas, like bogs and *Molinia*-dominated vegetation types, were well correlated to most of the ISODATA strata. Other, lesser represented types of the area, were distributed on few strata with higher variance (see table 4.3).

For future investigations, it can be proposed to raise the number of samples of strata with high variances even more to ensure that each type is sampled sufficiently. Also, some categories were underrepresented by the relevés data in strata with low variance. This happened in particular in habitat types with high cover values of *Phragmites communis*. Here, dominant reed overgrew the existing variance, which could not be detected on a coarse ISODATA classification level.

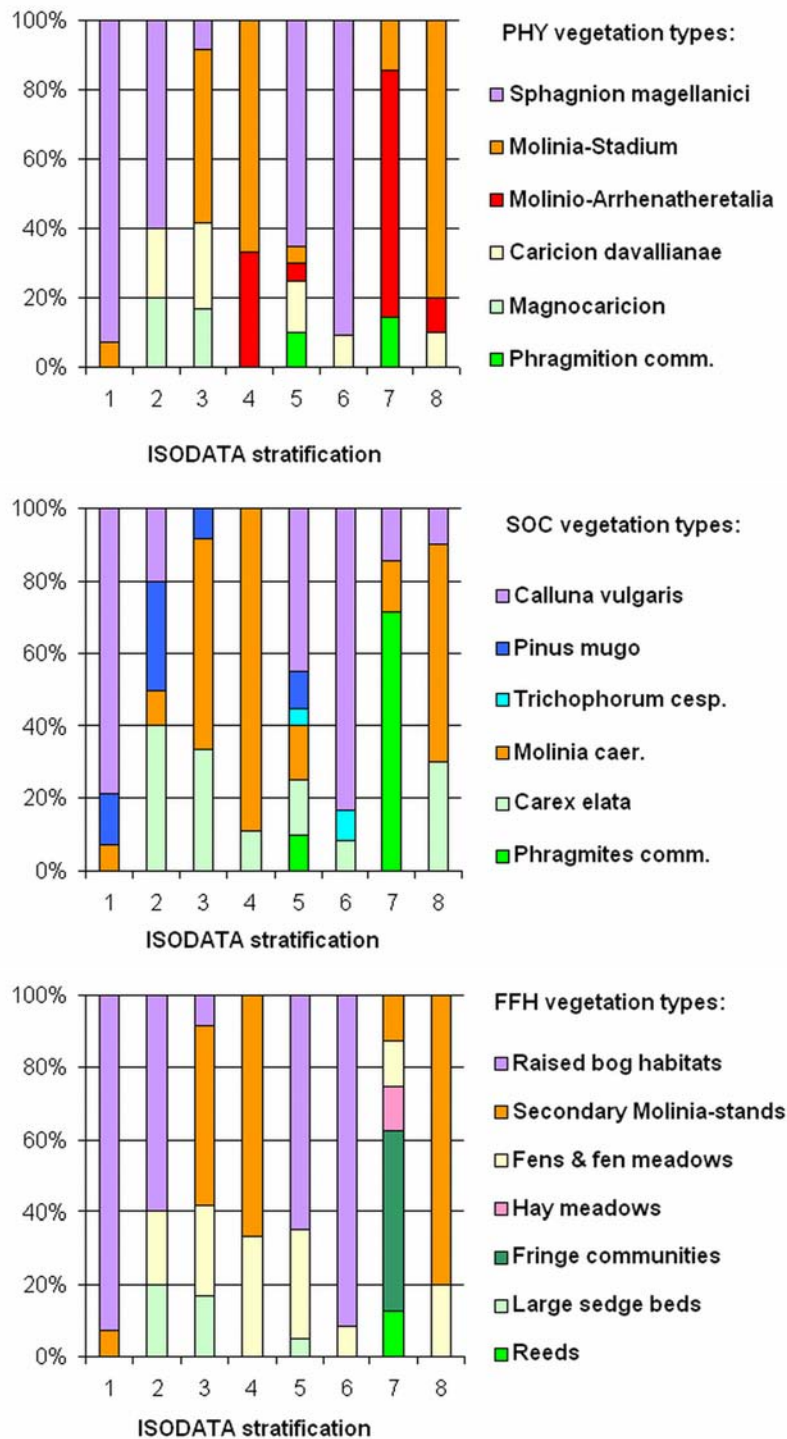


Figure 6.1: Fractions of phytosociological (PHY, top), Sociation- (SOC, middle) and FFH-vegetation types (bottom) within the predefined ISODATA strata of the sampling design 2005

6.2 Ordination and its Mapping

NMS Ordination

The used ordination method NMS (see section 4.3.1) bears two important advantages in respect of this project: on the one hand, it mirrors real structures. Other possible ordination methods, e.g. eigenvector methods like the DCA (Detrended Correspondence Analysis, Hill and Gauch 1980), lose some variance explanation to a first determination of gradients in the data set. Although this enables a better axis interpretation, i.e. the parallelisation with environmental gradients (Glavac, 1996, 159), it does not enhance the resulting maps.

Map interpretation is based on overlaid classification polygons and colour composition in the end, i.e. the distances in colour space. Therefore, distances should represent true variances as best as possible which is done by NMS ordination. In DCA, distances in ordination space are not interpretable in terms of similarity. It shows compression of real distances between data points on the second axis. If axis interpretation plays a more important role in some application, it can be considered to execute a rotation of the NMS data space by Principal Component analysis (PCA, Greig-Smith 1983).

After PCA rotation (proposed by Clarke 1993), although relative positions of relevés are not affected, the main floristic variation is displayed by the first axis (Legendre and Legendre 1998, 391ff and McCune and Mefford 1999, 132ff). A second important feature of the NMS is the possibility to choose the number of dimensions. Certainly, a three dimensional solution would represent more variance of the data set and has been applied before (Zimmermann, 2005; Schmidtlein et al., 2007). However, the main aspect of developing a mapping method for conservancy purposes can be best fulfilled by a two-dimensional NMS solution. Easy and fast map interpretation with a two-dimensional legend is of main focus here.

Problems arise if the stress value for a two-dimensional solution exceeds the well-established limit of 20 (Clarke, 1993). In these cases, two possibilities are thinkable: if the data set features well-defined strata, we propose to divide into subdata sets with each individual NMS calculations. Or, ordination methods that are able to deal with non-linearities and high variances can be used, like Isomap (Isometric feature mapping, introduced by Tenenbaum 1998, and Tenenbaum et al. 2000, and e.g. applied by Mahecha and Schmidtlein 2008) or SOMs (Self-Organising Maps, a neural network algorithm introduced by Kohonen 2001). Here lies potential for further studies to investigate the applicability of the mentioned algorithms in conservation monitoring.

PLS Regression Models

The ordination axis values were regressed against scene spectra of the relevé pixels by PLS regression method (see section 4.3.3). The resulting regression equations could be applied to the full scene. The resulting borderless maps (see fig. 5.9) show as much variance of the sampled vegetation as possible to be displayed by two dimensions. Homogeneous habitats as well as mixed stands and transition zones can be made out.

After applying the PLS regression method to three different data sets, following statements can be made: Very good model results, indicated by R^2 , can be yielded with scores of axes that explain much of the data variance, i.e. with long floristic gradients. This can be seen from all data sets 2004 and 2005. Axes with less explanatory power (less than 70 %) cannot be mapped in the same quality.

The data set 2004 south is best described by NMS ordination values in comparison to the data sets 2004 north and 2005, and gives very good (second axis) to good (first axis) model results. This is due to the fact that this data set represents a small area with relatively discrete boundaries. Due to its discrete inventory, reference spectra correspond very well to the underlying vegetation.

The extensive data sets of 2004 north and 2005 represent many different habitats with many transition zones. Still, the northern data set gives good results in the PLS regression. The wholeplot structure of the underlying samples, and therefore a better correlation between vegetation and spectral data seems to be the reason.

The data set 2005 does not perform as good. Here, some reasons are to be considered. First of all, between-type confusion was more likely as this large area contained more vegetation types that had to be separated, e.g. 10 phytosociological categories (data set 2005) versus 6 respectively 5 phytosociological vegetation types (data sets 2004 north and south). Secondly, samples were taken without wholeplot design, which means that only one relevé met an averaged spectrum of four pixels. Also relevé location by GPS console did not happen in the same accuracy as 2004. Due to geocorrection, wrong pixel allocations were possible. Thirdly, two years lay between the scene acquisition and vegetation sampling. This time delay may have caused some structure development amongst growing of *Phragmites communis* and *Molinia caerulea*, the most dominant plant species in the data set.

Validation results have to be seen critical to some point. Ideally, samples would be divided into training and validation data. In this case, the number of relevés was not sufficient. With leave-one-out cross-validation, the spatial dependency of the samples may cause some optimistic error (Labovitz,

1986), as relevés of 2004 are allocated in a dense grid with approx. 80 m distances. Zimmermann (2005) tested the model prediction with thinned out vegetation data of the data set 2004 south. Good model results (80% of the R^2 a full model would yield) could still be reached with half the number of samples (approx. 20 relevés). In respect to the application of the method in conservancy, this means a step in the direction of reducing cost-consuming field work. Further investigations would be of interest in this matter.

Regular PLS regression modelling accounts for linear relationships between variables (Huon de Kermadec et al., 1997), but – following Haaland and Thomas (1988) – it can handle some non-linear relationships as well. Therefore, it is not possible to gain information on the presence and source of linear relationships. True non-linearities cannot be regressed properly with the common PLS method, and lead to unsatisfying results. Then, non-linear PLS regressions can be used, e.g. ASPLS (Additive Splines for PLS Durand and Sabatier 1994). In case of this study, satisfying PLS modelling results were obtained with small numbers of principal components of the spectrometer bands in relation to the number of input samples. This indicated linear relationships, and therefore, the regular PLS method could be used.

6.3 Classification and its Mapping

Three common vegetation classification schemes have been applied to the same data sets for comparison reasons (see section 5.2). The phytosociological classification put the resulting categories into the context of plant communities of Central Europe. Dominance aspects were taken into account by the sociation concept. Fauna-Flora-Habitats within their ecosystems were of main interest regarding the motivation of this project.

All three applied vegetation classification schemes could be used for supervised classifications. The different outputs mirrored different aspects of the structures of the area under investigation. At large, the objective sampling hindered vegetation classification. Mixed stands and transitions were represented by a large number of relevés. This mirrored the real vegetation structure of the sampled part of the area of investigation, but lead to weak reference spectra. If existent, well defined structures could be found in the data sets with systematic samples, as high numbers of relevés were taken.

The data set 2004 south showed discrete formations where each classification scheme could be applied easily. However, a preferential sampling would have ensured that small, but important vegetation units like the stands with *Cladium mariscus*, or fen communities of the *Orchido-Schoenetum nigricantis*, had been represented by more relevés.

Classifying and Mapping Phytosociological Communities

Classifying phytosociological communities on association level means to classify on a high level of detail. It reverts to the system of diagnostic and differential species that have been defined by expert knowledge of vegetation scientists of Central Europe. It allows for complexity, as diagnostic species define the vegetation type but depending on attendants (that e.g. refer to the vegetation type genesis and land-use) manifold subassociations and formations can be differentiated. Therefore, the categorisation by abundances of diagnostic species allows for mixtures of species.

Unfortunately, phytosociological communities often were weakly defined, some relevés had to be classified on alliance level due to lack of association character species (e.g. the alliance *Arrhenatherion*). A subdivision on the level of local differential taxa was not done. More relevés, or a preferential sampling design, would have been necessary. Image classification results indicated that weakly defined communities could not be detected, e.g. relevés assigned to the *Primulo-Schoenetum ferruginei* of the data set 2004 north showed very high cover values of *Molinia caerulea*. In contrast, the very same community could be well classified by the relevés of the data set 2005, where *Schoenus* species dominated or co-dominated with *Molinia caerulea*. Other well characterised associations, e.g. the *Phragmitetum communis*, *Sphagnetum magellanicum*, and relevés of the *Eriophoro-Trichophoretum* showed similar results.

In this regard, good image classification results may as well depend on other attributes like soil signal, water or biomass, which may serve as proxies in the classification procedure. Occurrences of diagnostic species from phytosociology may be closely related to such variables.

Relevés that were problematical in phytosociological classifications showed equal problems in image classifications. As above mentioned, the categorisation by abundances of diagnostic species allows for mixtures of species. Relevés can therefore be well represented by the imagery with a spatial resolution of $4 \times 4 \text{ m}^2$ where the spectral information per pixel is a mixture (of endmembers) as well. Heterogeneity can be outbalanced by using SAM ISD method. This leads to the conclusion that with the given scene data phytosociological vegetation types are appropriate to spectrally differentiate natural vegetation on a stand level, if stands are well defined by diagnostic species. Otherwise, reference spectra are not pure enough to differentiate vegetation types properly.

Classifying and Mapping of Dominance Aspects

Dominance aspects mirror the main visible aspects of the area. Two important advantages can be lined out: First, a classification for dominance aspects can be applied very fast to vegetation data, in contrast to classifying phytosociology or Fauna-Flora-Habitats. For producing a first overview map, this means a simple and very fast way in cases, where time is scarce.

Second, it bears the easy possibility to define transitions and ecotones as own vegetation types. In contrast, Fauna-Flora-Habitat mapping manuals advise to combine habitats, and the transition zones within, to complexes in such cases. Hence, loose of information is the result. Although exceptions have been published (e.g. Schmidtlein 2000), a classical phytosociological classification does not provide for ecotone classification at all.

The vegetation classification by dominance aspects showed that only few taxa dominate in the sampled part of the area of investigation. This means, however, that this concept bears the disadvantage that it does not separate into vegetation types as detail-rich as the other vegetation classification schemes applied in this study that are based on abundances of character species.

Mainly *Molinia caerulea*, steady attendance of *Phragmites communis* and occurrences of *Carex elata*, *Calluna vulgaris*, and *Sphagnum* species define the relevés. Where the data sets show homogeneous dominances, relevé assignment can be done easily. When monitoring the spread of single species with high dominance power, like *Phragmites communis* or *Molinia caerulea*, the dominance classification approach seems most advantageous to be used, and performs with high accuracy in validation with the given imagery.

Classifying and Mapping Fauna-Flora-Habitats

Mapping Fauna-Flora-Habitats means to map according to habitats defined by ecosystem factors, e.g. abiotic factors like light, moisture, trophic status, and biotic factors like fauna and flora species. Habitat classification is strongly correlated to phytosociological vegetation types, because categorisation of FFH types is based on phytosociological communities that occur in these habitats. Some emphasis lies upon cover values of important species (e.g. *Cladium mariscus* or *Pinus mugo* agg.), and on the differentiation of habitat conditions.

Separations between 7110 (active raised bogs) and 7120 (degraded raised bogs still capable of natural regeneration) was not possible by pure spectral discrimination of the pixels. This could be done by visualising degraded plot structures on the scene before image classification (see fig. 5.15).

In general, Fauna-Flora-Habitats of the investigated areas were possible to be image classified by the utilised imagery, if they were well defined by their species inventory. Problems occurred regarding image classification of *Molinia* rich stands. As well, bog woods with *Pinus mugo agg.* showed no satisfying results. The demand of assigning relevés to this very vegetation type if *Pinus mugo agg.* covers at least 10 % could not be classified properly by image classification. To detect such structures, spatial resolution seems to be too low. Here, a combination with other imagery is suggested, i.e. high spatial resolution orthophotos with a spatial resolution of $0.4 \times 0.4 \text{ m}^2$ where single trees can be made out, or with LIDAR data for structural properties of the canopy.

Relevés of transition zones as well as mixed stands that could not be properly assigned to vegetation types showed also confusions in image classifications. Hence, as already mentioned, they were not appropriate to be used as reference spectra. These critical zones are visible in the maps of PLS regression models, and can therefore be better detected and monitored by a Synthesis map of both discrete and non-discrete mapping approaches.

According to mapping phytosociological vegetation types, within-stand heterogeneity could be outbalanced by using SAM ISD method. With the given scene data it was possible to spectrally differentiate Fauna-Flora-Habitats, if underlying spectra were well defined by diagnostic and / or dominant species.

From the Viewpoint of Image Classification

Two pixelbased and supervised image classification algorithms have been applied to the same data sets (SAM and MESMA, see section 5.2.4). At large, results showed that SAM classifications performed best if ISD spectra determination was used. This possibility of referencing pixels allows for heterogeneity within types which is an important factor when mapping natural vegetation. The homogeneous community *Phragmitetum communis* of the data set 2004 north built an exception and could be better image classified if MSD or BRSD spectra were used as reference.

The MESMA classification algorithm produced not as good results regarding κ values derived from validation. This was due to several facts: the so-called input endmember spectra should represent pure, and not mixed information. As reference data were taken from the scene itself, only mixed signals were used to unmix. Here, working with field spectra is common. In case of this project, no field spectra were taken during scene data acquisition.

Secondly, MESMA was designed as a fuzzy method. Its crisp usage means a decrease of information that can be gained. Fuzzy outputs were obtained

and gave good optical results but were difficult to validate. Field spectra can be used for accuracy assessment of MESMA classification outputs (e.g. Bachmann et al. (2005)). Also, the validation of fuzzy outputs could be done if also fuzzy input data were used. Hence, by distance matrices of both input and output data, the quality of image classification results could be measured, e.g. *z* – test or *Mantel* – test (Kent and Ballard, 1988; Foody and Arora, 1996). A possibility was to work with subplot information of the data set 2004 as fuzzy input. First results did not show promising results. Furthermore, PLS regression models delivered the continuous maps needed for this study. Hence, concentration was put on crisp outputs.

Thirdly, MESMA was used in this project only with BRSD reference spectra. κ results were comparable to SAM classifications with BRSD. Further investigations seem promising using ISD reference. This would include, certainly, high computational efforts. Therefore, in consideration of these constraints, SAM resulted as the more convenient tool regarding this project.

First tests to iteratively set individual thresholds (see section 4.4.2) for different vegetation types in SAM image classification showed promising results. In case of the MSD and ISD methods, some vegetation types could be better differentiated with specific thresholds set. Certainly, this kind of time consuming efforts would only be reasonable if individual stands were in the focus of deeper investigations. However, it would be an interesting matter in further investigations.

Apart from SAM and MESMA, three common image classification algorithms have been tested. Minimum Distance to Means classifier (MD, see Lillesand and Kiefer 2004, 539 for more information), Maximum Likelihood (ML, of Fisher 1922, insights given by Aldrich 1997), as well as Parallelepiped classifier (PP, details in Richards 1999) were tested on PCA outputs of the scene, MNF-rotation outputs of the scene (Minimum Noise Fraction, see Green et al. 1988) as well as on the PLS regression models that were gained within this project. As MD and PP classifier did not yield comparable results to those of the upper mentioned methods SAM and MESMA, focus was hence put on the latter. ML did perform nearly as good as SAM and MESMA. Further investigations will show how ML performs with different reference spectra determination methods (as described in section 4.4.2).

Other interesting possibilities to classify natural vegetation are Neural Nets (e.g. applications of Carpenter et al. 1999) and Support Vector Machines (e.g. Huang et al. 2002) that show promising results when applied to complex structures. Also object-based methods (e.g. delivered by the software eCognition) are to consider. Applications on the differentiation of landscape patterns are shown by Schneider et al. (1997), of forest vegetation (Buck et al., 1999; De Kok et al., 1999), and in conservancy (Blaschke, 2002).

It is to be tested in further analyses, if the combination of pixels according to some textual criteria improves classification results, or if due to the object formation too much information of the single pixels will be lost.

Accuracy Assessment

Cross-validation results are to be interpreted with caution due to above mentioned reasons (see section 6.2). With the unparted data, some communities were already under-represented by the given relevés. Therefore, the division into training and validation data was not possible within the classification steps. Leave-one-out cross-validation was the only possibility to validate without reducing the data set. Alternatives like ten-fold cross-validation would have decreased autocorrelation effects in feature space, but decreased the data set. Hence, more sampling would have been necessary.

6.4 Synthesis

Aim of this project was to produce maps that include as well informations on the continuous attributes of natural vegetation as well as on vegetation types. The resulting Synthesis maps (see maps B in the Appendix) of combining discrete with non-discrete mapping approaches display both information.

On the one hand, PLS regression models define all existing vegetation types that have been sampled in their variance. Homogeneous as well as heterogeneous areas with transitions inbetween can be made out by a (two-dimensional) colour-space. All colours can be referred to positions among ordination axes that indicate habitat definition and species composition. The quality of the models is given by the squared correlation coefficient R^2 for each axis as well as explanatory power of the ordination.

On the other hand, for all three applied vegetation classification schemes, vegetation types are mapped by polygons derived from image classifications. Vegetation type colours in the map depend on the colour space of the NMS ordination. Homogeneous areas show more or less homogeneous colours whereas transition zones and mixed stands show graduated colours, and Salt-and-Pepper-Effects. Vegetation types that are closely related to each other, show similar colour space positions and are difficult to separate. Therefore, different hatchures are overlaid. Similar types are provided with the same hatchure in a different colour, e.g. in case of *Molinia*-dominated vegetation types. This certainly influences the colour impression of the map reader, as the hatchure colour does optically give another impression of the original colours derived from regression models underneath. But still, graduated

colours can be detected, and each pixel can be assigned to a vegetation type by its hatchure.

The quality of image classifications can be projected for each vegetation type in % of correctly classified relevés. This enables for deeper research, if wanted structures shall be mapped in more detail.

6.5 Usage for Conservancy Purposes

If we come back to the motivation of the project, mapping Fauna-Flora-Habitat types of large conservation areas is in the main focus. Methods must be reproducible for monitoring reasons, as well as stay within moderate costs (see section 2.1). The introduced Synthesis map is a reproducible method. It delivers two-fold information on pixel basis: habitat type membership on the one side, stand position in the context of the continuous field of the vegetation on the other. Hence, ecotones can be monitored within habitats, which allows for the important roles of ecotones in monitoring (see section 2.2). Due to the use of high spatial and spectral resolution of the imagery, this information is given in the same spatial detail for a large area, and the quality of the given details is measurable. Producing maps with these qualities is not possible by traditional field methods.

Apart from scene imagery, main costs are due to field work. Field data are an important component, as PLS regression models are based on ordination axes that have been calculated from relevés data. Also, they cannot be replaced by the usage of extant spectral libraries in the context of image classifications. For each monitoring study, a new spectral library has to be formed by the collection of samples to account for the local realities of vegetation.

Field data can be reduced (see section 6.2), or taken from extant mapping projects in the area under investigation, if sampling and scene acquisition interval allows for. A combined relevé utilisation is supposable in the context of systematic inventarisations of biotopes (Stellmach and Langensiepen, 2006, 2007). For a complete map, the sampling design should ensure that all habitats are included in the relevés data that occur in the area of investigation, and well characterised samples should ensure a spectral differentiation. To base mapping on objective data, but best allow for the mentioned conditions, we propose a restricted random sampling design, where unsupervised image classifications of the image data deliver the stratum informations. The number of samples for each stratum should be calculated according to the variance of each stratum, with high sample numbers for strata with high variances.

Bibliography

- Abdi, H. (2003). *Partial Least Squares (PLS) regression*. Sage, Thousand Oaks, CA.
- Aber, J. and Martin, M. (1995). High spectral resolution remote sensing of canopy chemistry. In Green, R., editor, *Summaries of the Fifth Annual JPL Airborne Earth Science Workshop*, Pasadena, California. Jet Propulsion Laboratory.
- Adams, J. B., Smith, M. O., and Johnson, P. E. (1986). Spectral mixture modeling: a new analysis of rock and soil types at the Viking Lander 1 site. *Journal of Geophysical Research*, 91:8098–8112.
- Alberotanza, L., Brando, V. E., Ravagnan, C., and Zandonella, A. (1999). Hyperspectral aerial images. A valuable tool for submerged vegetation recognition in the Orbetello Lagoons, Italy. *International Journal of Remote Sensing*, 20(3):523–533.
- Albertz, J. (1996). *Einführung in die Fernerkundung - Grundlagen der Interpretation von Luft- und Satellitenbildern*. Wissenschaftliche Buchgesellschaft, Darmstadt.
- Aldrich, J. (1997). R.A. Fisher and the Making of Maximum Likelihood 1912-1922. *Statistical Science*, 3:162–176.
- Anderson, D. J. (1965). Classification and Ordination in Vegetation Science: Controversy over a Non-Existent Problem? *Journal of Ecology*, 53(2):521–526.
- Armitage, R. P., Kent, M., and Weaver, R. E. (2005). Identification of the spectral characteristics of British semi-natural upland vegetation using direct ordination: a case study from Dartmoor, UK. *International Journal of Remote Sensing*, 25(17):3369–3388.
- Asner, G. P. (1998). Biophysical and biochemical sources of variability in canopy reflectance. *Remote Sensing of Environment*, 64:234–253.

- Asner, G. P., Wessman, C. A., and Schimel, D. S. (1998). Heterogeneity of savanna canopy structure and function from imaging spectrometry and inverse modeling. *Ecological Applications*, 8:1022–1036.
- Aspinall, R. J., Marcus, W. A., and Boardman, J. W. (2002). Considerations in collecting, processing, and analysing high spatial resolution hyperspectral data for environmental investigations. *Journal of Geographical Systems*, 4:15–29.
- Austin, M. P. (1985). Continuum concept, ordination methods, and niche theory. *Annual Reviews of Ecological Systems*, 16:39–61.
- Bachmann, M., Müller, A., Habermeyer, M., Schmidt, M., and Dech, S. (2005). Iterative MESMA unmixing for fractional cover estimates - evaluating the probability. *Proceedings of the 4th EARSeL Workshop on Imaging Spectroscopy (Warsaw)*, 4:467–473.
- Balzer, S., Schröder, E., Ssymank, A., Ellwanger, G., Kehrein, A., and Rost, S. (2004). Ergänzung der Anhänge zur FFH-Richtlinie auf Grund der EU-Osterweiterung: Beschreibung der Lebensraumtypen mit Vorkommen in Deutschland. *Natur und Landschaft*, 79(8):341–349.
- Banner, A., Meidinger, D. V., LEA, E. C., Maxwell, R. E., and von Sacken, B. C. (1996). Ecosystem mapping methods for British Columbia. *Environmental Monitoring and Assessment*, 39:97–117.
- Barkman, J. J., Doing, H., and Segal, S. (1964). Kritische Bemerkungen und Vorschläge zur quantitativen Vegetationsanalyse. *Acta Botanica Neerlandica*, 13:394–419.
- Belward, A. S. (1991). Spectral characteristics of vegetation, soil and water invisible, near infrared and middle-infrared wavelengths. In Belward, A. S. and Valenzuela, C. R., editors, *Remote sensing and geographical information systems of resource management in developing countries*, E Applied Sciences, pages 31–53. NATO Asi Series, Washington, D.C.
- Beyer, H. L. (2006). Hawth's Analysis Tools for ArcGIS. <http://www.spataleecology.com/htools>.
- Billeter, R., Hooftman, D. A. P., and Diemer, M. (2003). Differential and reversible responses of common fen meadow species to abandonment. *Applied Vegetation Science*, 6:3–12.

- Biondini, M. E., Bonham, C. D., and Redente, E. F. (1985). Secondary successional patterns in a sagebrush (*Artemisia tridentata*) community as they relate to soil disturbance and soil biological activity. *Vegetatio*, 65:25–36.
- Birger, J. (1998). Das Monitoring der Bergbaufolgelandschaften Mitteldeutschlands mit Hilfe von Fernerkundungsdaten. In Frühauf, M. and Hardenbicker, U., editors, *Geowissenschaftliche Umweltforschung im mitteleuropäischen Raum. Beiträge der 3. Tagung zur Geographischen Umweltforschung in Mitteldeutschland im Rahmen des Universitätsverbandes Halle - Jena - Leipzig*, pages 77–85.
- Blackburn, G. A. (1998). Quantifying chlorophylls and carotenoids at leaf and canopy scales: An evaluation of some hyperspectral approaches. *Remote Sensing of Environment*, 66:273–285.
- Blaschke, T., editor (2002). *Fernerkundung und GIS. Neue Sensoren - innovative Sensoren*. Herber Wichmann-Verlag, Heidelberg.
- Boardman, J. W. and Green, R. O. (2000). Exploring the spectral variability of the Earth as measured by AVIRIS in 1999. <http://hdl.handle.net/2014/16602>.
- Bosshard, A., Andres, F., Stromeyer, S., and Wohlgemuth, T. (1988). Wirkung einer kurzfristigen Brache auf das Ökosystem eines anthropogenen Kleinseggenriedes - Folgerungen für den Naturschutz. *Bulletin des Geobotanischen Instituts ETH Zürich*, 54:181–220.
- Braun, W. (1983). *Vegetationskundliche Skizze des Murnauer Moooses. Geologische Karte von Bayern - Blatt 8333 - Erläuterungen*. Bayerisches Geologisches Landesamt, München.
- Braun, W., Künne, H., and Lotto, R. (1984). Liste der Farn- und Blütenpflanzen des Naturschutzgebiets "Murnauer Moos". *Berichte der Bayerischen Botanischen Gesellschaft*, 55:121–130.
- Braun-Blanquet, J. (1921). Prinzipien einer Systematik der Pflanzengesellschaften auf floristischer Grundlage. *Berichtbände der naturwissenschaftlichen Gesellschaft St. Gallen*, 57:305–351.
- Braun-Blanquet, J. (1928). *Pflanzensoziologie : Grundzüge der Vegetationskunde*. Springer, Berlin.

- Brisco, B., Brown, R. J., Hirose, T., McNairn, H., and Staenz, K. (1998). Precision agriculture and the role of remote sensing: a review. *Canadian Journal of Remote Sensing*, 24(3):273–285.
- Broge, N. H. and Leblanc, E. (2000). Comparing prediction power and stability of broadband and hyperspectral vegetation indices for estimation of green leaf area index and canopy chlorophyll density. *Remote Sensing of Environment*, 76:156–172.
- Buck, A., de Kok, R., Schneider, T., and Ammer, U. (1999). Integration von Fernerkundungsdaten und GIS zur Beobachtung und Inventur von Schutzwäldern in den Bayerischen Alpen. In Strobl, J. and Blaschke, T., editors, *Angewandte Geographische Informationsverarbeitung XI*, pages 94–101. Herber Wichmann-Verlag, Heidelberg.
- Burmeister, E. G. (1982). Die erste faunistische Bestandsaufnahme im Mur-nauer Moos. *Entomofauna – Zeitschrift für Entomologie*, 1:5–22.
- Campbell, J. B. (2002). *Introduction to Remote Sensing*. Guilford Publications, New York, 3 edition.
- Carpenter, G. A., Gopal, S., Macomber, S., Martens, S., Woodcock, C. E., and Franklin, J. (1999). A neural network method for efficient vegetation mapping. *Remote Sensing of Environment*, 70:326–338.
- Carter, G. A. (1993). Responses of leaf spectral reflectance to plant stress. *American Journal of Botany*, 80:239–243.
- Cherril, A. and McClean, C. (1999). Between-observer variation in the application of a standard method of habitat mapping by environmental consultants in the UK. *Journal of Applied Ecology*, 36:989–1008.
- Clark, R. N. (1999). Spectroscopy of rocks and minerals and principles of spectrometry. In Rencz, A., editor, *Remote sensing for the earth science*, number 3 in Manual of remote sensing, pages 3–58. John Wiley and Sons.
- Clarke, K. R. (1993). Non-parametric multivariate analyses of changes in community structure. *Australian Journal of Ecology*, 18:117–143.
- Clements, F. E. (1916). *Plant Succession: An Analysis of the Development of Vegetation*, volume 242. Carnegie Institution of Washington.
- Cohen, J. (1960). A coefficient of agreement for nominal scales. *Educational and Psychological Measurement*, 20(1):37–46.

- Collins, W. (1978). Remote sensing of crop type and maturity. *Photogrammetric Engineering and Remote Sensing*, 44:43–55.
- Congalton, R. (1991). A Review of Assessing the Accuracy of Classifications of Remotely Sensed Data. *Remote Sensing of Environment*, 37:35–46.
- Cooper, W. S. (1926). The Fundamentals of Vegetational Change. *Ecology*, 7:391–413.
- Cornelius, J. M. and Reynolds, J. F. (1991). On determining the statistical significance of discontinuities within ordered ecological data. *Ecology*, 72:2057–2070.
- Council, N. (1998). *Precision Agriculture in the 21st Century: Geospatial and Information Technologies in Crop Management. Committee, Assessing Crop Yield: Site-specific farming, information systems, and research opportunities*. National Academy Press, Washington, D.C.
- Council of the European Union/ Der Rat der Europäischen Gemeinschaften (1992). Richtlinie 92/43/EWG des Rates vom 21. Mai 1992 zur Erhaltung der natürlichen Lebensräume sowie der wildlebenden Tiere und Pflanzen. In *Amtsblatt der Europäischen Gemeinschaften*, volume 206 of L, pages 7–50.
- Curran, P. J., Kupiec, J. A., and Smith, G. M. (1998). Biochemical Composition of a Slash Pine Canopy. *IEEE Transactions on Geoscience and Remote Sensing*, 35(2):415–420.
- Daubenmire, R. F. (1960). Some major problems in vegetation classification. *Silva Fennica*, 105:22–25.
- Daubenmire, R. F. (1968). *Plant Communities: A Textbook of Plant Synecology*. Harper and Row, New York.
- Davies, A. M. C. (2001). Uncertainty testing in PLS regression. *Spectroscopy Europe*, 13:16–19.
- De Kok, R., Schneider, T., Baatz, M., and Ammer, U. (1999). Object-Based classification and applications in the alpine forest environment. *International Archives of Photogrammetry and Remote Sensing*, 32:7–4–3 W6.
- de Lange, R., van Til, M., and Dury, S. (2004). The use of hyperspectral data in coastal zone vegetation monitoring. *EARSeL eProceedings 3*, 2:143–153.

- Dennison, P. E., Halligan, K. Q., and Roberts, D. A. (2004). A comparison of error metrics and constraints for multiple endmember spectral mixture analysis and spectral angle mapper. *Remote Sensing of Environment*, 93:359–367.
- Dennison, P. E. and Roberts, D. A. (2003a). Endmember selection for multiple endmember spectral mixture analysis using endmember average RMSE. *Remote Sensing of Environment*, 87:123–135.
- Dennison, P. E. and Roberts, D. A. (2003b). The effects of vegetation phenology on endmember selection and species mapping in southern California chaparral. *Remote Sensing of Environment*, 87:295–309.
- Deutscher Wetterdienst (2007). http://www.dwd.de/de/FundE/Klima/KLIS/daten/online/nat/index_mittelwerte.htm.
- Dierßen, B. and Dierßen, K. (1982). Kiefernreiche Phytocoenosen oligotropher Moore im mittleren und nordwestlichen Europa. Überlegungen zur Problematik ihrer Zuordnung zu höheren synsystematischen Einheiten. In Dierschke, H., editor, *Struktur und Dynamik von Wäldern*, pages 299–331, Berichte d. Internationalen Symposiums d. IVV.
- Dierßen, K. and Dierßen, B. (2001). *Moore*. Ulmer, Stuttgart.
- Dingler, M., Paul, H., and Vollmar, F. (1943). *Das Murnauer Moor, eine kurzgefaßte Darstellung*. Gerber, München, 2 edition.
- Dobrowski, S., Anderson, M., Greenspan, M., Ustin, S., and Wolpert, J. A. (2000). Aerial image analysis in evaluating vineyard canopy parameters. *American Journal of Enology and Viticulture*, 51:288–289.
- Du Rietz, G. E. (1921). *Zur methodologischen Grundlage der modernen Pflanzensoziologie*. PhD thesis, Uppsala.
- Du Rietz, G. E. (1930). *Vegetationsforschung auf soziationsanalytischer Grundlage*. Abderhalden, E.: Handbuch der biologischen Arbeitsmethoden 11, Berlin.
- Du Rietz, G. E. (1954). Die Mineralbodenwasssergrenze als Grundlage einer natürlichen Zweigliederung der Nord- und Mitteleuropäischen Moore. *Plant Ecology*, 5/6(1):571–585.
- Duda, R. D. and Hart, P. E. (1973). *Pattern Classification and Scene Analysis*. John Wiley and Sons, New York.

- Durand, J. F. and Sabatier, R. (1994). Additive Splines for PLS Regression. *Rapport technique, unite de biometric*, (9405).
- Edom, F. (2001). Revitalisierung von Regenmooren an ihrer klimatischen Arealgrenze. In Succow, M. and Joosten, H., editors, *Landschaftsökologische Moorkunde*, volume 2, pages 534–543, Stuttgart. E. Schweizerbart'sche Verlagsbuchhandlung.
- Efron, B. (1983). Estimating the Error Rate of a Prediction Rule: Improvement on Cross-Validation. *Journal of the American Statistical Association*, 78(382):316–331.
- Efron, B. and Tibshirani, R. J. (1993). *An introduction to the bootstrap*. Chapman and Hill, New York.
- Egler, F. E. (1942). Vegetation as an object of study. *Philosophy Sci.*, 9:245–260.
- Ellenberg, H. (1956). *Grundlagen der Vegetationsgliederung : Einführung in die Vegetationskunde f. Studierende der Hochschulen, 1. Teil: Aufgaben und Methoden der Vegetationskunde*. Ulmer, Stuttgart.
- Ellenberg, H. (1996). *Vegetation Mitteleuropas mit den Alpen in ökologischer, dynamischer und historischer Sicht*. Ulmer, Stuttgart, 5 edition.
- Elvidge, C. D. (1990). Visible and near infrared reflectance characteristics of dry plant materials. *International Journal of Remote Sensing*, 11:1775–1795.
- Engelbrecht, H. (2003). Erdgeschichte und Umweltgeologie am Geotop "Langer Köchel" im Murnau-Eschenloher Moos (Oberbayern). In Jordan, P., Heinz, R., Heitzmann, P., Hipp, R., and Imper, D., editors, *Geotope - wie schützen/ wie nutzen?*, volume 31, pages 126–133, Hannover. Deutsche Geologische Gesellschaft.
- European Commission (2007). <http://ec.europa.eu/environment/nature/natura2000/barometer/docs/sci.pdf>.
- European Commission DG Environment (2003). *Interpretation Manual of European Union Habitats*. Version EUR 25, Brüssel.
- Fartmann, T., Gunnemann, H., Salm, P., and Schröder, E. (2001). Berichtspflichten in Natura-2000-Gebieten. *Angewandte Landschaftsökologie*, 42:1–725.

- Fernandes, R. A., Miller, J. R., Hu, B., and Rubinstein, I. G. (2002). A Multi-Scale Approach to Mapping Effective Leaf Area Index in Boreal *Picea mariana* Stands using High Spatial Resolution CASI Imagery. *International Journal of Remote Sensing*, 23(18):3547–3568.
- Fisher, R. A. (1922). On the mathematical foundations of theoretical statistics. *Philosophical Transactions of the Royal Society London A*, 222:309–368.
- Fogel, D. N. and Tinney, L. R. (1996). *Image Registration using Multiquadric Functions, the Finite Element Method, Bivariate Mapping Polynomials and the Thin Plate Spline*. National Center for Geographic Information and Analysis. Technical Report 96-1.
- Foody, G. M. (1996). Fuzzy modelling of vegetation from remotely sensed imagery. *Ecological Modelling*, 85:3–45.
- Foody, G. M. (1999). The continuum of classification fuzziness in thematic mapping. *Photogrammetric Engineering and Remote Sensing*, 65:443–451.
- Foody, M. G. (2002). Status of land cover classification accuracy assessment. *Remote Sensing of Environment*, 80:185–201.
- Foody, M. G. and Arora, M. K. (1996). Incorporating mixed pixels in the training, allocation and testing stages of supervised classifications. *Pattern Recognition Letters*, 17:1389–1398.
- Fortin, M. J., Olson, R. J., Ferson, S., Iverson, L., Hunsaker, C., Edwards, G., Levine, D., Butera, K., and Klemas, V. (2000). Issues related to the detection of boundaries. *Landscape Ecology*, 15:453–466.
- Frahm, J. P. and Frey, W. (2004). *Moosflora*. UTB, 4 edition.
- Friedel, U. (2005). Hyperspektrale Fernerkundung zur Kartierung der Vegetation des Murnauer Moores. Master's thesis, Universität Bayreuth.
- Fritz, S. and See, L. (2004). Improving quality and minimising uncertainty of land cover maps using fuzzy logic. In *GISRUK 2004*.
- Gamon, J. A., Field, C. B., Roberts, D. A., Ustin, S. L., and Valentini, R. (1993). Functional Patterns in Annual Grassland during a AVIRIS Overflight. *Remote Sensing of Environment*, 44:239–253.

- Gams, H. (1918). Prinzipienfragen der Vegetationsforschung. Ein Beitrag zur Begriffserklärung und Methodik der Biocoenologie. *Vierteljahresschrift der Naturforschenden Gesellschaft Zürich*, 63(3-4):239–493.
- Gams, H. (1947). Die Fortschritte der alpinen Moorforschung von 1932 bis 1946. *Plant Systematics and Evolution*, 94(1/2):235–264.
- García-Haro, F. J., Sommer, S., and Kemper, T. (2005). A new tool for variable multiple endmember spectral mixture analysis (VMESMA). *International Journal of Remote Sensing*, 26(10):2135–2162.
- Gates, D. M., Gates, H. J., Gates, J. C., and Gates, V. (1965). Spectral properties of plants. *Applied Optics*, 4:11–20.
- Gauch, H. G. (1982). *Multivariate analysis in community ecology*. Cambridge University Press, Cambridge.
- Gauch, H. G. and Whittaker, R. H. (1981). Hierarchical classification of community data. *Journal of Ecology*, 69(2):537–557.
- Gausman, H. W., Allen, W. A., and Cardenas, R. (1969). Reflectance of cotton leaves and their structure. *Remote Sensing of Environment*, 1:19–22.
- Gausman, H. W., Allen, W. A., Gardenas, R., and Richardson, A. J. (1973). Reflectance discrimination of cotton and corn at four growth stages. *Agronomy Journal*, 65:194–198.
- Gauss, C. F. (1795). Method of Least Squares. unpublished.
- Geiersberger, I. (2002). Das Murnauer Moos. In *Markt Murnau am Staffelsee - Beiträge zur Geschichte, Band 1*, Murnau a. Staffelsee.
- Geisser, S. (1975). The Predictive Sample Reuse Method with Applications. *Journal of the American Statistical Association*, 70(350):320–328.
- Gillison, A. N. and Brewer, K. R. W. (1985). The use of gradient directed transects in natural resource surveys. *Journal of Environmental Management*, 20:103–127.
- Glavac, V. (1992). On the nature of vegetation boundaries, undisturbed flood plain forest communities as an example - a contribution to the continuum/discontinuum controversy. *Vegetatio*, 101:123–144.

- Glavac, V. (1996). *Vegetationsökologie: Grundfragen, Aufgaben, Methoden*. Gustav Fischer Verlag, Jena.
- Gleason, H. A. (1926). The individualistic concept of the plant association. *Bulletin of the Torrey Club*, 53:7–26.
- Goodall, D. W. (1954). Objective methods for the classification of vegetation. III. An essay in the use of factor analysis. *Australian Journal of Botany*, 2:304–324.
- Goodall, D. W. (1963). The continuum and the individualistic association. *Vegetatio*, 11:297–316.
- Goodin, D. G. and Henebrey, G. M. (1997). A Technique for Monitoring Ecological Variables in Tallgrass Prairie Seasonal NDVI Trajectories and a Discriminant Function Mixture Model. *Remote Sensing of Environment*, 61:270–278.
- Gosz, J. R. (1993). Ecotone Hierarchies. *Ecological Applications*, 3(3):369–376.
- Green, A. A., Switzer, P., and Craig, M. D. (1988). A Transformation of Ordering Multispectral Data in Terms of Image Quality with Implications for Noise Removal. *IEEE Transactions on Geoscience and Remote Sensing*, 26(1):65–74.
- Greig-Smith, P. (1983). *Quantitative plant ecology*. University of California Press, 3 edition.
- Gremer, D. (2001). Zur Standorts- und Vegetationsveränderung von Regenmooren. In Succow, M. and Joosten, H., editors, *Landschaftsökologische Moorkunde*, volume 2, pages 457–463, Stuttgart. E. Schweizerbart'sche Verlagsbuchhandlung.
- Griggs, R. F. (1938). Timberlines in the northern Rocky Mountains. *Ecology*, 19:548–564.
- Haaland, D. M. and Thomas, E. V. (1988). Partial Least Squares Methods for Spectral Analyses. 1. Relation to Other Quantitative Calibration Methods and the Extraction of Qualitative Information. *Analytical Chemistry*, 60(11):1202–1208.

- Habbe, K. A. (1995). Zur Diskussion über die Chronostratigraphie des Pleistozäns im Alpenvorland und zu einigen daraus resultierenden Schlußfolgerungen für die Geomorphologie. *Regensburger Geographische Schriften*, 25:49–36.
- Hansen, A. J. and diCastri, F., editors (1992). *Landscape Boundaries: Consequences for Biotic Diversity and Landscape Flows. Ecological Studies 92*. Springer Verlag, New York.
- Hennekens, S. M. and Schaminée, J. H. J. (2001). TURBOVEG, a comprehensive data base management system for vegetation data. *Journal of Vegetation Science*, 12:589–591.
- Hill, M. O. (1979). TWINSPAN - A FORTRAN program for arranging multivariate data in an ordered two-way table by classification of the individuals and attributes.
- Hill, M. O. and Gauch, H. G. (1980). Detrended correspondence analysis: an improved technique. *Vegetatio*, 42:47–58.
- Hirano, A., Madden, M., and Welch, R. (2003). Hyperspectral image data for mapping wetland vegetation. *Wetlands*, 23(2):436–448.
- Hoeskuldsson, A. (1988). PLS regression methods. *Journal of Chemometrics*, 2(3):211–228.
- Hoffer, A. M. (1978). Biological and physical considerations in applying computer-aided analysis techniques to remote sensor data. In Swain, P. and Davis, S., editors, *Remote Sensing: The Quantitative Approach*, pages 227–289. McGraw-Hill Book Company.
- Holland, M. M., Risser, P. G., and Naiman, R. J., editors (1991). *Ecotones*. Chapman and Hall, New York.
- Hruschka, W. R. (1987). Data analysis: Wavelength selection methods. In Williams, P. and Norris, K. H., editors, *Near-infrared technology in the agriculture and food institutes*, pages 35–53. American Association of Cereal Chemists, St. Paul, MN.
- Huang, C., Davies, L. S., and Townshend, J. R. G. (2002). An assessment of support vector machines for land cover classification. *International Journal of Remote Sensing*, 23(4):725–749.

- Huon de Kermadec, F., Durand, J. F., and Sabatier, R. (1997). Comparison between linear and nonlinear PLS methods to explain overall liking from sensor characteristics. *Food Quality and Preference*, 8(5/6):395–402.
- Innanen, K. and Miller, J. R. (1998). On the direct extraction of scene component fractions and crown cover distribution in open forest canopies using high spatial resolution winter imagery. In *International Forum: Automated Interpretation of High Spatial Resolution Digital Imagery for Forestry*, Victoria, B.C.
- Jacobsen, A. (2000). *Analysing Airborne Optical Remote Sensing Data from a Hyperspectral Scanner and Implications for Environmental Mapping and Monitoring - results from a study of CASI data and Danish semi-natural, dry grasslands*. PhD thesis, National Environmental Research Institute, Denmark.
- Jacobsen, A., Nielsen, A. A., Ejrnaes, R., and Groom, G. (2000). Spectral Identification of Plant Communities for Mapping of Semi-Natural Grasslands. *Canadian Journal of Remote Sensing*, 26(2):370–383.
- Jago, R. A., Cutler, M. E. J., and Curran, P. J. (1999). Estimating chlorophyll concentration from field and airborne spectra. *Remote Sensing of Environment*, 68:217–224.
- Jensen, J. R. (1996). *Introductory Digital Image Processing - A Remote Sensing Perspective*. Prentice Hall Inc., New Jersey, 2 edition.
- Jeschke, L. (2003). Filze, Möser und Dosen : Ein Plädoyer für Moornationalparke in Deutschland. *Nationalpark : Wildnis - Mensch - Landschaft*, 122(1):9–12.
- Jäger, E. J. and Werner, K. (1999). *Rothmaler, Exkursionsflora von Deutschland - Gefäßpflanzen: Atlasband*. Spektrum Akademischer Verlag, Stuttgart, 10 edition.
- Jäger, E. J. and Werner, K. (2002). *Rothmaler, Exkursionsflora von Deutschland - Gefäßpflanzen: kritischer Band*. Spektrum Akademischer Verlag, Heidelberg, 9 edition.
- Kaptein, A., Thiemann, S., and Schäfer, A. (1999). Biotope and land-use monitoring. In *Proceedings of IGARSS'99*, volume 2, pages 1206–1207.

- Kaule, G. (1974). *Die Übergangs- und Hochmoore Süddeutschlands und der Vogesen: Landschaftsökologische Untersuchungen mit besonderer Berücksichtigung der Ziele der Raumordnung und des Naturschutzes*. Verlag J. Cramer, Lehre, Dissertationes Botanicae 27.
- Küchler, A. W. (1967). *Vegetation Mapping*. Ronald Press, New York.
- Kehrein, A. (2002). Aktueller Stand und Perspektiven der Umsetzung von Natura 2000 in Deutschland. *Natur und Landschaft*, 77(1):2–9.
- Kennedy, R. E., Cohen, W. B., and Takao, G. (1997). Empirical Methods to Compensate for a View-Angle-Dependent Brightness Gradient in AVIRIS imagery. *Remote Sensing of Environment*, 62:277–291.
- Kent, M. and Ballard, J. (1988). Trends and problems in the application of classification and ordination methods in plant ecology. *Vegetatio*, 78:109–124.
- Kent, M. and Coker, P. (1992). *Vegetation description and analysis: a practical approach*. Belhaven Press, London.
- Keshava, N. and Mustard, J. F. (2002). Spectral Unmixing. *IEEE Signal Processing Magazine, Exploiting Hyperspectral Imagery*, 19:44–57.
- König, P. (2007). Torfstich im Murnauer Moos. unpublished.
- Kohonen, T. (2001). *Self-Organizing Maps*. Springer, Berlin, 3 edition.
- Kruse, F. A., Lefkoff, A. B., Boardman, J. W., Heidebrecht, K. B., Shapiro, A. T., Barloon, P., J., and Goetz, A. F. H. (1993). The spectral image processing system (SIPS) - Interactive visualization and analysis of imaging spectrometer data. *Remote Sensing of Environment*, 44:145–163.
- Kruskal, J. B. (1964). Nonmetric multidimensional scaling: a numerical method. *Psychometrika*, 29:115–129.
- Kuchler, A. W. (1973). Problems in Classifying and Mapping Vegetation for Ecological Regionalization. *Ecology*, 54(3):512–523.
- Kuisle, A. (2000). *Sprengen - Brechen - Sieben. 70 Jahre Steinbruch-Technik im Hartsteinwerk Werdenfels*, pages 97–122. Ausstellungskatalog, Schloßmuseum Murnau.

- Kumar, L., Schmidt, K., Dury, S., and Skidmore, A. (2001). Imaging spectrometry and vegetation science. In Van Der Meer, F. and De Jong, S., editors, *Imaging spectrometry. Basic principles and prospective applications*, pages 111–155. Kluwer Academic Publishers.
- Labovitz, M. L. (1986). Issues arising from sampling designs and band selection in discriminating ground reference attributes using remotely sensed data. *Photogrammetric Engineering and Remote Sensing*, 52:201–211.
- Lachenbruch, P. A. (1968). On Expected Probabilities of Misclassification in Discriminant Analysis, Necessary Sample Size, and a Relation with the Multiple Correlation Coefficient. *Biometrics*, 24(4):823–834.
- Lachenbruch, P. A. and Mickey, M. R. (1968). Estimation of Error Rates in Discriminant Analysis. *Technometrics*, 10(1):1–11.
- Lagally, U., Kube, W., and Frank, H. (1994). *Geowissenschaftlich schutzwürdige Objekte in Oberbayern. Ergebnisse einer Erstaufnahme. Erdwissenschaftliche Beiträge zum Naturschutz*. Bayerisches Geologisches Landesamt, München.
- Lang, A. and Walentowski, H. (2007). *Handbuch der Lebensraumtypen nach Anhang I der Fauna-Flora-Habitat-Richtlinie in Bayern*. Bayerisches Landesamt für Umwelt und Bayerische Landesanstalt für Wald und Forstwirtschaft, Augsburg and Freising-Weißenstephan.
- Lauber, K. and Wagner, G. (1998). *Flora Helvetica*. Haupt Verlag, Bern, 2 edition.
- Legendre, A. M. (1805). *Nouvelles méthodes pour la détermination des orbites des comètes*. Courcier.
- Legendre, P. and Legendre, L. (1998). *Numerical Ecology*. Elsevier Science B.V., Amsterdam, 2 edition.
- Leopold, A. (1933). *Game Management*. Charles Scribner's & Sons, New York.
- Lewis, M. (1994). Species composition related to spectral classification in an Australian spinifex hummock grassland. *International Journal of Remote Sensing*, 15:3223–3239.
- Lewis, M. (1998). Numeric classification as an aid to spectral mapping of vegetation communities. *Plant Ecology*, 136:133–150.

- Lewis, M. (2000). Discrimination of arid vegetation composition with high resolution CASI imagery . *The Rangeland Journal*, 22(1):141–167.
- Lillesand, T. M. and Kiefer, R. W. (2004). *Imaging Spectrometry*. John Wiley and Sons, Inc., New York, 5 edition.
- Maas, D. (1988). Keimung und Etablierung von Streuwiesenpflanzen nach experimenteller Ansaat. *Natur und Landschaft*, 63:411–415.
- Mahecha, M. D. and Schmidtlein, S. (2008). Revealing biogeographical patterns by nonlinear ordinations and derived anisotropic spatial filters. *Global Ecology and Biogeography*, 17:284–296.
- Malmer, N. (1956). The southern mires. *Acta Phytogeographica Suecica*, 50:149–158.
- Mariscal, M. J., Orgaz, F., and Villalobos, F. J. (2000). Modelling and measurement of radiation interception by olive canopies . *Agricultural and Forest Meteorology*, 100:183–197.
- Martens, H. and Martens, M. (2000). Modified Jack-knife estimation of parameter uncertainty in bilinear modelling by partial least squares regression (PLS). *Food Quality and Preference*, 11:5–16.
- Mausser, W. (2003). The Airborne Visible/Infrared Imaging Spectrometer AVIS-2 - multiangular and hyperspectral data for environmental analysis. In *Proceedings of IGARSS*, volume 3, pages 2020–2022, Toulouse.
- McCune, B. and Mefford, M. J. (1999). *PC-ORD. Multivariate Analysis of Ecological Data, Version 4*. MjM Software Design, Gleneden Beach, Oregon, U.S.A.
- Merényi, E., Farrand, W. H., Stevens, L. E., Melis, T. S., and Chhibber, K. (2000). Mapping Colorado River Ecosystem Resources In Glen Canyon: Analysis of Hyperspectral Low-Altitude AVIRIS Imagery. In *Proc. ERIM 14th International Conference and Workshops on Applied Geologic Remote Sensing*, pages 44–51, Las Vegas, Nevada.
- Mueller-Dombois, D. and Ellenberg, H. (1974). *Aims and Methods of Vegetation Ecology*. Wiley, New York.
- Myers, V. I. (1970). Soil, water, and plant relations. In *Remote Sensing with Special Reference to Agriculture and Forestry (National Research Council Committee on Remote Sensing for Agricultural Purposes)*, pages 253–267. National Academy of Sciences, Washington, D.C.

- Myneni, R., Hall, F., Sellers, P., and Marshak, A. (1995). The interpretation of spectral vegetation indexes. *IEEE Transactions on Geoscience and Remote Sensing*, 33:481–486.
- Neuenschwander, A. L., Crawford, M. M., and Provanca, M. J. (1998). Mapping of coastal wetlands via hyperspectral AVIRIS data. In *Proceedings of the 1998 IGARSS Conference*, Seattle, Washington.
- Nowotny, G. and Tröster, B. (2002). Zur Bestandesentwicklung der Sumpfgladiole (*Gladiolus palustris* Gaudin) im Bundesland Salzburg. In *10. Österreichisches Botanikertreffen*, pages 45–50, BAL Gumpenstein, Irnding.
- Oberdorfer, E. (1977a). *Süddeutsche Pflanzengesellschaften zwischen Alpen und Main - Teil I: Fels- und Mauergesellschaften, alpine Fluren, Wasser-, Verlandungs- und Moorgesellschaften*. Gustav Fischer Verlag, Jena, 2 edition.
- Oberdorfer, E. (1977b). *Süddeutsche Pflanzengesellschaften zwischen Alpen und Main - Teil III: Wirtschaftswiesen und Unkrautgesellschaften*. Gustav Fischer Verlag, Jena, 2 edition.
- Oberdorfer, E. (1994). *Pflanzensoziologische Exkursionsflora*. Ulmer, Stuttgart, 7 edition.
- Okin, G. S., Roberts, D. A., Murraya, B., and Okin, W. J. (2001). Practical limits on hyperspectral vegetation discrimination in arid and semiarid environments. *Remote Sensing of Environment*, 77:212–225.
- Oppelt, N. and Mauser, W. (2004). Hyperspectral Monitoring of Physiological Parameters of Wheat during a Vegetation Period Using AVIS Data. *International Journal of Remote Sensing*, 25(1):145–159.
- Peñuelas, J., Filella, I., Biel, C., Serrano, L., and Savé, R. (1993). The Reflectance at the 950-970 Region as an Indicator of Plant Water Status. *International Journal of Remote Sensing*, 14(10):1887–1905.
- Peñuelas, J., Pinol, J., Ogaya, R., and Filella, I. (1997). Estimation of plant water concentration by reflectance Water Index WI (R900/R970). *International Journal of Remote Sensing*, 18(13):2869–2875.
- Pfadenhauer, J. (1997). *Vegetationsökologie: ein Skriptum*. IHW-Verlag, Eching, 2 edition.

- Ponyatovskaya, V. M. (1961). On two trends in phytocoenology. *Vegetatio*, 10(5/ 6):373–385. translated by Major, J.
- Quinger, B. (1986). Nachtrag zur Liste der Farn- und Blütenpflanzen des Naturschutzgebietes "Murnauer Moos". *Berichte der Bayerischen Botanischen Gesellschaft*, 57:111–112.
- Ramenski, L. G. (1930). Zur Methodik der vergleichenden Bearbeitung und Ordnung von Pflanzenlisten und anderen Objekten, die durch mehrere verschiedenartig wirkende Faktoren bestimmt werden. *Beiträge zur Biologie der Pflanzen*, 18:269–304.
- Rückriem, C. and Roscher, S. (1999). Empfehlungen zur Umsetzung der Berichtspflicht gemäß Artikel 17 der Fauna-Flora-Habitat-Richtlinie. *Angewandte Landschaftsökologie*, 22:1–456.
- Reitter-Welter, B. (2004). Wo der Wachtelkönig ruft. *Nationalpark*, 4:46–47.
- Richards, J. A. (1999). *Remote Sensing Digital Image Analysis*. Springer-Verlag, Berlin.
- Risser, P. G. (1995). The status of Science examining ecotones. *BioScience*, 45(5):318–325.
- Roberts, D. A., Gardner, M., Church, R., Ustin, S., Scheer, G., and Green, R. O. (1998). Mapping Chaparral in the Santa Monica Mountains Using Multiple Endmember Spectral Mixture Models. *Remote Sensing of Environment*, 65:267–279.
- Sampson, P. H., Mohammed, G. H., Zarco-Tejada, P. J., Miller, J. R., Noland, T. L., Irving, D., Treitz, P. M., Colombo, S. J., and Freemantle, J. (2001). The bioindicators of forest condition project : A physiological, remote sensing approach. *The Forestry Chronicle*, 76:941–952.
- Scharl, I. (2000a). *Kooperation und Gegnerschaft - zur gemeinsamen Geschichte von Hartsteinwerk und Naturschutz am Langen Köchel*, pages 123–132. Ausstellungskatalog, Schloßmuseum Murnau.
- Scharl, I. (2000b). *Unternehmensgeschichte des Hartsteinwerkes Werdenfels. - In: Industrie und Natur. Zur Geschichte des Hartsteinwerkes Werdenfels im Murnauer Moos*. Ausstellungskatalog, Schloßmuseum Murnau.
- Schloßmuseum des Marktes Murnau am Staffelsee (2002). Zur Geschichte des Hartsteinwerkes Werdenfels im Murnauer Moos.

http://www.schlossmuseum-murnau.de/Sonderausstellungen/Industrie_und_Natur/Industrie_und_Natur.htm.

- Schmidt, K. S. and Skidmore, A. K. (2001). Exploring spectral discrimination of grass species in African rangelands. *International Journal of Remote Sensing*, 22:3421–3434.
- Schmidt, K. S. and Skidmore, A. K. (2003). Spectral discrimination of vegetation types in a coastal wetland. *Remote Sensing of Environment*, 85(1):92–108.
- Schmidtlein, S. (2000). *Aufnahme von Vegetationsmustern auf Landschaftsebene*. PhD thesis, Ludwig-Maximilians-Universität München, published: Nationalparkverwaltung Berchtesgaden, Forschungsbericht 44.
- Schmidtlein, S. (2003). Raster-based detection of vegetation patterns at landscape scale levels. *Phytocoenologia*, 33:603–623.
- Schmidtlein, S. and Sassin, J. (2004). Mapping of continuous floristic gradients in grasslands using hyperspectral imagery. *Remote Sensing of Environment*, 92:126–138.
- Schmidtlein, S., Zimmermann, P., Schüpferling, R., and Weiß, C. (2007). Mapping the floristic continuum: Ordination space position estimated from imaging spectroscopy. *Journal of Vegetation Science*, 18:131–140.
- Schneider, W., Suppan, E., Steinwendner, J., and Bartl, R. (1997). Automatic Extraction of Landscape Ecology Features from Satellite Imagery by Computer Vision Techniques. In *Proceedings of Geospatial Information Age*, volume 4, pages 630–639, Washington state convention and trade center.
- Schouten, M. C. G. (1984). Some aspects of the ecogeographical gradient in Irish ombrotrophic bogs. *Peat Congress, Dublin*, 1:414–432.
- Schuckert, U. (1998). *Monitoring der Hoch- und Zwischenmoorvegetation mit Methoden der Fernerkundung am Beispiel des Wurzacher Riedes*. PhD thesis, University Hohenheim, published: Verlag Dr. Kovac, Hamburg.
- Scott, C. T. and Köhl, M. (1994). Sampling with partial replacement and stratification. *Forest Science*, 40:30–46.
- Serrano, L., Ustin, S. L., Roberts, D. A., Gamon, J. A., and Peñuelas, J. (2000). Deriving water content of chaparral vegetation from AVIRIS data. *Remote Sensing of Environment*, 74:570–581.

- Shepard, R. N. (1962). The analysis of proximities: Multidimensional scaling with an unknown distance function. *Psychometrika*, 27:125–139, 219–246.
- Sinclair, T. R., Hoffer, R. M., and Schreiber, M. M. (1971). Reflectance and internal structure of leaves from several crops during a growing season. *Agronomy Journal*, 63:864–868.
- Smith, A. J. E. (2004). *The moss flora of Britain and Ireland*. University Press, Cambridge, 3 edition.
- Smith, M. L. and Carpenter, C. (1996). Application of the USDA Forest service national hierarchical framework of ecological units at the sub-regional level: the New England - New York example. *Environmental Monitoring and Assessment*, 39:187–198.
- Smith, M. L., Ollinger, S. V., Martin, M. E., Aber, J. D., Hallett, R. H., and Goodale, C. L. (2002). Direct estimation of aboveground forest productivity through hyperspectral remote sensing of canopy nitrogen. *Ecological Applications*, 12(5):1286–1302.
- Smits, P. C., Dellepiane, S. G., and Schowengerdt, R. A. (1999). Quality assessment of image classification algorithms for land-cover mapping: a review and a proposal for a cost-based approach. *International Journal of Remote Sensing*, 20(8):1461–1486.
- Spanglet, H. J., Ustin, S. L., and Rejmankova, E. (1998). Spectral reflectance characteristics of california subalpine marsh plant communities. *Wetlands*, 18(3):307–319.
- Ssymank, A. (1997). Anforderungen an die Datenqualität für die Bewertung des Erhaltungszustandes gemäß den Berichtspflichten der FFH-Richtlinie. *Natur und Landschaft*, 72(11):477–480.
- Ssymank, A., Hauke, U., Rückriem, C., Schröder, E., and Messer, D. (1998). Das europäische Schutzgebietssystem Natura 2000. BfN-Handbuch zur Umsetzung der Fauna-Flora-Habitat-Richtlinie und der Vogelschutz-Richtlinie. *Landschaftspflege und Naturschutz*, 53.
- Ssymank, A., Petersen, B., Ellwanger, G., Biewald, G., Hauke, U., Ludwig, G., Pretscher, P., and Schröder, E. (2003). Das europäische Schutzgebietssystem Natura 2000. Ökologie und Verbreitung von Arten der FFH-Richtlinie in Deutschland. Band 1: Pflanzen und Wirbellose. *Landschaftspflege und Naturschutz*, 69.

- Steele, B. M., Patterson, D. A., and Redmond, R. L. (2003). Toward estimation of map accuracy without a probability test sample. *Environmental and Ecological Statistics*, 10:333–356.
- Stehman, S. V. (1992). Comparison of systematic and random sampling for estimating the accuracy of maps generated from remotely sensed data. *Photogrammetric Engineering and Remote Sensing*, 58(9):1343–1355.
- Stehman, S. V. (1996). Cross-Validatory Choice and Assessment of Statistical Predictions. *Photogrammetric Engineering and Remote Sensing*, 62(4):401–407.
- Stellmach, M. and Langensiepen, I. (2006). Kartieranleitung Biotopkartierung Bayern Teil 2: Biotoptypen. <http://www.bayern.de/lfu/natur/Biotopkartierung/index.html>.
- Stellmach, M. and Langensiepen, I. (2007). Kartieranleitung Biotopkartierung Bayern Teil 1: Arbeitsmethodik. <http://www.bayern.de/lfu/natur/Biotopkartierung/index.html>.
- Stohlgren, T. J., Owen, A. J., and Lee, M. (2000). Monitoring shifts in plant diversity in response to climate change: a method for landscapes. *Biodiversity and Conservation*, 9:65–86.
- Stone, M. (1974). Cross-Validatory Choice and Assessment of Statistical Predictions. *Journal of the Royal Statistical Society. Series B (Methodological)*, 36(2):111–147.
- Strahler, A. (2002). Global Land Cover: Approaches to Validation. In *GLC2000 Meeting*, Ispra. JRC.
- Strohwasser, P. (1990). Ergänzungen zur Liste der Farn- und Blütenpflanzen des Naturschutzgebietes Murnauer Moos. unveröffentlichtes Manuskript.
- Strohwasser, P. (1994). Errichtung und Sicherung schutzwürdiger Teile von Natur und Landschaft mit gesamtstaatlich repräsentativer Bedeutung. Projekt: Murnauer Moos, Moore westlich des Staffelsees, Bayern. *Natur und Landschaft*, 69:326–368.
- Strohwasser, P. (2006). Kartierung von Naturschutzgebieten. unpublished. personal communication.
- Succow, M. and Jeschle, L. (1990). *Moore in der Landschaft. Entstehung, Haushalt, Lebewelt, Verbreitung, Nutzung und Erhaltung der Moore*. Verlag Harri Deutsch, Thun, 2 edition.

- Swanson, F. J. and Sparks, R. E. (1990). Long-term ecological research and the invisible place. *Bioscience*, 40:502–508.
- Tansley, A. G. and Chipp, T. F. (1926). *Aims and Methods in the study of vegetation*. British Empire Vegetation Committee, London, 6 edition.
- Tenenbaum, J. B. (1998). *Mapping a manifold of perceptual observations. Advances in neural information processing systems*. MIT Press, Cambridge, MA.
- Tenenbaum, J. B., de Silva, V., and Langford, J. C. (2000). A global geometric framework for nonlinear dimensionality reduction. *Science*, 290:2319–2323.
- Thessler, S., Ruokolainen, K., and Tuomisto, H. (2005). Mapping gradual landscape-scale floristic changes in Amazonian primary rain forests by combining ordination and remote sensing. *Global Ecology and Biogeography*, 14:315–325.
- Thichy, L. (2002). JUICE, software for vegetation classification. *Journal of Vegetation Science*, 13:451–453.
- Thomas, V., Treitz, P., Jelinski, D., Miller, J., Lafleur, P., and McCaughey, J. H. (2002). Image classification of a northern peatland complex using spectral and plant community data. *Remote Sensing of Environment*, 84:83–99.
- Tompkins, S., Mustard, J. F., Pieters, C. M., and Forsyth, D. W. (1997). Optimization of Endmembers for Spectral Mixture Analysis. *Remote Sensing of Environment*, 59:472–489.
- Townsend, P. A. (2000). A Quantitative Fuzzy Approach to Assess Mapped Vegetation Classifications for Ecological Applications. *Remote Sensing of Environment*, 72:253–267.
- Townsend, P. A. and Walsh, S. J. (2001). Remote sensing of forested wetlands: application of multitemporal and multispectral satellite imagery to determine plant community composition and structure in southeastern USA. *Plant Ecology*, 157:129–149 A.
- Traxler, A. (1998). *Handbuch des vegetationsökologischen Monitorings; Teil A: Methoden*. Umweltbundesamt Wien.

- Treitz, P. M., Howarth, P. J., and Suffling, R. C. (1992). Application of detailed ground information to vegetation mapping with high spatial resolution digital imagery . *Remote Sensing of Environment*, 42:65–82.
- Tüxen, R., Miyawaki, A., and Fujiwara, K. (1972). Eine erweiterte Gliederung der Oxycocco-Sphagnetea. In Tüxen, R., editor, *Grundfragen und Methoden in der Pflanzensoziologie*, pages 500–520, Junk, Den Haag.
- Uhlig, P. W. C. and Jordan, J. K. (1996). A spatial hierarchical framework for the co-management of ecosystems in Canada and the United States for the Upper Great Lakes Region. *Environmental Monitoring and Assessment*, 39:59–73.
- Underwood, E., Ustin, S. L., and DiPietro, D. (2003). Mapping nonnative plants using hyperspectral imagery . *Remote Sensing of Environment*, 86(2):150–161.
- Ustin, S., Roberts, D. A., Gamon, J. A., Asner, G. P., and Green, R. O. (2004). Using imaging spectroscopy to study ecosystem processes and properties. *BioScience*, 54:523–533.
- Ustin, S. L., Roberts, D. A., Pinzon, J., Jacquemoud, S., Gardner, M., Scheer, G., Castañeda, C., and Palacios-Orueta, A. (1998). Estimating Canopy Water Content of Chaparral Shrubs Using Optical Methods . *Remote Sensing of Environment*, 65:280–291.
- van der Meer, F. D. and de Jong, S. M. (2001). *Imaging Spectrometry: Remote sensing and digital image processing*. Kluwer Academic Publishers, Dordrecht, 4 edition.
- Verdebout, J., Jacquemoud, S., Andreoli, G., Hosgood, B., and Schmuck, G. (1994). Investigations on the biochemical components NIR absorption features in AVIRIS and laboratory reflectance spectra of vegetation. In *IGARSS Geoscience and Remote Sensing Symposium - Surface and Atmospheric Remote Sensing: Technologies, Data Analysis and Interpretation*, volume 2, pages 993–995, Ispra, Italy.
- Vollmar, F. (1947). Die Pflanzengesellschaften des Murnauer Mooses. *Berichte der Bayerischen Botanischen Gesellschaft*, 27:13–97.
- Wagner, A., Wagner, I., and Georgii, B. (2000a). *Pflege- und Entwicklungsplan Murnauer Moos, Moore westlich des Staffelsees und Umgebung*. Unveröffentlichtes Gutachten im Auftrag des Landkreises Garmisch-Partenkirchen, Garmisch-Partenkirchen.

- Wagner, A., Wagner, I., and Georgii, B. (2000b). *Pflege- und Entwicklungsplan Murnauer Moos, Moore westlich des Staffelsees und Umgebung, Band II E: Floristisch-vegetationskundliche Grundlagen*. Landratsamt Garmisch-Partenkirchen.
- Walter, H. and Lieth, H. (1967). *Klima-Diagramm-Atlas*. Gustav Fischer Verlag, Jena.
- Wang, F. (1990). Improving Remote Sensing Image Analysis through Fuzzy Information Representation. *Photogrammetric Engineering and Remote Sensing*, 56 /8:1163–1169.
- Weiss, C. (2003). Zur Standortbindung und zu Einflüssen der Beweidung in alpinen Phytozönosen am Beispiel Frauenalpl im Wettersteingebirge. Master's thesis, Ludwig-Maximilians-Universität München.
- Wenkel, K. O., Wegehenkel, M., and Lutze, G. (2003). Einsatzmöglichkeiten für und Anforderungen an die Fernerkundung aus der Sicht der Landschaftsforschung und des Landschaftsmonitoring. In Dech, S. W. e. a., editor, *DFD-Nutzerseminar*, volume 20, pages 167–177.
- Wessman, C. A. (1994). Estimation Canopy Biochemistry through Imaging Spectrometry. In Hill, J. and Mégier, J., editors, *Imaging Spectrometry - a Tool for Environmental Observations*, pages 57–69. Kluwer, Dordrecht.
- Wessman, C. A., Bateson, C. A., and Benning, T. L. (1997). Detecting fire and grazing patterns in tallgrass prairie using spectral mixture analysis. *Ecological Applications*, 7:493–511.
- Whittaker, R. H. (1956). Vegetation of the Great Smoky Mountains. *Ecological Monographs*, 26:1–80.
- Wiegand, G. (1992). Explorative Datenanalyse und räumliche Skalierung - eine kritische Evaluation. *Verhandlungen der Gesellschaft für Ökologie*, 21:327–338.
- Wieneke, F., Dietz, K. R., Sachweh, M., and Strahtmann, F.-W. (1988). Satellitenbilddauswertung - Methodische Grundlagen und ausgewählte Beispiele. In *Münchener Geographische Abhandlungen*, volume A 38. Institut für Geographie der Universität München.
- Williams, D. J., Rybicki, N. B., Lombana, A. V., O'Brien, T. M., and Gomez, R. B. (2003). Preliminary investigation of submerged aquatic vegetation mapping using hyperspectral remote sensing. *Environmental Monitoring and Assessment*, 81(1):383–392.

- Williams, W. T. and Lambert, J. M. (1939). Plant associations on land. *American Midland Naturalist*, 21:1–27.
- Williams, W. T. and Lambert, J. M. (1959). Multivariate methods in plant ecology. I. Association analysis in plant communities. *Journal of ecology*, 47:83–101.
- Wold, H. (1966). Estimation of principal components and related models by iterative least squares . In Krishnaiah, P., editor, *Multivariate analysis*, pages 391–420. Academic Press.
- Wold, S., Sjöström, M., and Eriksson, L. (2001). PLS-regression: a basic tool of chemometrics. *Chemometrics and Intelligent Laboratory Systems*, 58:109–130.
- Wooley, J. T. (1971). Reflectance and Transmittance of Light by Leaves. *Plant Physiology*, 47:656–662.
- Wunsch, J. (2006). Hyperspektrale Fernerkundung zur Kartierung von FFH-Lebensraumtypen mit multipler Regression (Murnauer Moos). Master's thesis, Ludwig-Maximilians-Universität München.
- Yamano, H., Chen, J., and Tamura, M. (2003). Hyperspectral identification of grassland vegetation in Xilinhot, Inner Mongolia, China. *International Journal of Remote Sensing*, 24(15):3171–3178.
- Zarco-Tejada, P. J., Miller, J. R., Noland, T. L., Mohammed, G. H., and Sampson, P. H. (2001). Scaling up and model inversion methods with narrow-band optical indices for Chlorophyll content estimation in closed forest canopies with hyperspectral data. *IEEE Transactions in Geosciences and Remote Sensing*, 39(7):1491–1507.
- Zimmermann, P. (2005). Abbildende Spektroskopie als Werkzeug für die Kartierung von Vegetationsübergängen im Murnauer Moos. Master's thesis, Universität Bayreuth.

Appendix A

Tables

A.1 MRPP: Tests on homogeneity

Table A.1: MRPP test: Floristic homogeneity among subplots 2004 - boldly printed plots were excluded from further analyses.

2004 rank order	Original				DCA axis values			
	Plot	Bray Curtis distance	Plot	$\log_{10}[\text{cover}]$ Bray Curtis distance	Plot	Euclidean distance	Plot	$\log_{10}[\text{cover}]$ Euclidean distance
1	S 18	0.82	S 18	0.81	S 18	434.80	S 18	306.40
2	N 77	0.72	N 64	0.59	S 06	166.50	N 64	161.35
3	N 79	0.63	N 77	0.51	N 16	114.32	N 77	118.59
4	N 76	0.59	N 65	0.46	N 07	108.16	S 13	109.10
5	N 25	0.59	N 79	0.45	N 04	105.20	S 06	100.10
6	N 09	0.58	N 22	0.44	N 79	98.34	N 22	95.47
7	N 07	0.57	S 13	0.43	N 77	95.34	N 65	75.26
8	N 38	0.57	N 04	0.41	N 03	90.29	N 79	72.66
9	N 13	0.55	N 21	0.40	N 13	89.69	S 42	67.80
10	N 03	0.53	N 33	0.39	N 08	88.13	N 78	64.39
11	N 04	0.53	N 38	0.38	N 05	86.68	S 29	62.00
12	N 16	0.51	N 76	0.38	N 53	85.46	N 33	61.07
13	N 33	0.51	N 09	0.37	N 22	84.86	S 09	60.10
14	N 24	0.51	S 40	0.36	N 18	84.39	N 53	58.67
15	N 19	0.50	S 03	0.36	N 24	82.03	S 03	54.80
16	N 21	0.47	N 03	0.36	N 02	76.02	N 21	54.27
17	N 18	0.47	N 13	0.36	N 09	71.96	N 70	51.85
18	S 34	0.47	N 78	0.35	N 14	69.21	N 66	51.10
19	N 14	0.46	N 16	0.35	N 38	68.37	S 41	49.20
20	N 05	0.45	N 80	0.35	N 33	67.33	N 16	48.57
21	N 22	0.45	N 18	0.34	N 25	65.88	S 02	46.50
22	N 27	0.44	S 29	0.34	N 65	64.01	N 03	45.21
23	N 53	0.43	N 75	0.34	N 78	62.02	N 38	45.01
24	S 06	0.42	N 25	0.33	N 21	61.01	N 09	44.75
25	S 20	0.42	N 05	0.33	S 42	54.30	S 30	44.60
26	N 75	0.42	N 07	0.32	N 11	53.21	N 02	43.47
27	N 51	0.41	N 60	0.32	S 24	52.20	N 73	42.97
28	N 02	0.40	N 67	0.32	S 40	51.70	S 26	42.90
29	N 65	0.40	S 23	0.32	N 27	50.03	S 14	42.80
30	S 13	0.40	N 66	0.31	S 02	49.30	S 10	41.90
31	N 20	0.40	N 19	0.31	N 75	47.43	S 40	41.20
32	N 11	0.39	N 53	0.31	S 13	47.10	N 68	41.07
33	N 64	0.38	S 06	0.30	N 30	46.54	N 63	40.85
34	N 43	0.37	S 42	0.30	S 20	45.10	N 80	38.27
35	N 30	0.37	N 59	0.30	N 19	44.33	S 04	37.60
36	S 10	0.36	N 11	0.30	N 76	41.61	N 25	37.34
37	N 08	0.36	S 37	0.30	N 64	40.95	N 74	37.22
38	S 33	0.33	N 08	0.30	N 20	38.82	N 62	36.88
39	N 26	0.33	N 20	0.29	S 29	38.50	N 60	36.76
40	N 78	0.33	N 24	0.29	S 34	38.00	S 23	36.00

2004	Original				DCA axis values			
			$\log_{10}[\text{cover}]$				$\log_{10}[\text{cover}]$	
rank order	Plot	Bray Curtis distance	Plot	Bray Curtis distance	Plot	Euclidean distance	Plot	Euclidean distance
41	N 62	0.32	N 51	0.29	N 62	37.92	S 20	35.70
42	N 36	0.32	S 34	0.28	S 25	37.40	S 01	34.80
43	S 42	0.31	N 29	0.28	N 41	34.44	S 37	34.60
44	N 63	0.31	S 41	0.27	N 49	34.36	N 59	34.53
45	N 41	0.31	S 10	0.27	S 31	34.10	N 55	33.97
46	N 60	0.30	S 20	0.27	N 26	30.65	S 21	33.40
47	S 39	0.30	N 14	0.27	S 36	29.90	N 67	33.05
48	S 21	0.29	N 27	0.26	N 80	28.13	N 19	33.00
49	N 80	0.28	N 73	0.25	N 63	28.08	N 24	32.93
50	N 52	0.28	N 62	0.25	N 47	28.01	S 15	32.90
51	N 35	0.28	S 02	0.25	N 43	27.57	N 51	32.38
52	S 38	0.27	N 71	0.25	S 26	27.30	N 58	32.34
53	S 02	0.26	N 41	0.25	S 15	26.80	N 13	32.01
54	S 24	0.25	S 21	0.25	N 35	26.06	N 04	31.35
55	N 46	0.24	N 26	0.24	N 10	26.00	N 54	31.18
56	N 10	0.24	S 27	0.24	S 10	25.90	N 48	30.81
57	S 15	0.24	S 12	0.24	N 60	25.57	N 76	30.75
58	S 40	0.24	N 02	0.24	N 71	24.69	N 41	30.69
59	N 32	0.24	N 44	0.23	N 31	24.11	N 42	30.28
60	N 40	0.23	N 36	0.23	S 41	23.80	S 25	28.90
:	:	:	:	:	:	:	:	:
80	S 44	0.19	N 54	0.20	N 46	17.09	N 14	21.07
81	N 47	0.18	N 32	0.20	S 09	16.30	N 11	20.59
82	S 32	0.18	S 32	0.20	N 66	16.17	N 46	19.63
83	S 16	0.18	S 07	0.20	S 33	15.70	S 33	19.20
84	N 70	0.17	S 35	0.19	S 03	14.80	S 24	18.60
85	S 26	0.17	N 70	0.19	N 73	14.74	N 71	18.10
86	S 41	0.16	N 55	0.19	S 05	14.60	N 30	18.08
87	S 22	0.16	S 17	0.19	S 37	14.40	N 44	17.69
88	S 25	0.15	S 30	0.18	N 68	14.27	N 52	17.49
89	S 03	0.15	N 35	0.18	N 54	14.08	S 36	17.00
90	S 09	0.15	N 30	0.18	N 37	13.76	N 35	16.41
91	S 19	0.15	N 48	0.17	S 11	13.70	N 15	16.01
92	N 55	0.14	S 39	0.17	N 40	13.52	S 16	16.00
93	S 07	0.14	S 33	0.17	N 57	13.46	S 17	14.90
94	N 37	0.13	N 52	0.17	S 27	12.40	N 31	14.83
95	S 28	0.13	S 38	0.17	S 39	12.20	N 20	14.54
96	S 05	0.12	N 46	0.17	S 44	11.30	N 18	13.77
97	S 17	0.12	S 19	0.17	S 14	11.20	S 44	12.20
98	S 36	0.12	N 15	0.17	S 12	10.80	N 40	11.24
99	S 14	0.12	S 16	0.17	S 32	10.70	S 19	11.20
100	S 08	0.11	N 47	0.17	N 55	10.63	N 49	11.13
101	S 12	0.11	S 25	0.16	N 58	10.28	S 27	10.50
102	S 04	0.11	N 74	0.16	S 35	10.10	S 39	9.50
103	N 73	0.11	S 31	0.15	S 28	8.80	S 22	9.00
104	S 11	0.10	S 43	0.15	S 22	7.80	S 34	8.70
105	N 58	0.10	N 31	0.14	S 07	7.30	S 43	8.20
106	N 68	0.09	N 69	0.13	S 17	6.80	N 37	7.55
107	S 30	0.09	S 05	0.13	N 74	6.45	S 32	6.80
108	S 35	0.09	S 22	0.13	N 69	4.94	N 26	6.37
109	N 74	0.06	S 44	0.12	S 43	4.50	N 32	6.04
110	S 01	0.05	N 37	0.11	S 01	4.10	S 38	5.10
111	N 69	0.04	S 36	0.08	S 08	3.50	S 08	1.10

Table A.2: MRPP test: Spectral homogeneity among subplots 2004 - boldly printed plots were excluded from further analyses

2004		original spectra		$\log_{10}[1/R]$		original spectra		$\log_{10}[1/R]$	
rank order	Plot	Euclidean distance	Plot	Euclidean distance	rank order	Plot	Euclidean distance	Plot	Euclidean distance
1	S 08	12731.00	N 10	4.67	57	N 15	1164.92	S 24	1.02
2	S 18	12445.00	S 15	2.80	58	N 42	1163.89	S 42	0.99
3	N 10	11082.54	S 08	2.53	59	N 53	1159.96	N 62	0.95
4	S 36	5468.00	S 41	2.30	60	N 65	1158.24	N 68	0.94
5	N 64	4370.58	N 54	2.24	61	N 69	1155.74	S 22	0.92
6	N 79	4073.89	N 07	2.24	62	S 40	1146.00	S 14	0.91
7	N 70	3722.22	N 38	2.18	63	S 17	1146.00	N 09	0.90
8	N 77	3233.20	N 51	2.06	64	S 07	1146.00	N 22	0.92
9	N 78	3223.22	N 31	2.04	65	S 12	1137.00	S 38	0.87
10	N 07	3159.14	N 67	2.04	66	S 41	1126.00	S 10	0.87
11	S 43	2964.00	N 11	2.01	67	S 01	1118.00	N 78	0.86
12	N 05	2706.83	N 03	2.00	68	N 38	1109.19	N 42	0.86
13	N 72	2678.93	N 69	1.88	69	N 80	1102.57	N 66	0.85
14	S 16	2671.00	S 18	1.86	70	N 24	1080.55	N 79	0.84
15	N 76	2604.88	S 35	1.84	71	N 44	1080.36	N 59	0.81
16	S 11	2308.00	N 65	1.80	72	S 05	1077.00	N 29	0.80
17	N 73	2171.34	S 19	1.75	73	N 03	1056.66	N 48	0.77
18	N 63	2155.67	N 20	1.67	74	S 27	1032.00	S 09	0.77
19	S 42	2135.00	N 33	1.62	75	N 67	989.41	S 11	0.76
20	S 34	2099.00	N 16	1.60	76	N 09	988.02	S 23	0.74
21	S 13	2045.00	S 39	1.59	77	N 16	975.61	N 55	0.72
22	N 33	2032.95	N 37	1.59	78	N 29	969.94	N 21	0.72
23	N 60	1982.44	N 77	1.55	79	N 04	911.82	N 05	0.70
24	S 31	1928.00	N 15	1.55	80	S 09	898.00	N 30	0.69
25	N 22	1919.28	N 60	1.55	81	N 11	880.68	N 40	0.69
26	N 74	1917.16	S 30	1.53	82	N 49	877.80	N 24	0.69
27	N 18	1825.57	S 02	1.52	83	N 51	868.78	S 01	0.68
28	N 48	1816.25	N 27	1.48	84	S 33	849.00	N 19	0.68
29	S 20	1789.00	S 16	1.46	85	S 10	830.00	S 36	0.66
30	N 54	1785.12	N 14	1.45	86	N 46	822.83	S 03	0.65
31	S 35	1781.00	N 74	1.44	87	N 36	815.33	S 07	0.62
32	S 15	1759.00	N 49	1.43	88	S 39	795.00	S 40	0.60
33	N 31	1733.06	N 41	1.42	89	N 37	780.15	N 73	0.56
34	S 23	1732.00	N 63	1.41	90	S 24	758.00	N 02	0.56
35	N 41	1727.61	N 47	1.40	91	N 14	757.25	N 44	0.55
36	S 14	1724.00	N 08	1.39	92	S 04	751.00	N 25	0.54
37	S 22	1706.00	S 20	1.38	93	S 26	749.00	S 25	0.54
38	N 02	1676.64	S 43	1.37	94	S 28	742.00	N 04	0.54
39	N 20	1667.95	N 80	1.36	95	N 71	730.80	N 58	0.53
40	S 44	1639.00	S 33	1.35	96	N 43	728.64	N 64	0.53
41	S 19	1600.00	S 34	1.34	97	N 58	724.56	S 21	0.53
42	S 30	1557.00	N 18	1.33	98	S 06	699.00	S 13	0.52
43	N 47	1553.34	N 72	1.29	99	N 59	655.91	N 46	0.51
44	N 08	1504.83	N 53	1.28	100	N 21	649.51	S 32	0.51
45	S 37	1495.00	S 12	1.28	101	N 35	620.50	S 05	0.49
46	S 25	1454.00	S 44	1.28	102	N 25	551.07	S 27	0.49
47	N 66	1453.48	N 52	1.26	103	N 13	542.43	S 06	0.44
48	N 40	1453.28	N 32	1.26	104	N 55	535.83	N 75	0.44
49	S 32	1434.00	N 43	1.25	105	N 57	509.19	N 13	0.43
50	N 68	1374.90	S 37	1.20	106	N 75	485.78	N 35	0.42
51	S 03	1373.00	S 17	1.19	107	N 27	483.76	N 71	0.36
52	S 21	1362.00	S 31	1.19	108	N 26	474.84	N 36	0.35
53	N 19	1244.76	S 04	1.17	109	S 29	453.00	S 26	0.35
54	N 30	1179.32	N 76	1.17	110	N 32	428.32	S 29	0.35
55	S 38	1175.00	S 28	1.12	111	N 62	380.90	N 57	0.33
56	S 02	1173.00	N 70	1.03	112	N 52	305.29	N 26	0.28

Table A.3: MRPP test: Spectral homogeneity among plots 2005 - boldly printed plots were excluded from further analyses

2005		original spectra		$\log_{10}[1/R]$		original spectra		$\log_{10}[1/R]$	
rank order	Plot	Euclidean distance	Plot	Euclidean distance	rank order	Plot	Euclidean distance	Plot	Euclidean distance
1	25	6149.69	70	3.07	51	90	1219.63	67	1.19
2	70	4910.06	23	2.27	52	68	1204.75	72	1.16
3	38	4203.94	26	2.17	53	14	1200.73	100	1.13
4	44	3295.69	59	2.14	54	16	1153.62	7	1.12
5	77	3235.92	18	2.00	55	83	1143.90	66	1.11
6	22	2972.11	5	1.94	56	1	1127.71	2	1.11
7	18	2958.82	52	1.93	57	13	1119.32	47	1.09
8	6	2734.60	37	1.79	58	31	1110.14	96	1.01
9	60	2475.84	22	1.75	59	78	1107.69	4	0.98
10	63	2367.48	81	1.74	60	27	1097.46	68	0.98
11	61	2316.67	60	1.68	61	41	1096.57	89	0.96
12	19	2270.88	93	1.67	62	93	1086.18	39	0.95
13	72	2179.77	99	1.67	63	24	1076.36	17	0.95
14	12	2153.41	6	1.65	64	88	1069.57	1	0.90
15	17	2108.83	77	1.63	65	4	1045.09	41	0.88
16	73	2102.67	9	1.61	66	23	1039.10	14	0.86
17	74	2084.28	88	1.59	67	92	1010.55	51	0.85
18	34	2069.27	71	1.58	68	66	1007.79	62	0.84
19	59	2055.12	78	1.57	69	43	1003.37	85	0.82
20	36	1947.07	44	1.57	70	29	996.05	64	0.80
21	21	1881.76	13	1.57	71	52	995.73	87	0.80
22	30	1879.38	57	1.53	72	2	972.47	97	0.77
23	49	1774.01	36	1.53	73	75	963.57	28	0.77
24	62	1739.84	45	1.52	74	8	951.13	40	0.75
25	39	1699.59	11	1.50	75	98	935.99	56	0.75
26	37	1695.66	15	1.49	76	15	913.62	31	0.74
27	71	1689.75	19	1.47	77	97	904.65	29	0.71
28	64	1682.10	21	1.44	78	54	889.73	65	0.64
29	9	1639.11	50	1.43	79	69	853.99	83	0.63
30	35	1622.68	24	1.42	80	42	836.49	54	0.62
31	26	1550.90	61	1.41	81	51	832.66	82	0.61
32	50	1544.33	33	1.41	82	11	829.67	63	0.60
33	45	1544.21	16	1.41	83	87	821.78	80	0.59
34	20	1540.56	84	1.40	84	79	804.38	53	0.58
35	99	1534.98	73	1.40	85	86	803.77	30	0.57
36	84	1522.60	69	1.40	86	81	799.26	3	0.56
37	65	1404.71	74	1.38	87	91	770.21	49	0.54
38	85	1362.34	42	1.37	88	10	768.56	86	0.53
39	80	1334.50	12	1.35	89	58	758.34	98	0.50
40	5	1327.33	32	1.33	90	82	687.48	43	0.47
41	40	1324.86	34	1.33	91	100	680.70	95	0.46
42	28	1298.45	75	1.32	92	47	653.28	79	0.45
43	67	1297.95	55	1.32	93	95	648.90	10	0.42
44	53	1294.97	90	1.31	94	94	640.97	27	0.40
45	32	1289.13	76	1.30	95	89	628.38	20	0.39
46	57	1272.18	8	1.26	96	7	603.37	46	0.39
47	46	1266.44	91	1.25	97	48	576.70	94	0.39
48	33	1264.08	38	1.23	98	76	494.96	35	0.38
49	56	1255.04	92	1.20	99	55	486.97	58	0.38
50	3	1222.00	25	1.19	100	96	391.80	48	0.34

A.2 NMS Axis Scores

A.2.1 Data 2004

Table A.4: Two-dimensional NMS ordination solution: axis scores for the subset 2004 north

plot	NMS axis 1	NMS axis 2	plot	NMS axis 1	NMS axis 2
N 02	-1.14485	0.69869	N 42	-0.12063	-0.39113
N 03	-0.8249	0.74019	N 43	0.10077	-0.39094
N 04	-0.60529	0.58423	N 44	0.3963	-0.26676
N 05	-0.31055	0.59537	N 46	0.00413	-0.41865
N 07	-1.52471	0.74481	N 47	0.5375	-0.2377
N 08	-1.06126	0.97088	N 48	0.55846	-0.43869
N 09	-0.53937	0.27621	N 49	0.45174	-0.30713
N 11	-0.67581	0.12183	N 51	0.28111	-0.74097
N 13	-0.94332	0.28338	N 52	0.25102	-0.51554
N 14	-0.76558	0.52082	N 53	0.68686	-0.35369
N 15	-0.67392	0.34315	N 54	0.77106	-0.18268
N 16	-0.74092	0.50023	N 55	0.89447	-0.1611
N 18	-0.99702	0.62104	N 57	0.17455	-0.66095
N 19	-0.9539	0.09505	N 58	0.41501	-0.63998
N 20	-0.58286	0.48082	N 59	1.75754	0.17618
N 21	-0.3876	-0.45128	N 60	1.85291	0.59552
N 22	0.30457	0.70813	N 62	0.73473	-0.25546
N 24	-0.79044	0.24748	N 63	1.64165	-0.08189
N 25	-0.6103	0.03548	N 65	2.02825	-0.0816
N 26	-0.33511	-0.05341	N 66	0.35819	0.01583
N 27	-1.02653	-0.07981	N 67	1.60189	0.00639
N 29	-0.55356	0.14145	N 68	1.58472	-0.24886
N 30	-0.40613	-0.27897	N 69	1.8086	0.0135
N 31	-0.44118	-0.18463	N 70	0.53177	-0.75118
N 32	-0.79377	-0.2956	N 71	-0.06124	0.26958
N 33	-0.45063	0.02186	N 73	1.64377	-0.22249
N 35	-0.00073	-0.24644	N 74	1.53167	-0.33688
N 36	-0.15123	-0.46015	N 75	-1.11125	0.24334
N 37	0.13112	-0.30944	N 76	-1.26553	0.38456
N 38	-0.81636	-0.08025	N 78	0.5252	0.57932
N 40	-0.44332	-0.72355	N 79	0.42802	0.12301
N 41	-0.55987	-0.57087	N 80	-1.31791	0.28035

Table A.5: Two-dimensional NMS ordination solution: axis scores for the subset 2004 south

plot	NMS axis 1	NMS axis 2	plot	NMS axis 1	NMS axis 2
S 01	-0.14547	0.99299	S 25	0.189	0.53335
S 02	-0.6584	1.01913	S 26	-0.28445	-0.72347
S 03	0.06646	1.01781	S 27	-0.21884	-1.19158
S 04	-0.03156	0.87192	S 28	-0.28888	-1.18498
S 05	-0.22425	0.94315	S 29	1.11895	0.44564
S 07	-0.05835	0.97725	S 30	0.8874	0.46327
S 09	0.08361	0.8901	S 31	-0.27665	-0.46104
S 10	-0.01277	0.37352	S 32	-0.43906	-1.26989
S 11	-0.02839	0.54869	S 33	-0.54583	-1.25651
S 12	0.1804	0.64405	S 34	0.9511	0.65746
S 14	0.14753	0.74855	S 35	1.02451	0.58047
S 15	0.03599	-0.01908	S 36	0.29308	0.69161
S 16	-0.14918	-0.143	S 37	-0.03419	-1.42849
S 17	-0.4031	-0.19721	S 38	-0.61375	-1.27736
S 19	0.22329	0.64442	S 39	-0.58892	-1.10024
S 20	0.01718	0.13394	S 40	1.23494	0.1987
S 21	-0.32289	-0.47743	S 41	0.89745	0.36024
S 22	-0.19975	-1.13113	S 42	-0.36309	-1.40737
S 23	-0.60753	1.08456	S 43	-0.63151	-1.1732
S 24	0.33802	0.68698	S 44	-0.56214	-1.06582

A.2.2 Data 2005

Table A.6: Two-dimensional NMS ordination solution: axis scores for the subset 2005

plot	NMS axis 1	NMS axis 2	plot	NMS axis 1	NMS axis 2
1	-1.05149	-0.7856	52	-1.06055	-0.05163
2	-0.02446	-0.37468	53	-0.58805	-0.42401
3	-1.1852	-0.42568	54	-0.36995	0.14474
4	-1.23769	-0.03199	55	0.22442	-1.45226
5	-1.03171	-0.65387	56	-1.17055	-0.44129
6	-1.17472	-0.21607	57	0.9566	0.82006
7	-1.23102	0.15923	58	-1.1428	-0.46643
8	-1.18351	-0.14833	59	-1.13183	-0.6106
9	-1.09285	-0.44138	60	-1.21015	-0.43558
10	-0.61611	0.12512	61	0.451	1.32963
11	0.67374	-0.046	62	0.53612	1.25264
12	-0.98641	-0.2355	63	0.30627	1.43002
13	0.68424	1.26302	64	-0.03065	0.16007
14	-0.42378	-0.44295	65	1.28372	-0.09369
15	0.69003	0.69506	66	1.23861	-0.35862
16	0.80773	0.73194	67	-0.17132	1.57654
17	-1.18787	-0.23646	68	1.06207	-0.18601
18	-1.18622	-0.20001	69	-0.03658	1.47423
19	-1.24887	-0.15069	71	0.87332	-0.17321
20	-0.95839	-0.67144	72	0.11525	0.11809
21	0.74761	0.1015	73	0.63818	-0.18743
22	-0.04214	-0.60107	74	0.67285	-0.53934
23	0.80129	-0.08973	75	-0.05475	-0.20292
24	0.96304	0.29156	76	0.59219	0.38841
26	0.48575	-0.14005	77	0.70885	-0.10738
27	0.76215	-0.20347	78	0.82663	0.80664
28	0.72318	0.41286	79	0.594	-0.33562
29	0.79062	-0.20342	80	0.20419	1.17939
30	0.50926	0.7644	81	-1.14132	-0.49973
31	0.77025	0.2457	82	-1.08361	-0.5252
32	0.72891	0.19348	83	-1.18004	-0.40512
33	1.08661	-0.05844	84	-0.8301	-0.38717
34	0.78011	-0.30514	85	0.74341	0.90687
35	0.8337	-0.04964	86	0.67527	0.83306
36	0.71285	-0.49849	87	0.86842	-0.02871
37	0.80125	0.35665	88	0.79622	0.40838
39	1.102	-0.45469	89	0.06497	-0.43601
40	0.28158	0.9951	90	-0.19488	-0.41385
41	-0.19761	-0.47282	91	0.03744	0.37761
42	-0.443	-0.37016	92	-0.90897	-0.01943
43	-0.59863	-0.17449	93	0.73247	1.08356
44	0.54906	-0.56568	94	0.41935	-0.00513
45	-0.35176	-0.11238	95	0.44107	0.96925
46	0.80888	0.19248	96	0.62375	-0.47236
47	-1.27175	-0.27079	97	-1.23893	-0.41286
48	0.56614	0.27885	98	-1.36642	-0.339
49	-0.47098	-0.10536	99	-0.01955	-0.74511
50	0.7564	-0.82973	100	-0.49822	-0.3585
51	-0.47767	-0.38577			

A.3 Plot Header Data

Figure A.1: Plot header data of the subarea 2004 north

PLOTS Subarea 2004 north	X Gauß-Krüger coordinates	Y Gauß-Krüger coordinates	Covers [%]										green mosses (ex Sphagnum)	red Sphagnum	green Sphagnum	white Sphagnum	av. height of herbs [cm]	av. height of trees [m]	# of Phragmites comm. individuals
			water	bare soil	litter	vegetation	tree layer	shrub layer	herb layer	moss layer									
N_02	4438523.73	5280226.26	0.17	0.33	28.3	99	0	0	63.3	85.7	4.33	8	0	1.33	27	0	25		
N_03	4438585.29	5280185.68	11	0.33	18.7	89.3	0	0	58.3	66.3	16	4	0	1	27.3	0	16.7		
N_04	4438650.61	5280143.42	1.67	0.83	42.6	94.7	1.67	3	67.3	69.3	7	2.67	0	0	40	1.67	72.7		
N_05	4438710.99	5280102.11	1.5	0	50	98.7	0	34.3	58.3	38.7	1.83	1.5	0	0	40.7	0	100		
N_07	4438453.01	5280183.1	0	0	15.3	99.3	23.3	21.7	56.7	78.3	21	3.33	0	0	25.7	1	1.67		
N_08	4438514.24	5280142.81	0	0	4	98.7	0	27.7	55	80	3.33	3.17	0	1.33	27.7	0	20		
N_09	4438576.01	5280100.14	0	0	62.7	85	0	0	75	34	1.33	0.67	0	0.33	32	0	147		
N_10	4438639.31	5280060.46	1.33	0.67	30.7	96.7	0	0	79	44.3	3.67	2	0	0	38.3	0	138		
N_11	4438702.59	5280019.78	5.33	0.67	41	81	0	0	67.7	32	1.67	1.33	0.17	0.33	31.7	0	272		
N_13	4438440.37	5280098.19	16	1.33	39	81	0	0	60.7	31	1.67	2.83	0	0	27.3	0	10.7		
N_14	4438502.99	5280060.05	2.67	0.67	19	97.7	0	0	68.3	75.7	10.3	1.33	0	3.33	22.3	0	10		
N_15	4438567.41	5280018.53	0	0	40	99.3	0	0	97	23.7	1.33	0	0	0	29	0	53.3		
N_16	4438628.82	5279976.31	0.17	0.33	45	97.3	0	0	74.7	73.3	8	1.33	0	0	28.3	0	66.7		
N_18	4438364.9	5280060.59	4.33	0.33	8.67	94.7	0	0	48	75.7	7	9	0	3.33	26	0	0		
N_19	4438429.89	5280017.16	0	0	62.3	99.3	0	0	59.7	72	10.3	1.67	0	2	29.7	0	8.33		
N_20	4438492.84	5279972.88	0	0	25	97.7	0	0	82.3	36.3	3.67	1.33	0	0	29.7	0	130		
N_21	4438553.81	5279939.17	4	2.67	69.3	66.7	0	0	61.7	5.67	1.33	0	0	0	41.7	0	147		
N_22	4438619.77	5279894.46	0	0.33	77.6	78	0	0.33	72.7	24.3	5.33	0	0	0	46.7	0	143		
N_24	4438356.86	5279973.79	0	0	62.3	96	0	0	53.3	55	7.67	0.5	0	5.33	28	0	39.3		
N_25	4438420.64	5279927.54	0	0	68.6	87.7	0	0	80.7	8.33	4	1	0	0.67	37.3	0	21.7		
N_26	4438482.81	5279891.68	0.33	0.33	88.3	96	0	0	71.7	55	9.33	2.33	0	3.33	40.7	0	91.7		
N_27	4438545.17	5279852.06	0	2.67	46.7	97	0	0	65	83.3	4	0.33	0	6.67	34	0	27.3		
N_29	4438287.38	5279930.35	0	0.33	77	99.7	0	0	38.3	89.3	0	4.33	7.67	3	39.7	0	52.7		
N_30	4438349.07	5279890.99	0	0	55.7	85	0	0	58.3	46.7	0	2	4.67	1.67	42	0	51.7		
N_31	4438411.7	5279850.93	0	0.67	88.3	78.3	0	0	69.7	20.3	0	1.33	2	0.17	37.7	0	35.7		
N_32	4438472.02	5279810.92	0	0	72.3	94.7	0	0	68.3	75	6	0.17	0	0.67	31.7	0	28.3		
N_33	4438538.23	5279768.67	0	0	78.3	91.7	0	0	63.7	47	6	0.67	0	0	41.3	0	117		
N_35	4438275.28	5279845.79	0	0.33	96.3	65.7	0	0	64	2.33	0	0.17	1	0.17	27.3	0	93.3		
N_36	4438340.26	5279807.76	0	3.33	94	60.3	0	0	60.3	1	0	0	0.5	0	37.3	0	48.7		
N_37	4438403.92	5279767.36	0.33	2.33	95	75	0	0	75	0	0	0	0	0	42.3	0	105		
N_38	4438464.11	5279725.9	0.67	0.67	77	90	0	0	58.3	49	0	3.67	5	3.67	30	0	61.7		
N_40	4438205.29	5279805.18	0	0.33	94.7	71.7	0	0	71.7	0.67	0	0	0.33	0	31	0	77.7		
N_41	4438268.85	5279767.04	0.17	0.17	90	69.3	0	0	62.3	11.7	0	0.67	7.33	0.67	28.7	0	63.3		
N_42	4438331.58	5279724.89	0	0	89.3	70	0	0	68.3	1.67	0	0	0	0	37.7	0	71		
N_43	4438393.12	5279682.76	0.33	0.17	82.3	70.7	0	1.33	70	0	0	0	0	0	41.3	0	110		
N_44	4438455.65	5279643.19	3.33	0	96.3	80.3	0	0	80.3	0.33	0	0	0	0	50	0	146		
N_46	4438194.09	5279724.04	0	0	97.3	75	0	0	74.7	0.33	0.33	0	0	0	39.3	0	98.3		
N_47	4438257.28	5279682.59	0	0	96.3	75	0	0	75	0	0	0	0	0	52.7	0	278		
N_48	4438319.46	5279641.58	0.67	1.67	95	75	0	0	75	0	0	0	0	0	46	0	210		
N_49	4438382.01	5279600.71	0.5	3.33	85	83	0	0	83	0.33	0	0	0	0	49.7	0	210		
N_51	4438121.93	5279679.43	3.67	0.33	93.3	62	0	0	62	1.33	0.33	0	0	0	40	0	160		
N_52	4438185.14	5279640.57	0.33	0	97	67.7	0	0	67.7	0	0	0	0	0	36.7	0	114		
N_53	4438248.47	5279601.28	0	0	97	56	0	0	56	0	0	0	0	0	52.3	0	214		
N_54	4438311.67	5279556.32	0.17	0	96	72	0	0	72	0.33	0	0	0	0	50.7	0	210		
N_55	4438373.05	5279515.97	0	0	82	90.7	0	0	90.7	0	0	0	0	0	46.7	0	129		
N_57	4438113.18	5279597.51	0	0	96.7	67.7	0	0	67.7	0	0	0	0	0	42	0	195		
N_58	4438176.1	5279555.28	0	0	97.7	78.3	0	0	78.3	0	0	0	0	0	45	0	147		
N_59	4438237.89	5279513.97	0	5	95	47.3	0	0	47.3	0.33	0	0	0	0	18.3	0	383		
N_60	4438302.52	5279473.17	0	0	99.7	60.7	0	0	60.7	0	0	0	0	0	33.3	0	30		
N_62	4438041.6	5279552.82	2	1.67	84.7	79	0	0	79	0	0	0	0	0	43.7	0	197		
N_63	4438101.25	5279510.98	0.33	33.3	51.7	43.3	0	0	43.3	0	0	0	0	0	35	0	100		
N_64	4438167.01	5279474.33	16.7	0	84	75	0	0	73.3	6.67	6.67	0	0	0	38.3	0	333		
N_65	4438229.45	5279430.28	23.3	1	91.7	37.7	0	0	37.7	1.67	0.17	0	0	0	18.3	0	167		
N_66	4438292.22	5279390.49	1.67	0	95	78.3	0	0	78.3	1.67	0	0	1	0	44	0	83.3		
N_67	4437968.05	5279508.69	0	1.33	96	48.7	0	0.33	48.7	0	0	0	0	0	16.7	0	413		
N_68	4438030.66	5279470.62	0	2.67	71	91.7	0	0	91.7	0	0	0	0	0	63.3	0	0		
N_69	4438092.77	5279429.63	0	9.33	88.3	50	0	0	50	0	0	0	0	0	47.3	0	500		
N_70	4438155.79	5279387.23	0	0	97	76	0	4	72.7	0	0	0	0	0	48.7	0	107		
N_71	4438218.43	5279349.2	0	0	90	71.7	0	0	71.7	3.67	0.83	0	0	0	35	0	65		
N_72	4437955.33	5279427.37	66.7	0	10	25	0	0	25	0	0	0	0	0	26.7	0	0		
N_73	4438022.54	5279389.02	0	3.33	86.7	78.3	0	0	78.3	0	0	0	0	0	76.7	0	20		
N_74	4438062.81	5279347	1.67	0	96.7	75	0	0	75	0	0	0	0	0	53.3	0	0		
N_75	4438144.98	5279307.03	0	0.33	31	89	0	0	81.3	37	7.67	6.83	0	0.33	23.3	0	0		
N_76	4438211.68	5279266.67	0	0.83	31.8	97.3	0	0	75	60	6.67	4.67	0	0.17	25	0	0		
N_77	4437949.76	5279347.64	0	0	71.7	89.3	36.3	3.33	56.7	4.67	0.67	0	0	0	100	0	140		
N_78	4438011.79	5279304.18	0	0	60.7	99	20	0.67	84.7	13.3	1	0	0	0	60	0	110		
N_79	4438075.69	5279266.23	1	0	76	97.3	0	0	97.3	2.33	0	0	0	0	81.7	0	100		
N_80	4438137.12	5279225.68	0	1.33	17.6	96.3	0	0	91.7	17	2.33	0	0	0.83	20	0	0		

Figure A.2: Plot header data of the subarea 2004 south

PLOTS Subarea 2004 south	X Gauß-Krüger coordinates	Y Gauß-Krüger coordinates	Covers [%]													av. height of herbs [cm]	av. height of trees [m]	# of <i>Phragmites comm.</i> individuals		
				water	bare soil	litter	vegetation	tree layer	shrub layer	herb layer	moss layer	green mosses (ex <i>Sphagnum</i>)	red <i>Sphagnum</i>	green <i>Sphagnum</i>	white <i>Sphagnum</i>					
S_01	4438750.73	5279239.96	0	0	0	97.3	92.7	0	0	62.7	0	0	0	0	0	0	0	67.7	0	96.7
S_02	4438812.54	5279201.07	0	0	88.7	56.7	0	0	56.7	0	0	0	0	0	0	0	0	36	0	127
S_03	4438873.64	5279160.31	2.17	0	92.7	79.7	0	0	79.7	0.67	0	0	0	0	0	0	0	32.7	0	100
S_04	4438939.48	5279114.75	0	0	93.7	74.3	0	0	74.3	0.33	0.17	0	0	0	0	0	0	37	0	157
S_05	4439000.38	5279073.83	0	0.33	93.3	70.3	0	0.33	70.3	0.33	0	0	0	0	0	0	0	41.3	0	213
S_06	4439061.84	5279030.6	1.33	0	92	74.3	0	0	74.3	1.33	0.17	0	0	0	0	0	0	53.3	0	163
S_07	4438741.37	5279156.55	0	1.33	96	85	0	0	85	0	0	0	0	0	0	0	0	53.7	0	123
S_08	4438803.98	5279121.1	58	7	83.3	23.3	0	0	23.3	0	0	0	0	0	0	0	0	83.3	0	0
S_09	4438866.25	5279074.98	0	0.5	93.3	75.7	0	0	75.7	0.33	0	0	0	0	0	0	0	36	0	122
S_10	4438926.64	5279032	0	0.17	89.3	77.7	0	0	77.7	0	0	0	0	0	0	0	0	25	0	133
S_11	4438992.02	5278989.38	0	0.17	91.3	75.7	0	0	75.7	0	0	0	0	0	0	0	0	33.3	0	127
S_12	4438670.18	5279116.85	0	0.67	96.3	77.7	0	0	77.7	0	0	0	0	0	0	0	0	50.7	0	90.7
S_13	4438730.3	5279076.29	13.3	1.67	65.7	68.3	0	0	68.3	0	0	0	0	0	0	0	0	59	0	38.3
S_14	4438793.68	5279035.43	1.33	0.33	90.7	69	0	0	69	0	0	0	0	0	0	0	0	33.3	0	213
S_15	4438858.54	5278992.94	1	0.33	92.3	64	0	0	64	1.33	0.33	0	0	0	0	0	0	28.7	0	61.7
S_16	4438924.08	5278952.13	1.67	0	89	55	0	0	55	0	0	0	0	0	0	0	0	24	0	34
S_17	4438977.61	5278917.33	0.17	0.33	89.3	50	0	0	49	2.33	0.17	0	0	0	0	0	0	20.7	0	1.33
S_18	4438657.98	5279034.49	3.33	0	0	79	66.7	0	37.3	0	0	0	0	0	0	0	0	43.3	2	80
S_19	4438721.41	5278990.1	0	0	94.3	77.7	0	0	77.7	0	0	0	0	0	0	0	0	30.3	0	223
S_20	4438782.9	5278949.55	0	0	97.3	75	0	0	75	0	0	0	0	0	0	0	0	25.7	0	46.7
S_21	4438839.13	5278908.7	0.33	2.67	80	85	0	2.33	85	2	0	0	0	0	0	0	0	22.3	0	0
S_22	4438904.5	5278861.62	0.83	5.67	44.2	90.7	0	0	89.7	2	0	0	1	0	0	0	0	17.7	0	0
S_23	4438583.6	5278992.34	0	0.83	184	80.7	0	0	80.7	0	0	0	0	0	0	0	0	42.7	0	90
S_24	4438647.89	5278950.79	0.33	0	95.7	76.7	0	0	76.7	0	0	0	0	0	0	0	0	45.7	0	197
S_25	4438709.68	5278909.6	0	0	95	77	0	0	77	0	0	0	0	0	0	0	0	30.7	0	237
S_26	4438772.88	5278864.27	2	7	53.3	89.7	0	0	89.3	2.33	0.33	0	0	0	0	0	0	19	0	0
S_27	4438836.54	5278826.25	1.33	3	38.8	89.7	0	5.67	87.7	3.67	0	0	0	0	0	0	0	18	0	0
S_28	4438896.51	5278786.14	0	2	24.8	90.7	0	6	86	3	0.17	0	0.33	0	0	0	0	22.3	0	0
S_29	4438572.89	5278907.03	39.3	3.67	0.83	87.7	0	0	87.7	14.3	0	0	0	0	0	0	0	45.3	0	42.7
S_30	4438635.39	5278867.11	68.3	3.5	15.5	70	0	0	70	0.67	0.33	0	0	0	0	0	0	43.3	0	44.3
S_31	4438704.01	5278830.43	0.17	0.83	83	66.7	0	0	66.7	3.67	0.17	0	0.67	0	0	0	0	19	0	0
S_32	4438767.2	5278792.81	0	1.5	24.3	94.3	0	2.33	93	8.67	0	0	1.33	0	0	0	0	24.3	0	0
S_33	4438823.52	5278740.62	0.33	0.33	25.7	94.3	0	10	78.3	33.3	0	0.5	4.33	0	0	0	0	22.7	0	0
S_34	4438502.65	5278865.59	3.33	8.33	5	87	0	0	81.7	11.3	5.67	0	0	0	0	0	0	48.3	0	86.7
S_35	4438563.8	5278825.8	48.3	8.33	3.5	73.3	0	0	73	3.67	0.33	0	0	0	0	0	0	41.7	0	47.3
S_36	4438628.36	5278785.81	0.33	0	94.7	88.3	0	0	88.3	0.33	0.17	0	0	0	0	0	0	33.3	0	220
S_37	4438691.34	5278747.95	0.17	0.33	24	97	0	0	92	16.3	3	0.33	0.33	0	0	0	0	20	0	0
S_38	4438752.95	5278700.17	0.67	2.67	31.3	94.3	0	0	83.3	45	0	2.83	3	0	0	0	0	20.3	0	0
S_39	4438812.7	5278662.06	0.5	0.17	45.3	99.3	0	0	74.7	66.7	0	2.17	3.17	0	0	0	0	20	0	0
S_40	4438488.93	5278782.3	1.67	11	5.33	87.3	0	0	70.3	34.3	8.33	0	0	0	0	0	0	36.7	0	0
S_41	4438556	5278742.36	0.17	30	4.67	70	0	0	62.7	10	6	0	0	0	0	0	0	33.3	0	0
S_42	4438623.73	5278703.33	0	0.5	19	88	0	0	87.3	28.3	0.5	0	0.17	0	0	0	0	23.3	0	0
S_43	4438678.2	5278656.15	0	0.33	21	88	0	2	77	80	0	4.67	5.67	0	0	0	0	28.3	0	0
S_44	4438742.09	5278619.14	1.17	0.17	48.7	89	0	6	84.7	76.7	0	1.33	2.33	0	0	0	0	23.3	0	0

Figure A.3: Plot header data of the subarea 2005, Plot1-50

PLOTS Subarea 2005	X Gauß-Krüger coordinates	Y Gauß-Krüger coordinates	Covers [%]								av. height of herbs [cm]	av. height of trees [m]
			water	bare soil	litter	vegetation	tree layer	shrub layer	herb layer	moss layer		
1	4438840.55	5278819.29	0	0	100	100	0	10	100	1	25	0
2	4439126.71	5278701.28	0	0	90	100	0	0	100	10	35	0
3	4438758	5278206.15	0	0	45	100	80	0	90	90	30	2
4	4438045.11	5278542.11	0	0	70	100	75	0	70	55	17	1
5	4438848.96	5278774.07	1	0	70	100	10	0	98	10	27	2
6	4438090.53	5278483.12	0	0	20	100	0	0	90	90	20	0
7	4438730.27	5278779.8	0	0	60	100	0	0	99	30	30	0
8	4437874.29	5278400.15	0	0	50	100	0	0	99	90	25	0
9	4438492.42	5278217.67	0	0	50	100	0	25	80	90	27	0
10	4439094.6	5278566.82	0	2	90	98	0	6	90	20	25	0
11	4438975.38	5278969.52	0	0	90	100	0	0	80	0	45	0
12	4438162.14	5278956.69	0	0	35	100	45	0	85	95	35	4
13	4438584.81	5278796.96	25	5	5	80	0	0	75	5	30	0
14	4438569.25	5279107.02	0	0	70	100	30	2	75	60	40	1
15	4438618.61	5278882.03	17	0	20	83	0	0	80	10	42	0
16	4438351.03	5278507.45	0	0	90	100	0	0	90	80	40	0
17	4437892.09	5278445.6	0	0	40	100	4	10	98	90	20	1
18	4438112.02	5278429.96	0	0	90	100	30	0	95	60	40	2
19	4437681.21	5278285.67	0	0	80	100	30	0	98	90	25	2
20	4438008.11	5278155.21	1	0	75	99	0	0	90	80	30	0
21	4438405.09	5279222.41	0	0	100	100	0	0	95	0	60	0
22	4438322.97	5279129.83	0	0	98	100	50	0	90	15	70	5
23	4438663.11	5278904.94	1	0	100	100	0	0	95	0	55	0
24	4438444.06	5278922.16	0	0	100	100	0	3	97	10	50	0
25	4438357.374	5278837.4	15	0	85	85	0	3	85	3	60	0
26	4439183.53	5278713.2	0	0	2	100	0	0	100	1	45	0
27	4438473.49	5278368.75	0	2	98	98	0	0	85	0	85	0
28	4438680.95	5278961.04	0	0	100	100	0	0	95	0	70	0
29	4438421.02	5278243.15	0	0	98	100	0	0	95	6	40	0
30	4438317.87	5278141.96	0	0	20	100	0	0	100	60	40	0
31	4438631.03	5278948.05	0	0	100	100	0	0	95	0	50	0
32	4438401.71	5278886.17	0	0	98	100	0	0	100	1	65	0
33	4438507.29	5278912.6	0	0	100	100	6	0	100	1	60	2
34	4438231.34	5278756.39	0	0	100	100	0	0	96	1	70	0
35	4437619.93	5278626.19	0	0	100	100	0	0	80	0	65	0
35	4438595.69	5278688.58	0	0	100	100	0	0	100	1	55	0
37	4439189.93	5278833.89	0	0	80	100	0	0	100	5	45	0
38	4438276.2	5278266.35	0	0	95	100	0	0	97	10	28	0
39	4438327.529	5278207.765	0	0	10	100	0	0	100	1	45	0
40	4438287.64	5277999.71	0	0	10	100	0	0	100	80	30	0
41	4438157.68	5278794.96	0	0	98	100	0	0	65	45	30	0
42	4437924.17	5278980.24	0	0	65	100	0	0	70	65	35	0
43	4438237.96	5279089.87	0	2	15	98	0	10	95	65	30	0
44	4438825.29	5278969.45	0	0	95	100	0	0	70	0	50	0
45	4437921.7	5279285.01	0	0	15	100	0	0	99	90	15	0
46	4437937.79	5278648.55	7	0	93	93	0	0	66	0	40	0
47	4437904.33	5278536.35	0	0	20	100	40	0	90	100	25	2
48	4437668.78	5278528.68	0	1	100	99	0	0	75	1	60	0
49	4437545.81	5278462.12	0	0	35	100	0	0	75	90	37	0
50	4438369.53	5278207.46	0	0	20	100	0	0	100	80	55	0

Figure A.4: Plot header data of the subarea 2005, Plot 51-100

PLOTS Subarea 2005	Gauß-Krüger coordinates		Covers [%]								av. height of herbs [cm]		av. height of trees [m]	
	X	Y	water	bare soil	litter	vegetation	tree layer	shrub layer	herb layer	moss layer				
51	4438034.88	5279010.63	0	0	85	100	0	0	95	70	30	0		
52	4438121.79	5278954.8	0	0	25	100	0	8	97	90	27	0		
53	4438145.28	5278906.05	0	0	90	100	0	0	75	95	30	0		
54	4437850.36	5278874.71	0	0	75	100	0	0	95	70	38	0		
55	4438031.271	5278891.763	10	0	50	90	0	0	90	0	40	0		
56	4438865.58	5278672.97	0	0	90	100	0	3	95	70	40	0		
57	4438350.62	5278653.35	0	0	60	94	0	0	80	30	40	0		
58	4438832.8	5278400.79	0	0	20	100	0	7	90	95	25	0		
59	4438635.53	5278182.31	0	0	40	100	0	15	75	95	15	0		
60	4438813.89	5278113.72	0	0	60	100	0	0	90	90	25	0		
61	4437905.31	5279446.045	0	0	100	100	60	0	35	0	85	3		
62	4438093.18	5279361.53	0	0	100	100	0	0	25	0	80	0		
63	4437750.38	5279004.42	0	0	100	100	80	0	35	3	95	7		
64	4438234.49	5278418.13	0	8	35	92	0	0	92	70	60	0		
65	4438448.97	5278871.14	0	0	90	100	0	0	100	15	115	0		
66	4438304.209	5278408.75	0	0	98	100	0	0	100	0	100	0		
67	4438314.9	5278448.42	0	0	90	100	0	0	90	5	65	0		
68	4438276.997	5278562.364	0	0	95	100	0	0	100	0	65	0		
69	4438283.696	5278515.801	0	0	95	100	0	0	100	25	80	0		
70	4438286.509	5278107.238	0	0	5	100	0	0	100	90	65	0		
71	4437543.98	5278529.4	1	9	90	90	4	0	80	12	65	1		
72	4438192.5	5279224.79	0	0	80	100	0	0	97	65	50	0		
73	4438688.19	5278852.93	0	0	95	100	0	0	90	1	50	0		
74	4438656.89	5278802.15	0	0	90	100	0	0	95	1	45	0		
75	4438266.85	5278796.5	0	0	95	100	0	0	96	10	50	0		
76	4437782.32	5278677.05	0	0	100	100	0	0	97	12	80	0		
77	4437979.45	5278655.21	0	0	100	100	0	0	94	3	60	0		
78	4438320.44	5278636.09	0	0	70	100	0	0	100	3	40	0		
79	4438510.35	5278531.42	0	0	95	100	0	0	100	50	60	0		
80	4438343.02	5277978.01	0	0	7	100	0	0	100	50	60	0		
81	4438869.24	5278297.96	0	0	100	100	0	10	100	60	35	0		
82	4438843.81	5278568.53	1	0	98	100	0	0	85	80	25	0		
83	4438753.29	5278091.71	0	0	90	100	0	0	95	35	30	0		
84	4438577.36	5278085.05	0	0	70	100	0	0	95	100	35	0		
85	4438544.89	5278695.19	23	2	5	75	0	0	75	10	35	0		
86	4438547.39	5278872.49	12	0	10	88	0	0	90	18	45	0		
87	4439071.13	5278749.09	99	0	99	100	0	0	85	0	40	0		
88	4438408.54	5278518.74	0	0	100	100	0	0	98	5	45	0		
89	4438002.1	5278738.47	0	0	98	100	0	0	80	7	40	0		
90	4438199.51	5279289.25	0	0	90	100	0	0	95	35	30	0		
91	4437801.13	5278935.24	15	0	80	85	0	0	65	65	35	0		
92	4438200.86	5279049.89	0	0	40	100	12	0	55	100	15	1		
93	4438458.4	5278792.52	19	1	10	80	0	0	80	4	0	0		
94	4438366.78	5278596.62	1	4	20	95	0	0	95	10	35	0		
95	4437613.7	5278511.42	0	0	99	100	0	0	96	2	75	0		
96	4438458.75	5278318.02	20	0	80	80	0	0	60	0	40	0		
97	4438081.71	5278109.34	0	0	10	100	5	3	50	100	30	2		
98	4438468.58	5277976.68	0	0	15	100	20	0	60	100	20	2		
99	4437892.42	5278773.12	1	0	18	100	0	0	75	70	28	0		
100	4438613.31	5278542.34	0	0	98	100	0	0	80	73	45	0		

A.4 Vegetation Classification Tables

A.4.1 Phytosociology

A.4.2 Sociation

A.4.3 Fauna-Flora-Habitats

A 4.1 (2005)

Categorisation to Phytosociological vegetation types

Table with columns for vegetation types (PC, CM, CE, PS, AR, MC, MS1, MS2, PM, ET, SM) and rows for species (Phragmites, Schoenus, Arctostaphylos, Euphorbia, Dryas, etc.). Includes abbreviations and tree formations on the right.

s1: Aconitum napellus ssp. neomontanum (066), Aconitum vulpina (064), Agropyron caninum (068, 069, 067, 066), Agrostis carina (086, 016, 057, 078, 027), Agrostis gigantea (026), Athyrium filix-femina (072), Awochloa pubescens (068), Carex feruginea (078), Carex rostrata (002), Epilobium palustre (072), Euphrasia rostkoviana (039), Filipendula ulmaria (027), Fraxinus excelsior (051), Galium album ssp. album (039), Galium aparine (067, 064), Galium verum (039, 065), Juncea articulata (086, 064), Kurzia pauciflora (081), Leontodon hispidus (039), Leucanthemum vulgare agg. (039), Pheum pratense (067, 069, 039), Plantago major ssp. major (065), Polygala selysbii (027, 029), Primula grandiflora (039), Urtica dioica (067), Valeriana officinalis (069)

A 4.2 (2005)

Categorisation to Sociation vegetation types

Table with columns for vegetation types (Ph, F, CI, CE, M, T, Pn, C, CS) and rows for various plant taxa across different layers (tree, shrub, herb, moss, etc.).

tree formations

Summary table with columns 012, 061, 063 and rows corresponding to the taxa in the main table, showing numerical values.

Appendix B

Synthesis Maps

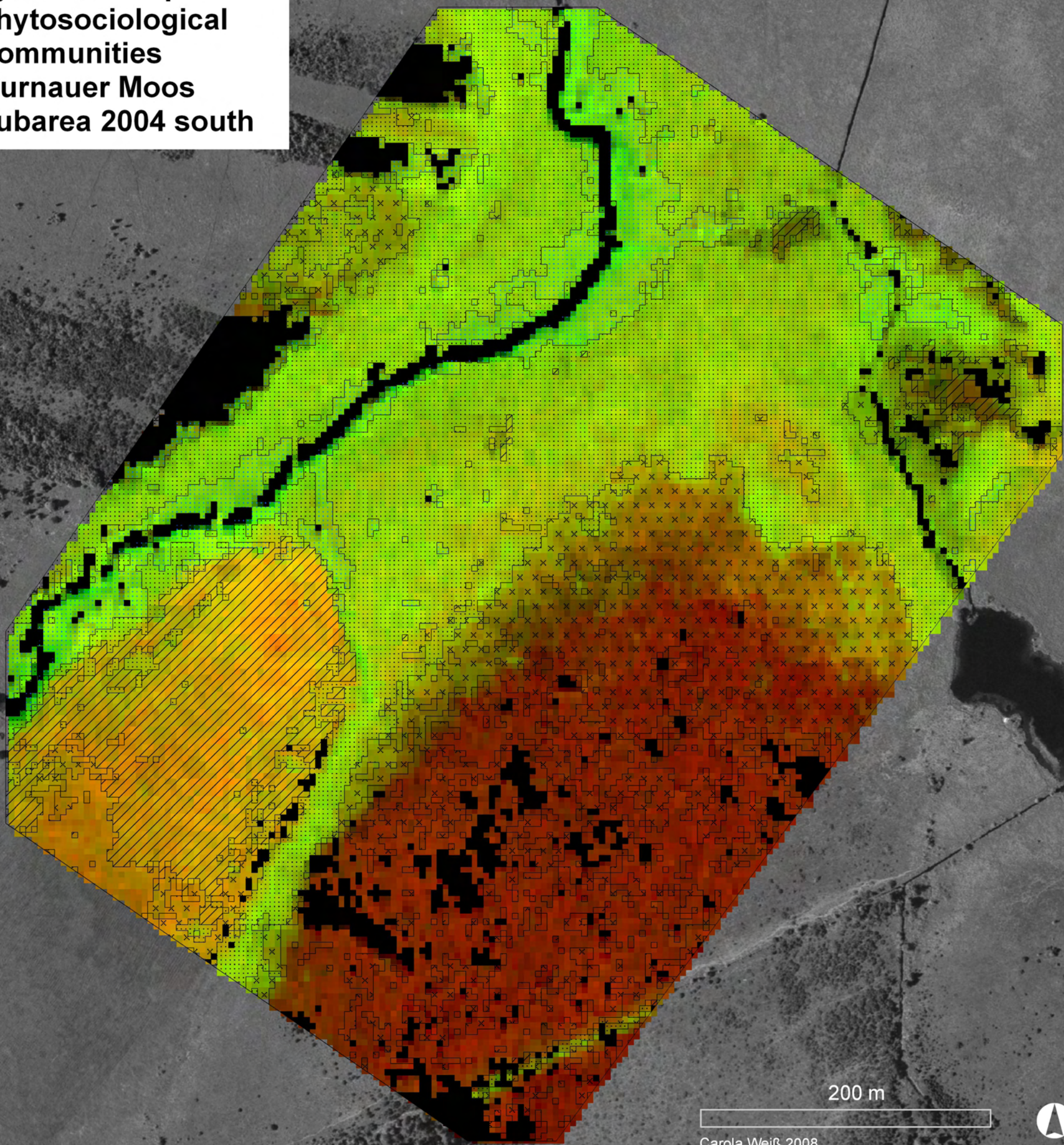
Synthesis Map of Phytosociological Communities Murnauer Moos Subarea 2004 south

5279190.000000

5279190.000000

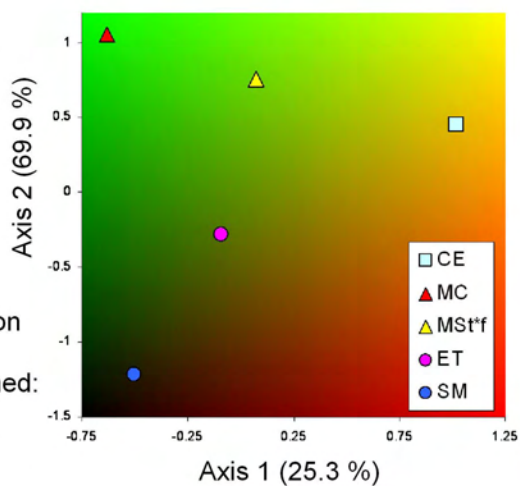
5278790.000000

5278790.000000



Carola Weiß 2008
Source of Orthophoto: Bavarian Survey Department (LVG)

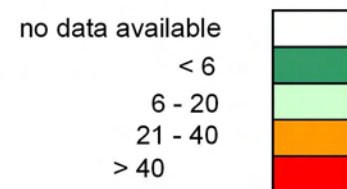
Colour Legend:
Colours derived from PLS regression models of NMS axis 1: red colour (R^2 0.68)
NMS axis 2: green colour (R^2 0.92)



Class Legend:
Classes derived from supervised image classification of HyMap™ scene with Spectral Angle Mapper ISD method
 κ : 0.83
Overall accuracy: 88 %

- Caricetum elatae* (CE)
- Molinetum caeruleae* (MC)
- Molinia*-Stadium (abandoned fen meadows) (MSt*f)
- Eriophoro-Trichophoretum cespitosi* (ET)
- Sphagnetum magellanici* (SM)
- Unclassified

Spectral separability:
wrong class assignment in [%]



	CE	MC	MSt*f	ET	SM
CE					
MC					
MSt					
ET					
SM					

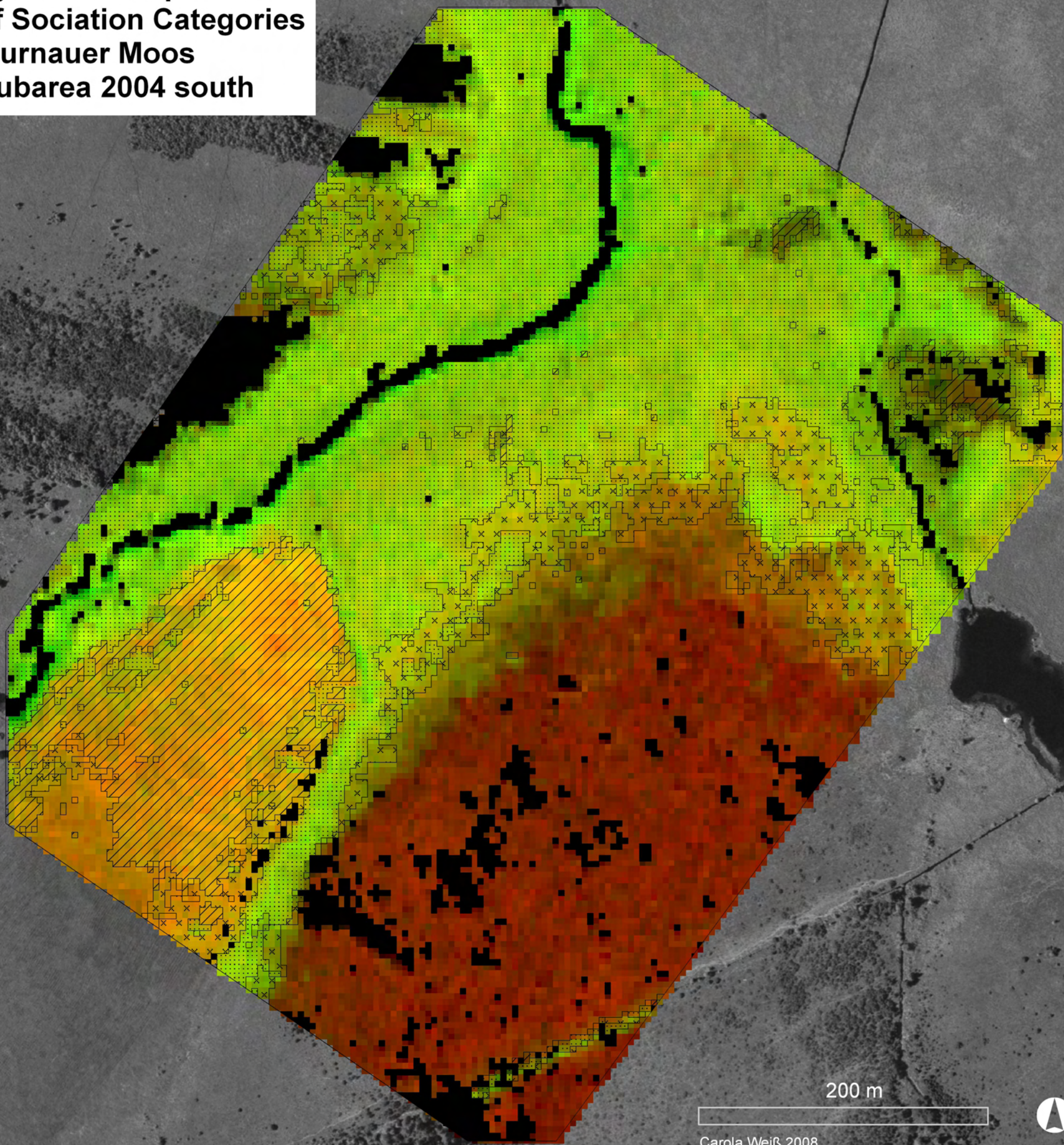
Synthesis Map of Sociation Categories Murnauer Moos Subarea 2004 south

5279190.000000

5279190.000000

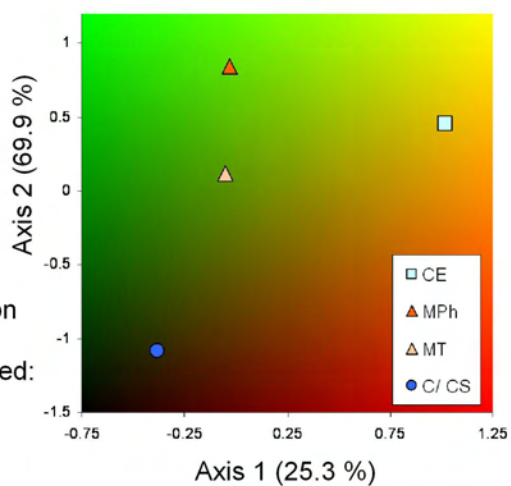
5278790.000000

5278790.000000



Carola Weiß 2008
Source of Orthophoto: Bavarian Survey Department (LVG)

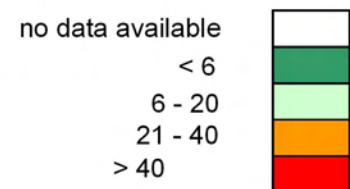
Colour Legend:
Colours derived from PLS regression models of
NMS axis 1: red colour (R^2 0,68)
NMS axis 2: green colour (R^2 0,92)



Class Legend:
Classes derived from supervised image classification
of HyMap™ scene with Spectral Angle Mapper ISD method
 κ : 0.93
Overall accuracy: 95 %

- Carex elata*-Sociation (CE)
- Phragmites communis*-*Molinia caerulea*-
Subconsociation (MPh)
- Molinia caerulea*-*Trichophorum cespitosum*-
Subconsociation (MT)
- Calluna vulgaris*-*Sphagnum*-Association (CS)
- Unclassified

Spectral separability:
wrong class assignment in [%]



	CE	MPh	MT	C/CS
CE				
MPh				
MT				
CS				

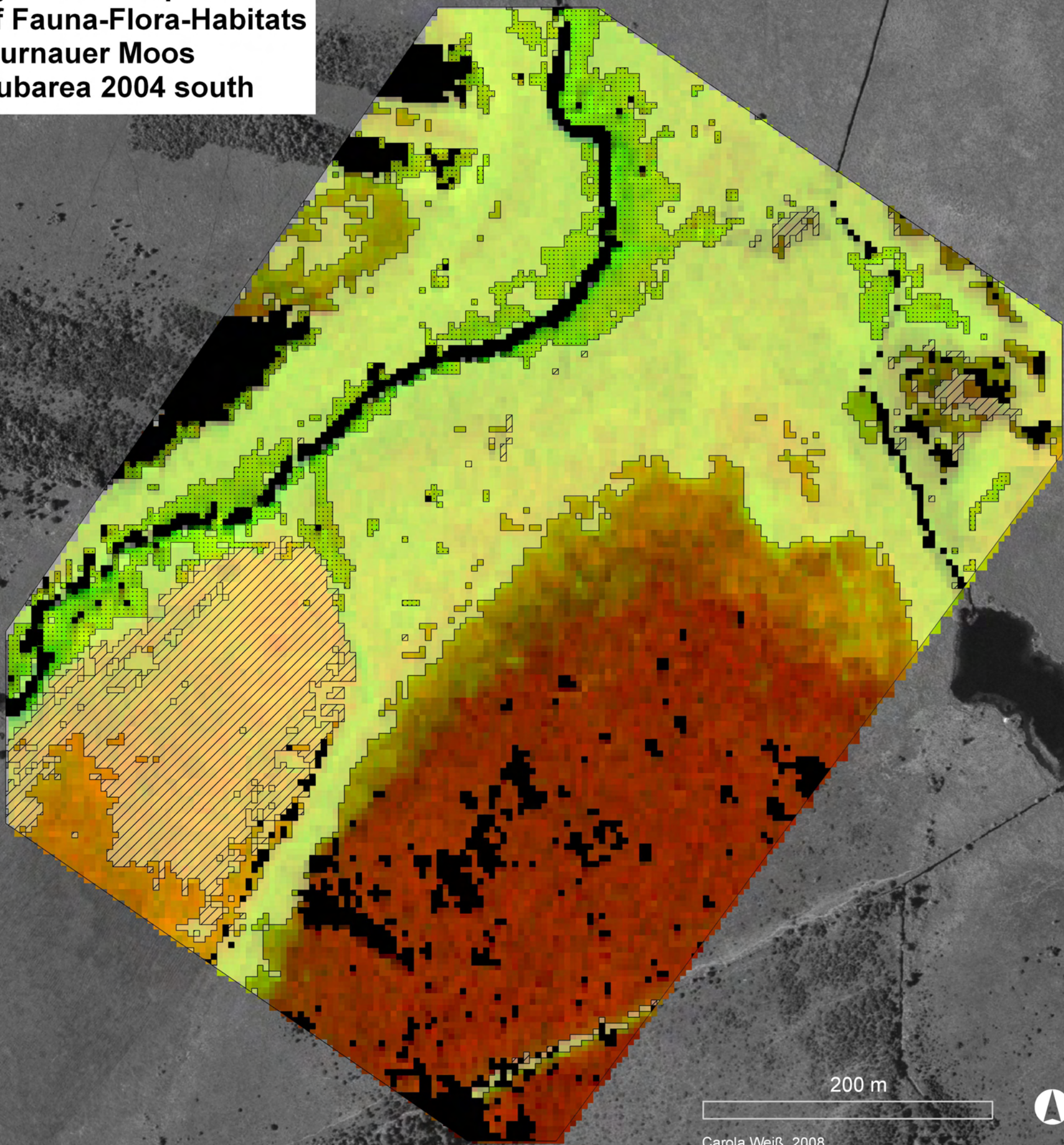
Synthesis Map of Fauna-Flora-Habitats Murnauer Moos Subarea 2004 south

5279190.000000

5279190.000000

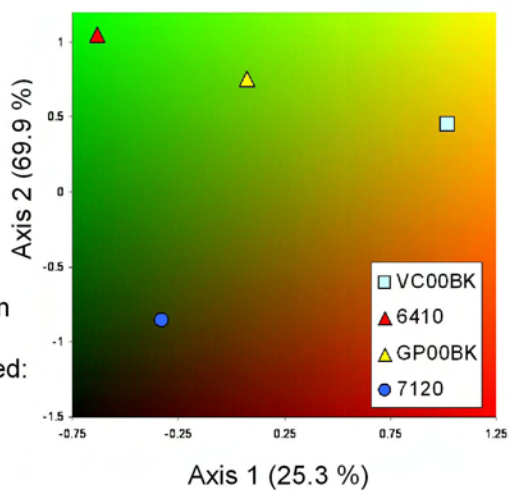
5278790.000000

5278790.000000



Carola Weiß 2008
Source of Orthophoto: Bavarian Survey Department (LVG)

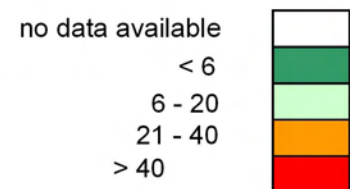
Colour Legend:
Colours derived from PLS regression models of
NMS axis 1: red colour (R^2 0.68)
NMS axis 2: green colour (R^2 0.92)



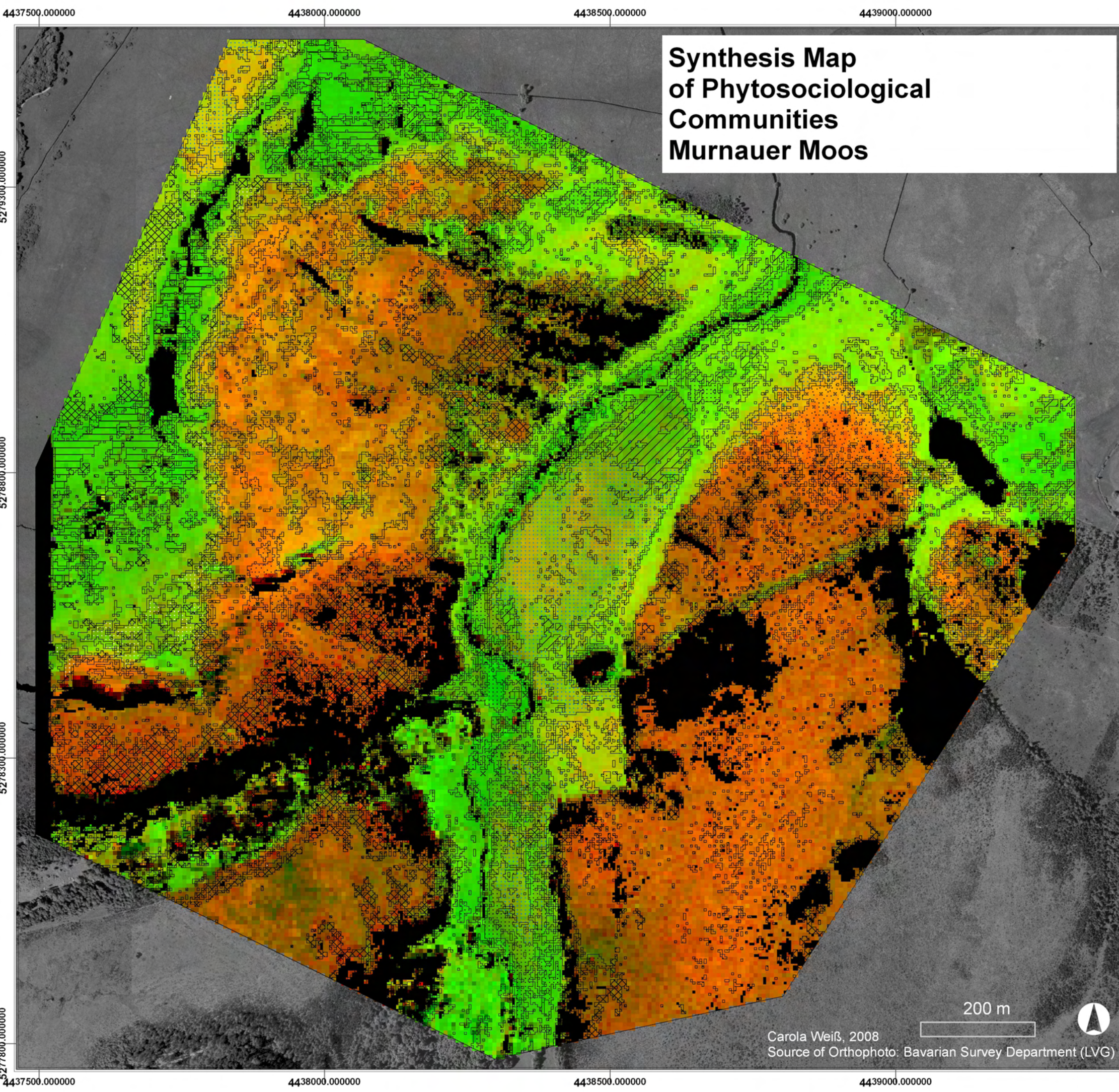
Class Legend:
Classes derived from supervised image classification
of HyMap™ scene with Spectral Angle Mapper ISD method
 $kappa$: 0.89
Overall accuracy: 93 %

- VC00BK (transparent 60 %)
- 6410
- GP00BK (transparent 60 %)
- 7120
- Unclassified

Spectral separability:
wrong class assignment in [%]



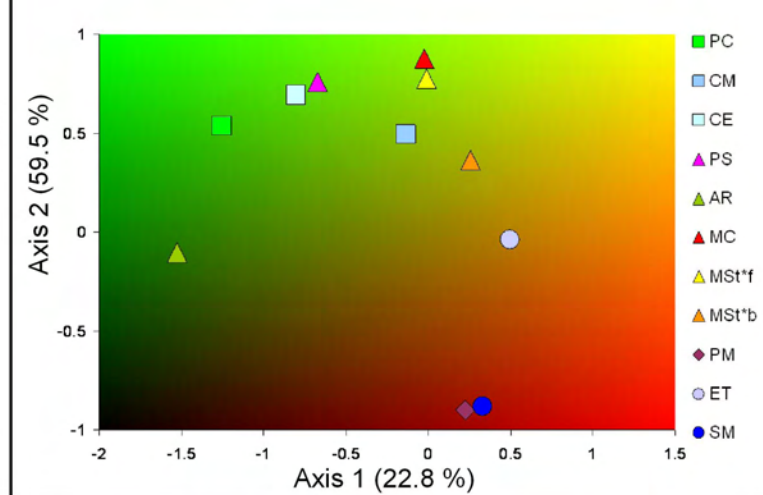
	VCO	6410	GP0	7120
VC00BK				
6410				
GP00BK				
7120				



Synthesis Map of Phytosociological Communities Murnauer Moos

Colour Legend:
Colours derived from PLS regression models of
NMS axis 1: red colour (R^2 0.29)
NMS axis 2: green colour (R^2 0.60)

Class centroids in NMS ordination space -
variance explained: 82.3 %

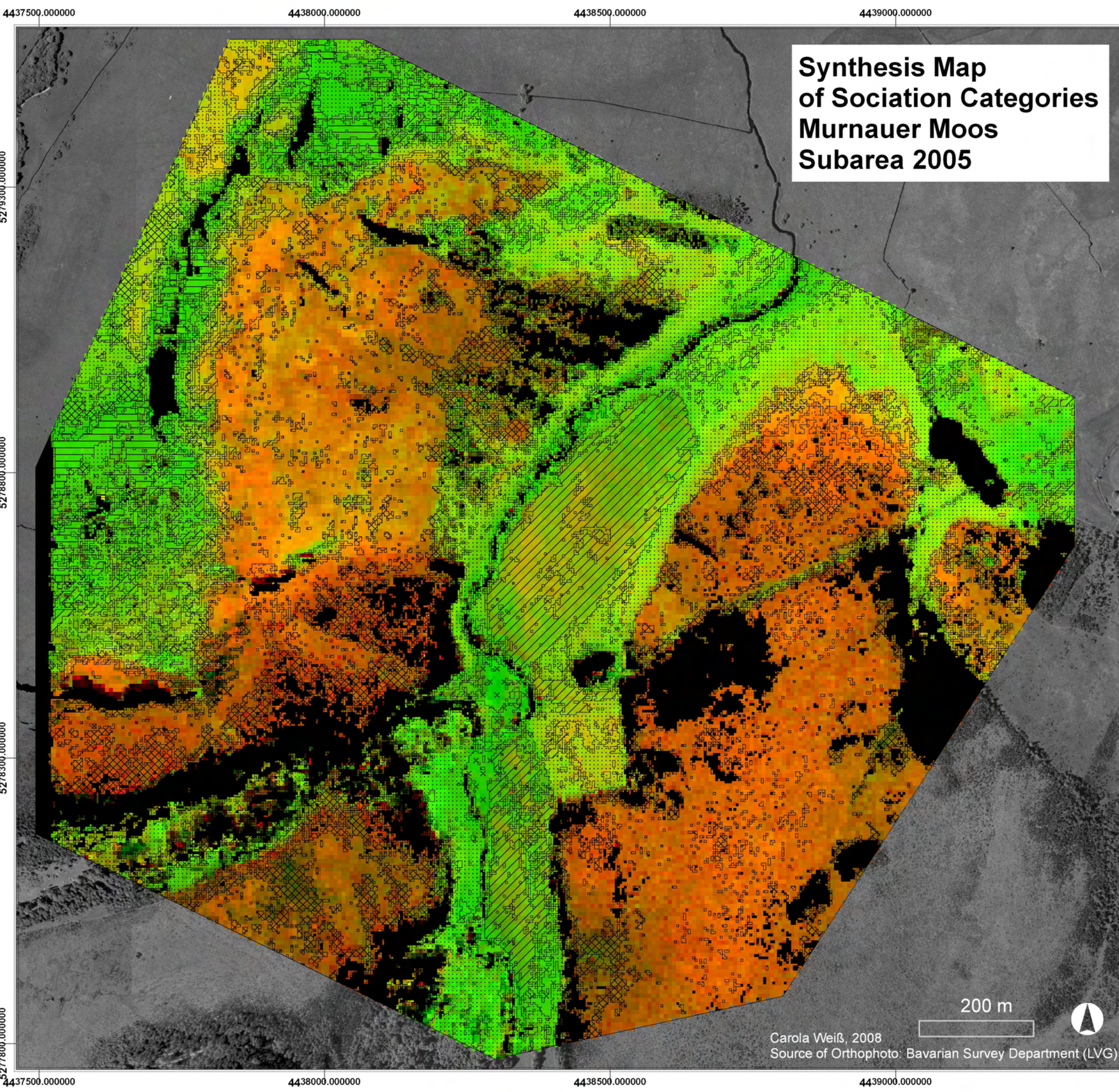


Class Legend:
Classes derived from supervised image classification
of HyMap™ scene with Spectral Angle Mapper ISD
method
 κ : 0.51

- Phragmitetum communis* (PC)
 - Cladietum marisci* (CM)
 - Caricetum elatae* (CE)
 - Primulo-Schoenetum ferruginei* (PS)
 - Arrhenatherion* (AR)
 - Molinietum caeruleae* (MC)
 - Molinia-Stadium* (MSt)
 - *f: abandoned fen meadows/ *b: desiccated bogs*
 - Pino mugo-Sphagnetum* (PM)
 - Eriophoro-Trichophoretum cespitosi* (ET)
 - Sphagnetum magellanicum* (SM)
 - Unclassified
- Spectral separability:
wrong class assignment in [%]
- no data available
 - < 6
 - 6 - 20
 - 21 - 40
 - > 40

	PC	CM	CE	PS	AR	MC	MSt*f	MSt*b	PM	ET	SM
PC											
CM											
CE											
PS											
AR											
MC											
MSt*f											
MSt*b											
PM											
ET											
SM											

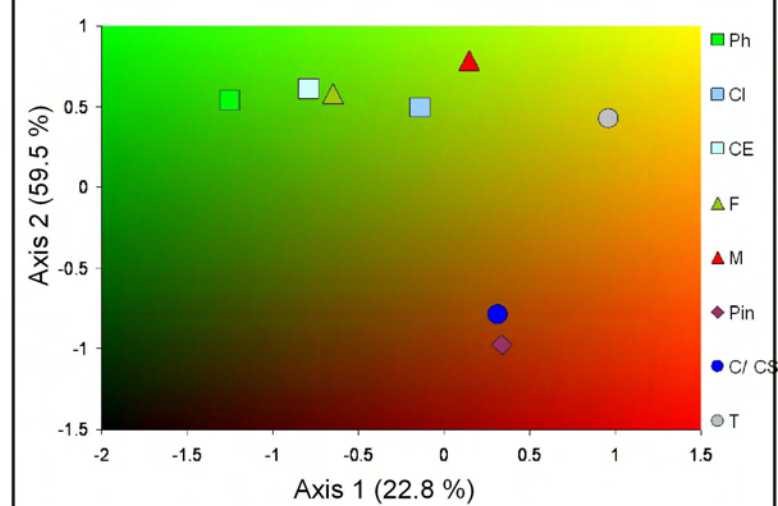
Carola Weiß, 2008
Source of Orthophoto: Bavarian Survey Department (LVG)



Synthesis Map of Sociation Categories Murnauer Moos Subarea 2005

Colour Legend:
Colours derived from PLS regression models of
NMS axis 1: red colour (R^2 0.29)
NMS axis 2: green colour (R^2 0.60)

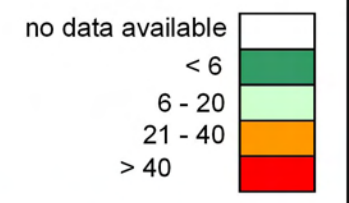
Class centroids in NMS ordination space -
variance explained: 82.3 %



Class Legend:
Classes derived from supervised image classification
of HyMap™ scene with Spectral Angle Mapper ISD
method
 $kappa$: 0.53

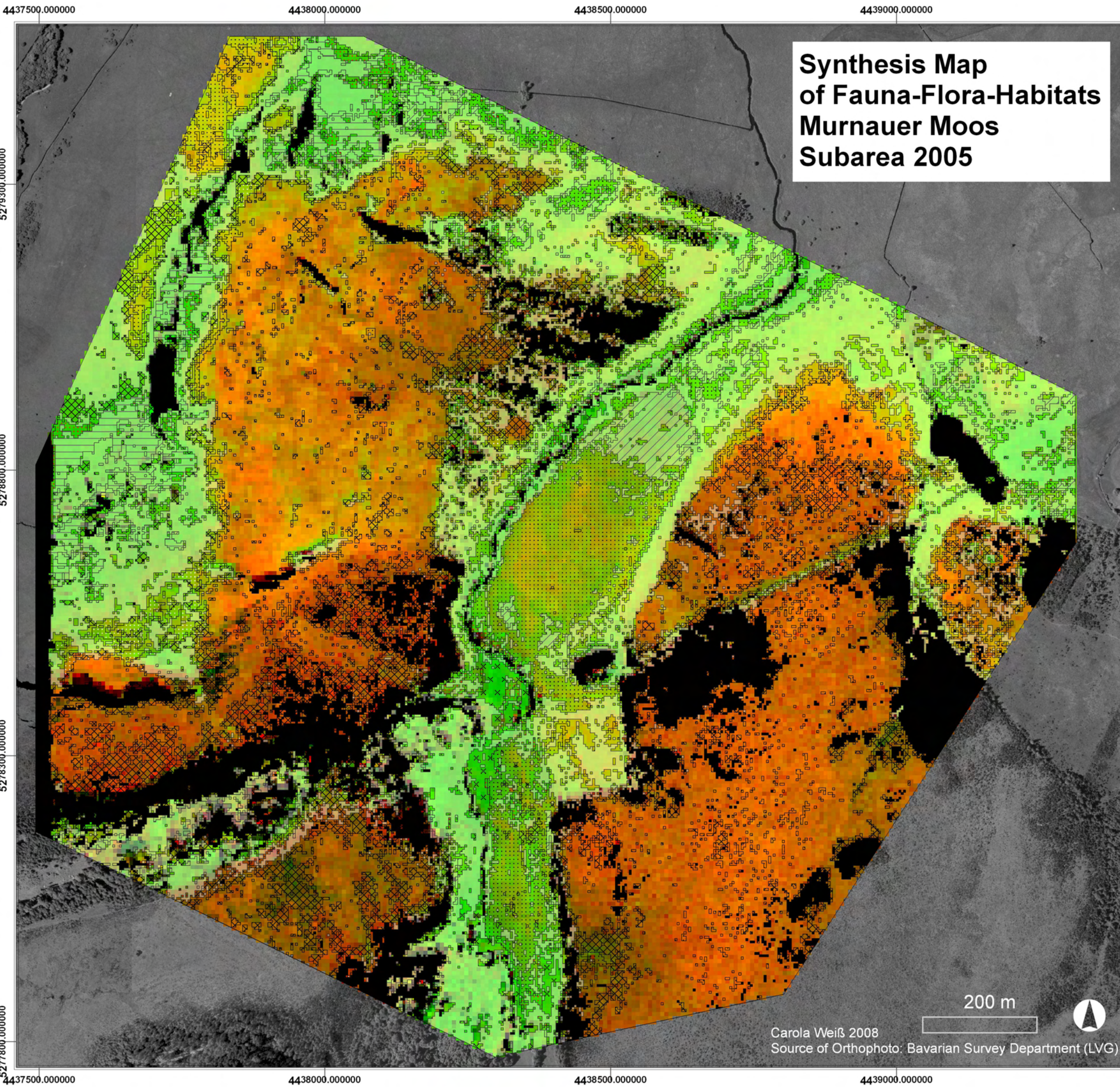
- Phragmites communis*-*Carex elata*-Sociation (Ph)
- Cladium mariscus*-*Molinia caerulea*-Subconsociation (CI)
- Carex elata*-Subconsociation (CE)
- Tall forb-Association (F)
- Molinia caerulea*-Consociation (M)
- Pinus mugo*-*Sphagnum*-Association (Pin)
- Calluna vulgaris*-Consociation (C)
- Trichophorum cespitosum*-Consociation (T)
- Unclassified

Spectral separability:
wrong class
assignment in [%]



	Ph	CI	CE	F	M	Pin	C/CS	T
Ph								
CI								
CE								
F								
M								
Pin								
C								
T								

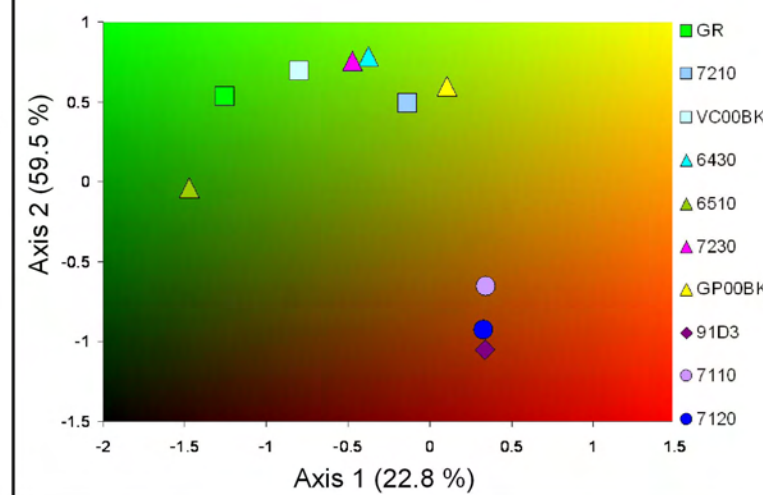
Carola Weiß, 2008
Source of Orthophoto: Bavarian Survey Department (LVG)



Synthesis Map of Fauna-Flora-Habitats Murnauer Moos Subarea 2005

Colour Legend:
Colours derived from PLS regression models of
NMS axis 1: red colour (R^2 0.29)
NMS axis 2: green colour (R^2 0.60)

Class centroids in NMS ordination space -
variance explained: 82.3 %



Class Legend:
Classes derived from supervised image classification
of HyMap™ scene with Spectral Angle Mapper ISD
method
kappa: 0.54

- GR (transparent 60 %)
 - 7210
 - VC00BK (transparent 60 %)
 - 6430
 - 6510-6520
 - 7230
 - GP00BK (transparent 60 %)
 - 91D3
 - 7110-7120
 - Unclassified
- Spectral separability:
wrong class
assignment in [%]
- no data available
 - < 6
 - 6 - 20
 - 21 - 40
 - > 40

	GR	7210	VC0	6430	6510	7230	GP0	91D3	7110	7120
GR										
7210										
VC00BK										
6430										
6510										
7230										
GP00BK										
91D3										
7110										
7120										

Carola Weiß 2008
Source of Orthophoto: Bavarian Survey Department (LVG)

Acknowledgements

First of all, I want to thank Prof Dr Friedrich Wieneke for supporting the project and providing valuable feedback, for encouragement, and for interesting discussions. Likewise, I want to thank Prof Dr Sebastian Schmidlein, who initialized and supervised this study, and who always gave inspirations if problems arose.

This research was supported by the Doctoral Scholarship Programme of the DBU (Deutsche Bundesstiftung Umwelt). I want to thank the DBU for three years of financing, interesting seminars, and to Mrs Dr Hedda Schlegel-Starmann in particular for her support in many questions. The equipment for the project was partially financed by the research funding of the DFG (Deutsche Forschungsgemeinschaft). Likewise, my thanks go to the LVG (Landesamt für Vermessung und Geoinformation Bayern) for the permission to use and publish highly resolved orthophotos (licence number 3272/ 08).

Especially during the last phases of this study I was provided and encouraged with companionship of my room colleagues Susan Niebergall, Monika Tepfenhardt, Florian Schlenz, and Johanna Dall'Amico, as well as by Andrea Reiter, Monika Prasch, and Dr Ulrich Strasser. Jens Neumeister carefully proof-read this work. My thanks are extended to Prof Dr Ralf Ludwig for referencing this thesis, and to Prof Dr Wolfram Mauser and all other colleagues at his Chair for Geography and Geographical Remote Sensing (Department of Geography, LMU München). It was a great pleasure to work there.

Andreas Müller at the Environment and Geoinformation Department at DLR Oberpfaffenhofen arranged the scene data acquisition. I want to thank him and his Department for preprocessing the data, for kind supports, and Martin Bachmann and Lena Liekfeld for discussions at milestones of this study.

I want to thank Uwe Friedel, Patrick Zimmermann, and Jörg Wunsch for the great work they did during relevé collection in summer 2004 and 2005, and for their evaluations and interesting discussions.

My thanks are extended to Prof Dr Carl Beierkuhnlein and his Chair of

Biogeography at University Bayreuth. Ralf Schüpferling aided the georeferencing of the scene, and GPS measurements. Very special thanks go to Prof Dr Eduard Hertel who post-classified all moss species, and to Dr Pedro Gerstberger who determined unassured classified vascular plants.

Thanks go to Peter Strohwasser at the LRA Garmisch-Partenkirchen, to Dr Alfred Wagner and Ingrid Wagner, and to Dr Martin Bucerius at the LfU Augsburg for discussing the application of the resulting methods that were developed during this study.

It is not possible to enumerate all who encouraged me emotionally during the last phase of this study. Many non phraseable thanks go to my parents who always helped if help was needed. I want to thank Rasmus and Emil for their patience, and Robert in particular, for his everlasting support.

curriculum vitæ

Personal Data

Name	Carola Weiß
Date of Birth	June 6, 1977
Place of Birth	Munich
Nationality	German
Education	1996: Abitur

Studies

1996/1999	Study of Lehramt an Gymnasien English and Geography at LMU, Munich
1999/2003	Study of Geography at LMU, Munich
2000	CIMO scholarship at University of Helsinki (Helsingin Yliopisto)
2003	Diploma of Geography with minor subjects Botany and Geology; Title of thesis: Untersuchungen zur Standortbindung und zu Einflüssen der Beweidung in alpinen Phytozönosen am Beispiel Frauenalpl im Wettersteingebirge
since 2004	PhD thesis in Geography at LMU, Munich

Employment

09-1997/07-1999	Student trainee at Siemens AG, Munich: Team assistance, documentations, and presentations
10/11-1999	Internship at ZAMG, Vienna: Development of a new guidance for phenological monitoring in Austria
05-2000/03-2001	Student trainee at Infineon Technologies AG, Munich: Conception, development and administration of internal network-shares
11/12-2001	Graduate assistant at Chair for Geography and Geographical Remote Sensing, LMU München: Support of current research projects
02/03-2002	Internship at GAF, Munich: Actualisation of in-house software LaFIS manual
04/2002	Internship at GLA, Munich: Quality assurance of digital maps, ArcObjects-programming
07-2002	Graduate assistant at Chair for Geography and Geographical Remote Sensing, LMU München: Support of field trips

- since 10-2002 Guide at Botanical Garden Munich, in German, English and Italian
- 10-2002/12-2003 Student trainee at GLA, Munich: Quality assurance of digital maps with ArcGIS and ArcInfo within the framework of the BIS-project
- 07-2003 Graduate assistant at Chair of Biogeography, University of Bayreuth: Support of field trips
- 04-2004/12-2004 Research associate at GLA, Munich: soil scientific works within the framework of the BIS-project
- 07-2004/12-2007 Raised by the DBU scholarship programme for doctorates
- 02-2008/05-2008 Research associate at Chair for Geography and Geographical Remote Sensing, LMU München: Modelling snow parameters

Publications and Conference Contributions

- 09-2004 Weiss, C. and Schmidtlein, S. *The Effects of Sheep Grazing on Alpine Meadows in the Bavarian Alps*. In Verhandlungen der Gesellschaft für Ökologie, 34, 400 (2004).
- 09-2005 Weiss, C. and Schmidtlein, S. *Combining Discrete and Non-discrete Approaches in vegetation Mapping for Monitoring*. In Verhandlungen der Gesellschaft für Ökologie, 35, 432 (2005).
- 2007 Schmidtlein, S.; Zimmermann, P.; Schüpferling, R.; Weiss, C. *Mapping the floristic continuum: Ordination Space Position Estimated from Imaging Spectroscopy*. In Journal of Vegetation Science, 18, 131-140 (2007).
- 04-2007 Weiss, C. and Schmidtlein, S. *Monitoring Conservation Areas with Imaging Spectroscopy: Combining Discrete and Non-discrete Approaches*. In 5th EARSeL SIG IS Conference, Bruges, Belgium (2007).
- 04-2008 Weiss, C. and Schmidtlein, S. *Monitoring großer FFH Gebiete mit hyperspektraler Fernerkundung*. In BfN Statusseminar Biodiversitätsmonitoring, Insel Vilm (2008).

Munich, June 2008